THE

The American Journal of ANATOMY

MANAGING EDITOR

DONALD DUNCAN

THE UNIVERSITY OF TEXAS
MEDICAL BRANCH
GALVESTON TEXAS

ASSOCIATE EDITORS

BURTON L. BAKER
UNIVERSITY OF MICHIGAN

SAM L. CLARK, JR.
WASHINGTON UNIVERSITY

C. P. LEBLOND
MCGILL UNIVERSITY

RICHARD J. BLANDAU
UNIVERSITY OF WASHINGTON

DON W. FAWCETT
HARVARD UNIVERSITY

HARLAND W. MOSSMAN
UNIVERSITY OF WISCONSIN

VOLUME 112

JANUARY MARCH, MAY 1963

PUBLISHED BY

THE WISTAR INSTITUTE OF ANATOMY AND BIOLOGY
PHILADELPHIA PA

CONTENTS

No 1 JANUARY 1963

No 2 MARCH 1963

No. 3 MAY 1963

The Thymus in Mice of Strain 129/J Studied with the Electron Microscope[1]

SAM L. CLARK, JR.
Department of Anatomy Washington University School of Medicine St. Louis, Missouri

The thymus has been called an endocrine gland and a lymphoid organ, but there is scant evidence that it functions as either (see the reviews by Marine, '32; Maximow and Bloom, '57; Tesseraux, '59). In embryonic origin it resembles the thyroid and parathyroid glands, being derived from the endoderm, and perhaps also the ectoderm, of the pharyngeal pouches (Norris, '38) Initially the thymus is a hollow epithelial structure but obliteration of the lumen and infiltration by small thymic cells alter its glandular appearance. Nevertheless vestiges of its original epithelial character remain in the Hassall's corpuscles and the cords of large pale cells that populate the thymic medulla. Some of the latter have fine intracellular fibrils and cilia; in places they assume an acinar arrangement (Deanesly '28 Hoshino '61). In the acute involution of disease or stress most of the small thymic cells degenerate which exaggerates the epithelioid appearance of the organ (Dougherty '52 Ito and Hoshino, '62) Despite these indications that the thymus may be glandular no secretory granules or inclusions have been described and the only extensive evidence for a thymic hormone is that of Metcalf ('59) He extracted a factor from the thymus which increased the production of lymphocytes by other lymphoid tissues. This factor accumulated to a measurable degree in the blood plasma of both human beings and of mice with lymphatic leukemia but the active principle has not yet been characterized chemically.

The small cells of the thymus resemble lymphoid cells and seem to be equivalent to them functionally. Thymic cells, injected intravenously have been traced to lymph nodes and spleen where they can restore immunological competence to lethally irradiated animals (Micklem and Ford, '60 Rankin, '60 Snell, Winn and Kandutsch, '61) Conversely transfused lymphocytes have been identified in the thymus (Gengozian, Urso, Congdon, Conger and Makinodan, '57; Popp, '61; Rankin, '60) Nevertheless the thymus differs from other lymphoid organs in both structure and function. It contains cells that appear to be epithelial. It lacks sinuses the blood vascular system is a capillary network and lymphatics drain only the interlobular connective tissue. Adrenal and gonadal hormones produce greater atrophy of the thymus than of other lymphoid organs (Dougherty '52) but thymic lymphocytes are more resistant to radiation than those elsewhere (Trowell, '61) Ordinarily the thymus lacks germinal centers and does not make antibody (Marshall and White '61) Its cells acquire little immunity to grafts of foreign tissue elsewhere in the body (Winn '61) and transplanted thymic cells rarely develop immunity against their host (Vos, de Vries Collenteur and van Bekkum, '59 Billingham, Defendi, Silvers and Steinmuller '62) However Marshall and White ('61) stimulated the thymus to make antibody by injecting antigen directly into the organ. They proposed that there is a barrier to the penetration of antigens from the blood into the thymus, and they demonstrated that subcutaneously injected trypan blue and pneumococcal polysaccharide failed to reach the thymic parenchyma unless it had been injured previously by cauterization.

[1] This work was supported in part by grants RG-3784 and RG-7178 from the National Institutes of Health, United States Public Health Service.
This work was performed during the tenure of Career Development Award of the National Institutes of Health, United States Public Health Service.

The fact that the thymus beginning at puberty slowly atrophies until in old age it is almost completely replaced by adipose tissue, together with the difficulty of detecting any functional deficit after thy mectomy have led to the conclusion that the thymus is a vestigial organ, of little use to mature animals. However before puberty and perhaps for some time after ward, it appears to be the chief site of lymphopoiesis in the body (Kindred 40 Andreasen and Ottesen, 44; Schooley Bry ant and Kelly '59) Furthermore thy mectomy in some species causes a more or less permanent reduction in the total volume of lymphoid tissue in the body and in the numbers of circulating lymphocytes (Bierring '60; Metcalf '59 Miller '61b; Schooley and Kelly '61) Thymectomy performed soon after birth limits the even tual competence of the lymphoid tissues to make both humoral and cellular antibodies (Miller '61b Archer and Pierce '61; Arnason Janković and Waksman '62 Szenberg and Warner '62) Thus the ymus seems to exert a formative influence on the development of the lymphoid system and may even play a role in its maintenance.

In an analogous way the thymus must be present for lymphatic leukemia to de velop in mice whether the cause of the leukemia be a virus, ionizing radiation or genetic predisposition (Law and Potter '56 Law '59 Gross '59 Miller '59 '60 '61a) Leukemic cells begin their proliferation in the thymus even though the thy mus may have been grafted from another animal and the cells which become leu kemic are the host s. Presumably the thymus protects the leukemic cells from homeostatic mechanisms which retard the development of leukemia elsewhere in the body Similarly the thymus may shelter forbidden clones (Burnet '58) of lym phoid cells capable of forming antibodies against antigenic constituents of the ani mal s own body As evidence for this Burnet and Holmes ('62) cite the presence of germinal centers in the thymuses of a strain of auto-immune mice and in cases of myasthenia gravis a disease attributed to auto-immunity (Castleman '5 Harvey and Johns '6) Perhaps the barrier which protects these cells from destruction is the same barrier that excludes antigens from the thymus (Marshall and White '61) but in any case the thymus provides a peculiar environment which affects the developmental potentialities of its lymphoid cells.

In adult animals thymic lymphocytes arise chiefly by mitosis of larger lymphocytes (Leblond and Sainte-Marie '60) but their embryonic origin remains obscure. Maximow ('09) concluded that lymphocytes invade the embryonic thymus from the surrounding mesenchyme but others believe they arise from thymic epithelial cells. Most of the evidence both for and against the latter hypothesis comes from attempts to produce lymphocytes from cul tures of thymic epithelium. Gregoire ('35) and Murray (47) failed, whereas Auer bach ('61a '61b) succeeded, but his cul tures might have been contaminated with mesenchymal reticular cells.

In this study the electron microscope has been used to examine the thymus in young adult mice paying particular atten tion to the reticular cells, their epithelial character and the environment which they provide for thymic lymphoid cells It has been found that the lymphoid cells are separated from connective tissue by a cellular barrier just as they are in lymph nodes (Clark, '62) but the structure of the barrier differs in the two organs

METHODS

Nine male mice three to nine months old of strain 129/J (a strain with low incidence of tumors and high resistance to radiation bred from stock obtained from the Roscoe B Jackson Memorial Laboratory Bar Harbor Maine) were killed by ethyl ether or a blow on the head bled, and the thymus prepared for electron mi croscopy Small blocks of tissue were fixed for one hour at room temperature in 1% osmium tetroxide dissolved in a balanced salt solution buffered to pH 7 4 containing a high concentration of cal cium nitrate The salt solution used was that of White (46) adapted for fixation by W C Bauer (personal communication '60) Extra calcium was added to improve the preservation of cell membranes (Palay McGee Russell Gordon and Grillo '62) but it precipitated when added to the salt

solution of White used in previous experiments (Clark, '62) By using an earlier formula published by White (46) which contains half as much phosphate and bicarbonate, calcium has been added to three times its prescribed value without precipitation, and good preservation of tissues has been obtained. Here is the formula now in use

Stock solution A

NaCl	14 0 gm
KCl	0 75
$MgSO_4$ (anhydrous)	0.55
$Ca(NO_3)_2 \cdot 4H_2O$	1.5
Distilled water to a volume of	100 ml

Stock solution B

Dextrose	17 0 gm
$NaHCO_3$	1 1
$Na_2HPO_4 \cdot 7H_2O$	0.22
KH_2PO_4 (anhydrous)	0.052
Phenol red	0 01
Distilled water to a volume of	100 ml.

Saturate with CO_2.

The stock solutions are stored at 5 C and diluted to 20 volumes for use To avoid precipitation, do not mix the stock solutions without dilution.

After fixation the tissues were dehydrated in ethanol and embedded in Epon 812 according to Luft's method ('61) Sections were cut for light and electron microscopy with a Porter-Blum microtome (Servall) and glass knives. Thin sections were stained with saturated aqueous uranyl acetate acidified with acetic acid or with the lead hydroxide stain of Millonig ('61) and examined in an RCA EMU 3C electron microscope

RESULTS

In these young adult mice of strain 129/J the thymus was white and firm, and filled the anterior mediastinum. In microscopic sections it appeared solid and cellular with distinct boundaries and no infiltrating adipose cells. The delicate stroma consisted of a thin capsule rudimentary interlobular septa, and a penetrating lacework of reticular fibers more concentrated in the medulla than in the cortex (figs. 1 9 10 11) The reticular fibers were comprised of collagen associated with a fine fibrillar material common to connective tissue elsewhere (Clark '62) Fibroblasts were present, even in some small reticular bundles. The blood vessels formed a sparse network, again more concentrated in the medulla, and no lymphatics were identified. Within this stroma, the thymic parenchyma formed an almost continuous mass of cells. On the basis of their appearance in the electron microscope these cells could be divided into three categories: (1) lymphoid cells which include the so-called thymocytes or small round cells of the thymus (2) macrophages, corresponding to what some authors have called mesenchymal reticular cells and (3) epithelial cells the proper reticular cells of the thymus (fig 1). The cortex, though not sharply demarcated from the medulla, could be distinguished by its great concentration of lymphoid cells and its sparse attenuated epithelial cells (fig. 2) In the medulla, where lymphoid cells were few epithelial cells were numerous, voluminous, and arranged in clumps, solid cords, or nests resembling acini (figs. 4 12 19) No Hassal's corpuscles were seen. The lymphoid cells of the thymus occupied a sequestered site, separated from connective tissue and blood vessels by the epithelial cells and their basement membrane (figs. 6 7) Venules with a thick endothelium infiltrated by lymphocytes were found in the thymus (figs 22, 23) similar to those already described in other lymphoid tissues (Smith and Hénon, '59 Clark, '62) A detailed description of these features follows.

The free cells of the thymus were indistinguishable in structure from lymphoid cells elsewhere (see Clark, 62) There were lymphocytes of various sizes and large cells appearing to be transitional between large lymphocytes and macrophages (figs. 1–7 11) Mitotic figures were numerous but scattered randomly there were no germinal centers. Plasma cells with ergastoplasmic sacs in all stages of dilatation, including some with very dense contents were concentrated near the surface of the cortex and around blood vessels (fig 5) Eosinophils were numerous near blood vessels. Mast cells were rare

Macrophages filled with numerous inclusions lay within the parenchyma of both

cortex and medulla as well as in the surrounding connective tissue (fig. 2) They could be distinguished from epithelial cells by their lack of desmosomes and tonofibrils. The inclusions varied in size and constitution. Most were less than one micron in diameter some were yellow brown by transmitted light and others stained with the periodic acid Schiff technique. As seen by electron microscopy they combined dense often lamellar structures and vacuolar spaces. Within some macrophages there appeared to be small lymphocytes in varying stages of decomposition (fig. 9) In the periphery of the cortex there were some very large macrophages tightly filled with small inclusions and deeply indented by the surrounding lymphocytes and plasma cells they did not appear to be multinuclear (fig 3)

Epithelial cells second only to small lymphocytes in numbers could be identified by their tonofibrils and desmosomes they varied greatly in shape and contents. Nuclei were uniformly large with finely divided chromatin, prominent nucleoli (figs. 1 2, 4 11 12) and in a few instances intranuclear ring-shaped structures (figs. 9 12) Mitotic figures were not observed. The cytoplasm was marked by unusually large mitochondria, numerous particles resembling ribonucleoprotein, and in some areas well-developed ergastoplasm. Tonofibrils were concentrated near the nucleus and at the periphery of the cell where they inserted into desmosomes connecting adjacent cells (figs 1 4 7 9 10 12 13 19 20) This arrangement was similar to that found in epidermis (Setälä, Merenmies Stjernvall and Nyholm '60) Wherever epithelial cells bordered upon connective tissue a basement membrane separated the two. At intervals along this border there were structures in the epithelial cells resembling half desmosomes each associated with a region of increased density in the adjacent basement membrane (fig. 21) These structures have also been described in epidermis (Setälä et al. '60 Munger and Brusilow '61)

Cytoplasmic inclusions in epithelial cells fell into three classes First there were dense inclusions containing various lamellar or vacuolar structures similar to those found in macrophages (figs. 2 4 10–13, 19) These were not numerous and there were no signs of phagocytosis of lymphocytes. Second there were small dense granules, spherical or oblong in shape and ranging from 75 millimicrons upward in smallest diameter These were found in close association with ergastoplasm and each granule was invested in a single membrane (figs. 13 14) There were similar granules in some macrophages and vascular endothelial cells but many of these granules were not associated with ergastoplasm and lacked an investing membrane (figs. 6–8) Third some epithelial cells contained nests of cytoplasmic vacuoles more or less spherical uniform in size, indented by microvillous projections of the surrounding membrane and enclosing an amorphous material of moderate density (figs. 15–18) In a few cells the vacuoles were large and irregular as if they had formed by coalescence of smaller vacuoles (fig. 4) In other cells amorphous material completely filled the vacuoles microvilli were few and the membranes separating adjacent vacuoles were indistinct; these clusters resembled the multilocular droplets of mucus in goblet cells of the intestine (fig. 17) In a few places amorphous material similar to that in the vacuoles occupied an extracellular position in what appeared to be the lumen of an acinus surrounded by epithelial cells which, in rare instances bore cilia (fig. 19) Some epithelial cells contained droplets that stained with the periodic acid Schiff technique but their correspondence with inclusions viewed in the electron microscope was not established.

The barrier interposed between lymphoid cells and connective tissue consisted of a continuous layer of epithelial cells closely joined by desmosomes and resting on a basement membrane This barrier extended completely around the periphery of each lobule and surrounded each of the penetrating blood vessels and reticular fibers (figs. 1 6 7 9–11) Some epithelial cells were tenuous and thin others were rounded and voluminous but they formed one interconnected whole with lymphoid cells lying in the intercellular interstices. In places lymphocytes lay athwart the bar

der extending from a space between epithelial cells, through a defect in the basement membrane into the adjacent connective tissue (fig. 6) The connective tissue around arterioles and most capillaries was narrow and almost acellular containing only a few fibroblasts or perivascular cells and a rare lymphoid cell, but around venules there was a wide space usually filled with lymphocytes. Leblond and Sainte-Marie ('60) called this perivascular space a doubled-walled lymphatic vessel but by electron microscopy no lymphatic endothelium could be seen, there being only thymic epithelium and venular endothelium on either side of a connective tissue space filled with lymphocytes.

The arterioles and capillaries of the *thymus were not unusual except that capil*lary endothelial cells were thicker and contained fewer small vesicles than those of many other capillaries (fig 6) (Palade '61) Each cross-section of a capillary consisted of four to six endothelial processes, interconnected by small desmosomes like those in other capillaries described by Muir and Peters ('62)

The venules of the thymic cortex resembled the so-called high endothelial post capillary venules of lymph nodes, tonsils, and Peyer's patches (Smith and Hénon '59 Clark, '62) They were vessels with wide lumens and tall endothelial cells interspersed with numerous small lymphocytes (fig. 22) Some lymphocytes lay partly surrounded by endothelial cells, and partly in the lumen of the vessel as if they were migrating through the vascular wall (fig. 23) It was not clear from single sections whether the lymphocytes lay between or within endothelial cells. Some endothelial cells contained inclusions similar to those in macrophages, but no degenerating lymphocytes were observed. The basement membrane of the endothelium without any surrounding smooth muscle was contiguous with the lymphocyte-filled perivascular connective tissue.

No forms intermediate between epithelial cells and lymphocytes were recognized. Where lymphocytes lay adjacent to epithelial cells, no syncytial, desmosomal or other form of attachment was seen.

DISCUSSION

These observations reinforce the conclusion that the thymus contains lymphoid cells that can migrate to and from other lymphoid tissues. Small lymphocytes seem to have a propensity for invading epithelia in the tonsils and small intestine. In the present study they were found occluding interruptions in the basement membrane of the thymic epithelium, as if in the process of passing through it. Perhaps small lymphocytes penetrate basement membranes more readily than do other types of cells. The venules with thick endothelium also included small lymphocytes in their walls. This type of venule not described previously in the thymus has been considered as a pathway for migration of small lymphocytes in other lymphoid tissues. Although most investigators had supposed that lymphocytes entered the venules from surrounding lymphoid tissue Gowans ('61) has obtained autoradiographic evidence that, in lymph nodes, intravenously injected lymphocytes cross the walls of these vessels in the opposite direction, completing the circuit from blood to thoracic duct which he had proposed earlier (Gowans, '59) The direction of migration in the thymus remains to be determined. In addition, it is not known whether the endothelial cells are specialized to trap lymphocytes or thicken secondarily as a result of their migration

Thymic lymphoid cells come from a unique environment which may determine their potentialities for function in the lymphoid system. Three features of this environment will be discussed the destruction of lymphoid cells secretion by epithelial cells and the hemato-thymic barrier.

The thymus more than other lymphoid tissues, undergoes acute involution in response to a variety of stresses. Many lymphoid cells are destroyed and large macrophages increase in number (Loewenthal and Smith '52 Ito and Hoshino '62) Concomitantly lysosomes — subcellular bodies rich in acid phosphatase and common in macrophages — can be isolated in increased numbers (Rahman, '62). It was in macrophages that signs of phagocytosis of lymphocytes were observed in

the present study; perhaps macrophages grow large in acute involution by ingesting lymphocytes. The products of lymphocytic degeneration mediated by macrophages may influence other lymphoid cells par ticularly those that surround the large macrophages. Metcalf and Ishidate ('62) found mitotic lymphoid cells clustered about such macrophages in mice of the AKR strain, hereditarily predisposed to lymphatic leukemia, but they were cau tious about concluding that macrophages play a primary role in the pathogenesis of leukemia.

Thymic epithelial cells presumably derived from the endoderm or ectoderm of the thymic primordium contain small dense granules and vacuoles with amor phous contents that might be the "lymphocytosis-stimulating factor of Metcalf ('59). The granules resemble those in the para thyroid gland judged to be secretory by Munger and Roth ('62) but similar gran ules occur in macrophages in both thymus and lymph nodes (see fig. 21 of Clark, '62) Amorphous material similar to that in epithelial vacuoles was found in inter cellular spaces that resembled the lumens of acini. If either of these materials stimulates lymphocytic proliferation it might do so in the thymus as well as at distant sites.

The epithelial barrier interposed be tween lymphoid cells and connective tissue in the thymus with its desmosomal junctions and basement membrane is more elaborate than that found in lymph nodes (Clark, '62) If it is the agency responsible for excluding antigens then it constitutes the hemato-thymic barrier proposed by Marshall and White ('61) The analogy with the hemato-encephalic barrier seems strained in that the thymus where connective tissue surrounds blood vessels corresponds in structure only to those regions of the brain supposedly de void of a blood brain barrier (Dempsey and Wislocki, '55) Nevertheless the brain and thymus both offer protection to the growth of unusual clones of cells grafts of foreign tissue sometimes urvive in the brain (Crouse '59) leukemic cells and "forbidden clones of auto-immune cells can grow in the thymus (Burnet and Holmes '62) Probably the word "barrier is too passive to describe adequately the partial exclusion of certain substances from either the brain or the thymus. Substances penetrate the brain at various rates by what seem to be active processes (Tschirgi, '62) and the thymus may use equally active means to exclude antigens and protect malignant or auto-immune cells from destruction.

The thymus does not seem to participate directly in immune responses but it probably supplies lymphocytes in quantity to the rest of the body (Bierring '60 Auer bach '61b) Removal of the thymus soon after birth cripples development of immunological competence and Miller ('61b) has proposed that the thymus provides the cells that produce immune responses in other lymphoid tissues, even though these tissues also make lymphocytes. That immunological competence may stem from the thymus is indicated by Kalmutz s ('62) demonstration of antibody synthesis by opossum embryos at an age when lymph oid cells are confined almost entirely to that organ. The thymus may serve as the primordial source of lymphocytes Auer bach ('61a) has concluded that they develop from thymic epithelial cells and Ackerman ('62) has proposed a similar epithelial origin in the bursa of Fabricius an organ in birds analogous to the thymus. In neither case does the evidence seem conclusive and no signs of such a transition were observed in the present study but embryonic thymus was not examined. Even if lymphocytes do originate from epi thelial cells they reproduce during most of life by mitosis of larger lymphocytes both in the thymus and elsewhere (Le blond and Sainte Marie '60) Further more the lymph nodes and spleen remain immunologically active and self-sufficient after the thymus has reached an advanced stage of atrophy Therefore whatever contribution the thymus makes to the development of immunological competence must be more specific than merely the production of large numbers of lymphocytes.

The production of lymphocytes by the thymus may come at a strategic stage in development when soon after birth the initial exposure to numerous antigens stimulates large numbers of lymphoid cells to become plasma cells Pla ma cells do

not seem to be capable of mitosis possibly their differentiation is irreversible (Nossal and Mäkelä, '62) Therefore unless lymphoid cells are replaced by mitosis as frequently as they differentiate into plasma cells the lymphoid system may fail to maintain itself This supposition is not supported by reports that the initial response to antigen is proliferation of lymphoid cells to form germinal centers (Congdon and Makinodan, '61) but the balance between differentiation and replacement may be a delicate one or in the final stages of a response, differentiation may continue after replacement ceases. If the lymphoid system is so vulnerable in young animals the thymus may contribute to its maintenance in two ways. First, a thymic hormone may stimulate mitosis in other lymphoid tissues (Metcalf '59) Second the thymus may provide lymphoid cells with an environment free from antigenic stimulation, where reproduction may proceed without competition from irreversible differentiation.

The latter proposal may be carried a step further in terms of Burnet's ('58) clonal selection hypothesis. According to Burnet, antigens provoke the evolution by mutation and natural selection, of clones of lymphoid cells adapted to the synthesis of specific antibody In the thymus free from antigenic stimulation, lymphoid cells might remain uncommitted to any one antigen; thus the thymus could provide a constant supply of lymphoid cells ready to respond to new antigenic experiences. If this supposition is correct, atrophy of the thymus with advancing age might be accompanied by immunologic senility in which the "memory of old antigenic experiences persists in the ability to make antibodies but the lymphoid system has lost the capacity to respond to new antigenic stimuli. Uncommitted clones of cells in the thymus might by chance develop immunological reactivity against some constituent of the animal's own body but as long as such potentially auto-immune cells remained within the thymus, unexposed to the proper iso-antigen no harm would result. Cells wandering from the thymus probably would be destroyed by excessive antigen or whatever homeostatic mechanism suppresses auto-immune cells. However should the hemato-thymic barrier be injured, the iso-antigen might reach the auto-immune clone in the proper concentration to elicit antibody synthesis, and auto-immune disease would ensue.

These speculations are not entirely self consistent, but regardless of their validity increased knowledge of the thymus should enhance our understanding of some of the activities of the lymphoid system — responses that can not be explained completely in terms of the activities of individual cells, such as immunological unresponsiveness, auto-immunity and possibly the resistance to cancer

SUMMARY

The thymus in these young adult male mice was a solid epithelial organ, infiltrated with lymphoid cells and perforated by delicate reticular fibers and blood vessels. The epithelial cells, presumably derived from the endoderm or ectoderm of the thymic primordium, were characterized by cytoplasmic tonofibrils and desmosomes connecting adjacent cells. Wherever the epithelium bordered connective tissue as at the periphery of the lobules and along reticular fibers and blood vessels, there was a basement membrane. No Hassal's corpuscles were seen but a few epithelial cells were arranged in acini and possessed cilia. Some epithelial cells contained small dense granules or clusters of vacuoles filled with amorphous material, either of which might represent a secretory product. No signs that epithelial cells produce lymphocytes were observed in these adult animals. There were large macrophages containing numerous inclusions and degenerating lymphocytes, but possessing none of the distinctive features of epithelial cells. Most of the lymphoid cells lay between epithelial cells in a space separated from connective tissue by a continuous barrier of epithelial cells and basement membrane This probably is the hemato-thymic barrier that prevents antigens and vital dyes from penetrating into the thymic parenchyma. Small lymphocytes were found occluding gaps in the epithelial basement membrane as if migrating through it, and others infiltrated the walls of peculiar venules with thick endothelial cells. This type of vessel, not described

previously in the thymus seems to be a site for migration of lymphocytes between lymphoid tissues and the blood stream In considering the physiological evidence that the thymus plays a necessary role in the development of immunological competence it was proposed that lymphocytes migrating from the secluded environment of the thymus possess unique potentialities for function in the lymphoid system.

LITERATURE CITED

Ackerman, G. A. 1962 Electron microscopy of the bursa of Fabricius of the embryonic chick with particular reference to the lympho-epithelial nodules. J Cell Biol., 13 127–146.

Andreasen, E., and J Ottesen 1944 Significance of the various lymphoid organs to the lymphocyte production in the albino rat. Acta Path. Microbiol. Scand. Suppl., 54 25–32.

Archer O., and J C. Pierce 1961 Role of thymus in development of the immune response. Fed. Proc., 20 26.

Arnason, B G., B. D Janković and B. H. Waksman 1962 Effect of thymectomy on "delayed" hypersensitive reactions. Nature 194 99–100.

Auerbach, R. 1961a Experimental analysis of of the origin of cell types in the development of the mouse thymus. Develop. Biol., 3 336–354

——— 1961b Genetic control of thymus lymphoid differentiation. Proc. N t. Acad. Sci., 47 1175–1181

Bierring, F 1960 Quantitative investigation on the lymphomyeloid system in thymectomized rats. In Ciba Foundation Symposium on Haemopoiesis. G. E. W Wolstenholme and M. O'Connor eds. Little Brown and Co., Boston pp 185–198.

Billingham R. E., V Defendi, W K. Silvers and D Steinmuller 1962 Quantitative studies on the induction of tolerance of skin homograft and on runt disease in neonatal rats. J N t. Cancer Inst., 28 365–435.

Burnet M. 1958 The Clonal Selection Theory of Acquired Immunity Vanderbilt University Press Nashville 1959

Burnet, F M., nd M. C. Holmes 1962 Thymus lesion in an uto-immune disease of mice. N ture 194 146.

C tleman, B 1955 Tumors of the thymus gland. In Atla of Tumor Pathology Armed Forces Institute of P thology W shington, D C., Section V f scicle 19

Clark, S L., J 1962 The reticulum f lymph nodes in mice tudied with the electron microscope Am J Anat 110 17 ...4

Congdon, C. C and T M kinodan 1961 Splenic white pulp alteration after tigen injection relation to time of serum antibody production. Am. J P th 39 697 710

Crouse G. S. 19 9 The effec of variation in the ge of the donor on homologous gr ft into the brain of the r t Ana Rec 135 215–223

Deanesly R. 1928 Experimental studies on the histology of the mammalian thymus. Quart. J Micro. Sci., 72: 247 273.

Dempsey E. W., and G. B. Wislocki 1955 An electron microscopic study of the blood-brain barrier in the rat, employing silver nitrate as a vital stain. J Biophys. and Biochem. Cytol., 1 245–256.

Dougherty T F 1952 Effect of hormones on lymphatic tissue. Physiol. Rev 32: 379–401.

Gengozian, N., I. S. Urso, C. C. Congdon, A. D. Conger and T Makinodan 1957 Thymus specificity in lethally irradiated mice treated with rat bone marrow Proc. Soc. Exp. Biol. and Med., 96 714–720.

Gowans, J L. 1959 The recirculation of lymphocytes from blood to lymph in the rat. J Physiol., 146: 54–69

——— 1961 Group Discussion. In: Biological Activity of the Leucocyte G. E. W Wolstenholme and M. O'Connor eds. Little Brown and Co., Boston, Ciba Foundation Study Group No. 10 pp. 107–108.

Gregoire, C. 1935 Recherches sur la symbiose lymphoépithéliale u niveau du thymus de mammifère. Arch. de Biol., 46 717–820.

Gross, L. 1959 Effect of thymectomy on development of leukemia in C3H mice inoculated with leukemic "passage" virus. Proc. Soc. Exp. Biol. and Med., 100 325–328.

Harvey A. M., and R. J John 1962 Myasthenia gravis and the thymus. Amer J Med., 32 1–5.

Hoshino, T 1961 Occurrence of ciliated vesicle-containing reticular cells in the mouse thymus. Okajimas Fol. Anat. J p., 37 209–213.

Ito, T., and T Hoshino 1962 Histological changes of the mouse thymus during involution and regeneration following administration of hydrocortisone. Z. Zellforsch., 56 445–464

Kalmutz, S. E. 1962 Antibody production in the opossum embryo. N ture 193 851–853.

Kindred J E. 1940 A quantitative study of the hemopoietic organs of young albino rats. Amer J Anat., 67 99–149

Law L. W., and M. Potter 1956 The behavior in transplant of lymphocytic neoplasms arising from parental thymic grafts in irradiated, thymectomized hybrid mice Proc N t. Acad. Sci., 42 160–167

Law L. W 1959 Some aspect of the etiology of leukemia. Can. Cancer Conf 3 145–169.

Leblond, C. P and G. Sainte-Marie 1960 Models for lymphocyte and plasmocyte formation. In Ciba Found tion Symposium on Haemopoiesis. G. E. W Wolstenholme nd M. O'Connor eds. Little Brown and Co Boston pp. 152 172.

Loewenthal, L. A., nd C. Smith 1952 Studies on the thymus of the mammal. IV Lipid laden foamy cell in the invol ting thymus of the mouse An t. Rec., 112 1 15.

Luft J H. 1961 Improvement in epoxy resin embedding methods. J Biophys nd Biochem. Cytol 9 409–414

M rine D. 1932 The thyroid, p rathyroid and thymus In Special Cytology E V Cowdry ed. P ul B Hoeber Inc New York, vol 2, pp 797–808

Marshall, A. H. E., and R. G. White 1961 The immunological reactivity of the thymus. Brit. J Exp. Path., 42: 379–385.

Maximow A. 1909 Untersuchungen über Blut und Bindegewebe. II. Über die Histogenese der Thymus Bei Säugetieren. Arch. Mikroskop. Anat. u. Entwicklungsmech., 74: 525–621.

Maximow A. A., and W Bloom 1957 A Text book of Histology W B. Saunders Co., Phila delphia, pp 276–281

Metcalf, D. 1959 The thymic lymphocytosis stimulating factor and its relation to lymphatic leukemia. Can. Cancer Conf 3 351–366.

Metcalf, D., and M. Ishidata, J 1962 PAS-positive reticulum cells in the thymus cortex of high and low leukaemia strains of mice. Austral. J Exp. Biol. Med. Sci., 40 57–72.

Micklem, H. S., and C. E. Ford 1960 Proliferation of injected lymph node and thymus cells in lethally irradiated mice. Transplant. Bull., 26 436–441.

Miller, J F A. P 1959 Fate of subcutaneous thymus grafts in thymectomized mice inoculated with leukaemic filtrate. N ture 184 (suppl. 23) 1809–1810.

——— 1960 Studies on mouse leukaemia. The fate of thymus homografts in immunologically tolerant mice. Brit. J Cancer 14 244–255.

——— 1961 Analysis of the thymus influence in leukaemogenesis. Nature, 191 248–249

——— 1961b Immunological function of the thymus. Lancet, 2. 748–749

Millonig, G. 1961 A modified procedure for lead staining of thin sections. J Biophys. and Biochem. Cytol., 11 736–739

Muir A. R., and A. Peters 1962 Quintuple-layered membrane junctions at terminal bars between endothelial cells. J Cell Biol., 12. 443–448.

Munger B. L., and S. W Brusilow 1961 An electron microscopic study of eccrine sweat glands of the cat foot and toe pads — evidence for ductal reabsorption in the human. J Biophys. and Biochem. Cytol., 11 403–417

Munger B. L., nd S I. Roth 1963 The mor phologic sequence of secretion in the parathy roid glands as compared to other endocrine organs. Anat. Rec., 142 261

Murray R. G. 1947 Pure cultures of rabbit thymus epithelium. Amer J Anat., 81 369–411.

Norris E. H. 1938 The morphogenesis and histogenesis of the thymus gland in man in which the origin of the Hassall' corpuscles of the human thymus is discovered. Contrib Embryol., Carnegie Inst., Wash 27 191–207

Nossal, G. J V and O Mäkelä 1962 Autoradiographic studies on the immune response I. The kinetics of plasma cell prolifer tion J Exp. Med., 115 209–230

Palade G. E. 1961 Blood capillaries of heart and other organs. Circulation 24 368–388

Palay S. L., S. M. McGee-Russell S Gordon Jr and M. A. Grillo 1962 Fixation of neural tissues for lectron microscopy by perfusion with solutions of osmium tetroxide. J Cell Biol., 12. 385–410

Popp R. A. 1961 Repopulation of thymus by immunologically competent cells derived from donor marrow Proc. Soc. Exp. Biol. and Med., 108 561–564

Rahman, Y E. 1962 Electron microscopy of lysosome-rich fractions from rat thymus isolated by density-gradient centrifugation before and after whole-body x irradiation. J Cell Biol., 13. 253–260.

Rankin, J J 1960 Circulation of lymphocytes and thymocytes in the normal and leukemic mouse. Acta Anat 40 221–230

Schooley J C., B J Bryant and L S. Kelly 1959 Preliminary autoradiographic observations of cellular proliferation in lymphoid tissues, using tritiated thymidine. In The Kinetics of Cellular Proliferation, F Stohlman, J ed. Grune and Stratton, New York, pp. 208–217

Schooley J C., and L. S. Kelly 1961 The thymus in lymphocyte production. Fed. Proc., 20 71

Setälä, K., L. Merenmies, L. Stjernvall and M. Nyholm 1960 Mechanism of experimental tumorigenesis. IV Ultrastructure of interfollicular epidermis of normal adult mouse. J N t. Cancer Inst., 24 329–353.

Smith, C., and B. K. Hénon 1959 Histological and histochemical study of high endothelium of post-capillary veins of the lymph node Anat. Rec., 135 207–214

Snell, G. D., H. J Winn and A. A. Kandutsch 1961 A quantitative study of cellular immunity J Immun., 87 1–17

Szenberg, A., and N L. Warner 1962 Dissociation of immunological responsiveness in fowls with hormonally arrested development of lymphoid tissues. N ture 194 146–147

Tesseraux, H. 1959 Physiologie und P thologie des Thymus. Zwanglose Abhandlungen us dem Gebiete der Inneren Sekretion, Johann Ambrosius Barth, Leipzig, 9 1–147

Trowell, O A. 1961 Radiosensitivity of the cortical and medullary lymphocytes in the thy mus. Int. J Radiat. Biol., 4 163–173.

Tschirgi, R. D. 1962 Blood-brain barrier fact or fancy? Fed. Proc., 21 665–671

Vos, O., M. J de Vries, J C. Collenteur and D W van Bekkum 1959 Transplantation of homologous and heterologous lymphoid cells in -irradiated and non-irradiated mice. J N t. Cancer Inst., 23 53–73.

White P R. 1946 Cultivation of animal tissues *in vitro* in nutrients of precisely known constitution. Growth, 10 231 260.

Winn, H. J 1961 Immune mechanisms in homotransplantation. II. Quantitative assay of the immunologic activity of lymphoid cells stimulated by tumor homografts J Immun., 86 228–239

Yoffey J M., and F C Courtice 1956 Lymphatics, Lymph and Lymphoid Tissue. Harvard University Press, Cambridge Mass.

previously in the thymus seems to be a site for migration of lymphocytes between lymphoid tissues and the blood stream. In considering the physiological evidence that the thymus plays a necessary role in the development of immunological competence it was proposed that lymphocytes migrating from the secluded environment of the thymus possess unique potentialities for function in the lymphoid system.

LITERATURE CITED

Ackerman, G. A. 1963 Electron microscopy of the bursa of Fabricius of the embryonic chick with particular reference to the lympho-epithelial nodules. J Cell Biol., 13 127–146.

Andreasen, E., and J Ottesen 1944 Significance of the various lymphoid organs to the lymphocyte production in the albino rat. Acta P th. Microbiol. Scand. Suppl., 54 25–32.

Archer O., and J C. Pierce 1961 Role of thymus in development of the immune response. Fed. Proc., 20: 26.

Arnason, B G., B. D Janković and B H. Waksman 1962 Effect of thymectomy on delayed" hypersensitive reactions. Nature 194 99–100.

Auerbach, R. 1961 Experimental analysis of of the origin of cell types in the development of the mouse thymus. Develop. Biol., 3 336–354.

——— 1961b Genetic control of thymus lymph cod differentiation. Proc. N t. Acad. Sci., 47 1175–1181

Bierring, F 1960 Quantitative investigation on the lymphomyeloid system in thymectomized ts. In Ciba Foundation Symposium on Haemopoiesis. G. E. W Wolstenholme and M. O'Connor eds. Little Brown and Co Boston pp. 185–196.

Billingham, R. E., \ Defendi, W K. Silvers and D. Steinmuller 1962 Quantitative tudies on the induction of tolerance of skin homografts and on runt disease in neonatal rats. J Nat. Cancer Inst 28 365–435.

Burnet, M. 1958 The Clonal Selection Theory of Acquired Immunity \ anderbilt University Press, Nashville 1959

Burnet F M., and M. C. Holmes 1962 Thymus lesions in an uto-immune dise se of mice N ture 194 146.

Ca tleman B. 1955 Tumors of the thymu gland. In Atla of Tumor P thology Armed Forces Institute of P thology W shington, D. C., Section V fascicle 19.

Clark, S. L., J 1962 The reticulum of lymph nodes in mice tudied with the lectron microscope Am J Anat 110 217 .38.

Congdon, C. C and T Makinodan 1961 Splenic whit pulp lteration fter antigen injection relation to time of serum antibody production. Am. J P th., 39 (7 10

Croose G. B. 1972 The effect of ri tion in the ge of the donor on homologous gr fts into the brain of the t An t Rec 135 215–223.

Deanesly R. 1928 Experimental studies on the histology of the mammalian thymus. Quart. J Micro. Sci., 72: 247–275.

Dempsey E. W., and G. B. Wislocki 1955 An electron microscopic study of the blood-brain barrier in the at, employing silver nitrate as a vital stain. J Biophys. and Biochem. Cytol., 1 245–256.

Dougherty T F 1952 Effect of hormones on lymphatic tissue. Physiol. Rev 32: 379–401.

Gengozian, N., I. S. Urso, C. C. Congdon A. D. Conger and T Makinodan 1957 Thymus specificity in lethally irradiated mice treated with rat bone marrow Proc. Soc. Exp. Biol. and Med., 96 714–720.

Gowans, J L. 1959 The recirculation of lymphocytes from blood to lymph in the rat. J Physiol., 146 54–69.

——— 1961 Group Discussion. In Biological Activity of the Leucocyte G. E. W Wolstenholme and M. O'Connor eds. Little, Brown and Co., Boston, Ciba Foundation Study Group No. 10, pp. 107–108.

Gregoire C. 1935 Recherches sur la symbiose lymphoépithéliale au niveau du thymus de mammifère. Arch. de Biol., 46 717–820.

Gross, L. 1959 Effect of thymectomy on development of leukemia in C3H mice inoculated with leukemic passage" virus. Proc Soc. Exp. Biol. and Med., 100 325–328

Harvey A. M., and R. J Johns 1962 Myasthenia gravis and the thymus. Amer J Med., 32: 1–5.

Hoshino, T 1961 Occurrence of ciliated vesicle-containing reticular cells in the mouse thymus. Okajimas Fol. Anat. Jap 37 209–213.

Ito, T and T Hoshino 1962 Histological changes of the mouse thymu during involution and regeneration following administration of hydrocortisone. Z. Zellforsch 56: 445–464

Kalmutz, S. E. 1962 Antibody production in the opossum embryo. Nature 193 851–853.

Kindred, J E. 1940 A quantitative tudy of the hemopoietic organs of young albino rats. Amer J Anat., 67 99–149

Law L. W., and M. Potter 1958 The behavior in transplant of lymphocytic neoplasms rising from parental thymic graft in irradiated, thymectomized hybrid mice. Proc N t. Acad. Sci., 42 160–167

Law L. W 1959 Some spect of the etiology of leukemia. Can. Cancer Conf 3 145–162.

Leblond, C. P and G. Sainte-Marie 1960 Models for lymphocyte and plasmocyte form tion. In Ciba Foundation Symposium on Haemopoiesis. G. E. W. Wolstenholme and M. O'Connor eds. Little Brown and Co Boston, pp. 152 172.

Loewenthal, L. A., and C. Smith 1952 Studies on the thymus of the mammal. IV Lipid laden foamy cell in the invol ting thymus of the mouse Anat. Rec 112 1 15.

Luft, J H. 1961 Improvement in epox resi embedding methods. J Biophys. nd Biochem. Cytol., 9 409–414

Marine D 1932 The thyroid, par thyroid nd thymus In Special Cytology E. V Cowdry ed. P ul B. Hoeber Inc New York, vol. 2, pp. 797–868.

Marshall, A. H. E., and R. G. White 1961 The immunological reactivity of the thymus. Brit. J. Exp. Path 42: 379–385.
Maximow A. 1909 Untersuchungen über Blut und Bindegewebe. II. Über die Histogenese der Thymus Bei Säugetieren. Arch. Mikroskop. Anat. u. Entwichlungsmech., 74 525–621.
Maximow A. A., and W Bloom 1957 A Text book of Histology W B. Saunders Co., Philadelphia, pp. 276–281.
Metcalf, D. 1959 The thymic lymphocytosis stimulating factor and its relation to lymphatic leukemia. Can. Cancer Conf., 3 351–366.
Metcalf, D., and M. Ishidate, Jr. 1962 PAS-positive reticulum cells in the thymus cortex of high and low leukaemia strains of mice. Austral. J Exp. Biol. Med. Sci., 40 57–72.
Micklem, H. S., and C. E. Ford 1960 Proliferation of injected lymph node and thymus cells in lethally irradiated mice. Transplant. Bull., 26 436–441.
Miller, J. F. A. P 1959 Fate of subcutaneous thymus grafts in thymectomized mice inoculated with leukaemic filtrate. Nature, 184 (suppl. 23) 1809–1810
——— 1960 Studies on mouse leukaemia. The fate of thymus homografts in immunologically tolerant mice. Brit. J Cancer 14: 244–255
——— 1961a Analysis of the thymus influence in leukaemogenesis. N ture, 191 248–249
——— 1961b Immunological function of the thymus. Lancet, 2: 748–749
Millonig, G. 1961 A modified procedure for lead staining of thin sections. J Biophys. and Biochem. Cytol., 11 736–739
Muir, A. R and A. Peters 1962 Quintuple-layered membrane junctions t terminal bars between endothelial cells. J Cell Biol., 12: 443–448.
Munger, B. L., and S. W Brusilow 1961 An electron microscopic study of eccrine sweat glands of the cat foot and toe pads — evidence for ductal reabsorption in the human. J Biophys. and Biochem. Cytol., 11 403–417
Munger, B. L., and S. I. Roth 1962 The morphologic sequence of secretion in the parathyroid glands as compared to other endocrine organs. Anat. Rec., 142: 261
Murray R. G. 1947 Pure cultures of rabbit thymus epithelium. Amer J Anat., 81 369–411.
Norris, E. H. 1938 The morphogenesis and histogenesis of the thymus gland in man in which the origin of the Hassall' corpuscles of the human thymus is discovered Contrib. Embryol., Carnegie Inst., Wash., 27 191 207
Nossal, G. J V and O Mäkelä 1962 Autoradiographic studies on the immune response. I. The kinetics of plasma cell proliferation J Exp. Med., 115 209–230.
Palade G. E. 1961 Blood capillaries of heart and other organs. Circulation, 24 368–388
Palay, S. L., S. M. McGee-Russell, S. Gordon, Jr and M A. Grillo 1962 Fixation of neural tissues for electron microscopy by perfusion with solutions of osmium tetroxide J Cell Biol., 12: 385–410.
Popp, R. A. 1961 Repopulation of thymus by immunologically competent cells derived from donor marrow Proc. Soc. Exp. Biol. and Med., 108 561–564
Rahman, Y E. 1962 Electron microscopy of lysosome-rich fractions from rat thymus isolated by density-gradient centrifugation before and after whole-body x-irradiation. J Cell Biol., 13 253–260.
Rankin, J J 1960 Circulation of lymphocytes and thymocytes in the normal and leukemic mouse. Acta Anat., 40: 221–230
Schooley J C., B. J Bryant and L. S. Kelly 1959 Preliminary utoradiographic observations of cellular proliferation in lymphoid tissues, using tritiated thymidine In The Kinetics of Cellular Proliferation, F Stohlman Jr ed. Grune and Stratton, New York, pp. 208–217
Schooley J C., and L. S. Kelly 1961 The thymus in lymphocyte production. Fed. Proc., 20: 71
Setälä, K., L. Merenmies, L. Stjernvall nd M. Nyholm 1960 Mechanism of experimental tumorigenesis. IV Ultrastructure of interfollicular epidermis of normal adult mouse. J Nat. Cancer Inst., 24 329–353.
Smith, C., and B K. Hénon 1959 Histological and histochemical study of high endothelium of post-capillary veins of the lymph node. Anat. Rec., 135 207–214.
Snell, G. D., H. J Winn and A. A. Kand tch 1961 A quantitative study of cell lar immunity J Immun., 87 1 17
Szenberg, A. and N L. Warner 1962 Dissociation of immunological responsiveness in fowls with hormonally arrested development of lymphoid tissues. N ture 194 146–147
Tesseraux, H 1959 Physiologie und P thologie des Thymus. Zwanglose Abhandlungen dem Gebiete der Inneren Sekretion Johann Ambrosius Barth, Leipzig, 9 1 147
Trowell, O. A. 1961 Radiosensitivity of the cortical and medullary lymphocytes in the thymus. Int. J Radiat. Biol., 4 163–173
Tschirgi, R. D 1962 Blood brain barrier fact or fancy? Fed. Proc., 21 665–671
Vos O M. J de Vries, J C. Collenteur and D W van Bekkum 1959 Transplantation of homologous and heterologous lymphoid c lls i irradiated and non-irradiated mice. J N t. Cancer Inst., 23: 53–73.
White P R. 1946 Cultivation of imal tissues in vetro in nutrients of precisely known constitution. Growth, 10 231 289
Winn, H. J 1961 Immune mechanism i homotransplantation. II. Quantitative ssay of the immunologic activity of lymphoid cell stimulated by tumor homografts. J Imm 86 228–239.
Yoffey J M., and F C. Courtice 1956 Lymphatics, Lymph and Lymphoid Tissue II rvard University Press, Cambridge M ss.

PLATE 2

EXPLANATION OF FIGURES

2 In addition to lymphocytes and plasma cell (P) this region of the thymic cortex contains two large cell an epithelial cell (E) and macrophage (M) Although similar in size and shape (note the extended processes of the epithelial cell and the long pseudopod of the macrophage outlined by rrows) they may be distinguished by several criteria and cells transitional in type between the two have not been found. The nucleu of the epithelial cell tend to be larger and less dense Its cytoplasm contains relatively few dense lipoid inclusions. There re cytoplasmic tonofibrils (T) and desmosomes connecting neighboring epithelial cells, although none can be discerned in thi micrograph. × 4,500.

3 Thi large luster of lipoid incl sion nd acuoles i contained i single macrophage which lies in the peripheral part of the thymic cortex Its nucleus i not to be seen, but indenting its cytopl sm are numerou lymphocytes and plasma cell (P) × 2,300

PLATE 2

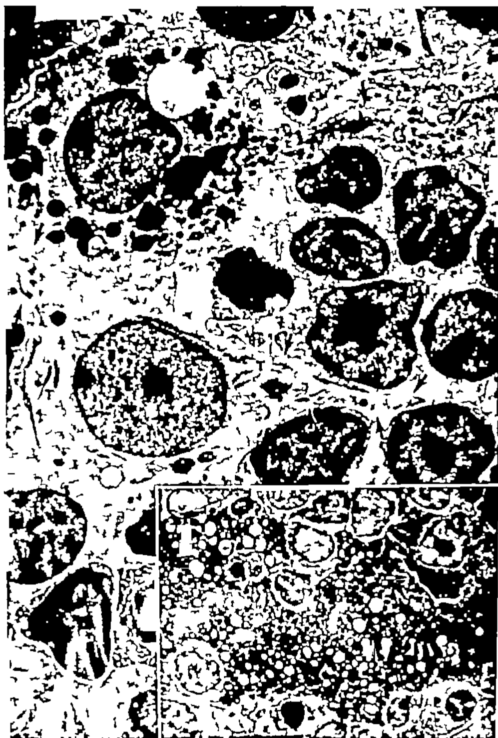


PLATE 3

EXPLANATION OF FIGURES

4 This i mall nest of epithelial cells (E) in the thymic medull sur rounded by large lymphoid cell (LL) The larger of the epithelial cell contains tonofibril (T) and a group of vacuoles with amorphou contents. These vacuoles are larger than those in figures 15 nd 16, nd look as if they had formed by coalescence of smalle acuoles. × 0 000.

5 These tw plasma cell in the thymic cortex differ in the content of *thei erg topla mic acs. I the upper left the sacs are distended* with amorphous material. In the center they contain condensed material. Still other pl sma cells had relati ly empty collapsed erg toplasm. 10,000

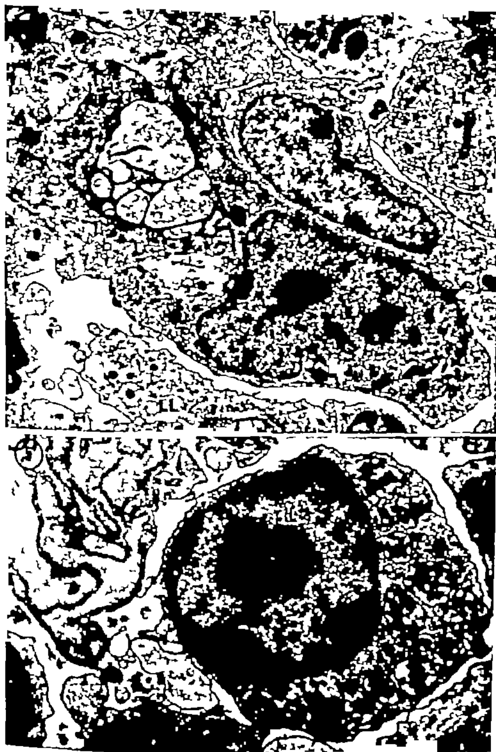


PLATE 4

EXPLAN TION OF FIGURE

6 This capillary in the thymic cortex, cut in cross-section, is lined by relatively thick endothelium made up of numerous cytoplasmic processes connected by desmosomes (D) There are few f the small cytoplasmic vesicles described in other capill ries by Palade ('61) In these features the vessel is typical of thymic pillaries. Surrounding the basement membrane of the endothelium is a space containing collagenous fibrils (C) and some adventitious cells. One (arrow) contains some small granules like those found in epithelial cells (see figs. 13 and 14) The space is enclosed by another basement membrane associated with l yer of tten ted epithelial cells (E) Beyond the epithelial cells lie lymphocytes (L) One in the pper left, occludes gap in the epithelium and it basement mem brane as if it were in the process of migrating from the parenchyma of the thymus to the connective tissue surrounding the capillary × 16,000.


C

PLATE 5

EXPLAN TION OF FIGURES

7 This is another view of the barrier that separates the blood stre m from the lymphocytes in the thymic cortex. At the bottom of th picture is the lumen of capillary or small venule containing erythrocyte (R) Between the blood and the lymphocytes (L) lie (1) a thick endothelium, (2) its basement membrane (3) space containing collagenous fibrils and fine fibrillar material (C) (4) the basement membrane of the thymic epithelium (B) and (5) the epithelial cells (E) The epithelial cells are joined by desmosome (D) and contain tonofibril (T) At the region marked "B" the epithelial cell is separated — probably artificially — from it basement membrane. The lymphocyte (L) in the upper right contains prominent centriole. The unlabeled cell lying in the connective tissue space (C) may be perivascular cell enclosed in its basement membrane There is dense cytoplasmic granule in the endothelium (G) similar to those found in some epithelial cells and macrophages (see figs. 6, 13 and 14) × 20,000.

8 This is another cytoplasmic granule in the endothelium of capillary × 23 000.


7
L
T
B
C
8

PLATE 6

EXPLAN TION OF FIGURES

9 The elongated epithelial cell (E) encloses one of the delicate reticular fibers that penetrate the thymic cortex t intervals. The reticular fiber (C) consists of extracellular fibrils and some amorphous material, wrapped in a basement membrane surrounded by the epithelial cell (E) The latter contains tonofibrils inserting into desmosomes (D) which ttach it to neighboring epithelial cell. In the nucleus of the epithelial cell is circular structure found in several types f cells in the thymus. On either side of the epithelial cell are lymphocyte (L) and macrophage (M) the latter containing an inclusion resembling lymphocyte undergoing dissol tion. Only in macrophages h ve such signs of phagocytosis of whole cells been observed in the thymus. × 14,000

10 This is another example of reticular fibers ensheathed in epithelial cells (E) as they traverse the thymic cortex. A basement membrane separates the epithelial cells from the space occupied by collagenous and other fibrillar material (C) The epithelial cells contai tonofibrils (T) concentrated near the cell membrane, and desmosomes (D) connecting adjacent cells. × 18,000.


D
C

PLATE 7

EXPLANATION O FIGURE

11 This region of the thymic medulla contains larger and more numerous reticular fibers than the cortex, but here too, they re enclosed in epithelial cells (E) with their basement membranes, which separate the connective tissue spaces (C) from the are occupied by lymphocytes (L) The epithelial cells form an ttem ted, spidery network which does not appear to be syncytial. They contain number of very dense inclusions. × 10,000.

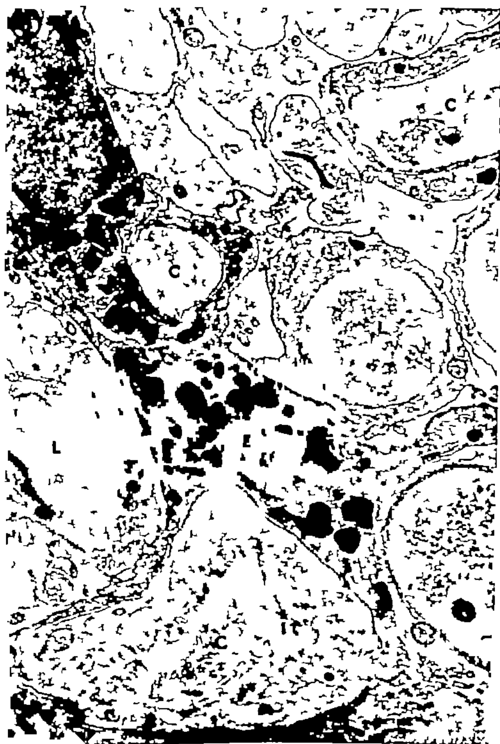
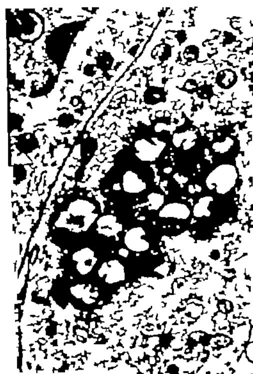

C
C
L
L
C

PLATE 8

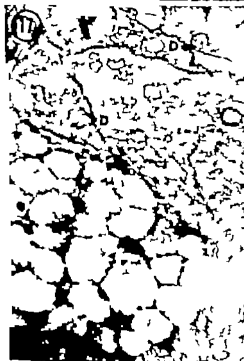
EXPLANATION OF FIGURE

12 In this region of the thymic medulla the reticular fibers are few and epithelial cells form solid nests which include only a few lymphocytes (L). The epithelial cells are larger with large nuclei containing finely dispersed chromatin and prominent nucleoli. In the lower right is a ring-shaped intranuclear structure (arrow) like that in figure 9. The epithelial mitochondria are large. Tonofibrils (T) occupy typical locations along the nuclear membrane and cellular border where they insert into desmosomes (D) joining adjacent cells. The thickened, palisaded appearance that tonofibrils give to cell borders may also be discerned in figure 1. × 10,000.


12
D
D
D
T
T
L
B






17
D
D


18

PLATE 10

EX LAN TION OF FIGURES

All four figures were taken from nests of epithelial cell i the medull of the thymus t demonstrat vari tions in the ppearance of cytoplasmic vacuoles.

15 These vacuoles are spherical but indented by microvillous projections of their surrounding membranes. They are partly filled by an mor phous material of intermediate density × 8,000

16 I these vacuoles microvilli predomin te and there i relatively little morphous material At the arrow terminal bar marks the junction with an adjacent epithelial cell th t contai dense rods and gran- les simil to those in figures 13 nd 14. × 16,000.

17 I this nest of epithelial cells connected by desmosomes (D) the cytoplasm of one cell is crowded with spherical vacuoles filled with homogeneous material. The membranes separating adjacent vac uoles are indistinct, and the group resembles droplet of mucus in goblet cell of the intestine. × 10,000.

18 The mate l in these m tually deformed acuoles is concentrated into small dense spheres. The cell contains tonofibrils (T) × 10,000.

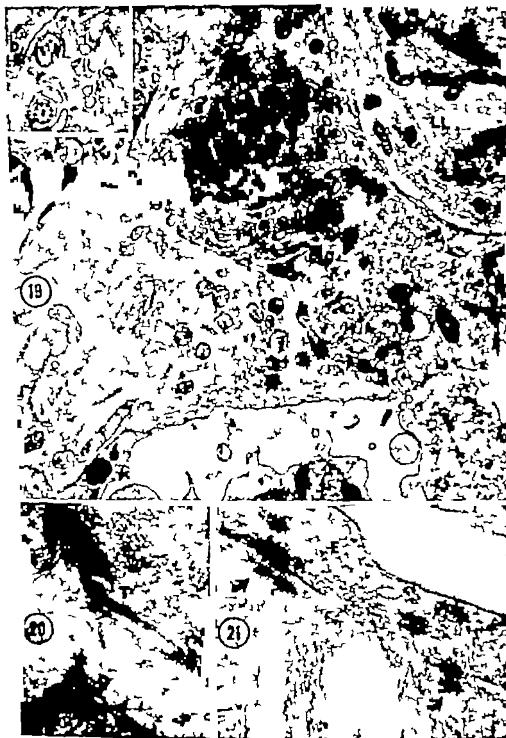

19
20
21
E

PLATE 12

EXPLANATION OF FIGURES

22 This is an oblique section of venule from the thymic cortex. Along the side of the vessel uppermost in the picture, the endothelial cell are thick, and there are lymphocytes between or within them (L) Two other lymphoid cells occupy the lumen of the vessel. The remainder of the vascular wall consists only of basement membrane separating the epithelium from the surrounding connective tissue space (C) × 7,000.

23 This is another venule with thick endothelium from the thymic cortex There is lymphocyte (L) in the lumen of the essel another squeezed between the outstretched processes of endothelial cell and third in the connective tissue space (C) between the basement membrane of the endothelium and the basement membrane of the thymic epithelium (E) These venules resemble those found in other lymphoid tissues and they appear t be routes for the migration of lymphocytes, but the direction of migration remains to be established. (R erythrocyte) × 7,000

The Cycle of the Seminiferous Epithelium in Man

YVES CLERMONT
Department of Anatomy, McGill University, Montreal, Canada

The histological appearance of the human seminiferous epithelium suggests a haphazard arrangement of its germ cell components, which is not easily systematized. This is in sharp contrast with what can be observed in most mammalian species and particularly in the rat where the various generations[1] of germ cells make up cellular associations of fixed composition. In the rat, spermatids at a given step of development are always associated with the same types of spermatocytes and spermatogonia. Consequently only a limited number of cell associations can be seen in various cross sections of seminiferous tubules. This characteristic arrangement of the germ cells implies that in any one area of the seminiferous epithelium the aforementioned cellular associations follow each other in time. The resulting orderly sequence gives rise to the so-called "cycle of the seminiferous epithelium,"[2] (see reviews in Leblond and Clermont, '52b; Roosen-Runge, '52).

Each typical cell association which may then be considered as a stage of the cycle can be classified and identified by using various arbitrary cytological or histological criteria. Our previous studies of the seminiferous epithelium in several mammals identified the stages by making use of the steps of development of the spermatids as seen in sections stained with the periodic acid-Schiff-hematoxylin technique — the periodic acid-Schiff component demonstrated particularly well the changes taking place in the acrosomic structure of the spermatids — (Leblond and Clermont '52a; Clermont, '54, '60; Clermont and Leblond, '59).

The remarkable arrangement of the germ cells described for most mammals is apparently lacking in man since typical cellular associations or stages of the cycle are difficult to identify. As early as 1902 Von Ebner impressed by the poor organization of the germ cells wrote that "the developmental stages of the sperm cells are less regularly arranged in the seminiferous tubules of man than in the testis of other mammals."[3] Branca ('11, '24) as well as Slotopolsky and Schinz ('24, '25) held similar views and stressed the variability in the histology of the human seminiferous epithelium from one tubule to the next and from one individual to another. Roosen-Runge ('52) although noticing as did Von Ebner that "over small areas, four generations (of germ cells), may be found together in combinations generally similar to those in the rat," insisted in a later article (Roosen-Runge and Barlow, '53) "that in man, in contrast to most other mammals, there is little if any correlation between the developmental stages of spermatogonia, spermatocytes, spermatids and spermatozoa in any restricted area of the seminiferous tubule." Roosen-Runge ('52) suggested that while in rats groups of spermatogonia develop synchronously, this is not the case in man, so that this lack of synchronicity in the development of spermatogonia would be in part responsible for the poor organization of the germ element in human seminiferous tubules.

The purpose of the present article is to examine whether there is a plan of organization in man corresponding to the cycle of the seminiferous epithelium observed in other mammals.

MATERIAL AND METHODS

This work was begun using well fixed testes from operation or from autopsy

[1] By generation, we mean a homogeneous group of cells at the same stage of development during spermatogenesis.

[2] The "cycle of the seminiferous epithelium" is fundamentally different from the "wave of the seminiferous epithelium," which concerns the distribution of the cellular associations along the length of the seminiferous tubules (see extensive discussion in Perey, Clermont and Leblond, '61).

[3] Quoted by Roosen-Runge ('52).

cases following accidental death Recently testicular biopsies were obtained from healthy prisoners through the kindness of Dr C G Heller Seattle Washington. The biopsies were collected in such a manner as to avoid touching or crushing the tubules. First the tunica albuginea was cut with a sharp scapel in a rectangle about 0 5 × 0.3 cm due to internal pressure, the underlying seminiferous tubules were raised a few millimeters above the surface of the testis. With a sharp razor blade, the protruding mass of tissue was cut in a stroke parallel to the surface of the tunica A section from such a biopsy (fig. 1) shows a well-preserved topographical arrangement with little damage to the tubules.



Fig. 1 Low power microphotograph of complete section from human testicular biopsy fixed in Zenker-formol. Staining hematoxylin-eosin. Magn. × 20. The topographical arrangement of the tubules as well as their histology is well preserved. The large number of obliquely or longitudinally cut sections reflects the extensive coiling of the tubules.

Of the several fixatives which were tried Zenker formol proved to be the best suited. Five micron sections were stained either with hematoxylin-eosin or with the periodic acid-Schiff-hematoxylin technique. The large amount of PA Schiff staining glycogen present in the cells of the seminiferous epithelium made it necessary to treat the sections with saliva before using the latter staining method.

To ascertain the presence or absence of stages of the cycle and to understand the nature of the apparently atypical cell associations observed over certain areas of tubules a systematic investigation of serial sections became essential Four particularly well fixed biopsies sectioned serially and stained with hematoxylin-eosin were used for this purpose

RESULTS

Description of cells composing the seminiferous epithelium

The following description of cells is made to facilitate the eventual identification of the cellular associations rather than to add new cytological characteristics to already well known elements (Painter '23 Winiwarter and Oguma '26 Stieve '30)

Sertoli cells

Although in histological sections it is impossible to delimit the cytoplasmic territory of a given Sertoli cell this element can be easily identified by its characteristic nucleus It has a polymorphous shape with a typically folded nuclear membrane and a large nucleolus The nucleolus is clearly divided into two zones a spherical eosinophilic core and an irregular basophilic fringe (figs. 3 7 Ser) The Sertoli nuclei are often separated from the limiting membrane of the tubule by an almost continuous layer of spermatogonia

Spermatogonia

In the description of spermatogonia special attention will be given to the nuclei as seen in the Zenker formol fixed testis. Following such fixation the chromatin or part of it remains finely granulated and diffusely distributed throughout the nucleus it is not precipitated into dark clumps as is the case with such fixa-

tives as Bouin, Flemming or formalin. The variability in nuclear sizes and chromatin distribution suggests a multiplicity of nuclear types which makes the classification of spermatogonia difficult. In the following description, however only the main types of spermatogonia will be mentioned. Since they closely resemble the spermatogonia found and described in the monkey (Clermont and Leblond '59) it is likely that the order in which they arise from one another is also the same as in the monkey They will be listed in this order

The first common type of spermatogonium may be called *dark type A spermatogonium* (Ad) The nucleus of this cell is spherical or ovoid, its finely granular chromatin is deeply stained and thus looks homogeneous (figs. 2, 3 Ad) In this dense chromatin mass one sometimes two or three clear cavities of various sizes are present. One or more of these vacuolar spaces contain a nucleolus which is free from adhering chromatin granulation.

The second common type of spermatogonium is designated *pale type A spermatogonium* (Ap) This cell is characterized by an ovoid nucleus containing a uniformly pale grey granular chromatin which gives a ground glass texture to the nucleus (figs. 2, 3 Ap) One or two nucleoli, free of chromophilic chromatin, are



Fig. 2 Microphotograph showing the two classes of type A spermatogonia. Staining hematoxylin-eosin. M fix. approx. × 1,200. The dark type A spermatogonium (Ad) contain nucleus with darkly stained chromatin in which paler vacuolar space may be distinguished The pale type A spermatogonium (Ap) shows ovoid nucleus containing pale grey chrom granulation.

seen attached to the nuclear membrane. In early prophase, some darkly stained crusts of chromatin appear on the inner surface of the nuclear membrane but not on the nucleolus. Such type Ap prophases are then difficult to differentiate from the next class the type B spermatogonia.

This third or *type B spermatogonium* is characterized by a nucleus containing, in addition to a fine chromatin granulation several heavily stained chromatin masses (fig. 3 Stage I B) Some of these chromatin clumps are attached to the nuclear membrane which then appears more clearly delineated others are applied to the nucleolus which has become detached from the nuclear envelope and is more or less centrally located.

It may be concluded that in Zenker formol fixed testes classification of spermatogonia into A and B types is possible this is contrary to the statement of Roosen-Runge and Barlow ('53) who claimed that type A and type B spermatogonia cannot be distinguished in man.

Spermatocytes

While the primary spermatocytes in meiotic prophase are easily identified, it is more difficult to recognize in man the equivalent of the so-called resting primary spermatocytes (also called preleptotene spermatocytes) described in several mammalian species (Clermont and Leblond, '53 '59 Oakberg, '56 and others)

Unlike the spermatogonium which lies in close proximity to the basement membrane the resting primary spermatocyte is usually detached from the tubular limiting membrane. Its spherical nucleus contains well stained chromatin granulation of uniform size which is distributed throughout the nuclear sap (figs. 3 6 Stage III R) A chromatin covered nucleolus and a few large chromatin flakes are however still visible When located along the limiting membrane this cell is admittedly difficult to differentiate from the type B spermatogonium.

When the chromatin granulations assume a filamentous texture and become deeply stained the cell is identified as a leptotene primary spermatocyte (figs 3 Stage V) In Bouin fixed biopsies

the filamentous character of the chromatin is more marked than in Zenker formol fixed material.) Following the leptotene the zygotene step of the meiotic prophase is characterized by the presence of coarser filaments (figs 3 14 Stage VI Z) which progressively shorten and thicken to give the typical pachytene configuration (figs 3 4–8 P) After a short diplotene step and diakinesis (fig 14 Di) the primary spermatocytes complete their first maturation division to yield secondary spermatocytes (figs. 3 11 Stage VI Spte II) These cells which are not always easily distinguished from the young spermatids have spherical nuclei which exhibit a well stained homogeneous chromatin and in addition have several large globular and deeply stained chromatin masses. These cells quickly complete the second maturation division to produce spermatids.

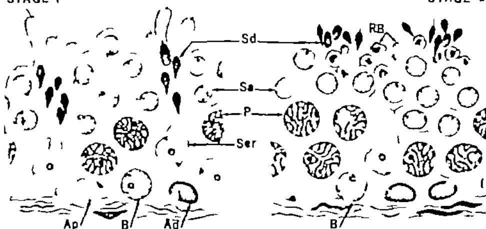
Spermatids

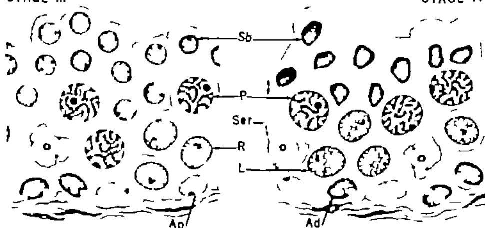
The steps of development of the spermatids in man have already been described (Clermont and Leblond '55) In this description spermiogenesis was divided into 12 steps which were defined in part by the stage of development of the PA Schiff positive acrosomic system (acrosomic granule plus head cap) These 12 steps were distributed over the following three phases A first or Golgi phase consisted of the first three steps during which the acrosomic granule arose in the Golgi zone of the spermatid. A second or cap phase was subdivided into four steps which showed the development of the head cap over the nucleus. A third or acrosomic and maturation phase was composed of the last five steps During that period the nucleus and overlying acrosomic structure of the spermatid elongated flattened and condensed, and the cell became a spermatozoon.

Unfortunately the PA Schiff staining of the acrosome is not as useful in man as in other species for the identification of the steps of spermiogenesis Firstly the delicate acrosomic structures are more difficult to preserve in man than in other mammalian species. Even in Zenker formol fixed testis the acrosomic granule and the head cap at its early stage of formation may dissolve away to be replaced by an unstained acrosomic vacuole," thus rendering the identification of the early steps of spermiogenesis quite difficult. Secondly the saliva treatment required to extract the large amount of PA Schiff positive glycogen present in the human seminiferous tubules reduces the stainability of the chromatin with hematoxylin thus making the recognition of the germ cell nuclei difficult Therefore it was felt that for routine work, and particularly in the following description of the cellular associations the morphological changes of the spermatid's nucleus as seen in hematoxylin-eosin stained sections would be used to identify characteristic steps of spermiogenesis.

The newly formed spermatid has a spherical nucleus which contains a few heavily stained granules in addition to a homogeneously pale stained chromatin (figs. 3 4 5 Stages I–II Sa). The nuclear surface is often depressed by a small acrosomic vacuole. As the spermatids mature the chromatin becomes more diffuse and more intensely stained the chromatin flakes disappear and the nucleus loses its perfectly spherical shape to elongate slightly (figs. 3 6 7 Stages III–IV Sb) Simultaneously the nucleus makes contact with the cytoplasmic membrane on the side of the cell nearest the limiting membrane. Later as the nucleus becomes more and more pointed the chromatin condenses and becomes heavily chromophilic (figs. 3 8 9 Stages V–VI Sc) During this condensation of the chromatin considerable variations in the nuclear shape can be observed, and frequent anomalies and signs of cell degen-

Fig. 3 Drawings diagrammatically representing the cellular composition and topography of the six typical cellular associations found repeatedly in human seminiferous tubules. These cell associations correspond to the stages of the cycle of the seminiferous epithelium they are numbered with Roman numerals, stages I–VI. Their complete description is given in the text. Lettering Ser Sertoli nuclei Ap and Ad, pale and dark type A spermatogonia; B type B spermatogonia; R, resting primary spermatocytes; L, leptotene primary spermatocytes Z, zygotene primary spermatocytes; P pachytene primary spermatocytes Di, diplotene primary spermatocytes Spto-Im, primary spermatocytes in division; Sptc-II, secondary spermatocytes in interphase; Sa, Sb, Sc, Sd, spermatids at various steps of spermiogenesis; RB residual bodies.


STAGE I
STAGE II
Sd
RB
Sa
P
Ser
Ap
B
Ad
B


STAGE III
STAGE IV
Sb
P
Ser
R
L
Ap
Ad

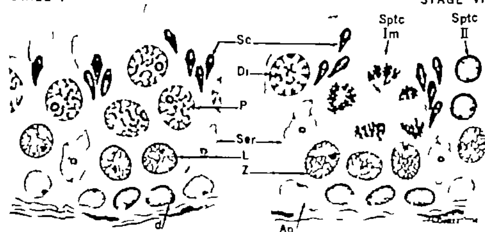

STAGE V
STAGE VI
Sptc Im
Sptc II
Sc
Di
P
Ser
L
Z
d
Ap

Figure 3

the filamentous character of the chromatin is more marked than in Zenker formol fixed material.) Following the leptotene the zygotene step of the meiotic prophase is characterized by the presence of coarser filaments (figs. 3 14 Stage VI Z) which progressively shorten and thicken to give the typical pachytene configuration (figs. 3 4–8 P) After a short diplotene step and diakinesis (fig 14 Di) the primary spermatocytes complete their first maturation division to yield secondary spermatocytes (figs. 3 11 Stage VI Sptc II) These cells which are not always easily distinguished from the young spermatids have spherical nuclei which exhibit a well stained homogeneous chromatin and in addition have several large globular and deeply stained chromatin masses. These cells quickly complete the second maturation division to produce spermatids.

Spermatids

The steps of development of the spermatids in man have already been described (Clermont and Leblond '55) In this description spermiogenesis was divided into 12 steps which were defined in part by the stage of development of the PA-Schiff positive acrosomic system (acrosomic granule plus head cap) These 12 steps were distributed over the following three phases. A first or Golgi phase consisted of the first three steps during which the acrosomic granule arose in the Golgi zone of the spermatid. A second or cap phase was subdivided into four steps which showed the development of the head cap over the nucleus. A third or acrosomic and maturation phase was composed of the last five steps. During that period the nucleus and overlying acrosomic structure of the spermatid elongated, flattened and condensed, and the cell became a spermatozoon

Unfortunately the PA Schiff staining of the acrosome is not as useful in man as in other species for the identification of the steps of spermiogenesis Firstly the delicate acrosomic structures are more difficult to preserve in man than in other mammalian species. Even in Zenker formol fixed testis the acrosomic granule and the head cap at its early stage of formation may dissolve away to be replaced by an unstained acrosomic vacuole, thus rendering the identification of the early steps of spermiogenesis quite difficult. Secondly the saliva treatment required to extract the large amount of PA Schiff positive glycogen present in the human seminiferous tubules reduces the stainability of the chromatin with hematoxylin thus making the recognition of the germ cell nuclei difficult. Therefore it was felt that for routine work, and particularly in the following description of the cellular associations the morphological changes of the spermatid s nucleus as seen in hematoxylin-eosin stained sections would be used to identify characteristic steps of spermiogenesis.

The newly formed spermatid has a spherical nucleus which contains a few heavily stained granules in addition to a homogeneously pale stained chromatin (figs 3 4 5 Stages I–II Sa) The nuclear surface is often depressed by a small acrosomic vacuole As the spermatids mature the chromatin becomes more diffuse and more intensely stained the chromatin flakes disappear and the nucleus loses its perfectly spherical shape to elongate slightly (figs. 3 6 7 Stages III–IV Sb) Simultaneously the nucleus makes contact with the cytoplasmic membrane on the side of the cell nearest the limiting membrane Later as the nucleus becomes more and more pointed the chromatin condenses and becomes heavily chromophilic (figs. 3 8 9 Stages V–VI Sc) During this condensation of the chromatin, considerable variations in the nuclear shape can be observed and frequent anomalies and signs of cell degen-

Fig. 3 Drawings diagrammatically representing the cellular composition and topography of the six typical cellular associations found repeatedly in human seminiferous tubules. These cell associations correspond to the stages f the cycle of the seminiferous epithelium they are umbered with Roman numerals, stages I–VI Their complete description is given in the text. Lettering Ser, Sertoli nuclei Ap and Ad, pale and dark type A spermatogonia; B, type B spermatogonia; R, resting primary spermatocytes; L, leptotene primary spermatocytes; Z, zygotene primary spermatocytes; P pachytene primary spermatocytes; Di, diplotene primary spermatocytes Sptc Im, primary spermatocytes in division; Sptc II, secondary spermatocyte in interphase Sa, Sb, Sc, Sd, spermatids t various steps of spermiogenesis RB residual bodies.

tene step of the meiotic prophase as judged by their large nucleus and thick chromosomes (P) The younger generation of spermatocytes may be seen in transition from the leptotene to the zygotene step of meiosis (L) The zygotene nuclei, whenever present are characterized by long chromosomal threads. Again the two types of spermatogonia are seen along the limiting membrane (Ap Ad)

Stage VI of the cycle (figs. 3 9) This stage is characterized by the primary and secondary spermatocytes undergoing the first and second maturation division and also by the presence of secondary spermatocytes in interphase (Sptc Im Sptc II) The division figures can be readily identified the chromosomes of the primary spermatocytes being thicker and longer than those of the secondary spermatocytes. The interphasic nuclei of secondary spermatocytes show a homogeneous chromatin with a few large globular chromatin masses. The maturing spermatids with their elongated nuclei are deeply inserted between the dividing spermatocytes (Sc) The younger generation of primary spermatocytes appears either at the zygotene step (Z) or at the very early pachytene step of the meiotic prophase The latter nuclei have thicker chromosomal threads. Type A spermatogonia are also seen along the basement membrane

Obviously the six cellular associations or stages of the cycle placed in the order given above would in time follow each other in sequence Following stage VI, stage I reappears, and a new cycle begins.

Deviations from the typical cellular associations

Minor variations in the cellular composition of the stages of the cycle Not infrequently in many locations minor deviations from the pattern just described for each stage of the cycle were observed. For example at stage VI of the cycle the young generation of spermatocytes instead of being at the zygotene step as indicated in figure 3 may be seen at th leptotene step of the meiotic proph s Similarly resting primary sperm tocytes instead of leptotene spermat c es are sometimes found at stag s IV or even V of the cycle (fig 3) Su h deviations indicate that, in man, the integration of the steps of development of the various generations of cells is not as rigid and precise as it is for example in the rat. These deviations are not sufficiently important however to disorganize entirely the pattern of stages composing a cycle of the seminiferous epithelium.

Heterogeneous cellular associations In the rat, one given cellular association usually occupies extensive portions or segments of a seminiferous tubule (Perey Clermont and Leblond '61) Consequently most tubular cross sections show only one cellular association (Leblond and Clermont, '52a, b) In man on the contrary a cellular association occupies a rather small portion of tubular epithelium, so that a cross section of the seminiferous tubules usually shows more than one (three on the average) cellular associations.

Since the stages of the cycle are distributed over small but numerous patches of the epithelial lining of the tubules the opportunities of observing borderline zones between stages is great and is, in fact, much greater than in any other mammalian species studied thus far The demarcation line between two adjacent stages of the cycle is usually sharp and clear (figs. 10–11 15–18) but there are exceptions. In such cases the cells belonging to the two adjacent typical cell groupings are intermixed and constitute what may be called an atypical or heterogeneous cellular association. This may be illustrated in the area photographed as figure 12, were mature spermatids (Sd) as well as young spermatids (Sa) are found associated with spermatocytes in division (Sptc Im) and with zygotene primary spermatocytes (Z) This cellular association does not fit any of the six stages described above It appears however that in this area the spermatids at the right (Sa and Sd) belong to stage II of the cycle hile th permatocytes at the left (Sptc Im and Z bel ng to stage VI of the cycle Consequentl there is here a zone of interpenetration of the two cellular associations identified as stages II and VI

Incomplete cellular associ tions One can also observe that in some areas of the

seminiferous epithelium a cellular association, which is otherwise typical completely lacks one sometimes two generations of cells. Thus in the stage I of the cycle shown in figure 13 the generation of pachytene spermatocytes is missing. In the majority of cases when such a cellular association is followed in serial sections the missing generation of cells can be found a few sections farther on, the number of cells composing this particular generation being evidently small In other instances however the generation of cells remained missing altogether and no trace of it was found in careful survey of serial sections. The frequency of these incomplete cellular associations varies considerably from one biopsy to another

Relative duration of the stages of the cycle

The frequency with which the various cellular associations appear in sections of tubules may be considered to give an index of their relative duration (Leblond and Clermont, '52) In the rat the relative duration of the stages expressed in percentage was obtained by estimating the frequency with which the various stages appeared in tubular cross sections the fact previously mentioned that each tubular cross section usually showed a single stage of the cycle simplified considerably the collection of data.

Due to the presence of several stages of the cycle per tubular section in man, the so-called paper cut-out method was used to obtain an estimate of the relative duration of each stage Well fixed cross and oblique sections were used (due to the extensive coiling of the tubules already mentioned, oblique are more frequently observed than transverse sections fig. 1) Each chosen tubular section was photographed at a magnification of approximately 50 times. With the help of the microscope the limits of a typical cellular association or stage of the cycle were defined and indicated on the photographs of the tubule as done in figures 15–17 Then using transparent tracing paper the tubular seminiferous epithelium outline was traced as well as the territory occupied in it by each stage of the cycle. The areas of paper showing the various stages of the cycle were cut and weighed the heterogeneous and incomplete cellular associations being excluded from this measurement

Data were collected from four sets of serial sections each set corresponding to sections of a biopsy taken from a different individual. However care was taken not to use any serial section of the same tubule at intervals less than 150 μ. Sections of a given tubule at these intervals showed a sufficiently great difference in the distribution of the stages of the cycle. For each biopsy all the pieces of paper belonging to the same stage of the cycle were weighed together The weight results were transformed into percentages giving an indication of the relative spatial importance of each stage in the cycle and consequently an index of the relative duration of these stages.

The results (table 1) show that the percentages obtained for a given stage of the cycle from each of the four individuals are variable but are of the same order of magnitude When the average percentage values for the various stages of the cycle are compared it is obvious that there are considerable variations between the stages.

TABLE 1

Percentage of the seminiferous epithelium area occupied by the various stages of the cycle (indicating relative duration of stages)

Specimen	Stages of the cycle I	II	III	IV	V	VI	Number of tubular sections surveyed
A	33.5	22.8	6.5	6.5	25.2	5.5	87
B	33 1	15.9	2.5	5.4	37 4	5.6	83
C	21.9	16.3	11.5	12.2	34.6	3.5	23
D	29 6	23 6	5.3	6.8	28.2	6.5	74
Averages	29.5	19 6	6.4	7 7	31.3	5.2	

Thus stages III, IV and VI are rather short (5.2 – 7.7%) while stages I, II and V are comparatively much longer (19.6 – 31.3%).

COMMENTS

From observations made on well preserved biopsies of normal adult human testis, it appears that in man as well as in other mammalian species there is a clear cut cycle of the seminiferous epithelium. The various generations of germ cells — spermatogonia, spermatocytes and spermatids — have an obvious tendency to form cellular associations of constant composition. *These cellular associations* — six were described here — may be considered as stages of the cycle. They would thus succeed each other in time in a fixed sequence (from stage I to stage VI) which repeats itself time and time again. In this respect, man is not fundamentally different from other mammals studied so far, a conclusion which is in opposition to the one arrived at by Roosen-Runge ('52) and others.

However, in man, the cycle of the seminiferous epithelium or rather the stages of the cycle which compose it are partly obscured by irregularities that may be classified under three headings.

The first type of irregularity results simply from the fact that any given typical cellular association covers numerous but rather small areas of the tubular epithelium. The immediate consequence of this is that over relatively small portions of tubule, the borderline zones where cells can intermix are much more numerous than in other mammalian species. Indeed such zones composed of so-called heterogeneous cell associations are frequently observed in tubular sections and contribute to the apparent disorganization of the histology of the seminiferous epithelium.

A second type of irregularity arises from the fact that one, sometimes two generations of cells are missing from a given cell association. Such an absence may be relative or absolute, relative when the cell type is missing in a given tubular section, but is present, although in reduced number in adjacent serial sections, absolute when the generation of cells is missing altogether. Such an irregularity of the seminiferous epithelium was observed more frequently in biopsies from individuals with lower sperm counts. This condition may have two possible causes, either partial or complete failure on the part of spermatogonia to produce a generation of spermatocytes, or else the degeneration and disappearance of a generation of spermatocytes or of spermatids which has been produced. The latter may be the most likely explanation in the case of the spermatids since the generation of maturing spermatids (Sc) are often seen to degenerate at stage V and are frequently missing from stages I and II of the cycle.

A third type of irregularity was observed at a finer level. It appears that the composition of the typical cell associations suffers a greater variability than was observed in the rat or other rodents (Leblond and Clermont, '52, Clermont '54, '60, Oakberg '56). Thus, the integration of the steps in development of the three or four generations of germ cells is not as accurate as it is in other species. One generation may be a little more or a little less advanced than shown in the drawings of the stages of the cycle (fig. 3). This shift in the developmental step of one generation of germ cells in relation to the developmental steps of the other generations is not important enough, however, to disturb seriously the fundamental pattern of the cycle of the seminiferous epithelium. This irregularity may have its origin at the time of the initiation of spermatogenesis which would start a little earlier or a little later than predicted (the developmental step of the preceding generation of germ cells serving as a landmark).

All the above mentioned factors acting together help to disorganize the histology of the human tubule and overshadow the plan of organization which we have demonstrated actually exists.

Not the least important factor which contributes to the disorganization of the structure of the seminiferous epithelium is purely mechanical and results from the rough handling of the biopsies at the time of collection. The seminiferous tubule in man is a small, apparently more fragile structure than that in other species. There seems to be less cohesion of the cells within the germinal epithelium so that any pressure on the tubules results in sloughing of cells into the tube lumen and/or to displacement of the cells from one area of the seminiferous epithelium to another. Even when such displacement artifacts are [illegible] they considerably complicate any characterization of the typical cellular associations.

While it was used here in a demonstration of the existence of the cycle of the seminiferous epithelium, the classification of the cellular associations into six stages of the cycle proposed above may now serve as a system of landmarks in more detailed histophysiological and histopathological studies on spermatogenesis.

SUMMARY

The normal histology of the seminiferous epithelium in man was reinvestigated on hematoxylin-eosin stained sections including serial sections, of Zenker formol fixed testes. Typical germ cell associations of fixed composition were described using the nuclear morphology of the germ cells and the topographical arrangement of the spermatids as the principal criteria. Thus one or two generations of spermatids at given steps of spermiogenesis had a clear-cut tendency to associate with one or two generations of spermatocytes and with spermatogonia at given steps of their respective development. Six such well-defined cellular groupings were found. These were classified as six stages of the cycle of the seminiferous epithelium since in a given area of seminiferous epithelium they follow each other in a cyclic manner

In man, the stages of the cycle occupy numerous small areas of the tubular epithelium as a consequence several such stages (three on the average) could be seen in a single tubular cross-section Furthermore at the borderline of such typical cellular associations, cells can intermingle giving irregular "heterogeneous associations which often locally disrupt the characteristic pattern of the stages of the cycle. The stages are also frequently disturbed by the absolute or relative absence of one or more generations of germ cells, and by an imperfect (comparative to rodents) integration of the developmental steps of the various generations of germ cells. The latter imperfections are not sufficiently important, however to obscure the pattern of the cycle of the seminiferous epithelium.

The relative durations of the stages of the cycle were estimated as percentages stages I, II and V were relatively long and stages III, IV and VI were comparatively much shorter.

ACKNOWLEDGMENT

This work was supported by a grant from the Population Council Inc. The author is indebted to Dr C. P Leblond and Miss C. Huckins for their help in the preparation of the manuscript. We gratefully acknowledge the help of Dr Carl G Heller Pacific Northwest Research Foundation Seattle Washington who provided us with many well fixed biopsies. The drawing was prepared by Mrs M. Oeltzschner.

LITERATURE CITED

Branca, A. 1911 Sur le caractère individuel du testicule humain. Compt. rend. Assoc. anat., 13 283–286.

——— 1924 Les canalicules testiculaires et la spermatogénèse de l'homme. Arch. Zool. exp., 62 53–252.

Clermont, Y 1954 Cycle de l'épithélium séminal et mode de renouvellement des spermatogonies chez le hamster Rev Canad. Biol., 13 208–245.

——— 1960 Cycle of the seminiferous epithelium of the guinea pig. Fertil. and Steril., 6 563–573.

Clermont, Y and C. P Leblond 1955 Spermiogenesis of man, monkey ram and other mammals as shown by the "periodic acid-Schiff" technique. Am. J Anat., 96 229–253

——— 1959 Differentiation and renewal of spermatogonia in the monkey Ibid., 104 237–274

Ebner V von 1902 Die Geschlechtsorgane A. Kolliker' Handbuch der Gewebelehre des Menschen. Vol. 3 6th Ed. Leipzig.

Leblond, C. P., and Y Clermont 1952a Spermiogenesis in rat, mouse, hamster and guinea pig as revealed by the periodic acid-Schiff-fuchsin sulfurous acid technique. Am. J Anat., 90 167–215.

——— 1952b Definition of the stages of the cycle of the seminiferous epithelium in the rat. Ann. N Y Acad. Sc., 55 548–573.

Oakberg, E. F 1956 A description of spermiogenesis in the mouse and its use in analysis of the cycle of the seminiferous epithelium and germ cell renewal. Am. J Anat., 99 391–414

Painter T S. 1923 Studies on mammalian spermatogenesis. II. The spermatogenesis in man. J Exp. Zool., 37 291–338.

Perey B., Y Clermont and C. P Leblond 1961 The wave of the seminiferous epithelium in the rat. Am. J Anat., 108 47–78.

Roosen-Runge E. C. 1955 Kinetics of spermatogenesis in mammals. Ann. N Y Acad. Sc 55 574–584

——— 1956 Quantitative investigations on human testicular biopsies. I. Normal testis Fertil. and Steril., 7 251–261

Roosen-Runge, E. C., and F D. Barlow 1953 Quantitative studies on human spermatogenesis. I. Spermatogonia. Am. J Anat., 93 143–170.

Steive H. 1930 Mannliche Genitalorgane. In Handbuch der. mikr Anat. des Menschen. W v Mollendorf, Berlin.
Slotopolsky B and H. R. Schinz 1924 Histologische Beobachtungen am menschlichen Hoden. Virchows Arch., 248 285–296.
——— 1925 Histologische Hodenbefunde bei sexual Verbrechen. Ibid., 257 294–355.
Winiwarter H. de, and K. Oguma 1926 Nouvelles recherches sur la spermatogénèse humaine. Arch. Biol 36 99–166.

PLATE 1

EXPLANATION O FIGURES

Microphotograph f areas of human seminiferous epithelium showing six typical cellular associations corresponding t the six stages of the cycle of the seminiferous epithelium. The number of the tage is indicated t the top of each picture on the lumen side of the tubular section Staining hematoxylin-eosin; Magn. pprox. × 900.

4 Stage I of the cycle howing newly formed spermatids (Sa) and maturing sperm tid (Sd); the latter are deeply inserted in the seminiferous epithelium between the younger spermatids. Also labeled are the generation of early pachytene primary spermatocytes (P) and the spermatogonia (G)

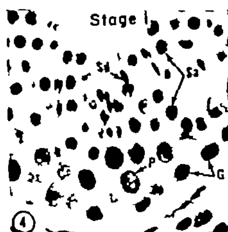
5 Stage II of the cycle shows generations of young spermatids (Sa) and of maturing spermatids (Sd) The latter now line the lumen of the tubule. Pachytene primary spermatocytes (P) and spermatogonia (G) are also indicated.

6 Stage III of the cycle in which one generation of spermatid (Sb) one of pachytene primary spermatocytes (P) and one of newly formed resting primary spermatocytes (R) are present and labeled.

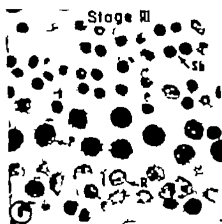
7 Stage IV of the cycle in which the generation of spermatids (Sb) hows the initial signs of elongation of their nuclei Also labeled are pachytene (P) and leptotene (L) primary perm tocytes and the Sertoli cell nuclei (Ser)

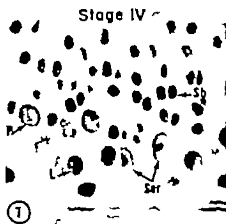
8 Stage V of the cycle showing groups of spermatids with elongated nuclei (Sc) late pachytene (P) and leptotene (L) primary spermatocytes. Several spermatogonia (G) line the limiting membrane.

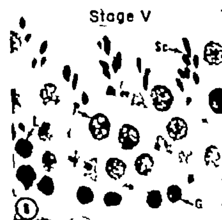
9 Stage VI of the cycle contains groups of maturing spermatids (Sc) between primary spermatocytes which are undergoing the first maturation division of meiosis (Sptc Im) A generation of zygotene primary spermatocytes (Z) present at this stage is also indicated.


Stage I
Sd
Sa
P
G
4


Stage II
Sd
Sa
P
G
5


Stage III
Sb
P
R
6


Stage IV
Sb
L
7


Stage V
Sc
P
L
G
8

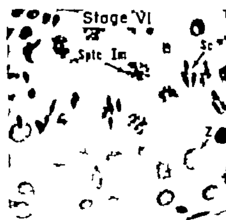

Stage VI
Sc
Z

PLATE 2

EXPLAN TION OF FIGURES

Microphotographs f arious characteristic areas in human seminiferous epithelium. Staining hematoxylin-eosin; M gn. approx. × 900

10 Photograph showing two adjacent typical cellular associations, their *sharp borderline being indicated by line On the left, the cells* which belong to stage I of the cycle are labeled as follows young spermatids (Sa) maturing spermatids (Sd); early pachytene primary spermatocytes (P) On the right the cell types present in stage V of the cycle are labeled as follows maturing spermatids (Sc) pachytene (P) and leptotene (L) primary spermatocytes.

11 Photograph of two adjacent stages of the cycle in which the sharp demarcation between the two is indicated by line On the left stage VI of the cycle is composed of the following elements maturing spermatids (Sc) secondary spermatocytes in interphase (Spte II) and early pachytene primary spermatocytes (P) On the right stage I of the cycle is composed of young spermatids (Sa) maturing spermatids (Sd) and pachytene primary spermatocytes (P)

12 Photograph from an area of the seminiferous epithelium showing heterogeneou cellular association composed of the following elements young (Sa) and maturing spermatids (Sc, Sd) primary spermatocytes in division (Spte Im) and zygotene primary spermatocytes (Z) This area represents zone of interpenetration of two tages of the cycle, tage VI on the left and stage II on the right, the demarcation between these two stages being tentatively indicated by dotted line.

13 Photograph of an area of the seminiferous epithelium corresponding to stage I of the cycle. Young (Sa) and maturing (Sd) spermatids are present as well as spermatogonia (G) but primary spermatocytes which are supposed to be present t this stage are completely absent from this so called "incomplete cell ssociation.

14 Photograph of an area of the seminiferous epithelium t late stage V *of the cycle The following elements can be seen maturing* spermatids (Sc) diplotene primary spermatocytes (D_1) zygotene primary spermatocytes (Z) and spermatogonia (G)

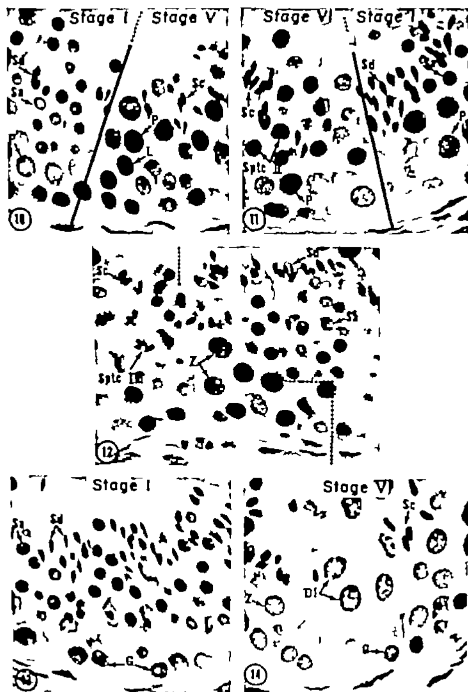

Stage I
Stage V
Stage VI
Stage I
Sd
Sa
Sc
P
L
Sptc II
Sd
Z
Sptc III
Stage I
Stage VI
Sa
Sd
Sc
Di
Z
G
10
11
12
14

PLATE 3

EXPLANATION OF FIGURES

Low power microphotographs of tubular sections to show the distribution of the arious typical cell associations or stages of the cycle (numbered with Roman numerals) as well as their demarcation lines. Fixation Zenker-formol; staining hematoxylin-eosin.

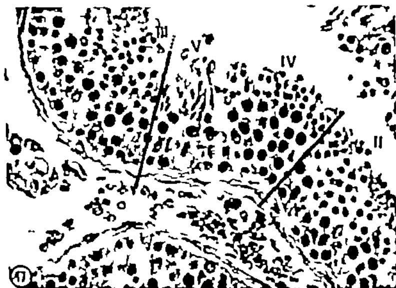
15 Photograph of tubule showing three typical stages of the cycle labeled I III and V respectively The unlabeled area on the left was difficult to characterize because it represents an oblique section through the epithelium. Magn. × 35.

16 Photograph of tubular cross section showing four different cellular associations corresponding respectively to stages VI, IV I and III of the cycle. Note that the numbers of the stages around the tubule are not consecutive. Magn. × 35.

17 Photograph of a portion from longitudinally cut tubule showing well demarcated stages of the cycle respectively labeled clockwise as III, V IV and II. Note that here also the number of the stages along the seminiferous epithelium are not consecutive. Magn. × 40.

18 Photograph of portion of seminiferous tubule showing well demarcated stage V of the cycle with stage VI of the cycle (with secondary spermatocytes in interphase) on its left and on its right stage I of the cycle Magn. × 40 (fig. 8 is microphotograph at higher magnification of the central area of this stage V of the cycle)


I
III
V
15
VI
IV
III
16


III
V
IV
II
I
17


VI
V
I
18

Electron Microscopic Description of a Third Cell Type in the Islets of the Rat Pancreas[1]

FELICE CARAMIA
Department of Anatomy Washington University School of Medicine St. Louis, Missouri

In spite of the numerous studies on the cytology of the pancreatic islets, there still is disagreement as to both the numbers and exact structure of their cells. This is particularly true of the D cell.

In 1931 Bloom was able to stain differentially three types of granular cells in the islets of the human pancreas fixed in Helly's fluid the alpha and beta types described by many other investigators, and a new type of granular cell which he called the D cell. In 1937 a more complete and extensive study of this third type was carried out on 41 different species of mammals by Thomas, who concluded that the D cells were a fundamental component of mammalian islets. Gomori ('39) using his modification of the Mallory azan stain could find D cells only in the dog, guinea pig and man whereas in the rat, cat, rabbit, mouse monkey and horse results were inconclusive. Subsequent investigations are in disagreement. Some investigators have described agranular D cells (Bencosme, '55) yet such do not correspond to Bloom's original description; others (Ferner '42) (Ferner and Stoeckenius '50) have interpreted them as degenerating alpha or beta cells and this latter interpretation appears to be predominant today

Previous electron microscopic studies of the pancreatic islets have failed to demonstrate the D cell described by Bloom with the exception of Bencosme ('58) who has described them in the cat. During our study of the ultrastructure of the different types of alpha cells in the rat pancreatic islets cells significantly different in structure to warrant consideration as being D cells were observed. These observations comprise the present report.

MATERIALS AND METHODS

Sprague-Dawley rats two days, 13 days, and six months old were used for this study The rats were anesthetized with ether and the pancreas exposed with proper technique was partially freed from the surrounding connective tissue and fat. Immediately excised, the tissue was transferred to a drop of 1% osmium tetroxide in White's balanced salt solution, and cut into minute fragments These were transferred into more fixative for periods varying from one to two hours. After fixation at room temperature they were washed in 10% ethanol, dehydrated in a series of increasing concentrations of ethyl alcohol and embedded in EPON 812 resin. The sections were cut with glass knives on a Porter Blum microtome and picked up on copper grids They were examined with and without the use of collodion supporting film in an RCA EMU 3C electron microscope at original magnifications of 1 400 to 7,000 Occasional sections were stained with lead hydroxide but a majority were examined without staining in order to demonstrate the inherent densities of the various granules.

RESULTS

Adult

The central portion of the pancreatic islet of the adult rat is composed predominantly of beta cells whereas the peripheral portion is composed almost entirely of alpha cells (fig 1) The beta cells are more dense than alpha cells this greater density being due to the relatively large amount of ergastoplasm as described by

[1] This work was supported in part by the United States Public Health Service Grant no. RG-3784.

Permanent address: Instituto di Patologia Generale, University of Perugia, Perugia, Italy

Lacy in the rat ('57) and Munger in the mouse ('58) In the beta cells (figs. 1 3) the ergastoplasm is composed of anastomosing membranous sacs and tubules of varying size with associated ribonucleoprotein granules The tubules do not display parallel orientation and are disposed between the vesicles containing the beta granules Sometimes in both alpha (fig 1) and beta cells (fig. 5) the ergastoplasmic sacs form a parallel array in part of the cell. The alpha granules are more electron dense than the beta (fig. 5) and are surrounded by closely applied limiting membranes in contrast to the large space that separates the surrounding membrane from the beta granule. Rod shaped mitochondria are few in alpha cells whereas in beta cells they are numerous (fig. 5)

The nuclei of alpha and beta cells also differ (figs 1 3) Those of the alpha cell are round or ovoid with fine uniformly dispersed chromatin that results in a relatively homogeneous dense nucleus. Occasionally larger dark particles are randomly distributed throughout the nucleus Nucleoli are also observed The nuclei of beta cells are larger than those of alpha cells and their chromatin is more clumped.

At the periphery of the islets interspersed among the alpha cells are occasional cells that are denser than either the alpha or beta cells (fig. 1) Usually they appear elongated and are radially disposed in the islet One end of such a cell abuts on an acinar cell the other on a capillary in the islet. Their cytoplasm contains a few scattered granules usually disposed on the side of the cell towards the capillary These granules vary in size and are slightly smaller than alpha granules although they have a similar density The ergastoplasm is formed by flattened sacs with associated granules the compact arrangement of which contributes to the cytoplasmic density (fig. 2) Their mitochondria are rod shaped scattered throughout the cytoplasm and more numerous than those of alpha cells. The prominent Golgi apparatus is formed by numerous vesicles, vacuoles and flattened cisternae. The nucleus is similar to that of alpha cells. These cells are considered to be an alpha cell variant and perhaps to be the correlate of the silver staining alpha cell of light microscopy

In addition to the granulated cells described above there is another distinct type of cell that is characterized by the presence of small granules of low electron density (figs. 3 4) These cells also are arranged close to capillaries. Their nuclei are somewhat ovoid and often contain nucleoli in the plane of section. The mitochondria are evenly distributed throughout the cytoplasm and of variable density usually being more dense than the secretory granules. The granules are of relatively similar size and density but are smaller than alpha and beta granules. The granules again are usually most numerous in the part of the cell nearest the blood vessel (fig 4) and are surrounded by a limiting membrane that is distinct but very closely applied and often is even more dense than the substance of the granule (fig 6) In contrast to other granulated cells (alpha or beta) the cytoplasm of these cells virtually is packed with secretory granules (fig. 6) The Golgi zone usually disposed on the opposite side of the cell from the capillary is rather prominent. In all of these cells the ergastoplasm is arranged at the margin of the cell These cells have been interpreted as D cells.

Three and thirteen days of age

At this stage all the cell types of the adult pancreas can be observed except the dark alpha cells The D cells at three and 13 days present the same characteristics as the adult D cells numerous small granules of evenly low electron density located close to the capillaries (figs. 7 8) The Golgi apparatus is more prominent and the nuclei, as seen in the alpha and beta cells, appear irregularly shaped tending toward an ovoid appearance and contain one or two nucleoli. Non-granulated cells can be seen at this stage although they tend to occur in greater number at two days than at 13 days

DISCUSSION

The characteristic ultrastructure permitting identification of alpha and beta cells in pancreatic islets of various species has



Fig. 1 A portion of an islet from adult rat p ncreas illustrating the two types of alph cell and beta cells. Dark alpha cells ( ) are characterized by dense cytoplasm with small granules concentrated near the capillary and numerous elong ed mitochondria. The clei are dense and regular in outline Clear alpha cells (A) have comparativ ly empty cytoplasm with lectron dense granules larger than those of the dark alph cells ( ) The beta cell (B) on ai sc ttered gra ules with prominent space present between the granule and it limiting membrear The uc f bet ell are round or ovoid and are less dense and larger than the nuclei of alph ll M hondria of all cells tend to be clumped at the side of the cell nex the pillary 4 000



Fig 2 Relatively high magnification of the two dark alpha cells illustrated in figure 1 The ergastoplasm in these cells is composed of large flattened sacs with associated granules. In addition to the granules associated with the membrane, there are numerous granules of similar size and density which ppear to be disposed in rosettes or irregular clusters. The secretory granules can be compared with those of the clear alpha cells better at this magnification. × 6,000



Fig. 3 Adult rat pancreas The arrow point part of D cell which is filled with small granules. These are less dense than alpha or beta granules and h ve losely applied limiting membrane. At the upper part of the field is part of an exocrine pancreatic cell. 9,000



Fig. 4 Adult rat pancreas D cell The cytoplasm of this cell contains granules of low electron density mitochondria, and an ergastoplasm formed of flattened sacs occasionally arranged in parallel array (arrow) The nucleus is slightly irregular in outline as compared t those of alpha or beta cells. × 13,000.



Fig. 5 Adult rat pancreas. This micrograph ill strates the differences between the specific granules of alpha and beta cells and whe compared to figure 6 the difference between these and the D cell granules. Alpha cell granules (A) are round, dense and have losely applied limiting membrane Beta cell granules (B) are lightly les electron dense and haracteristically have wide lear zone between the granule and it surrounding membrane × 23,000.



Fig. 6 An electron micrograph of portion of D cell showing numerous granules less dense than those of alpha and beta cells The granules are closely packed almost filling the cytoplasm. At the upper left is part of beta cell (B) × 32,000.



Fig. 7 A portion of an islet f newborn rat in which D cell is seen. The cytoplasm filled of granules of low electron density concentrated near the capillary and simila to D ll in the adult. Alpha cells (A) and undifferentiated cells are also present. × 10,000

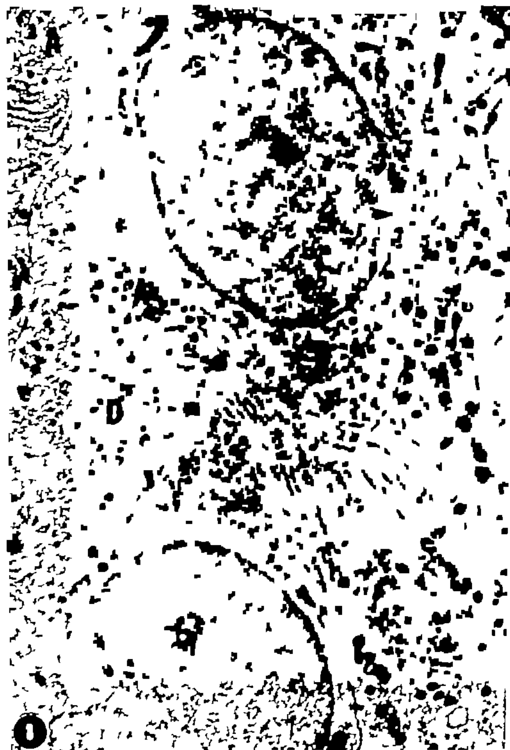


Fig. 8 Tw D cells in an islet from 13-day-old rat are present. The ultrastructural characteristics are comparable to those of D cells in new born and adult animals. Alpha cells (A) are also present. × 10,000.

been defined previously (Lacy '57). In the present study these characteristics have been confirmed. In addition a third cell type distinctly different in structure from alpha and beta cells consistently has been seen. This cell has a cytoplasm filled with small granules of low electron density and a nucleus which is round or ovoid.

On the basis of light microscopic studies on the identification of cell types in the pancreatic islets of various species this third granulated cell type most likely is the D cell of Bloom. In Bloom's ('31) original description the D cells in human pancreatic islets were observed to be granular a finding confirmed by Thomas ('37) in several other species, including the rat. The fact that other investigators have failed to confirm this observation and the granular nature of the D cell cytoplasm is not surprising. This disagreement may perhaps be explained by the use of different fixatives by these investigators Bloom and Thomas used Zenker-formol and Mallory-azan stain. Gomori ('39) used Bouin's fluid which is not a good fixative for the D cells and then stained with Mallory azan after oxidation with permanganate. Similar difficulties were encountered by Simard ('45) who also used Bouin's fixative, and Hard ('44) who used Gomori's modification of the Mallory-azan stain.

Our results also demonstrate that these cells cannot be considered degenerating cells as has been claimed by Ferner ('42) among others. Such a concept is not in accord with the following observations (1) these cells are present in young animals (three and 13 days of age) (2) the secretory granule of the D cell has a distinct ultrastructure different from that of alpha and beta cells and (3) intermediate types of granules have not been seen.

The electron dense alpha cells observed in the adult pancreatic islets differ in some characteristics from previously described alpha cells, and may be related to the current concept of a heterogeneous population of alpha cells Hultquist Dahlen and Helander ('48), using the Gros-Schultze method, reported that in the cat pancreatic islets 7% of the cells can be impregnated with silver salts. Differences were also reported by Goldner and Volk ('56) using a modified Davenport technique They confirmed that not all alpha cells visualized by the phloxin procedure are argentophilic, and they raise the question as to whether the Gomori stain identified two different kinds of cells or two different functional stages of the same cell type. A similar observation (Caramia, '62) was made on the adult human pancreas using the Goldner modification of the Davenport technique. Alternate serial sections of fresh tissue fixed in Bouin were stained with Mallory's phosphotungstic acid hematoxylin and by silver impregnation Only 6 – 8% of the islet cells were argentophilic in contrast to 22 to 34% of islet cells that were PTAH positive. Since in the newborn pancreas all Mallory hematoxylin positive alpha cells are also argentophilic, it is concluded that the difference in staining property observed in the adult alpha cells can be due to an aging alteration. It is possible that the difference in ultrastructure found in the two types of alpha cells identified in adult rat pancreas may account for the difference in staining properties of these cells

SUMMARY

(1) Evidence has been presented that two types of alpha cells can be distinguished in the adult rat pancreas the clear alpha cells described by other authors and dark alpha cells with few granules and compact ergastoplasm that probably correspond to the argentophilic alpha cells

(2) Cells significantly different from the clear and dark alpha cells and from the beta cells were also observed in the pancreatic islets of both young (two days 13 days old) and mature animals. These cells have cytoplasm filled with closely packed granules of low electron density and have a round nucleus. It is proposed that these are the D type cells as originally described by Bloom in the human pancreas.

LITERATURE CITED

Bencosme, S A. 1955 The histogenesis and cytology of the pancreatic islets in the rabbit Am. J f Anat 96 103–151

Bencosme S A and D C Pease 1958 Electron microscopy of the pancreatic islets. Endocrinology 63 1 13

Bloom W 1931 New type of granular cell in islets of Langerhans of man. Anat Rec 49 363–371.

Ferner H. 1942 Beitrage zur Histobiologie der Langerhansschen Inseln des Menschen mit besonderer Berucksichtigung der Silberzellen und ihrer Beziehung zum Pankreasdiabetes. Virchows Arch. f path. Anat., 309 87–136.
Ferner W., and W Stoeckenius J 1950 Die Cytogenesee des Inselsystem beim Menschen. Ztschr Zellforsch. u. mikr Anat., 35 147–175
Goldner M. G., and B W Volk 1956 The effect of hypophysectomy and of prolonged growth hormone administration on the pancreatic alpha cells of the rat. Colloquia on Endocrinology 9 75–88.
Gomori, G. 1939 Studies on the cell of the pancreatic islets. Anat. Rec 74 439–459
Hard, W L 1944 The origin nd differentiation of the A and B cells in the pancreatic islets of the rat. Am. J Anat., 75 369–403.
Hultquist, G. T M Dahlen and C. G. Helander 1948 Über die Technik bei Darstellung und Zahlung der Sogen. Silberzellen in den Langerhansschen Inseln. Schweiz. Ztschr f Path. u. Bakt., 11 570–589
Lacy P E. 1957 Electron microscopic identification of different cell types in the islets of Langerhans of the guinea pig, rat, rabbit and dog. Anat. Rec., 128 255–268
——— 1957 Electron microscopy of the normal islets of Langerhans. Diabetes, 6 498–507
Millonig, G. 1961 A modified procedure for lead staining of thin sections. J Bioph. Bioch. Cytol., 11 736–739
Munger B L. 1958 A light nd electron microscopic study of cellular differentiation in the pancreatic islets of the mouse. Am. J Anat., 103; 275–312.
Simard, L. C. 1945 Etude histologique de pancreas greffes dan la paroi abdominale chez le chien. Rev Can. de Biol., 4 264–287
Thomas, Thurlo B. 1937 Cellular components of the mammalian islets of Langerhans. Am J Anat., 62: 31–57

Morphological and Histochemical Studies of Experimentally Enlarged and Atrophied Salivary Glands of Rats[1]

CHESTER R. HANDELMAN[2] AND HERBERT WELLS
Biological Research Laboratories, Harvard School of Dental Medicine
Department of Pharmacology Harvard Medical School

The factors which regulate the rate of growth and size of the salivary glands are largely unknown. A new approach to the investigation of this problem was opened by the discovery that a marked increase in the weight of the submandibular salivary glands of rats follows repeated amputation of the lower incisor teeth (Wells et al., '59; Wells and Munson, '60) On the other hand, a marked decrease in the weight of the submandibular glands follows the administration of Dibenamine (dibenzylchlorethylamine) a potent adrenergic blocking agent (Wells '60) Wells Handelman and Milgram ('61) suggest that the sympathetic nervous system is involved not only in the response to incisor amputation but in the regulation of the normal growth and size of the salivary glands as well.

Preliminary morphologic studies of the enlarged glands indicate that the increase in gland weight is due to hypertrophy of the acinar cells (Wells et al., '59) The present report summarizes the results of a more detailed morphologic examination of the enlarged glands, and of glands made atrophic by administration of Dibenamine. A variety of histochemical techniques were also utilized in order to characterize the morphological changes further and for possible insights into the mechanism whereby these alterations in salivary gland size occur

METHODS AND MATERIALS

The experimental animals were male albino rats obtained from the Holtzman Co. Madison, Wisconsin. The rats in each experiment had been born on the same day and were between 70 to 80 days of age when used. The diet consisted of Purina Laboratory Chow (ground for the rats with amputated incisors) and water ad lib.

The lower incisor teeth were amputated at the gingival margin with a toenail clipper The amputations were performed at two-day intervals for a total of four times in eight days. The rats were autopsied 24 hours after the last amputation.

Dibenamine (dibenzylchlorethylamine) dissolved in distilled water to which a small amount of ethanol had been added, was injected intraperitoneally in a dose of 40 mg/kg twice daily for two days. Control injections consisted of distilled water and ethanol alone The rats were autopsied 16 hours after the last injection.

At the end of an experiment the rats were quickly killed with an excess of ether and the submaxillary and major sublingual glands removed and dissected free of extraneous connective tissue. The right submaxillary and sublingual glands were then weighed together on a torsion balance as the submandibular gland. Parts of the parotid glands were also removed and cleaned. The tissues were then bisected and either placed in an appropriate fixative or quick frozen in isopentane cooled by dry ice and ethanol for sectioning in the cold microtome (cryostat) The fixed tissues were embedded in paraffin and sectioned at 5 µ. The unfixed frozen tissues were sectioned at 10 µ in a cold microtome

HISTOCHEMICAL METHODS

Ribonucleic acid. The tissues were fixed for eight hours in neutral formalin. Sec

[1] This work was supported in part by a research grant (D-[illegible]) from the National Institute for Dental Research.

[2] Present address Forsyth Dental Infirmary Boston, Massachusetts.

Ferner H. 1942 Beitrage zur Histobiologie der Langerhansschen Inseln des Menschen mit besonderer Berucksichtigung der Silberzellen und ihrer Beziehung zum Pankreasdiabetes. Virchows Arch. f. path. Anat. 309 87–136.
Ferner W., and W Stoeckenius, J 1950 Die Cytogenese des Inselsystem beim Menschen. Ztschr Zellforsch. u. mikr Anat., 35: 147–175.
Goldner M. G and B W Volk 1956 The effect of hypophysectomy and of prolonged growth hormone administration on the pancreatic alpha cells of the rat. Colloquia on Endocrinology 9 75–88.
Gomori, G. 1939 Studies on the cells of the pancreatic islets. Anat. Rec., 74 439–459
Hard, W L. 1944 The origin and differentiation of the A and B cells in the pancreatic islets of the rat. Am. J Anat., 75 369–403
Hultquist, G. T M. Dahlen and C. G Helander 1948 Über die Technik bei Darstellung und Zahlung der Sogen. Silberzellen in den Langerhansschen Inseln. Schweiz. Ztschr f Path. u. Bakt., 11 570–580.
Lacy P E. 1957 Electron microscopic identification of different cell types in the islets of Langerhans of the guinea pig, rat, rabbit and dog. Anat. Rec., 128 255–268.
——— 1957 Electron microscopy of the normal islets of Langerhans. Diabetes, 6 498–507
Millonig, G. 1961 A modified procedure for lead staining of thin sections. J Bioph. Bioch. Cytol 11 736–739
Munger B L. 1958 A light and electron microscopic study of cellular differentiation in the pancreatic islets of the mouse. Am. J Anat., 103 275–312.
Simard L. C. 1945 Etude histologique de pancreas greffes dans la paroi bdominale chez le chien. Rev Can. de Biol., 4 264–287
Thomas, Thurlo B 1937 Cellular components of the mammalian islets of Langerhans. Am. J Anat., 62: 31–57

larged glands there was a significant ($P < 0.001$) decrease of approximately 30% in the number of acinar nuclei per high power field. The decrease in number of nuclei indicated that there were fewer cells to count in a high power field because each of the cells had enlarged.

The diameter of the granular tubules of the submaxillary glands was measured under oil immersion with an ocular micrometer. For these measurements 20 random tubular diameters were chosen from a number of sections from the glands of each of the six experimental and control rats. The results, in table 1 indicate that there was no significant alteration in the diameter of the granular tubules of the enlarged glands.

Effects of Dibenamine Administration of Dibenamine resulted in a significant ($P < 0.001$) decrease in submandibular gland weight (table 2) The rats receiving Dibenamine also lost a significant amount of body weight. However the decrease in body weight was 18% while the decrease in gland weight was 33% This indicated that the reduction in gland weight was far in excess of the loss in body weight.

The acinar cells of the atrophic submaxillary and parotid glands were clearly reduced in size (figs. 1 3 7 9) Acinar nuclei also appeared to be smaller and to have an irregular contour in contrast to the spherical appearance of nuclei from control acinar cells. In some sections there were areas where the glandular architecture appeared to be disturbed for the acinar cells were formed in cords with scanty cytoplasm and fragmented nuclei (figs. 6 9) Because of the atrophy of the acinar cells of the submaxillary gland there was a relative increase in the contribution of the granular tubules and ducts to the total composition of these glands (figs. 13 15) The acinar cells of the atrophic sublingual glands also appeared smaller than control acinar cells (figs. 10 12) The nuclei of these atrophic cells also appeared smaller

The results of a histometric evaluation of glands from Dibenamine-treated rats are shown in table 2. There was a significant ($P < 0.001$) increase of approximately 40% in the number of acinar nuclei per high power field. The increase in the cell population density indicated that there were more nuclei to count in each field because each of the acinar cells had decreased in size There was a small (8%) but significant ($P < 0.01$) reduction in the diameter of the granular tubules.

Ribonucleic acid. In salivary gland sections stained with methyl green-pyronin, only that pyronin staining material that was digested by ribonuclease was interpreted as ribonucleic acid (RNA) RNA appeared to be concentrated in the basilar and perinuclear regions and nucleoli of the acinar cells of control submaxillary and parotid glands (figs 4 7) In the remaining cytoplasm RNA was present as finely dispersed granules. In the control sublingual glands RNA was concentrated in the cytoplasm of the demilune cells while in the sublingual acinar cells it was distributed throughout the cytoplasm (fig. 10)

In the enlarged acinar cells there appeared to be a marked increase in the

TABLE 2

Effect of Dibenamine on submandibular gland weight, counts of acinar cell nuclei and submaxillary gland tubular diameter[1,2]

Treatment	No. of rats	Final body weight	Submandibular gland weight (right gland)	Acinar cell nuclei (counts/10 high power fields)			Submaxillary gland tubular diameter[3]
				Submaxillary	Sublingual	Parotid	
		gm	mg				μ
Control injection	6	257 ± 11	284 ± 5	164 ± 7	115 ± 2	278 ± 17	33 ± 0.1
Dibenamine 20 mg/kg	6	210 ± 14	190 ± 7	235 ± 17	158 ± 5	384 ± 12	30 ± 0.1

[1] Values are means ± standard error
[2] Initial body weight 240 ± 1 gm.
[3] Mean of 20 measurements/6 glands.

amount of RNA (figs. 5 8) The basilar and perinuclear regions of the submaxillary and parotid acinar cells contained material which stained intensely with pyronin. The nucleoli of these cells were enlarged and rich in RNA. The demilune and mucous acinar cells of the enlarged sublingual glands also had an increased content of RNA (fig. 11)

In all three glands administration of Dibenamine resulted in a marked decrease in the RNA content of the atrophic acinar cells (figs. 6 9 12)

The granular tubules of control submaxillary glands were found to contain *large pyronin-staining granules Digestion* with ribonuclease did not alter this intense staining reaction (fig. 19) These granules were still present in the tubules of the atrophic glands after administration of Dibenamine although the concentration of the granules was slightly reduced. On the other hand in the enlarged glands the tubules were almost completely devoid of the pyronin-positive ribonuclease resistant granules (fig. 20)

Carbohydrates A relatively high con- of PAS-positive granules was u in the apical portion of the acinar cells of the submaxillary and parotid glands from control rats (fig. 16) A similar staining pattern was observed in the acinar cells of enlarged glands from incisor-amputated rats In these glands, however the basilar and perinuclear regions where the RNA was located, were unstained and appeared to have widened (fig 17) In the acinar cells of the atrophic submaxillary and parotid glands from Dibenamine-treated rats most areas stained well with PAS although some areas exhibited a loss of PAS-positive granules (fig. 18)

The mucous acinar cells of the control sublingual glands were strongly PAS-positive A similar staining pattern was observed in enlarged glands from tooth-amputated rats and in atrophic glands from rats treated with Dibenamine

Large, weakly staining PAS positive granules were observed in the granular tubules of the submaxillary glands The presence of these granules apparently was not affected by either experimental procedure.

The mucous acinar cells of the sublingual glands stained intensely with alcian blue. Neither tooth amputation nor administration of Dibenamine significantly altered the pattern or intensity of this staining reaction.

Succinic dehydrogenase Intense succinic dehydrogenase activity was observed in the tubules and ducts of control glands. The presence of this enzyme in the tubules and ducts was not appreciably altered by either incisor amputation or administration of Dibenamine (figs. 13 14 15) Moderate enzyme activity was noted in the acinar cells of all control glands (fig. 21) *This enzyme activity appeared as small* blue-colored bodies often mitochondrial in shape. Present in the basilar portion of the acinar cytoplasm of only the atrophic glands, in addition to the small blue bodies, were larger and more deeply staining granules. These granules were especially prominent in atrophied sublingual glands (fig 22) If the tissue sections were treated with a lipid solvent (cold acetone) prior to incubation, the large deeply staining, cytoplasmic granules disappeared. On the other hand the blue staining of the mitochondrial-shaped bodies in the ducts and acinar cytoplasm was only slightly inhibited by treatment with cold acetone.

Lipids Some sudan staining of the phospholipid-rich mitochondria in the tubules and ducts was observed. While the mitochondria of the control acinar cells were moderately stained no cytoplasmic granular staining was noted (fig 23) The pattern of staining of the enlarged glands was essentially the same as that of control glands Sudanophilic granules were observed, however in the basal portion of the acinar cells of the atrophied glands from Dibenamine-treated rats (fig 24) These sudanophilic granules were similar in location and concentration to the large acetone-extractable granules observed in the sections stained for succinic dehydrogenase.

DISCUSSION

The morphologic and histometric data presented above indicate that the increase in weight of the submandibular glands that follows incisor amputation is due to a highly specific hypertrophy of the acinar

cells of the submaxillary and sublingual glands. The size of the tubules and ducts is not affected in any obvious way by amputation of the incisors. The reduction in weight of the submandibular glands which results from administration of Dibenamine is due primarily to a marked decreased in size of the acinar cells, and to some decrease in the width of the granular tubules.

In the albino rat the parotid glands are not, like the submandibular glands discrete, encapsulated organs. Hence it is extremely difficult to remove and weigh these glands with any degree of reliability However by means of histometric techniques, the acinar cells of the parotid glands were found to respond in much the same way as submaxillary and sublingual acinar cells to the experimental procedures.

Although incisor amputation does not enlarge the granular tubules or ducts the tubules exhibited a loss of the pyronin-positive ribonuclease-resistant granules. Tubular degranulation may be a non-specific response which follows exposure of the rats to a variety of metabolic alterations (Stahl, '60) Because the succinic dehydrogenase activity of the tubules is unaltered during hypertrophy or atrophy of the glands, the ability of the tubules to carry on many of their functions is probably not impaired.

The mitotic index of the salivary glands of adult rats is quite low (Leblond and Walker '56) The results of the present investigations indicate that the rate of cell division is not appreciably altered during enlargement or atrophy of the glands.

Jacoby and Leeson ('59) observed that the acini of the rat submaxillary gland have achieved their maximum width by six weeks of age and, as the glands continue to grow the granular tubules come to make up an increasing portion of the gland. The enlargement which results from incisor amputation thus alters the normal trend in a significant way for it is the acinar cells which contribute to the increase in size after incisor amputation.

The increased amount of RNA in the hypertrophied acinar cells as well as the enlarged nuclei and nucleoli are probably reflections of accelerated protein synthesis (Steich '59) On the other hand the decrease in RNA content and small irregularly shaped nuclei of the atrophic cells are indicative of a decreased protein synthetic activity These findings are in agreement with the idea that an increase in RNA is essential during periods of accelerated cell growth (Brachet, '55)

In his description of the PAS reactive substances in the adult rat salivary gland, Leblond ('50) concludes that these substances are largely mucopolysaccharides and mucoproteins. The present data with the PAS and alcian blue stains indicate that the apparent concentration of these substances in the enlarged or atrophic glands was not significantly different from controls. It appears likely that the change in weight of the glands resulting from the experimental procedures is not due to either excessive accumulation or loss of mucoprotein and mucopolysaccharide substances from the glands.

In agreement with Padykula ('52) and Dewey ('58) most of the succinic dehydrogenase activity was found to be concentrated in the granular tubules and ducts. The experimental procedures did not alter the concentration of the enzyme in these structures Moderate enzyme activity was also demonstrable in the basilar portion of the acinar cells. In addition, large, deeply staining granules were observed in the acinar cells of the atrophied glands following administration of Dibenamine. Novikoff ('59) points out that in the dehydrogenase techniques the formazan of the nitro blue tetrazolium can crystallize upon lipid material and produce the blue color in forms which are easily mistaken for mitochondria. Since the deeply staining granules in the atrophied glands were acetone-extractable and sudanophilic, they probably represent lipid droplets rather than structures possessing true succinic dehydrogenase activity The mechanism whereby lipid droplets accumulate in the atrophic acinar cells is not clear

The evidence thus far tends to support the hypothesis that the sympathetic nervous system is involved not only in the hypertrophic response to incisor amputation, but in the regulation of normal salivary gland size as well (Wells et al. '61) The size of the glands would thus depend

on the level of sympathetic stimulation received. The glands atrophy after Dibenamine because they receive less sympathetic stimulation as a result of the adrenergic blocking action of the drug The glands hypertrophy because, in some way the intensity of sympathetic stimulation which they normally receive is increased by incisor amputation. This idea has recently received support from Selye et al. ('61) They administered high doses of a sympathomimetic drug, isoproterenol, to rats and observed a five-fold enlargement of the submaxillary glands. This effect on gland weight has been confirmed in mice by Brown-Grant ('61) Wells ('62) has also confirmed Selye et al. and shown that the response of the glands to isoproterenol is similar in many respects to the response which follows amputation of the incisor teeth The fact that RNA accumulates in the hypertrophied cells while the atrophic cells are almost devoid of RNA, suggests that the sympathetic nervous system in some way regulates the metabolism of RNA in the salivary glands. In this respect the salivary glands may resemble various endocrine glands in which cell volume and RNA content are altered in response to changes in the level of stimulation. The acinar cells of the salivary glands may also be analogous to the cells of skeletal muscle where cell volume depends on the level of nervous activity

SUMMARY

A marked enlargement of the submandibular salivary glands of rats results from repeated amputation of the lower incisor teeth. On the other hand atrophy of the salivary glands follows administration of of Dibenamine a potent adrenergic blocking agent. The present studies utilized histological and histochemical techniques to describe these phenomena in detail and for possble insights into the underlying mechanisms. The enlarged glands showed a very marked increase in the size of the acinar cells. Acinar nuclei and nucleoli were also enlarged. There was no alteration in mitotic rate In the atrophic glands the acinar cells were markedly reduced in size and had smaller nuclei. Histometric analyses confirmed the visual impressions and indicated a slight reduction in tubular diameter in the atrophic glands but no change in tubular diameter in the enlarged glands. It was concluded that the enlargement of the glands following incisor amputation is due to a specific hypertrophy of the acinar cells. The atrophy produced by Dibenamine is due to atrophy of the acinar cells and a slight decrease in tubular size.

There was an accumulation of RNA in the hypertrophic cells while the atrophic cells were almost devoid of RNA. The changes in RNA content were interpreted as mirroring the rate of protein synthesis of the acinar cells. Incisor amputations, but not Dibenamine, depleted the tubules of their usual content of pyronin-positive, ribonuclease-resistant granules. However neither experimental procedure altered the concentration of succinic dehydrogenase in the tubules and ducts. The amount of PAS and alcian blue positive material in the acinar cells was unchanged. The atrophic acinar cells contained large acetone-extractable sudanophilic granules which are probably lipid in nature. The significance of these large lipid granules is not clear

ACKNOWLEDGMENTS

The authors wish to thank Dr J T Irving for his advice in the preparation of this manuscript, and Miss Anna Morse for excellent instruction in technical procedures.

LITERATURE CITED

Brachet, J 1955 The biological role of pentose nucleic acids. In The Nucleic Acids, volume 2. Editors E. Chargraff and J N. Davidson, pp. 475–519 Academic Press, New York

Brown-Grant, K. 1961 Enlargement of salivary glands in mice treated with isopropyl noradrenaline. Nature, Lond., 191 1076–1078.

Dewey M. M. 1958 A histochemical and biochemical study of the parotid gland in normal and hypophysectomized rats. Am. J Anat 102 243–271

Jacoby F and C. R. Leeson 1959 The post-natal development of the rat submaxillary gland. J Anat., Lond., 93: 201 216.

Leblond, C. P 1950 Distribution of periodic acid-reactive carbohydrates in the adult rat. Am. J Anat 86: 1–50.

Leblond, C. P and W E Walker 1956 Renewal of cell populations. Physiol. Rev 36 255–276.

McManus, J F A. 1948 Histological and histochemical uses of periodic acid. Stain Tech., 23: 99–108.
Mowry R. W 1960 Revised method producing improved coloration of acidic polysaccharides with Alcian blue 8GX supplied currently J Histochem. Cytochem., 8 323.
Nachlas, M. M., K. D. Tsou, E. De Souza, C. S. Cheng and A. M. Seligman 1957 Cytochemical demonstration of succinic dehydrogenase by the use of new p-nitrophenyl ditetrazol. Ibid., 5: 420–436.
Novikoff, A. B. 1959 Enzyme cytochemistry pitfalls in the current use of the tetrazolium technique. Ibid., 7 301–302.
Padykula, H. A. 1952 Localization of succinic dehydrogenase in tissue sections of the rat. Am. J. Anat., 91 107–146.
Pearse, E. A. G. 1960 Histochemistry Theoretical and Applied, pp. 825. Little, Brown and Company Boston.
Selye, H., R. Veilleux and M. Cantin 1961 Excessive stimulation of salivary gland growth by isoproterenol. Science, 133 44–45.
Stahl, S. S. 1961 Response of the periodontium, pulp and salivary glands to gingival and tooth injury in young adult male rats. III. Submaxillary glands. Oral Surg., Oral Med., Oral Path., 13: 870–874.
Steich, H. 1959 Changes in nucleoli related to alterations in cellular metabolism. In Society for the Study of Development and Growth XVI. Editor: Rudnick, pp. 105–122. Ronald Press, New York.
Wells, H., S. J Zackin, P Goldhaber and P L. Munson 1959 Increase in weight of the submandibular salivary glands of rats following periodic amputation of the erupted portion of the incisor teeth. Am. J Physiol., 196: 827–830.
Wells, H., and P L. Munson 1960 Experimental enlargement of the submandibular salivary glands of rats. Ibid., 199 63–66.
Wells, H. 1960 Inhibition by surgical procedures and drugs of the accelerated growth of salivary glands of rats. Ibid., 199 1037–1040.
——— 1962 Submandibular salivary gland weight increase by administration of isoproterenol to rats. Ibid., 202: 425–428.
Wells, H., C. Handelman and E. Milgram 1961 Regulation by the sympathetic nervous system of the accelerated growth of salivary glands of rats. Ibid., 201 707–710.

PLATE 1

EXPLANATION OF FIGURES

Figures 1, 2 and 3 are submaxillary gland sections stained with H. and E. × 460.

1 Control gland. Arrow points to granular tubule.

2 Hypertrophied gland. The acinar cells and their nuclei are enlarged. The nucleoli are prominent. The size of the granular tubules is unchanged.

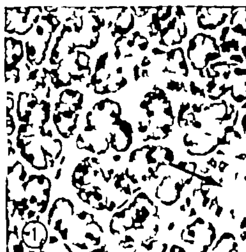
3 Atrophied gland. The cinar cells are reduced in size and have smaller nuclei. The arrow points to granular tubule which is reduced in size.

Figures 4, 5 and 6 are submaxillary gland sections stained with methyl green-pyronin. Only that material stained by pyronin and digestable by ribonuclease was interpreted as RNA. × 460.

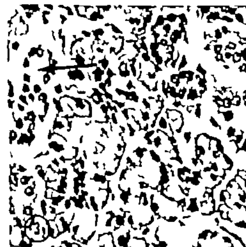
4 Control gland. RNA is present within the nucleu and in the perinuclear and basilar regions of the acinar cells. The remaining cytoplasm displays moderate amount of RNA.

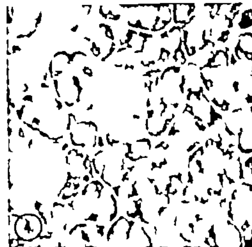
5 Hypertrophied gland. The enlarged nuclei of the acinar cells contain an increased amount of RNA. The nucleoli are also enlarged and rich in RNA. There is marked increase in perinuclear and basilar RNA.

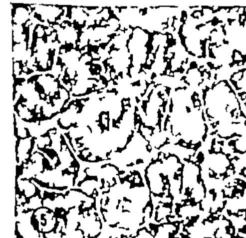
6 Atrophied gland. There is an overall decrease in cytoplasmic RNA. Arrow points to fragmented nucleus.


1


2


3


4


5


6

PLATE 2

EXPLAN TION O FIGURES

Figures 7 8 and 9 are parotid gland sections stained with methyl green-pyronin. × 460.

7 Control gland. RNA is present in the basilar regions of the acinar cells. The remaining acinar cytoplasm contains moderate amount of RNA.

8 Hypertrophied gland. The acinar cells are enlarged and show an increased amount of nucleolar and basilar RNA.

9 Atrophied gland. The acinar cells are smaller and contain little RNA. Arrow point t fragmented nuclei.

Figures 10, 11 and 12 are sublingual gland sections stained with methyl green-pyronin. × 290.

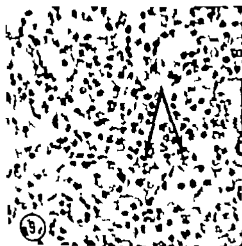
10 Control gland. The RNA is concentrated in the demilune cell (arrow) The cytoplasm of the mucous acinar cells contains moderate amount of RNA.

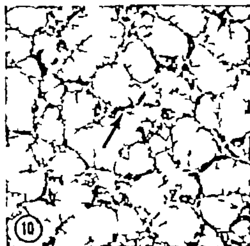
11 Hypertrophied gland. The acinar cells are enlarged. There is an over all increase in RNA which is especially prominent in the demilune cells (arrow)

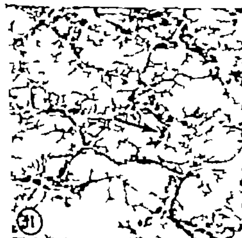
12 Atrophied gland. The acinar cells are smaller There is an overall reduction in the amount of RNA.


7


8


9


10



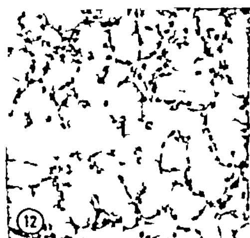

12

PLATE 3

EXPLANATION OF FIGURES

Figures 13 14 and 15 are submaxillary gland sections stained for succinic dehydrogenase. × 42.

13 There is intense enzymatic activity in the tubules and ducts, and moderate activity in the acinar cells.

14 Hypertrophied gland. The staining pattern is similar to that of the control gland. Hypertrophy of the acinar cells has reduced the number of tubules and ducts in the section.

15 Atrophied gland. At this magnification (× 42) the staining pattern is similar to th t of control and enlarged glands. Atrophy of the cinar cells has increased the number of tubules and ducts in the section.

Figures 16, 17 and 18 are submaxillary gland sections stained with the PAS technique × 460.

16 Control gland. The apical portion of the acinar cells is rich in PAS positive material. Th granular tubules contain weakly PAS positive granules (arrow)

17 Hypertrophied gland. The staining pattern is the same in the control gland except that the basilar portion of the cell is widened and unstained (arrow)

18 Atrophied gland. The amount and distribution of PAS positive material is unchanged.


13


14


15


16


17


18

PLATE 4

EXPLANATION OF FIGURES

Figures 19 and 20 are submaxillary gland sections incubated with ribonuclease and then stained with methyl green-pyronin. × 460.

19 Control gland. The acinar tissue is not stained with pyronin (compare with fig. 4) The granular tubules, however retain large numbers of ribonuclease-resistant, pyronin-positive granules.

20 Hypertrophied gland. Neither acinar cytoplasm nor nucleoli are stained with pyronin (compare with fig. 5) The tubules in the center of the figure are almost devoid of granules.

Figures 21 and 22 are sublingual gland sections stained for succinic dehydrogenase. × 460

21 Control gland. The ducts are stained intensely while the acinar cytoplasm shows only minimal staining.

22 Atrophied gland. Along with intense ductal staining, deeply staining granules are present in the basilar region of the acinar cells (arrow)

Figures 23 and 24 are sublingual gland sections stained with Sudan black B × 460.

23 Control gland. There is minimal staining of the acinar cytoplasm.

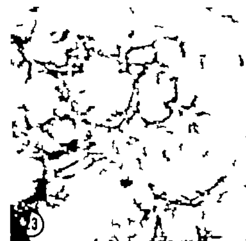
24 Atrophied gland. Large Sudanophilic granules are present in the basilar portion of the acinar cells.


19


20


21


22


23


24

Radioautographic Studies with Tritiated Thymidine of Cell Migration in the Mouse Adrenal after a Carbon Tetrachloride Stress[1]

ROBERT M. BRENNER
Department of Biology Brown University Providence Rhode Island

The extensive debate in the literature concerning the presence or absence of cell migration in the adrenal cortex has recently been reviewed by Bachmann ('54) Chester Jones ('57) and Skelton ('59) They have outlined the evolution of several conflicting concepts in this field. The oldest concept, orginally expressed by Gottschau (1883) is that the adrenal cortex of mammals is constantly being renewed by virtue of a steady centripetal flow of cells from the periphery of the gland towards the center with cell division restricted to the periphery of the gland and cell degeneration restricted to the central regions. This view was supported by the work of Hoerr ('31 '36) on the guinea pig adrenal. Hoerr found a large number of mitoses in the glomerulosa fasciculata regions and a large number of degenerating cells in the zona reticularis conditions that would naturally be present if migration were occurring

Associated with this migration concept was the idea that morphologically unspecialized cells in the connective tissue capsule of the gland may become progressively transformed into cells of the zona glomerulosa and enter into the migratory stream (Zwemer '36 Zwemer Wotton and Norkus, '38) This view was originally based upon the presence of apparently transitional cell types in the subcapsular regions of the gland; Salmon and Zwemer ('41) later claimed that studies with trypan blue had revealed a specific initial incorporation of label into capsule cells and that such cells were seen to migrate centripetally as predicted. Other workers (Calma and Foster '43; Baxter '46) were unable to repeat Salmon and Zwemer's work, however and claimed that trypan blue was not specifically incorporated into capsule cells but was found initially distributed among many of the parenchymal cells of the inner cortical zones. They therefore suggested that trypan blue was an inadequate tool for the study of cell migration in the adrenal.

A more recent concept supported by Greep and Deane ('49) and referred to as the zonal theory by Chester Jones ('48) is that there is no cell migration in the cortex of the mature animal, but that after the adult cortex is established, cells originate, function independently and may degenerate in each of the cortical zones. There is very strong evidence for the functional independence of each of the cortical zones (Giroud et al. '58 Greep and Deane '49) and the morphological evidence includes the fact that mitoses have been seen in quantity in all cortical zones including the zona reticularis in normal and in stressed rats (Baxter '46 Mitchell, '48) Degenerating cells have also been detected throughout the cortex, particularly in the zona fasciculata (Bennett, '40) Thus although most mitoses occur at the periphery of the gland and most degeneration occurs at the center considerable mitosis and some degeneration has been observed throughout the cortex, and this evidence is not compatible with a simple escalator theory

A third view has been presented by Tonutti ('42) namely that the cortex consists of inner and outer transformation fields the reticularis and glomerulosa respectively either of which can become progressively transformed into zona fasciculata under conditions of constant high demand for cortical hormones. Support

[1] This investigation was supported by research grant A-3784(C-3) from the National Institutes of Health, U. S. Public Health Service.

ing evidence for this view is that prolonged stimulation of the rat adrenal cortex with ACTH results in extension of the radial columns of the fasciculata up to the capsular border with the complete extinction of the zona glomerulosa (Chester Jones, '57).

A fourth and most inclusive concept was suggested by Chester Jones ('57) on the basis of the comparative morphology of the adrenal cortex. He suggested that the primary morphological unit of the cortex was a cord of cells which has the capacity to form loops coils and branching anastomoses that cell division normally goes on in only one portion of this cord, and that cells are pushed away from this region in both directions by pressure from dividing cells.

He further suggested that the arrangement of the cords in the mature adrenal resulted from the restrictions on growth provided by a confining connective tissue capsule and the capacity of the cords to loop and twist as they grew. Thus in many teleosts elasmobranchs, amphibians and reptiles, whose adrenals have extremely thin mesothelial capsules, the [illegible] are found in longitudinally running columns which may show extensive coiling, branching and anastamosing, without the formation of a zona glomerulosa or zona reticularis.

In birds and mammals, however the connective tissue capsule is quite thick and resistant, and the growing cortical cords form loops against this barrier and form a characteristic zona glomerulosa. The centrally located adrenal medulla is assumed to present a second rigid barrier to growth and the cortical cords are compressed and thus forced into torturously shaped columns which form the zona reticularis. This concept includes the idea of a centripetal migration of cells but Chester Jones stated ('57) that there was no unequivocal evidence for such migration.

In view of the variety of interpretations which have been placed upon the behavior of adrenocortical cells, it is important to continue efforts to analyse their movements. With the advent of tritiated thymidine (thymidine-H^3) which specifically labels DNA and produces high resolution radioautographs (Reichard and Estborn '51; Taylor Woods and Hughes '57) a powerful new tool for the study of the kinetics of cell populations has become available (Hughes et al. '58 Messier and Leblond, '60) and a few studies of adrenal cells labeled with thymidine-H^3 have now been reported.

Messier and Leblond ('60) studied cell proliferation with thymidine-H^3 in a variety of tissues in the mouse and rat and reported that the adrenal cortex had a slowly expanding cell population which showed none of the characteristics of active cell migration. Diderholm and Hellman ('60) administered thymidine-H^3 to immature, 21 day old rats and found a high rate of uptake of label in the zona glomerulosa and fasciculata indicating rapid cell renewal in these zones but they did not sacrifice animals at intervals in order to study the fate of the labeled cells. Walker and Rennels ('61) reported a study of mature female mice which had been injected during proestrus with a large dose of thymidine-H^3 (600 μc/mouse) and then been killed at intervals up to three weeks. They found a considerable incorporation of label into cells of the glomerulosa fasciculata region, but these labeled cells did not leave the periphery of the cortex in the time period studied. They suggested, therefore that the escalator theory be abandoned.

In preliminary radioautographic studies we had learned that a subcutaneous injection of CCl_4 in female BUA mice provoked a maximal incorporation of label into the zona glomerulosa and upper zona fasciculata if thymidine-H^3 was injected on the third or fourth days post-stress. The rate of uptake of label subsided to basal levels by the seventh day post-stress. The current investigation was designed to determine the fate of those adrenocortical cells which were labeled by thymidine-H^3 in such CCl_4-stressed females.

MATERIALS AND METHODS

Twenty-eight female BUA mice ranging from 72–84 days in age and 21–27 gms in weight were used in the following experiment. All mice were injected subcutaneously in the lower abdominal region with

a freshly prepared mixture of 0 1 ml of a 40% solution of CCl_4 in sesame oil at 9–11 AM on day zero. On day three all mice were placed in a safety glove box and were given two doses of thymidine-H^3 (specific activity 0.36 μc/mmole) at a dose rate of 0 75 μc/gm for each dose. The first dose was given between 11–11:30 AM and the second dose between 3–3:30 PM. Four animals were killed at 4–4:30 PM to serve as controls on the initial distribution of the label. Both adrenals, a piece of liver and a section of duodenum were fixed in Allen's fluid for 6–16 hours and then held for varying periods of time in 70% alcohol prior to paraffin imbedding. The rest of the mice were sacrificed and autopsied similarly in groups of three at each of the following times: 1 2, 3 4 6 10 16 and 24 weeks after the administration of thymidine-H^3 The labeled animals were kept in the safety glove box for at least two weeks prior to being transferred back to the colony room, in order to permit ample time for the excretion of radioactive wastes.

Paraffin imbedded tissues were sectioned at 3 μ and radioautographs were prepared with Eastman Kodak A.R.10 autoradiographic stripping film. Exposure times varied from two weeks to four months.

A special technique was used to prepare radioautographs of maximum density to permit study and photography of the distribution pattern of labeled cells at scanning magnifications. Well-exposed radioautographs were overdeveloped with a very strong developing solution and background grains were bleached by subtractive reduction (Mees, 42) with a mixture of potassium ferricyanide ($K_3Fe(CN)_6$) and sodium thiosulfate ($Na_2S_2O_3 \cdot 5H_2O$) (Lester and Carroll, '39)

The following modification of the Kodak D-8 developer formula was used

Distilled water	100	cm^3
Sodium Sulfite	9.0	gm
Hydroquinone	4.5	gm
Sodium Hydroxide	3.75	gm
Potassium Bromide	3.0	gm
Benzotriazole	0.024	gm

The above stock solution was kept refrigerated to prevent oxidation and was diluted to a 35% working solution prior to use Slides were developed five minutes at a temperature of 18 C with occasional agitation.

After the development period the slides were placed without rinsing into fresh Kodak Acid Fixer at 16–18 C for five minutes and then washed for 15 minutes in running water at a temperature of 16–18 C. Radioautographs prepared in this manner had a dense background as well as a dense deposit of silver over the radioactive nuclei. The background was bleached by inserting the slides, one at a time in a freshly prepared mixture of 20 ml of a 11.5% solution of $Na_2S_2O_3 \cdot 5H_2O$ and 0 5 ml of a 10% solution of $K_3Fe(CN)_6$. The bleaching action of the ferricyanide stops automatically in this mixture after 45–60 seconds at room temperatures. The slides can then be examined if the film is scraped off the back with a razor blade. If the bleaching action in inadequate the procedure can be repeated using the same or smaller amounts of $K_3Fe(CN)_6$. Caution must be exercised since excessive bleaching can completely remove the nuclear radioautograph

After bleaching, the slides were washed in running water for one-half hour stained in Harris Hematoxylin for three minutes differentiated in cold (12–15 C) dilute hydrochloric acid (pH 4) for five minutes blued in cold, dilute ammonium hydroxide (pH 9) for five minutes and rinsed in running water for one-half hour They were then dehydrated in cellosolve, cleared first in a one to one mixture of cellosolve and cedarwood oil for 15 minutes with constant gentle agitation and second in a one to one mixture of cedarwood oil and xylene for 15 minutes with similar agitation. Finally they were covered with Permount. This particular clearing procedure minimizes the tendency for the covered preparations to aspirate air

All the radioautographs were studied at various magnifications, and a series of photomicrographs was made to permit a qualitative analysis of the changes in the distribution of labeled cells with time No quantitative analyses were done although estimates of the relative numbers of labeled cells present in the different cortical zones at different times were made.

The photomicrographs were all made using a Wratten no. 45A blue-green filter

with Kodak Contrast Process Ortho film which was developed eight minutes in D-19 at 68°F

OBSERVATIONS

Initial distribution of the labeled cells

On day zero the heaviest concentration of labeled parenchymal cells occurred at the periphery of the cortex (fig. 1) Labeled nuclei were scattered in varying proportions between the zona glomerulosa and the upper portions of the zona fasciculata (figs. 3–4) Other labeled cells in the cortex were, for the most part, sinusoidal lining cells. Close observation of figure 1 will show that the great majority of silver deposits in the inner cortical zones were small, spindle-shaped masses of silver· the deposits over the parenchymal nuclei visible in figures 1 3 and 4 were more spherical. Many of the labeled parenchymal cells were obviously telophase pairs (figs. 3–4) indicating that mitosis had occurred after labeling.

There were some capsular fibroblasts which had been labeled, but these were very few in number and only an occasional cell in the adrenal medulla was labeled.

Between the cortex and the adrenal medulla lay the remnants of the X-zone (fig. 1) Scattered throughout the bulk of the degenerating X zone were numerous labeled fibroblasts and endothelial cells, all of which were clearly distinguishable as non-parenchymal elements. At the boundary between the degenerating X-zone and the lower zona fasciculata, there were no labeled parenchymal cells to be seen (figs. 1 3 and 4) This boundary region is the only viable remnant of the original X-zone and it consists of large numbers of small non-vacuolated cells with a high nucleo : cytoplasmic ratio In BUA females, the boundary region eventually becomes the zona reticularis although such a transformation does not become evident until the end of the first year of life (Brenner unpublished)

Changes in the distribution of the label with time

One week after administration of the label there was a striking increase in the number of labeled cells found in the periphery particularly in the upper portions of the fasciculata (fig 5) Obviously a considerable amount of mitotic activity had occurred during the first week, much of which was probably due to the influence of the CCl_4 stress. Most of this activity seemed confined to the upper fasciculata. Many telophase pairs were located in that region and their alignment clearly showed that the axis of mitosis had been centripetally oriented. There was no equivalent increase in the number of labeled cells in the glomerulosa. In most of the animals there was no dilution of label per nucleus in spite of the cell division during the first week. In one animal however there were a great many faint radioautographs (fig 14) In this case either the initial incorporation of label had been minimal or the rate of cell division had been inordinately high. Fortunately for this study such rapid dilution of the label was not the rule.

By the second week after labeling, heavily labeled cells could be found in the central regions of the cortex (fig 6) The glomerulosa did not yet reveal any significant changes in either the number or distribution of labeled cells, while the upper fasciculata was populated almost entirely by weakly labeled cells.

During the third and fourth weeks after labeling, heavily labeled cells were found at progressively deeper levels of the cortex. Large numbers of heavily labeled telophase pairs were located within the innermost portions of the zona fasciculata including the boundary of the degenerating X zone (figs. 7–10)

By the sixth week after labeling the boundary region was heavily populated by both heavily and weakly labeled cells, while the rest of the cortex, except the glomerulosa, contained only weakly labeled cells (figs. 2, 11 and 16) The continued cell division in the upper fasciculata and in cells which migrated out of that region finally resulted in a cortex in which almost no heavily labeled cells could be seen at 100 × magnifications on the tenth week of migration (fig. 12) Considerable dilution of label in the glomerulosa had also occurred by that time (fig. 15) indicating that cell division had been going on in this

region throughout this study By 16 and 24 weeks after labeling dilution had increased considerably in all cortical zones, but there had been no change in the distribution of labeled cells. The ultimate fate of labeled cells in the boundary region was difficult to determine because of dilution, but small numbers of labeled degenerating cells were present in this region.

An incidental observation was the finding of a large number of labeled fibroblasts and endothelial cells in the connective tissue which was slowly penetrating the boundary region in the process of encapsulating the shrinking X zone from the rest of the cortex. The origin of these labeled connective tissue cells was not immediately apparent, but they may have been either descendants of labeled cortical sinusoidal cells, or fibroblasts which had been labeled outside the adrenal and then migrated into the cortex during the process of repair

DISCUSSION

The observations presented here provide direct evidence for the centripetal migration of adrenocortical cells in the intact gland subsequent to an acute stress. The evidence supports the hypothesis of Chester Jones ('57) that the upper portion of the zona fasciculata is a mitotically active region from which cells may migrate centripetally Considerable numbers of glomerulosa cells had become labeled subsequent to stress but these cells did not appear to leave the glomerulosa at anywhere near the rate at which cells left the upper fasciculata, if indeed they left the glomerulosa at all. The exact contribution which the glomerulosa may have made to the migratory movement was impossible to determine in this experiment.

The evidence also shows that those cells which did migrate towards the inner cortical zones did not become mitotically quiescent but, on the contrary entered into several cell divisions with subsequent dilution of their radioactivity as judged by the increasing faintness of the radioautographs produced by such cells with time. The central region of the gland in this strain was occupied with a large slowly collapsing X zone (figs. 1–2) and the slow shrinkage of this zone was undoubtedly one of the factors which permitted centripetal migration to occur

The failure of Walker and Rennels ('61) to detect centripetal migration in female A/Jax mice is difficult to explain. Aside from possible strain differences, two factors may be mentioned. The first is that Walker and Rennels used a dose rate of 600 µc/mouse, and this dose may have adversely affected cell division and cell migration. The dose rate used in the present study was 37.5 µc/mouse (1.5 µc/gm) which is similar to the dose rate of 20–30 µc/mouse (1 µc/gm) used by Messier and Leblond ('60) and Hughes et al. ('58) in their analyses of cell migration in intestine and skin. Thymidine-H^3 has been shown to produce chromosome damage and growth inhibition in onion seedlings (Mc Quade and Friedkin, '60) and HeLa tissue culture cells (Painter Drew and Hughes '58) and it remains to be determined whether any inhibition of growth was present in the experiment reported by Walker and Rennels.

The second possibility is that the migration detected in the present experiment was provoked solely by the stress of CCl_4 administration and may not be a natural component of the growth pattern of the adrenal of either the BUA or the A/Jax mouse. Preliminary work cited previously showed, however that the rate of thymidine-H^3 incorporation into the adrenal reached a maximum on the third and fourth days after the injection of CCl_4 and then subsided to pre-stress levels by the seventh day indicating that mitotic rate in the cortex had returned to basal levels by that time. The severe damage to the liver which is produced by CCl_4 is completely repaired within five to six days (Myren, '56) and this also supports the concept that the mice had returned to approximately normal physiological balance by the end of the first week after the stress. The mitoses which subsequently occurred in the adrenal may have been dependent on the original stress but a conclusive answer to such a contention requires continued study of the migration phenomenon in a quantitative way under a variety of conditions.

The current investigation is probably best interpreted as providing an illustra

tion of the potential of the mouse adrenal cortex to expand its population by means of centripetal migration of mitotically active cells subsequent to the acute stress of CCl_4 administration. Whether centripetal migration can be detected in unstressed, thymidine-H^3 labeled BUA mice can only be determined by further work. Such studies are currently under way in our laboratory

SUMMARY

Virgin female BUA mice were stressed with a subcutaneous injection of CCl_4 and three days later were given intraperitoneal injections of thymidine-H^3 in order to incorporate label into a large number of DNA-synthesizing cells. Animals were sacrificed immediately after labeling and at intervals of 1 2, 3 4 6 10 18 and 24 weeks. Stripping film radioautographs were prepared of both adrenals from each animal and the changes in the distribution of the labeled cells with time were studied and photographed.

Labeled cells were initially distributed at the periphery of the cortex scattered between the glomerulosa and the upper fasciculata, but within four to six weeks heavily labeled cells were found deep within the cortex indicating that centripetal migration had occurred. The upper fasciculata was judged to be a region of maximum cell turnover from which cells had migrated centripetally but migration of cells from the glomerulosa seemed to be minimal.

ACKNOWLEDGMENT

The author wishes to express his thanks to Mrs. Theresa Bienieki for her excellent technical assistance during the course of this investigation.

LITERATURE CITED

Bachmann, R. 1954 Die Nebenniere. Handbuch der mikr Anat. des Menschen. Springer Verlag, Berlin., 6: 1–952.

Bennett, H. S. 1940 The life history and secretion of the cells of the adrenal cortex of the cat. Amer. J Anat., 67 151 227

Baxter, J S. 1946 The growth cycle of the cells of the adrenal cortex in the adult rat. J Anat., London, 80 139–146.

Calma, L., and C. L. Foster 1943 Trypan blue and cell migration in adrenal cortex of rats. N ture 152, 536.

Chester Jones, I. 1948 Variation in the mouse adrenal cortex with special reference to the zona reticularis and to brown degeneration, together with a discussion of the cell migration theory Quart. J Micr. Sci., 89 53–74.

——— 1957 The Adrenal Cortex. Cambridge University Press, Chap. 8.

Diderholm, H., and B. Hellman 1960 The cell renewal in the rat adrenals studied with tritiated thymidine. Acta Path. Microbiol. Scand., 49 82–88.

Giroud, C. J P M. Saffran, A. V Schally J Stachenko and E. H. Venning 1956 Production of aldosterone by rat adrenal glands in vitro. Proc. Soc. Exp. Biol. and Med., 92: 855–859

Gottschau M. 1883 Struktur und embryonale Entwickelung der Nebennieren bei Saugethieren. His. u. Braune Archiv für Anat. und Entwick., 9: 412–458.

Greep, R. O., and H. W Deane 1949 The cytology and cytochemistry of the adrenal cortex. Ann. N Y Acad. Sci., 50: 596–615.

Hoerr, N L. 1931 The cells of the suprarenal cortex in the guinea pig. Their reaction to injury and their replacement. Am. J Anat., 48: 139–197

——— 1936 Histological studies on lipins. II. A cytological analysis of the liposomes in the adrenal cortex of the guinea pig. Anat. Rec., 66 317–342.

Hughes, W L., V P Bond, G. Brecher E. P Cronkite, R. B Painter H. Quastler and F G. Sherman 1958 Cellular proliferation in the mouse as revealed by autoradiography with tritiated thymidine. Proc. Nat. Acad. Sci., 44 476–483.

Lester H. M., and J S. Carroll 1959 Photo-Lab-Index. Morgan and Morgan, Inc., New York. Chap. 21, p. 21

Mees, C. E. K. 1942 The Theory of the Photographic Process. The Macmillan Co., New York. Chap 14

Messier B and C. P Leblond 1960 Cell proliferation and migration as revealed by radioautography after injection of thymidine-H^3 into male rats and mice. Amer. J Anat., 106: 247–285.

Mitchell, R. M. 1948 Histological changes and *mitotic activity in rat adrenal during* post natal development. Anat. Rec., *101* 161–185.

Myren, J 1956 Injury of liver tissue in mice after single injection of carbon tetrachloride. Acta Path. Microbiol. Scand. Supp., *116:* 5–64.

McQuade, H. A., and M. Friedkin 1960 Radiation effects of thymidine-H^3 and thymidine-C^{14} Ex. Cell Res., *21* 118–125.

Painter R. B R. M. Drew and W L. Hughes 1958 Inhibition of HeLa growth by intranuclear tritium. Science, *127* 1244–1245.

Reichard, P and B Estborn 1951 Utilization of desoxyribosides in the synthesis of polynucleotides. J Biol. Chem., *188* 839–846.

Salmon, T N., and R. L. Zwemer 1941 Life history of cortico-adrenal cells of the rat by means of trypan blue injections. Anat. Rec., 80 421–429

Skelton, F R. 1959 Adrenal regeneration and adrenal-regeneration hypertension. Physiol. Rev 39 162–182.

Taylor J H., P S. Woods and W L. Hughes 1957 The organization and duplication of chromosomes as revealed by autoradiographic studies using tritium-labeled thymidine. Proc. Nat. Acad. Sci., 43 122–128.

Tonutti, E. 1942 Die Umbauvorgänge in den Transformationsfeldern der Nebennierenrinde als Grundlage der Beurteilung der Nebennierenrindenarbeit. Z. Mikr.-anat. Forsch., 52: 32–86.

Walker B. E., and E. G. Rennels 1961 Adrenal cortical cell replacement in the mouse. Endocrinology 68 365–374.

Zwemer R. L. 1936 A study of adrenal cortex morphology Am. J Path., 12: 107–114

Zwemer, R. L., R. M. Wotton and M. G. Norkus 1938 A study of cortico-adrenal cells. Anat. Rec., 72 249–263.

All figures in this and the succeeding plates are stripping film radioautographs which were developed and bleached as described in the text (except figs. 11–12) and stained with Harris' Hematoxylin.

Abbreviations (Plates 1–4)

B boundary region between fasciculata and degenerating X-zone
C, capsule of the adrenal gland
F zona fasciculata
M, adrenal medulla
X, degenerating portion of X-zone

PLATE 1

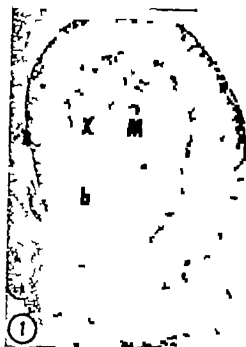
EXPLANATION OF FIGURES

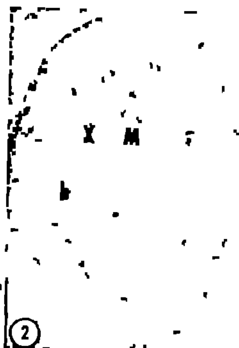
1 Initial distribution of label on day 0 The great majority of labeled cells are at the periphery of the gland in the zona glomerulosa and the upper portion of the zon fasciculata. Most labeled cells in the inner cortical zones are not parenchymal cells but sinusoidal lining cells. The boundary region is free of label. The degenerating portion of the X-zone contains large number of labeled fibroblasts. The adrenal medulla has only few labeled cells. The adrenal capsule has only a rare labeled cell. × 35.

2 Six weeks after labeling The inner cortical zones including the boundary region now contain a large number of labeled parenchymal cells. A considerable number of heavily labeled cells are still present in the zona glomerulosa indicating slow turnover in this region. N other significant changes are to be seen. × 35.

3 Initial distribution of label on day 0 This figure shows predominance of label in the upper fasciculata. The arrow points out a telophase pair which is centripetally oriented. × 100.

4 Initial distribution of label on day 0 This figure shows predominance of label in the glomerulosa. The arrow denotes another centripetally oriented telophase pair Note bsence of label in boundary region in both figures 3 and 4. × 100.


X
M
b
1


X
M
b
2


3
b


4
b
X

PLATE 2

EXPLANATION OF FIGURES

5 Distribution of label after one week. There has been a considerable increase in the number of labeled cells in the upper fasciculata. Many telophase pairs are grouped in clusters indicating centers of mitotic activity. The axis of mitosis is centripetal. × 100.

6 Distribution of label after two weeks. Labeled cells are now present in the central regions of the fasciculata. Heavily labeled cells still remain in the glomerulosa while broad band of very weakly labeled cells is present in the upper fasciculata. × 100.

7 Distribution of label after three weeks. Most of the heavily labeled cells are now found spread throughout the inner cortical zones. Heavily labeled cells are still present in the glomerulosa. The upper fasciculata is populated by weakly labeled cells. × 100.

8 Distribution of label after four weeks. N great change from distribution t three weeks is noticeable. The arrows point out telophase pairs located deep within the cortex indicating that mitotic activity is present in these inner regions. × 100.

5

6

7

8

PLATE 3

EXPLANATION OF FIGURES

9 Distribution of label t four weeks Adrenal from different animal than in figure 8 Label is similarly distributed but here one can see that heavily labeled cells have reached the boundary region. Arrow denotes mitosis at periphery of boundary region. × 150.

10 Distribution of label at four weeks Adrenal from a different animal than in figures 8–9. Here the distribution of label is slightly different, with considerable number of heavily labeled cells still in the upper portions of the fasciculata, but a large number of labeled cells also t the periphery of the boundary region. Arrow denotes cluster of telophase pairs at boundary region. × 150.

11 Distribution of label at six weeks The three large arrows indicate the approximate limits of the boundary region within which can be seen large number of both heavily and weakly labeled cells. Most of the cells in all other regions of the cortex are weakly labeled although few heavily labeled cells are still present at the periphery This preparation was not bleached and the excessive background is noticeable. × 100.

12 Distribution of label t ten weeks The boundary region now contains only a few heavily labeled cells Most of the labeled cells in the cortex are very weakly labeled at this time. × 100.

9

10

11

12

PLATE 4

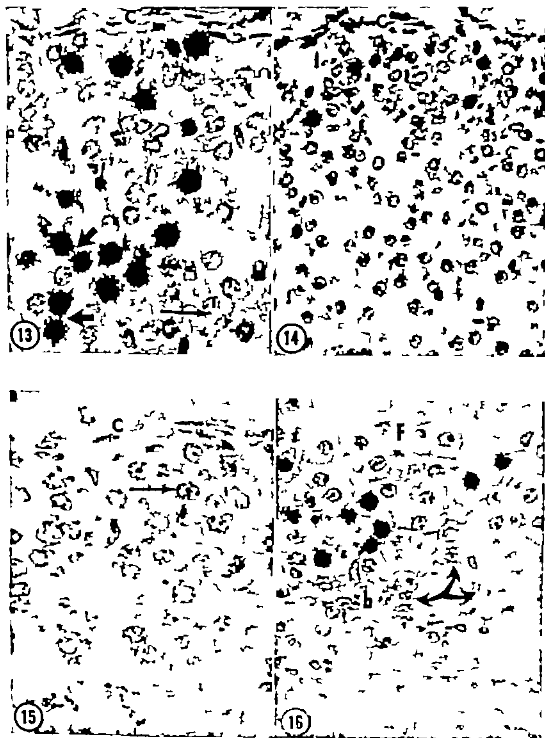
EXPLANATION OF FIGURES

13 A high magnification of the periphery of the cortex one week after the administration of label The heavy arrows denote pairs of heavily labeled cells. The thin arrow denotes cluster of weakly labeled cells in the fasciculata. These may be the descendants of cells which were initially very weakly labeled. × 430.

14 Periphery of the drenal from different animal than in figure 13 one week after labeling Practically all of the cells i the upper fasciculata are weakly labeled. This may indicate either that the original uptake of label was minimal in this adrenal, or th t the rate of cell division in the fasciculata was extremely high. × 200.

15 A high magnification of the periphery of the cortex ten weeks after labeling The arrow denotes a weakly labeled cell in the zona glomerulosa. × 430

16 The inner cortical regions six weeks after labeling The three curved arrows point to three weakly labeled cells in the boundary region. This zone is clearly seen here to consi t of small non-vacuolated cells located between the degenerating X-zone and the fasciculata. Heavily labeled cells are visible in the lower reaches of the fasciculata. × 430.


C
13
14
15
16
F
b

New Observations on the Structure of the Pacinian Corpuscle and its Relation to the Perineural Epithelium of Peripheral Nerves[1]

T. R. SHANTHAVEERAPPA AND G. H. BOURNE
Department of Anatomy, Emory University, Atlanta, Georgia

The Pacinian corpuscle was noted for the first time in the fingers of man in 1741 by Vater and the histological structure was described first by Pacini (1835, 1840) and later by Henle and Kolliker (1844), Herbst (1848), Krause (1881), Schumacher ('11), Glees et al. ('49), Quilliam and Sato ('55) and Cauna and Mannan ('58).

Electron microscopic studies were made by Pease and Quilliam ('57). They described the complex arrangement of the Pacinian corpuscle at ultramicroscopic levels.

The characteristic feature of all types of Pacinian corpuscle is their lamellated structure giving the appearance of cabbage leaves or onion peel. It has been said that the lamellar cells of the outer zone which give the onion peel appearance are made up of modified fibroblasts (Quilliam, '58; Cauna and Mannan, '58) and the innermost core of cells surrounding the nerve terminal is said to resemble both the Schwann cell and fibroblast, and thus are classified under neurofibroblasts (Quilliam, '58).

Our studies, however, have given a new significance to the morphology of this end-organ.

MATERIAL AND METHODS

A piece of the mesentery of the small intestine containing a Pacinian corpuscle was removed from adult cats and treated with the appropriate fixatives and reagents. The Pacinian corpuscle along with the nerve fiber was dissected out under a stereo-binocular dissection microscope, and after removal from the mesentery was separated from its connective tissue components and the lamellar sheath carefully isolated. Standard hematoxylin and eosin methods were applied on corpuscles and nerve fibers which had been formalin fixed. Sex chromatin studies were made by staining with 0.5% aqueous cresyl violet. The cellular borders were stained by dropping fresh tissue into 1% silver nitrate solution and keeping it in the dark for 24 hours; the Pacinian corpuscle was then isolated and dissection of the lamellar sheath was performed as usual and mounted in glycerine and exposed to sunlight. Some tissues, after exposure to sunlight, were dehydrated and cleared in xylol and mounted in DPX mounting medium.

RESULTS

With hematoxylin and eosin staining the mounts of whole Pacinian corpuscle looked like nucleated cellular bags; no cellular borders were demarcated and the usual onion peel appearance was seen in cross and longitudinal sections (figs. 1, 2a and b).

The tissues treated in silver nitrate, after removing the pericorpuscular connective tissue (fig. 3) revealed that the lamellar sheath, hitherto described as layers of fibroblasts, was not in fact composed of fibroblasts, but of flat, stratified squamous epithelium. A whole mount, after removing the pericorpuscular connective tissue, reveals the Pacinian corpuscle as a bag composed of stratified squamous epithelium (figs. 3, 4, 7, 8 and 9). The lamellae can be peeled off layer by layer until the inner core of the nerve terminal is revealed. Each lamella is a continuous sheet of squamous epithelium with serrated borders (figs. 10 and 11). When the superficial layers of squamous epithelium are peeled back they are found to be continuous with the outermost layers of

[1] Supported by grant B-1914 of the National Institute of Neurological Diseases and Blindness and by funds from Anatomy Training Grant 2G-305 of the National Institutes of Health, Division of General Medical Sciences.

the "perineural epithelium surrounding the nerve fiber (figs. 2a, 3 6 12 and 13) which innervated the corpuscle (see Shanthaveerappa and Bourne, '62a, b) The deeper layers of the lamellae were not continuous with those of the nerve fiber but were almost certainly derived from the more superficial layers of epithelium of the corpuscle (figs. 3 4)

The nerve fiber which supplies the Pacinian corpuscle, when cleared of its perineural connective tissue, clearly demonstrates perineural epithelium surrounding the nerve fiber completely (figs. 15 16).

There is a little connective tissue element between the squamous epithelial lamellae of the corpuscle. Our serial isolation of different components of the Pacinian corpuscle and nerve fiber which supplies it, showed that the endoneurium which surrounds the myelin sheath enters the Pacinian corpuscle along with the nerve fiber following it up to the termination of the myelin sheath (fig. 2a, b c and 5)

It has also been a constant histological as well as electron microscopical finding (Pease and Quilliam '57) that in between the lamellae of the Pacinian corpuscle connective tissue elements are also found the lamellae being formed by thin flat cells with flat nuclei. Our electron microscope studies (Shanthaveerappa et al. in preparation) on sciatic nerve of rat have indicated that there are collagen bundles in between the layers of squamous epithelium and that the cells of the perineural epithelium are extremely flat, with flat nuclei. We have observed up to six layers of this perineural epithelium surrounding sciatic nerve fasciculi. This seems to further support the evidence that the lamellae of the corpuscle are extensions of the perineural epithelium.

In female cats cresyl violet staining of the corpuscle showed the presence of sex chromatin in the nuclei of the epithelial cells (fig. 14) These nuclei were identical in appearance with those of the cells composing the perineural epithelium (figs. 12 and 14)

DISCUSSION

The presence of an epithelial-like structure around the nerve trunk has been recorded previously by Key and Retzius (1876) Lehmann ('53 '57) Krenjevic ('54) and Rohlich and Weiss ('55)

The present authors (Shanthaveerappa and Bourne, '62a, b c) have shown this epithelium to be a constant feature of all nerve fasciculi and that it is a stratified squamous structure which is five layers thick in the sciatic nerve of rat, cat and guinea pig and two layers thick in frog. The number of layers becomes less and less as the nerve fasciculus goes on dividing. This epithelium was described by Shanthaveerappa and Bourne ('62b) as a perineural epithelium. They also suggested that this perineural epithelium is a continuation of the pia-arachnoid membrane of the central nervous system. In motor nerves it appears that this epithelium follows the nerve, dividing up and surrounding the fasciculi as they become smaller and smaller until finally it surrounds the terminal fiber as an epithelial sheet (bell mouth of Henle) The epithelium finally fuses with the muscle fiber membrane around the motor end-plate so that the motor nerve is completely enclosed in a sheet of epithelium from its origin in the central nervous system to its termination. The present study demonstrates that the same holds true for sensory nerves and that the extension of the perineural epithelium contributes to a major degree to the structure of the end organs in this case the Pacinian corpuscle. The superficial lamellae of the corpuscle represent the direct continuous layers of the pia-arachnoid membrane, and the deeper layers are presumably formed by a continuous multiplication of the superficial layers, which have their own type of embryological development, peculiar to this type of end organ. The size and shape and borders of these squamous epithelial cells their nuclear content and sex chromatin distribution and staining character are identical with those of the pia-arachnoid membrane and the perineural epithelium indicating that they are continuous sheets of cells starting from the pia arachnoid and terminating in the end organs

It is of interest that Cauna and Mannan ('59) have observed that when the vascular relationship between the corpuscle and arteriovenous anastomosis is disturbed, a new receptor is formed on the same axon

TABLE 1

Nerve fasciculus	Nerve fiber entering pacinian corpuscle	Pacinian corpuscle
1 Perineurium (connective tissue surrounding the fasciculi) (See text fig. 1 a,b,c,d Shanthaveerappa and Bourne '62b.)	Perineural connective tissue surrounding the single nerve fiber (text fig. pl. 1 figs. 1, 2a,c)	Pericorpuscular connective tissue surrounding the end-organ (text fig. pl. 1, figs. 1, 2a,b)
2. Perineural epithelium, squamous epithelial sheets of cells surrounding multiple nerve fibers with blood vessels and connective tissue in between the epithelial sheets.	Perineural epithelium surrounding the single nerve fiber with blood vessels and connective tissue in between these squamous epithelial sheets (text fig. pl. 1, figs. 2a,c; pl. 2, fig. 3).	Squamous epithelial cell lamellae surrounding nerve terminal with blood vessels and connective tissue in between the lamellae (text fig. pl. 1 figs. 2a,b; pl. 2, figs. 3,4)
3. Endoneurium in between nerve fibers, surrounding each nerve fiber	Endoneurium surrounding the single nerve fiber (text fig. pl. 1 figs. 2a,c)	Endoneurium entering the corpuscle along with the nerve fiber (text fig. pl. 1 fig. 2a; pl. 2, figs. 4,5)
4 Myelin sheath along with the neurilemmal sheath surrounding the individual fiber.	Same as nerve fasciculus.	Myelin sheath along with the neurilemma ending in proximal part of corpuscle.
5. Axon of each nerve fiber	Axon entering the corpuscle.	Axon situated in center of corpuscle, distal part being devoid of the myelin sheath (text fig. pl. 2, fig. 5)

The summary given above shows how the structural arrangements of the nerve fasciculus, the nerve fiber entering the Pacinian corpuscle and the Pacinian corpuscle itself are similar and show definite relationship with each other.

the existing corpuscle undergoing involution indicating the potentiality of the perineural epithelium to multiply and form a new corpuscle on the same axon.

A summary of the characteristics of the Pacinian corpuscle and nerves is shown in table 1

SUMMARY AND CONCLUSIONS

These studies of Pacinian corpuscles have revealed that the lamellar sheets of these structures are made up of flat squamous epithelial cells. The superficial layers are the extension of the perineural epithelium, which is in turn the continuation of the pia-arachnoid membrane of the central nervous system. The deeper layers of lamellae probably arise from multiplication of the superficial lamellae of squamous cells. In view of the origin of the pia-arachnoid membrane and its continuation as perineural epithelium on peripheral nerves (Harvey and Burr '26; Harvey et al. '33; Shanthaveerappa and Bourne '62a,b,c) we consider that the squamous epithelium is ectodermal in origin.

The structural arrangement and the relationship between the Pacinian corpuscle the nerve fibers supplying the corpuscles, and the nerve fasciculus has been shown. It appears that the Pacinian corpuscle is nothing more than a localized enlargement at the end of the nerve fiber of the perineural epithelium.

Sex chromatin has been demonstrated in these squamous cell lamellae of the Pacinian corpuscle in the female cat.

It is probable also that the capsule which surrounds the heat receptor organs of Ruffini, cold end-bulbs of Krause Meissner s corpuscle and the muscle spindle and the lamellae of Herbst corpuscle is also made up of squamous epithelial cells representing an extension of the perineural epithelium.

LITERATURE CITED

Cauna, N., and G. Mannan 1958 The structure of human digital Pacinian corpuscles and its functional significance. J Anat., (Lond.) 92 1–14

——— 1959 Development and postnatal changes of digital Pacinian corpuscles (corpuscula

lamellosa) in the human hand. Ibid., (Lond.) 93 271–280.
Glees, P. A., A. Mohiuddin and A. G. Smith 1949 Transplantation of Pacinian corpuscle in the brain and thigh of the cat. An experimental study Acta Anat., 7 213–224
Harvey S. C., and S. H. Burr 1926 The development of meninges. Arch. Neurol. Psychiat., Chicago, 15 545–567
Harvey S. C., S. H. Burr and E. Van Campenhout 1933 Development of meninges. Ibid., 29 683–690.
Henle, F., and A. Kölliker 1844 Ueber die Pacinischen Körperchen an den Nerven des Menschen und der Säugethiere. Zurich 40 pp. (English review in the British and Foreign Medical Review 1845 19 78–83)
Herbst, G. 1848 Die Pacinischen Korper und ihre Bedeutung, Vol. IV 143 pp. Vandenhoeck and Ruprecht, Göttingen.
Key A. 1876 Studies in der anatomie des nervensystems und des Bindegewebes. Vol. 2, pp. 103–112, Samson and Wallin, Stockholm.
Krause, W 1881 Die Nervenendigung innerhalt der terminalen Körperchen. Arch. mikr Anat., 19 53–136.
Kranjevic, K. 1954 The connective tissue of the frog sciatic nerve. Quart. J Exper Physiol., 39 55–72.
Lehmann, H. J 1953 The epineurium as a diffusion barrier. Nature, 172 1045–1046.
——— 1957 Uber struktur und funktion der perineuralen diffusions barriere. Z. Zellforsch. Mikr Anat., 46 232–241
Pacini, F 1835 Sopra un particolar genere di piccoli corpi globulosi scoperti nel corpo umano da Filippo Pacini alunno interno degli Spedali riunti di Pistoia. (Letter to Accademia Medico-fisica di Firenze)
——— 1840 Nuovi organi scoperti nel corpo umano. 60 pp. Tipografia Cino, Pistoja.
Pease, D C., and T A. Quilliam 1957 Electron microscopy of the Pacinian corpuscle. J Biophys. Biochem. Cytol., 3 331–342.
Quilliam, T A. 1958 New problems in the functional activity of the Pacinian corpuscle. Ibid., 4 341–342.
Quilliam, T A., and M. Sato 1955 The distribution of myelin on nerve fibers from Pacinian corpuscles. J Physiol., 129 167–176.
Rohlich, P and U M. Weiss 1955 Studies on the histology and permeability of peripheral nervous barrier Acta Morphol. Budapest, 5 335–347
Schumacher S. v 1911 Beiträge zur Kenntnis des Baues und der Funktion der Lamellenkörperchen. Arch. mikr Anat., 77 157–193.
Shanthaveerappa, T R., and G. H. Bourne 1962a A perineural epithelium. J Cell. Biol., 14: 343–346.
——— 1962b The perineural epithelium metabolically active, continuous, protoplasmic cell barrier surrounding peripheral nerve fasciculi. J Anat. (Lond.) 96 527–537
——— 1962c Demonstration of perineural epithelium in whale and shark. N ture (in press)
Vater Abraham 1741 Dissertatio de consensu partium corporis humani. Haller Disputationum Anatomicarum selectarum. Vol. II, pp. 953–972, Göttingen.

PLATE 1

EXPLANATION O FIGURES

Artist' conception of the relationship of the various components of the Pacinian corpuscle and the nerve fiber which supplies it diagrammatically viewed following serial isolation of various components and longitudinal and cross sections.

1 Shows intact Pacinian corpuscle with the attached nerve fiber. Note that the whole corpuscle and the nerve fiber is surrounded by perineural and pericorpuscular connective tissue.

2a Longitudinal section of the whole Pacinian corpuscle and its nerve fiber showing arious structural components of the Pacinian cor puscle and nerve fiber Note the perineural epithelium and its ex tension on the corpuscle as squamous lamellae giving an onion peel ppearance.

2b Transverse section of the Pacinian corpuscle t its middle part, show ing various structural components. Note the absence of the myelin sheath in the nerve fiber and the multiple fl t squamous cell lamellae (epithelial cell sheets) giving an onion peel appearance

2c Transverse section of the nerve fiber which supplies the Pacinian corpuscle. Compare with 2a and 2b. Except for the smaller number of perineural epithelial cell lamellae (epithelial sheets) and the presence of the myelin sheath, all the structural components are identical with those of the corpuscle.

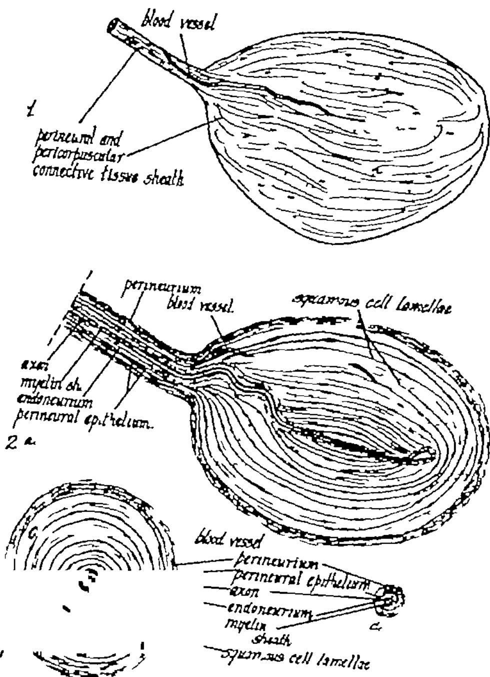

blood vessel
1
perineural and
pericorpuscular
connective tissue sheath
perineurium
blood vessel
squamous cell lamellae
axon
myelin sh.
endoneurium
perineural epithelium
2 a.
c
blood vessel
perineurium
perineural epithelium
axon
endoneurium
myelin
sheath
d
squamous cell lamellae

PLATE 2

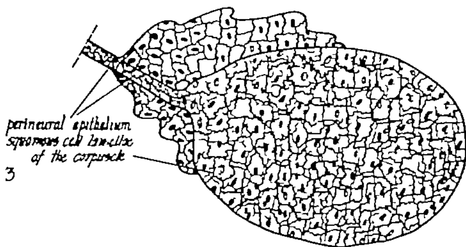
EXPLANATION OF FIGURES

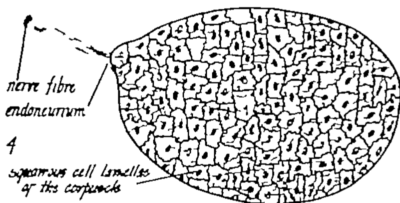
Artist's conception of the relationship of the various components of the Pacinian corpuscle and the nerve fiber which supplies it diagrammatically viewed following a serial isolation of various components and longitudinal and cross sections.

3 Whole Pacinian corpuscle removed from its connective tissue covering, showing that the entire corpuscle is made up of squamous epithelial cell lamellae and that the more superficial of these lamellae represent continuation of the perineural epithelium. The outermost lamella is shown reflected back from the corpuscle.

4 Whole Pacinian corpuscle removed from its connective tissue sheath and its superficial squamous epithelial cell sheet. The perineural pithelium which is continuous with this sheet is also removed from the associated nerve fiber exposing the endoneurium. The deeper squamous cell lamellae of the corpuscle are also shown. Note that the deeper layers of squamous cell lamellae are not continuous with the perineural epithelium, they are separate sheets covering the endorgans giving complexity to the structure of the corpuscle.

5 Semi-diagrammatic presentation of the Pacinian corpuscle and its nerve fiber from which the surface connective tissue covering, the perineural epithelium, and the squamous cell lamellae of the cor puscle have been completely removed, leaving the nerve fiber with its axon, myelin sheath and endoneural coverings. The relationships of the various constituents with each other up to the termination of the nerve fiber are demonstrated in this figure.


perineural epithelium
squamous cell lamellae
of the corpuscle
3


nerve fibre
endoneurium
4
squamous cell lamellae
of the corpuscle

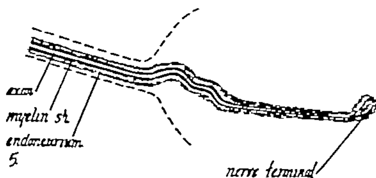

axon
myelin sh.
endoneurium
5
nerve terminal

PLATE 3

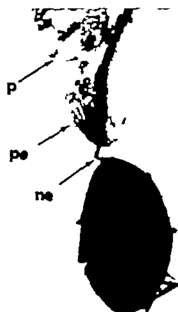
EXPLANATION OF FIGURES

6 Pacinian corpuscle from mesentery of cat, isolated under binocular dissecting microscope and fixed in formalin. Pericorpuscular connective tissue and perineurium (arrow p) cleared from corpuscle, and superficial squamous cell lamellae (arrow pe) of corpuscle reflected back on to nerve fiber (arrow ne) indicating that it extends over the nerve fiber. Thus the superficial lamellae of the corpuscle represent the continuation of the perineural epithelium. × 12.

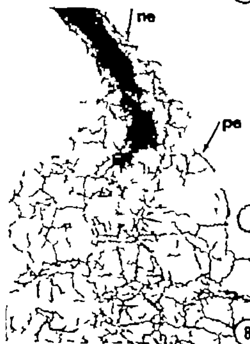
7 Whole mount of Pacinian corpuscle removed from its connective tissue covering. Treated in 1% aqueous silver nitrate to demonstrate cellular borders then dehydrated, cleared and mounted in DPX. Note that the Pacinian corpuscle is composed of squamous epithelial cells. × 136.

8 Region of attachment of nerve fiber to corpuscle at higher magnification. Method same as figure 7. Note innumerable sheets of squamous epithelial cell lamellae (arrow pe) lying beneath each other and extension of superficial lamellae over the nerve fiber (arrow ne) × 340.

9 Portion of corpuscle treated with 1% aqueous silver nitrate to demonstrate cell boundaries and counter-stained with cresyl violet to demonstrate the nuclei (arrows) × 340


p
pe
ne
6


7


ne
pe
8


9

PLATE 4

EXPLANATION OF FIGURES

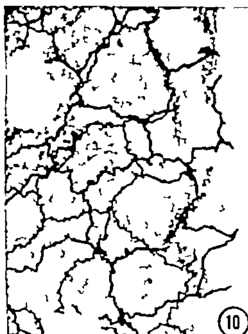
10 Superficial lamellae of corpuscle isolated and treated to demonstrate cell borders, and mounted flat on glass slide. Note squamous nature of the cells with well-defined serrated borders. × 340.

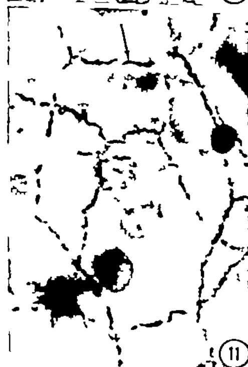
11 Higher magnification of portion of isolated lamellae. Method same as figure 9 Note the layers of squamous cells and their well defined serrated borders (arrow) and nuclei. × 1360.

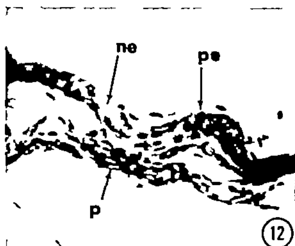
12 Whole mount of the nerve fiber which supplies the Pacinian corpuscle, enveloping connective tissue (perineurium) removed; treated with cresyl violet. Perineural connective tissue (arrow p) shown lying by the side of the nerve fiber The perineural epithelial nuclei (arrow pe) stained with cresyl violet, can be seen surrounding the nerve fiber (arrow ne) × 340

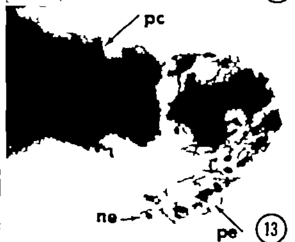
13 Whole mount of Pacinian corpuscle with portion of the nerve fiber which supplies it. Method same as figure 9 Superficial connective tissue removed. Note that the nerve fiber (arrow ne) which enters the corpuscle is covered by squamous epithelium (perineural epithelium, arrow pe) continuous with the squamous epithelial lamellae of the corpuscle (pc) × 340

14 Squamous cell lamella from the Pacinian corpuscle of adult female cat, isolated under dissection microscope, stained by 0.5% aqueous cresyl violet. Note the sex chromatin in nucleus (arrows) situ ted at one edge of the nuclear membrane, planoconvex in shape. × 1360


10


11


ne
pe
p
12


pc
ne
pe
13

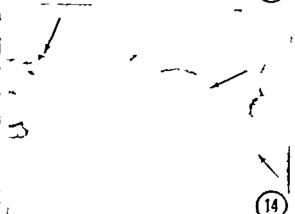

14

PLATE 5

EXPLANATION OF FIGURES

15 Whole mount of single nerve fiber which supplies the Pacinian corpuscle, the connective tissue sheath has been removed under the binocular dissecting microscope revealing the nuclei of the squamous epithelium surrounding the nerve stained by 0.5% aqueous cresyl violet, (arrows) × 1360.

16 Whole mount of single nerve fiber which supplies the Pacinian corpuscle the connective tissue investing the fiber has been removed under the binocular dissecting microscope and the fiber has been stained by silver nitrate to demonstrate cellular borders of the investing squamous epithelium which completely surrounds the fiber (arrows) × 410.

NEW OBSERVATIONS ON THE PACINIAN CORPUSCLE
T. R. Shanthaveerappa and G. H. Bourne

PLATE 6





Similarities Between Oligodendrocyte and Cerebellar Granule Cell Nuclei in *Mammalia* and *Aves*

JAN CAMMERMEYER

Laboratory of Neuropathology, National Institute of Neurological Diseases and Blindness, Bethesda, Maryland[1]

The nuclei of oligodendrocytes and cerebellar granule cells are so alike that in preceding studies on the regional distribution of oligodendrocytes, the cerebellar cortex was excluded (Cammermeyer '60d, g, h). In a subsequent comparison between Purkinje cells of various animals, reference was made to the granule cells, and their resemblance to oligodendrocytes both in structure and in arrangement around blood vessels; this was regarded as suggestive evidence of some function in common, possibly the intrinsic control of blood flow (Cammermeyer '62b). During these investigations conspicuous species variations in nuclear structure became apparent, as previously demonstrated in studies on the cerebellar granule cell nuclei by Levi (1897) and Olszewski ('47). No similar studies on oligodendrocyte nuclei are available.

The present analysis of a number of animal species intends to assemble all anatomical evidences of structural similarities between the two types of nuclei which may imply but not prove a close association in their function. Since the objective is to compare nuclear appearance, then in order to assure the identity of nuclear structures throughout the central nervous system and in the smaller as well as larger animal species, all materials were prepared under strict standard conditions (compare Cammermeyer '61). Since this material includes many animals of unknown age, the suitability of such material for comparative cytologic study depends on the stability of the nuclear structures with aging; the effect of an aging process is sought in a few animals of known age (compare Cammermeyer '63). Since the animals cannot be maintained under standard conditions of rest, an inquiry is made about the nuclear structures under somewhat extreme conditions of muscular activity caused by forced swimming, depressed functional spontaneity induced by reserpine treatment, and suppressed activity by daily barbiturate injections.

MATERIAL AND METHOD

Most animals, adult males, were obtained from various sources without specification of birth date, as cynomolgus macaque, ferret, golden hamster, mulatta macaque, opossum, raccoon, skunk, squirrel monkey, two-toed sloth and woodchuck. A few animals were raised in the animal quarters of the National Institutes of Health, as the brown mouse, Hartley guinea pig, New Zealand white rabbits and Sprague-Dawley rat. On rare occasions animals of known age, as cats, chinchilla, dogs, mink and Silver Carneau pigeons, were obtained from other sources.

Some animal material used herein as normal representatives has been employed previously (Cammermeyer '60b, e, g, h, '62b) and other material is derived from experiments which are described at the appropriate place in the text.

The animals were anesthetized either by intravenous injection of sodium pentobarbital mixed with heparin or by inhalation of chloroform. The latter, immediately after opening the chest, were given heparin intracardially. The blood vessels were flushed with a composite salt solution (Elliott's "B" of Baxter Co.) with the addition of 5% formalin, its total amount in ml corresponding to 14% of body weight in gm, and then perfused with an equal or larger amount of a modified Heidenhain's Susa solution (Cammermeyer '60-

[1] National Institutes of Health, U. S. Public Health Service, Department of Health, Education and Welfare, Bethesda, Maryland.

f) After the lapse of at least four hours the skull and vertebral canal were opened and the brain with spinal cord removed. Pieces from representative parts were placed in 95% ethyl alcohol for dehydration and then embedded in paraffin for staining with the combined procedures of periodic acid-Schiff and gallocyaninchrome alum abbreviated henceforth PASG (Cammermeyer '60f) and other routine methods

All nuclei were photographed at magnification × 2 500 linear enlargement under immersion oil optic and green filter over the light source using Agfa Isopan IFF 13 Plan film. In most instances the pictures were developed for high degree of contrast. Whenever the magnification is different it is indicated in the legends. Some pictures are composites of several in order to depict the various nuclei in sharp focus.

MICROSCOPIC EXAMINATION

A. *Identification criteria for distinguishing between various nuclei in the cat cerebellar cortex*

A brief description of the nucleus in each cell type gives the criteria by which nuclei are selected for the following comparative studies. The 144 day old cat (C1 101659C) is chosen because each cell type is distinct.

Neurons are usually easy to classify because of their large nucleus with relatively sparse chromatin content and conspicuous nucleolus. It is limited by a poorly stained outer membrane in which minute basophil dots appearing at regular intervals are responsible for a beaded appearance. A delicate circular line often forms an inner membrane. Attached to these membranes are several thin basophilic lines which radiate from the nucleolus A small number of chromatin granules occur along these lines. Larger chromatin bodies tend more or less to cover the nucleolus. The perikarya contain basophil masses or Nissl-substance of varying size all attached to extremely delicate curved parallel lines. A peripheral zone is usually free of basophil masses but traversed by thin lines attaching to the surface membrane Among Purkinje cells one type contains mostly small granules of basophil substance arranged in rings around the nucleus and another contains several coarse granules (compare Cammermeyer 62b) The Golgi type II neurons in the granular layer (fig. 1) and the small neurons in the molecular layer have only a moderate amount of basophil substance peripherally (compare Cammermeyer '63a) The cytoplasmic membrane contacts a blood vessel for varying lengths or is covered by faintly pink stained granules.

The *astrocyte* nucleus is characterized by its large size and sparse chromatin content with relatively small central chromatin masses surrounding the nucleolus (*a* in fig 2) Its shape varies greatly The nuclear membrane and a system of lines are faintly stained. In the cerebellar granule cell layer the astrocytes contain a few small pink PAS-stained granules which are arranged in rows and sometimes deposited in irregular spaces around the nucleus and other times next to vascular walls (arrow in figs 6 13 36) In the Bergmann s cell layer these granules form large clusters near the nucleus but in other parts a PAS-stained rounded body occurs. Delicate and faintly stained glial fibers are detected around the nucleus of astrocytes within the granule cell layer when the sections are stained by Mallory s phosphotungstic acid hematoxylin method (arrows in fig 3)

The *microglia cell* has a *nucleus of a* very irregular shape (*m* in fig. 4) Its membrane is heavily stained and its nucleoplasm contains many small and a few coarse chromatin granules Its cytoplasm covers each pole of the nucleus and is usually filled with PAS-stained granules making it possible to discern its shape and to determine whether the cell is attached to a vascular wall or a neuronal membrane.

Other mesodermal elements are identified by their association with vascular walls and their content of PAS-stained material The basement membrane of vascular walls is pink. The capillaries free of blood stand out as smooth parallel lines, and at intervals the space between is occupied by endothelial nuclei which when viewed from the inside are rounded kidney shaped or irregular (*e* in fig 5) their nucleoplasm seemingly is a faded blue

with myriads of poorly stained basophil granules of varying size. The same nucleus seen in a cross section of the capillary displays a clear nucleoplasm limited by a thick and heavily stained membrane (*e* in fig. 2); it is the heavily stained membrane which lends a diffuse blue hue to the nucleus in a flattened view In the granular layer twig-like fibers go off the membrane of venules and veins for a short distance (*t* in fig. 6) Elongated perivascular cells or histiocytes attached to the vascular walls have a clear cytoplasm filled with coarse PAS-stained granules and an elongated nucleus with a densely stained thick membrane and several coarse chromatin granules (*h* in fig. 7) Another similarly stained nucleus, delta nucleus, is usually located on the convex side of a vascular curvature where an intervascular strand of PAS-stained connective tissue fibers is seen. The shape of the nucleus situated within the fan-shaped, delta -like attachment varies from round and triangular to elongated (*d* in figs. 8–10) The nucleus, usually resting upon the vascular basement membrane, may dislocate for a varying distance inside the intervascular strands of connective tissue fibers (fig. 13) On rare occasions PAS-stained granules of varying size appear next to the nucleus (fig. 14) The intervascular strand may fracture or be cut off during preparation but usually enough remains to identify it (arrow in fig. 12) If two blood vessels are close together a short intervascular strand of connective tissue fibers may be overlooked and the delta nucleus ignored (fig. 11) Similar nuclei, eccentrically placed in a faint blue homogeneous cytoplasm (macrophages?) occasionally occur singly or in pairs near the surface of blood vessels (*x* in fig. 15) Larger groups are more rare.

Oligodendrocyte nuclei are identified by their round shape heavily stained outer membrane delicate inner membrane small chromatin granules attached to spoke-like fine basophil lines, and a rim of faintly blue cytoplasm (*o* in fig 16) They are more easily recognized among astrocytes of Bergmann's layer than among the granule cells. Their structure varies insignificantly in gray matter as the floor of the fourth ventricle (figs. 17–19)

The cerebellar granule cell nuclei, which resemble large-sized oligodendrocyte nuclei without cytoplasm, have an outer membrane containing basophil inclusions at regular intervals (*g* in fig. 16) An inner membrane is barely visible and several chromatin granules of varying size are suspended in a network of delicate basophil lines. These lines radiate from a medium-sized dark central chromatin mass covering the entire nucleolus, but this mass may divide into smaller granules which adhere to the surface of a pale nucleolus.

Conclusion. When tissues are prepared according to principles specified herein, the various cell types of the cerebellar cortex are recognized by their distinctive nuclear and cytoplasmic features:

The neurons by extremely large pale nuclei with a conspicuous nucleolus

The astrocytes by strikingly pleomorphic nuclei in a pale or clear cytoplasm with some PAS-stained material,

The microglia cells histiocytes and delta cells (and macrophages?) by intensely stained variously shaped nuclei and frequent inclusion of PAS-stained granules in their cytoplasm

And the oligodendrocytes, as well as cerebellar granule cells by spheroid nuclei relatively rich in chromatin and a moderate amount of cytoplasm which is faintly basophilic in the former only

Another basis for recognition of cell types is their relationship to vasculature

The neurons contact blood vessels for varying lengths

The astrocytes are in contact via processes

The microglia cells are detached and may contact neurons

The histiocytes adhere to vascular walls

The delta cells are entrapped in intervascular connective tissue fibers;

And both oligodendrocytes and cerebellar granule cells tend to aggregate near and along blood vessels.

B *The appearance of oligodendrocyte nuclei and granule cell nuclei in various regions of the macaque brain and spinal cord*

Nuclei in different regions were studied in order to establish whether a specific

pattern of chromatin distribution could be ascertained The central nervous system of the mulatta macaque (M1 121158C) was selected because of its profuse supply of oligodendrocytes (Cammermeyer '60e,g)

Oligodendrocyte nuclei of gray matter have many features in common (figs 20–36) A relatively small or medium sized chromatin mass usually hides a more or less eccentric small nucleolus. Radiating from it are several delicate basophil lines which cross a number of other lines forming an ill-defined network. Sometimes these lines end in small masses of chromatin which occasionally appear triangular and adhere to the inner aspect of the beaded outer membrane. The peripheral granules round when viewed in the equatorial plane (juxtavascular nucleus in fig. 29) appear irregular when seen at the surface of the nucleus (same nucleus in fig. 28) Usually around 1 mm inside the heavily stained membrane in the present pictures (corresponds to a distance of 0 4 μ in the microscopic section) occurs another faint circular line, referred to herein as an inner membrane (*o* in fig. 23 figs. 33 45 51 69 82, and others) Only parts of this delicate membrane are visible other pictures (indicated by arrow in figs. 20 35) The size of nuclei varies within a small (figs. 28 29) or large group (figs. 30 31 and 32) In general, the larger nuclei have a less intensely stained outer membrane and the nucleoplasm appears clear (*o* in fig. 20 fig 24) the smaller nuclei (figs. 21 25) have a more densely stained outer membrane (its chromatin material packed together!) and the nucleoplasm has a bluish tone (shadow effect of *the thickened outer membrane!)* Dispersed through the nucleoplasm are a few small chromatin granules held in place by basophil lines. The nuclei of different gray matter regions, except for insignificant quantitative differences retain their structural characteristics as e.g. in the fifth layer of motor cortical region (*o* in fig 20) in the pyramidal cell layer of Sommer sector or hippocampal H2 region (fig. 21) in the thalamic reticular nucleus (fig. 22) in the caudate nucleus (*o* in fig. 23) in gray matter bridge between caudate nucleus and putamen (fig. 27) in the floor of fourth ventricle (fig. 24) in the medial gray matter of pons (fig. 25) near "blue" neuron of dentate nucleus (fig. 26) near "pink" neuron of reticular formation (figs. 28 29) near blood vessel next to pink" motor neuron of ambiguous nucleus (*n* in fig. 30 fig. 31) next to pink" and "blue motor neuron of spinal cord C7 (*n* in figs. 32, 33 respectively) near "pink" and "blue neuron of spinal cord T12 (figs. 34 35 respectively) and along a blood vessel *at a short distance from pink neuron of* intermedio-lateral substance of spinal cord T12 (fig 36) Nuclei were selected from representative regions and from the neighborhood of different cell types, as "pink" and "blue neurons in cross sections of the brain stem and in longitudinal sections of the spinal cord (compare Cammermeyer '62b '63a,b)

The oligodendrocyte nuclei of white matter resemble the preceding ones. Their cytoplasm is faintly basophil and more readily noticed than in the gray matter; within the same region one cell has a shadow-like cytoplasm at one side of the nucleus (fig 37) and another has a long process attaching to a vascular wall (fig 38) or in other regions the cytoplasm is prominent and surrounds the entire nucleus (figs. 48 49 52) Since the amount of cytoplasm can vary greatly and since the size and chromatin content of nuclei can differ an exact identification and selection of comparable nuclei even within the same region may be quite difficult (figs. 45 48) The admixture of microglia cell nuclei which resemble the other nuclei (fig. 46) will augment difficulties in identification. Well preserved centrum ovale with no signs of maldevelopment *harbors isolated normal neurons which* have a large nucleus with relatively sparse chromatin, a distinct nucleolus and a large perikaryon with scattered basophil granules or Nissl-substance (*n* in fig. 43) Similar neurons in longitudinal section of the spinal cord appear unusually large in

"Pink" and "blue" neurons are distinguished by the reaction of their cytoplasm to PAS treatment; it becomes pink or remains unstained respectively. The identity of the two types of neurons is evidenced by their differential response to aging and anoxemia and by their varying ratio in regions and in species (relatively more "pink" neurons in the two-toed sloth than in the mink and other agile mammals). Although their functional role is not determined (discussed in Cammermeyer '60b), for purpose of comparison, oligodendrocyte nuclei near each type of neuron were studied separately

the ventrolateral funicle (fig. 90) Their nuclei are so different from those of oligodendrocytes that no diagnostic problems arise without well outlined cytoplasmic contours, some confusion with astrocytes may occur In oligodendrocyte nuclei, a conspicuous amount of chromatin is often seen covering the nucleolus. Except for variations in size they are noted for a uniformity in appearance with numerous chromatin granules in all white matter regions, as in the optic tract (figs. 37 38) fimbria (fig. 39) alveus over the Sommer sector (fig. 40) corpus callosum (fig. 41) white matter subjacent to motor cortex (fig. 42) centrum ovale (o in fig. 43) internal capsule (fig. 47) cortico-spinal tract in pons (fig. 44) lateral funicle of spinal cord C7 (figs. 45 48) lateral (fig. 49) and anterior funicles of spinal cord T12 (fig. 50) and cerebellar white matter of hemisphere (fig. 51) and vermis (fig. 52) Within the same system of corticospinal fibers the nuclei subjacent to the cerebral cortex resemble those in gray matter (compare figs. 20 and 42) Nuclei are of smallest size in optic tract, fimbria, alveus and corpus callosum (compare Cammermeyer '60d)

The cerebellar granule cell nuclei have a beaded outer membrane with irregular basophil masses *attached to its inner aspect* and a thin inner membrane. Delicate basophil lines from the peripherally situated masses converge upon a medium sized central chromatin structure which covers the nucleolus. When the peripheral part of the nucleus is viewed in a tangential plane the basophil masses appear elongated and greater in number. In general the nuclei are of uniform size and structure as depicted e.g., in the lobulus simplex (fig. 53) around the bottom of fissura prima (fig. 54) in the top of crus I (fig. 55) around the bottom of a secondary sulcus of crus I (fig. 56) in the vermis (fig. 57) and in the top of flocculus (fig. 58) These nuclei resemble more closely oligodendrocyte nuclei of gray matter than those of white matter

Conclusion. Oligodendrocyte nuclei situated in various gray matter regions have in common a more sparse storage of chromatin granules than noted for nuclei throughout white matter There is a considerable individual variation in content of chromatin but there are no major differences in nuclear structure or pattern of chromatin distribution from region to region. The cerebellar granule cell nuclei are of uniform appearance and resemble the oligodendrocyte nuclei of gray matter more than those of white matter.

C *The structure of the two nuclear types in cats rabbits pigeons and dogs of varying age*

In order to decide the usefulness of animals of unknown age for a comparative study of nuclear characteristics it was necessary to establish nuclear structures in animals of known age. There were four animal series covering various but overlapping age periods, namely cats from 1 to 20 weeks of age, rabbits from 1 to 31 months of age, pigeons from around 1 year to 6 years of age and two dogs, 4 and 15 years of age.

The brain stem of the one-week-old cat (pink tiger; blind, 8 days wt. 170 gm C4-081359C) has a population of nuclei which is difficult to classify even in the most mature portions. Many round to ovoid nuclei, richly supplied with chromatin, are situated eccentrically in a cytoplasm with peripheral minute basophil *granules (figs 62, 63) these cells mimic* oligodendrocytes by their perivascular arrangements in rows. Elsewhere as in the more developed reticular formation perivascular round nuclei with a moderate amount of faint blue cytoplasm resemble more mature oligodendrocyte nuclei (fig. 59) In the cerebellar granule cell layer excepting the fetal outer granule cell layer the nuclei vary greatly in size and shape (fig 64) and there are many mitotic figures among them. The five week-old cat (gray; 33 days wt. 430 gm C3-081259C) has a fully developed central nervous system, but rather few oligodendrocyte nuclei are identified in the floor of the fourth ventricle (fig. 60) The granule cell nuclei vary in size; they are rich in chromatin material dispersed in small granules and *accumulated around the nucleolus* (fig. 65) In the 20-week-old cat (144 days; wt. 1,050 gm; C1 101559C) the oligodendrocyte nuclei are of small size and their content of fine granular chromatin is less-

ened from that of preceding ages (*o* in fig 16 figs. 17–19 61) Several medium basophil masses are attached to a relatively thick heavily stained membrane (shadowing the nucleoplasm!) and a single large mass occupies the center The granule cell nuclei undergo a similar lessening in amount of their chromatin granules (fig. 2, *g* in fig. 16 fig. 66)

Age differences between rabbits are noticeable but not always equally striking. The entire oligodendrocyte nucleus in figure 67 is filled with minute chromatin granules at one month (36 days wt. 480 gm Ra4-040561C) the chromatin material accumulates in figure 68 in slightly larger masses along the membrane at two months (70 days wt. 1,880 gm, Ra1 050561C) and appear less abundant in figure 69 at 6 months (185 days wt. 3 860 gm Ra1-021661C) and in figure 70 at 12 months (344 days; wt. 3 770 gm Ra4-040461C) but some more granules occur in figure 71 at 22 months (658 days; wt. 6,070 gm Ra1-040461C) and in figure 72 at 31 months of age (929 days wt. 4 450 gm; Ra2 122057C) A diminution in size of the central chromatin mass is noticeable by comparing the last three stages with the two preceding stages. A moderate decrease in size of the nucleus is noted from 2 to 6 and from 22 to 31 months of age. Whereas granule cell nuclei have a relatively sparse amount of chromatin material at one month (fig 73) they contain many coarse granules at two months (fig 74) numerous smaller granules at six months (fig. 75) and relatively fewer and smaller at 12 (fig 76) 22 (fig. 77) and 31 months of age (fig 78) Between the two last stages a moderate enlargement of scattered chromatin granules seems to have taken place. The central chromatin material is small at one month largest at two and six months and smallest in the oldest age groups. Similarly the over all size of nuclei appears greater in the two and six month old animals than in the others. Neither oligodendrocytes nor cerebellar granule cells display inclusions like the red PAS-stained juxtanuclear bodies occurring in astrocytes of old rabbits.

The nuclear alteration in aging pigeons is recognized by changes in amount of chromatin material. The oligodendrocyte nucleus has an almost evenly thick membrane in figure 79 in the ten month old pigeon (P1-090861C) the chromatin material aggregates in small granules along the thick membrane which attains a beaded structure in figure 80 at one and one-half years (P3-090861C) and the membrane, having retained less chromatin, appears less thick with a more clear nucleoplasm in figure 81 in the six year old pigeon (P2 120258C) The granule cell nuclei have membranes with more chromatin material in the two younger (figs. 84 85) than in the oldest pigeon (fig. 86); the size of both the peripheral granules and the central mass decreases with aging.

The last series is of a four and three-quarter year old dog, Irish setter (D1 021159C) and a fifteen and one-third year old dog, dachshund (D1-081761C)· both the oligodendrocyte and granule cell nuclei are larger with more chromatin granules in the younger (figs. 82 and 87 respectively) than in the older dog (figs. 83 and 88 respectively) The oligodendrocytes and cerebellar granule cells are free of the red PAS-stained juxtanuclear inclusions which in the old dogs are conspicuous in astrocytes throughout the granule cell layer (fig. 89) as well as in the Bergmann s cell layer

Measurements with a planimeter controlled microscopically with camera lucida (Cammermeyer '60e), were bilaterally performed on the area of nuclei of astrocytes, oligodendrocytes and neurons in the facial nucleus in two rabbits 27 months (Ra21 010658C) and 35 months (Ra12-072657C) of age. After transection of the left facial nerve and a lapse of 5 and 12 days, respectively the animals were killed by the present two-step perfusion technique with delayed autopsy No significant difference in area was noted between the two sides. However a statistically significant difference is apparent between oligodendrocyte nuclei of the younger and of the older rabbit (table 1) in the course of eight months, equivalent to a 30% increase in age, the nuclei on the non-operated or normal" side decrease in area by around 10%

Conclusion. The oligodendrocyte nucleus and cerebellar granule cell nucleus, after reaching fully matured stages retain

TABLE 1

Area of oligodendrocyte nuclei in rabbit facial nucleus after transection of facial nerve (20 μ thick PASG stained serial sections)

Age	Weight	Average area ± standard error (Number of nuclei)	
		Operated side	Non-operated side
mos	kg	μ^2	μ^2
27	4 05	22.01 ± 0.34 (273)	31.65 ± 0.36 (264)
33	4 45	25.96 ± 0.60 (256)	28.56 ± 0.37 (265)

their general structural characteristics with aging. This preliminary survey suggests that aging is characterized by quantitative changes as decreasing size of nuclei with a diminishing content of chromatin in their membranes scattered granules and juxtanuclear masses. PAS-stained material does not accumulate in adjacent cytoplasm as it does in astrocytes of numerous species.

D *The appearance of the two nuclei with varying conditions of motor activity*

In animals the status of rest or activity is difficult to control. Depending on size of their cages and degree of docility an animal may or may not exercise, and when handled may become excited, as the rabbit, or remain quiet, as the dog. Animals like the monkey dog, cat and rabbit after intravenous injection of pentobarbital become instantaneously and deeply narcotized, but others exposed to chloroform go through a phase of great excitation, before deep narcosis is reached in two to ten minutes. Since standard conditions of rest could not be prescribed, material was collected from three experiments to determine whether nuclear structures were influenced by mode of behavior One series of cats of same age was allowed to swim to deter mine the effect of forced muscular activity or fatigue; one series of monkeys was treated with reserpine to depress spontaneous activity and one series of litter mate cats was treated with sodium barbital for long periods to study effects of inactivity

Cats, 144 to 148 days old, unable to escape from a water-filled tank, were forced to swim continuously for ten minutes (wt. 1,350 gm C4-092459C) 30 minutes (black, wt. 1 780 gm; C3-092459C), one hour (gray tiger; wt. 1 680 gm C1 092559C) two hours (red tiger; wt. 1,900 gm; C2-092459C) and four hours (gray tiger; wt. 1,980 gm C1-092459C) All were narcotized with chloroform immediately after termination of the experiment and then prepared by the two-step perfusion procedure with delayed autopsy All three cats with tiger" patterned fur swam quietly and continuously with regular foot strokes. The other two were nervous and excited when put in the water exhausted after two minutes of swimming, floated a little while, swam wildly for another short period floated and so on throughout the experimental period.

Four cats of the same litter kept in a light controlled room from the age of one month, at the age of 162–168 days were killed as above. One was forced to swim ten minutes daily the last 68 days (blue-gray tiger; male; wt. 2 080 gm; C1 100359C) the second swam 60 minutes daily the last 69 days (male wt. 1,550 gm; C4-100359C) the third swam four hours on the day of sacrifice (gray tiger; female; C3-100359C) and the fourth was fasted for a period of four hours before sacrifice (gray tiger- male; wt. 2 140 gm C2 100359C)

A single cat of unknown age (wt. 4 100 gm C1-040660C) received a subcutaneous injection of sodium pentobarbital (1 ml "Nembutal per kg body wt.) and remained narcotized for 48 hours. Then four litter mate cats were for a period of one month placed on a regimen of one sodium pentobarbital injection daily (0 75 ml "Nembutal" subcutaneously) starting at varying times so that when sacrificed at ages between 319 and 327 days the animals were in varying stages of recovery In one animal the last injection preceded sacrifice by two hours (wt. 2,845 gm; C1-042660C); in one the last injection was given 24 hours prior to sacrifice (wt. 2,705 gm; C2-042660C) in one seven days prior to sacrifice (wt. 2,800 gm C1-041960C) and in one 28 days prior to sacrifice (wt. 2,825 gm; C1-040560C) They were sacrificed by an intravenous injection of sodium pentobarbital with heparin followed by the

two-step perfusion procedure and delayed autopsy

From a larger series of reserpine (Serpasil, Ciba) treated cynomolgus macaques a few were selected. All exhibited during treatment the classical parkinsonian syndrome of tremor in activated muscles muscular rigidity with hunched position, increased salivation and lacrimation, and reduced behavioral spontaneity interrupted by sudden movements or bursts of agility In one a small dose of reserpine (0 75 mg per kg body wt.) was injected three times every eight hours; the experiment lasted a total of 24 hours (wt. 1,880 gm; M2 011260C) In one, a large dose (3 mg per kg body wt.) was given in a similar manner and the experiment lasted 24 hours (wt. 2,285 gm, M1-011360C) In one, a daily small dose (0 75 mg per kg body wt.) was given over a period of 84 days and the experiment terminated six hours after last injection (wt. 2,340 gm; M2 010660C) In one after two days of pretreatment with amphetamine four large injections of reserpine (3 mg per kg body wt.) were given over a period of 24 hours and the animal killed three and one-half hours after the last injection (wt. 2 670 gm M1-062760C) All experiments were terminated by an intravenous injection of pentobarbital with heparin immediately followed by the two-step perfusion procedure with delayed autopsy

Neither microscopic examination nor scrutiny of photomicrographic pictures (none of which is included herein) reveals any change in the nuclear structure of oligodendrocytes or cerebellar granule cells The nuclei conform to those of the normal ones already described and depicted herein Other changes as in the content of PAS-stained material of intervening tissue (in astrocytes!) are of complex nature but since the cells under study *are not involved a detailed description of* these changes is considered to be beyond the scope of the present investigation.

Conclusion. In animals some of known age exposed to acute and chronic, light and severe experiments, neither oligodendrocytes nor cerebellar granule cells display evidence of nuclear reaction. It is apparently of no consequence that the animals performed moderate or severe muscular activity leading to slight fatigue or chronically exercised to train muscles. It is equally apparent that nuclei show no change in distribution of chromatin with varying degree of inactivity due to narcosis or lack of spontaneity

E. *Topographic characteristics of oligodendrocyte and cerebellar granule cell nuclei in the cat*

Large areas may have to be searched in order to ascertain a spatial relationship between various cell types and blood vessels because the tissue is rarely cut in such a manner that this relationship is retained in a microscopic section. Thus the oligodendrocytes are seen to be arranged perivascularly near a nerve cell or vascular bifurcation (fig. 91); they vary greatly in number The nuclei in a cluster packed so closely that their membranes abut, often arrange themselves around an astrocyte nucleus and are separated from a neuron by a capillary (fig. 92) A blood vessel may pass between a contacting neuron and a single oligodendrocyte (fig. 91) There is a considerable regional variation in the perivascular arrangement of this cell type (Cammermeyer '60g h)

The laminar architecture of the cerebellar cortex is the same in various parts the thickness of the granule cell layer shows a regular thinning and thickening around sulci and the top of leaflets respectively; and the molecular and Purkinje cell layers are of uniform appearance In all animal species the top of several leaflets shows signs of local atrophy restricted to the molecular layer (fig. 93) or more severe damage affecting the granule cell layer without (fig. 94) or with subjacent white matter (fig. 95); defects due to tearing or abrasion during autopsy are ruled out because the surface of this molecular layer is covered by a delicate connective tissue *membrane with blood vessels* and/or the more severe cortical lesion is covered by a narrow zone of glial fibers. The Purkinje cells are distributed at regular intervals in a single layer with astrocyte nuclei interspersed (astrocytes of Bergmann's layer) Among the many species the rabbit cerebellar cortex is characterized by a large number of Purkinje cells with a cluster of granule cell-like nuclei displaced in the

molecular layer; rare ectopic Purkinje cells occur in the mulatta and cynomolgus macaques and squirrel monkey the 15 year old dog, the raccoon, woodchuck and pigeon but none is observed in the four year old dog, the chinchilla ferret, mink, skunk and sloth.

The densely packed nuclei in the granule cell layer are unevenly distributed so that rounded or elongated cell free spaces occur; accordingly an impression of alveoli (arrow in fig. 93) or rows (arrows in fig. 95) of nuclei emerges. With higher power it is readily seen that the congregation of nuclei follows the course of blood vessels which thereby influence the architecture of this layer (fig 96) The nuclei also conglomerate next to or along intervascular strands of connective tissue fibers (s and s in fig. 96) Astrocyte nuclei are scattered through the granule cell layer but in many instances they locate within a cluster of granule cell nuclei (arrows in fig. 96) The intervening tissue has a finely granular appearance with many bright red granules which are enclosed in astrocyte processes (figs. 6, 13)

Conclusion. The oligodendrocytes and cerebellar granule cells share several topographical characteristics they are arranged in clusters along blood vessels (compare Cammermeyer, '60d) many of the intervascular strands of connective tissue fibers form guidelines for their distribution (compare Cammermeyer '60b) and an astrocyte often takes a central position in these clusters. The nuclei often contact each other or the vascular walls the greatest number of them appear at varying but relatively short distances from the blood vessels.

F Comparison of the structure of oligodendrocyte and cerebellar granule cell nuclei in various species

This comparative study concerns randomly selected oligodendrocyte nuclei, located perivascularly in gray matter subjacent to the fourth ventricle and cerebellar granule cell nuclei from one hemisphere (compare previous section B) The material consists of adult male animals of known and unknown ages (compare preceding section C) from several orders Columbiformes Marsupialia, Edentata, Lagomorpha, Rodentia, Primates and Carnivora. The animals variety names will be used herein. Since amount and size of chromatin material throughout the nucleus vary with age quantitative differences between species are not taken into consideration. The distribution of nuclear chromatin which is not influenced by age, will be found to vary somewhat, individually and from one species to another but in general it will be noticed to follow one of three distinct patterns and accordingly the material is divided into three groups.

Type 1 Nuclei with chromatin aggregated predominantly in a large central mass. Among the two representatives included herein, the guinea pig (GP2 112558C) has a much larger central mass than the pigeons (compare p. 116) The accumulation of chromatin may be so great and homogeneous that the nucleolus is completely covered (figs. 97 99). Scattered nuclei among both oligodendrocytes (fig 98) and cerebellar granule cells around the bottom of fissures (fig 101) have a dense central chromatin accumulation with small or large round to oval perforations through which the pale nucleolus is recognized. A varying number of delicate basophil lines radiate from the central mass to the thick outer membrane and along them may appear diminutive chromatin granules. Often the lines may merge to form densely stained and short bands. The outer membrane in both species is thicker in the oligodendrocyte nuclei (figs. 97 and 79–81 respectively) than in the cerebellar granule cell nuclei (figs. 99 100 and 84–86 respectively) and small granular masses attach along its inner aspect to give it a beaded appearance. A delicate inner membrane is identified microscopically but is only vaguely depicted in the figures. The granule cell nucleus of the cochlear nucleus mimics the cerebellar type, except for its slightly larger size in the guinea pig (fig. 102)

Type 2. Nuclei with a conspicuous accumulation of chromatin material both centrally and peripherally and a quite regular spoke-like formation of basophil lines. This arrangement is present more strikingly in both nuclear types of the mouse (Ms1-010459C) hamster (Ham2 121758C) and rat (R5-011361CuC) than in those of

the raccoon (Rac1-032659C) woodchuck (Woc1-090861C) and mulatta macaque (M1 121158C)

The oligodendrocyte nuclei are made conspicuous by the prominent cone- or cornucopia-like chromatin structures attached to a densely stained outer membrane as seen in the mouse (fig. 103) the hamster (fig. 104) the rat (fig. 106) and the raccoon (bottom nucleus in fig 107) The chromatin structures attached to nuclear membranes are of slightly different shape when depicted in a plane through the center of the nucleus and its nucleolus (fig. 106 bottom nucleus in fig. 107) than when depicted in a tangential view of the nucleus (fig. 105 top nucleus in fig. 107) In the nuclei of both the woodchuck (fig. 108) and the mulatta macaque (compare B p 113 and figs 20–36) the peripheral structures are of smaller size and more basophil lines are formed.

The cerebellar granule cell nuclei in general have less striking peripheral chromatin granules attached to a thin outer membrane, as in the mouse (fig. 109) hamster (fig. 110) rat (fig 111) raccoon (fig. 112) woodchuck (fig. 113) and mulatta macaque (figs. 53–58) The cere- granule cell nuclei seem to be more y supplied with basophil lines and with scattered small chromatin granules.

Type 3 Nuclei with a moderate to minimal central accumulation, some peripheral aggregation considerable dispersion of small granular chromatin masses and conspicuous network of basophil lines. This group comprises cat (compare p. 115 and p. 113) mink (Mink1 103161C) opossum (OpVa1-020557C) cynomolgus macaque (M1-092358C) two-toed sloth (Slo1 112261C) ferret (Fer2 110361C) chinchilla (9 months Chin2-092358C) skunk (Skk1-030961C) squirrel monkey (SqM1-040460C) rabbits (compare p. 116) and dogs (compare p. 116)

The nuclei in general have a well developed network of basophil lines with numerous granules of varying size along them as well as along the inner aspect of the outer membrane This structure may not be equally well formed in both types of nuclei at times the oligodendrocyte nucleus may more closely resemble the preceding type 2, as seen in the cat (figs. 16–19 61 66) mink (figs. 114 119) and opossum (figs. 115 120) and at times the granule cell nucleus may look more like one of type 2, as in cynomolgus macaque (figs. 116 121) Otherwise, the two nuclear types conform in their pattern of chromatin arrangement, as in the two-toed sloth (figs. 117 118 122) ferret (figs. 123 126) chinchilla (figs. 124 127) skunk (figs 128 129) squirrel monkey (figs. 125 130) rabbits (figs 67–78) and dogs (figs. 82 83 87 88)

Conclusion. A material, comprising 19 different animals is divided into three groups on the basis of the structural characteristics of nuclei in oligodendrocytes and cerebellar granule cells. In type 1 most of the chromatin is placed centrally (guinea pig and pigeon); in type 2, chromatin accumulates under the outer membrane while the central mass is of medium size (mouse hamster rat, raccoon woodchuck and mulatta macaque) and in type 3 the chromatin material is more finely dispersed in and along a delicate basophil network (cat, mink, opossum, cynomolgus macaque two-toed sloth, ferret, chinchilla, skunk, squirrel monkey rabbit and dog)

Representatives of the small-sized rodents are noted for nuclei of the first and second types and those of small and large-sized primates and carnivores with few exceptions for nuclei of the third type.

DISCUSSION

Factors influencing nuclear chromatin content

The comparative study of nuclei in various species was preceded by an inquiry about factors which might influence the structure of these nuclei. The first factor to consider is to be found in the procedures of fixation and histological preparation of tissue A specific procedure must be rigidly adhered to in order both to preserve uniformly the various nuclei throughout the organ and to avoid artifactual cytoplasmic and nuclear changes. The quality of preservation must be judged by a number of microscopic characteristics which the tissue must have and the microscopic analysis must be restricted to adequately prepared regions. When these prerequisites are satisfied, the criteria used for dif

ferential diagnosis of nuclear types can be *defined* (Cammermeyer '58 '60e,f '61) Equally important is use of a stain ing method which brings out connective tissue fibers along the vasculature the granular material of cytoplasm, and the various mesodermal cells, specifically the delta cell type (figs. 8–14) which by the frequently used Nissl methods escape correct identification (Cammermeyer '60b). On the basis of these efforts, the method for selection of comparable nuclei is controlled, and this is particularly significant when studying, in small and large animals such a complex and compact cell population as in the cerebellar granule cell layer (figs. 1–19) The specificity of nuclei as a means of diagnosing a cell became evident during the *study of this material, in* contrast to ambivalent interpretations rendered after studying material fixed by immersion (compare Smart and Leblond, '61) The ease with which nuclei are classified varies with species; in some the distinction between astrocytes and oligodendrocyte nuclei is easy and in others difficult or impossible (Cammermeyer '60a,d) Small oligodendrocyte nuclei are dark in appearance because their thickened membranes shadow the nucleoplasm they should not be confused with nuclear pyknosis in which the chromatin is compacted within the shrunken nucleoplasm. Neither the so-called acute swollen oligodendrocyte (Penfield and Cone, '26) nor the pyknotic oligodendrocyte nucleus (Kryspin-Exner 43; Pannese, '58; Smart, '61; Smart and Leblond, '61) occurred in the present material as expected from views recently developed concerning the artifactual origin of these nuclear changes (Cammermeyer '60f '62a) In none of the animals did I find any anatomical evidence to support views that oligodendrocytes may give origin to macrophages (Kryspin-Exner 43) microneurons (Weber '59) or astrocytes (Smart and Leblond, '61)

The second factor is associated with regional peculiarities. The shape and size vary most among white matter oligodendrocyte nuclei (figs. 37–42, 44–52); they tend to be oblong in the direction of fibers and they are of smallest size in the optic tract, fimbria and alveus (Cammermeyer '60d) In general they are richly supplied with chromatin which makes separation *between nuclear types less distinct. Sometimes* a microglia cell nucleus may be mistaken for an oligodendrocyte nucleus or vice versa; the presence of PAS-stained granules should help distinguish between them. Many white matter nuclei assumed to be of oligodendrocytes are surrounded by more cytoplasm than elsewhere and the prominence of cytoplasm may be reminiscent of fibrous astrocytes. The differential effect of dehydrating agents, as al*cohol, on gray and white matter may also* contribute to their varied appearance (Cammermeyer '60e) If the region to be investigated is undergoing degenerative changes, criteria of identification may be disputed (compare Koenig and Barron '62) The presence of neurons in the centrum ovale is intriguing but offers no differential diagnostic problem in this material, with other techniques their nuclei might be confused with those of astrocytes. Similar isolated white matter neurons are extremely large in longitudinal sections of the spinal cord, possibly as the consequence of stretching from rostral to caudal (compare Kreyssig, 1885 Weil, '26) they have been described in man and cynomolgus macaque (Duncan, '53) but differ according to site from those in the lateral cervical nucleus (Rexed and Brodal, '51; Brodal and Rexed '53) and in the marginal nucleus (compare Kappers, Huber and Crosby '36 Anderson Meadows and *Chambers '61) Since the oligodendrocyte* nuclei are of fairly uniform appearance through gray matter (figs. 20–36) and since this comparison concerns cerebellar cortex (figs. 53–58) the oligodendrocyte in gray matter subjacent to the floor of the fourth ventricle is regarded as representative and suitable for ascertaining accurate classification. In such a survey also the duality of neuronal population in nuclei of brain stem and ventral horns of spinal cord has to be taken into consideration (Cammermeyer '62b '63a,b) and oligodendrocyte nuclei adjacent to both pink and "blue neurons be compared In order to assure correct selection of these nuclei, and in conformity with present views about their characteristic sites only those along

See footnote 2.

blood vessels should be chosen (Cammermeyer '60a,c,d,g,h)

The third factor is aging. The area of oligodendrocyte nuclei, determined planimetrically *is smaller in older than in* younger adult rabbits. A study of the pictures of randomly selected nuclei arranged in order of increasing age suggests a moderate reduction in content of chromatin material and in size of both oligodendrocyte and granule cell nuclei; however the pattern of chromatin distribution is not altered whether it is of the type seen in pigeons or that in rabbits and dogs (figs. 67–88) These observations led to a special investigation published elsewhere, in which the animals, the tissue the microscopic sections and the photographs were treated alike; the conclusion was that the Feulgen stained chromatin was continuously reduced in amount implicating an aging process which acts on synthesis but not on pattern of distribution (Cammermeyer '63a) Other information can be obtained by the study of these two separate series of rabbits of known age namely that in the ten animals no appreciable individual variation in distribution of chromatin takes place. When a more conspicuous nuclear structure is on hand as in the guinea pig, its constant appearance in a large animal material is readily established Thus with animals of unknown age, provided their nervous system is fully developed, a comparative study and classification of nuclei on the basis of chromatin distribution is permissible. As demonstrated in kittens (figs. 62–65) before maturation of the brain stem and the cerebellar cortex is completed, the attempt to identify nuclei is futile (compare Roback and Scherer '35 Lumsden '58) other techniques are required to discern the life history and determine the identity of the perivascular cells with a large nucleus situated in a cytoplasm rich in basophil granules As already stated there is no evidence to confirm the contention that pyknotic oligodendrocyte nuclei occur during maturation (Smart '61 Smart and Leblond '61) or aging (Pannese '58)

The fourth factor is behavior A survey of animals some of known age used in experiments with short or prolonged activity and inactivity indicated that no alteration of nuclear structures takes place. Thus animals in which the level of motor activity is not controlled (compare Cammermeyer '60d) may still be used for the projected purpose. No attempt was made to quantitate chromatin content or size of nuclei. There are no changes to support other views either that nuclei as part of normal life cycle go through a phase of pyknosis (Pannese, '58) or that neurons as the consequence of treatment with psychotropic drugs undergo hyerchromatosis or so-called dysmorphia (Terranova Vanni and Spiazzi, '62)

Similarities in topographical arrangement and nuclear structure

During these studies, each of the two cell types was found to partake equally in the organization of gray matter and cerebellar cortex in various animal species (figs. 91–96) Both types of nuclei, whether in an isolated cluster (fig 92) or within a cerebellar layer (fig 96) tend to lie close together and next to vascular walls but even more striking is the similarity of the manner in which they surround astrocytes and follow along blood vessels and intervascular connective tissue strands (compare oligodendrocytes in Cammermeyer '60b,d). This arrangement of granule cells, made conspicuous by the PASG-staining method, is at variance with alveolar type of arrangement around the cell free spaces, glomeruli or islands referred to when one of the modified Nissl methods is used (Fox and Barnard '37) How intimately the nuclei abut is depicted in a recent study with electron microscope (Gray '61); the space between nuclei narrows to 0 1–0.2 μ.

This comparative study of nuclei in the 19 animal species reveals three distinctive types of chromatin distribution which recur in gray matter oligodendrocytes and cerebellar granule cells. A few exceptions are noted which may not be significant because they are single representatives of unknown age; for a conclusive classification of nuclei a series of adult animals of varied known age should be examined as done for the rabbit, pigeon and dog. There is no close correlation between either the order or size of animal and the chromatin structure of nuclei; among Rodentia all three nuclear types occur and among

Primates and Carnivora two types are demonstrated. The orders are divided as follows Most representatives of the small sized Rodentia are noted for nuclei of first and second type in which chromatin tend to accumulate in larger masses and the basophil lines are less numerous. Small and large sized species of the Primates and Carnivora, including the more primitive mammals as Edentata and Marsupialia, tend to have nuclei of type 3 with dispersion of chromatin substance along a net work of basophil lines.

Somewhat similar results have been obtained in two other investigations concerning the cerebellar granule cell nuclei of material fixed by immersion. Levi (1897) described in mammals both a large central mass as in the guinea pig, ox, and human child and a reticular structure, as in the bat, dormouse dog and rabbit. Olszewski ('47) described a dispersion of chromatin granules in man, radiating fibers with few peripheral granules in pigeon, fibers radiating from a large central nucleolus in ox, a delicate network of basophil fibers in rabbit and pig, and four or more large masses attached to the nuclear membrane and connected by fibers crossing the central part in mouse A single report on spinal cord oligodendrocytes by Kamimura ('33) concluded that there was no structural differences observable in man ox, rabbit, mouse, guinea pig, hen, pigeon, amphibian, fish and cyclostomes.

In summary certain characteristics of the nuclei of gray matter oligodendrocytes (Cammermeyer '60d) recur in the nuclei of cerebellar granule cells (A) In their topographic arrangement, the nuclei tend to (1) cluster along blood vessels (2) follow intervascular strands of connective tissue fibers (3) adhere to the vascular wall (4) be so closely packed that their membranes seem to abut, and (5) to surround astrocyte nuclei. (B) Cytologically these nuclei are characterized (6) by being situated in cells with scant cytoplasm, and (7) by being free of intensely PAS-stained inclusions in adjacent cytoplasm. (C) In nuclei of both cells, the pattern of chromatin distribution (8) is usually the same in a given animal, (9) shows no individual variation when several animals of the same species are studied (10) varies in the same manner from one species to another (11) is retained with aging while the total content of chromatin diminishes and (12) remains unaltered under experimental conditions of short or prolonged changes in behavior.

Functional significance of the two cell types

It is customary to determine the identity of each cell in the central nervous system by the appearance of its nucleus. The reliability and success of such classification depends primarily on the quality of tissue preservation, as previously stated. Since the preparation of this material satisfied the stipulation set for obtaining standard conditions not only are the present results considered significant, but the twelve morphological features common to both gray matter oligodendrocyte and cerebellar granule cell nuclei become strong evidence of similarities in functions. In view of both cells close proximity to blood vessels it may be appropriate to advocate an intrinsic blood flow control for cerebellar granule cells (Cammermeyer '62b) as first proposed, but not yet established, for oligodendrocytes (Cammermeyer '60a,c,d).

The identity of cell types may be obscured by regional and species peculiarities which in turn may modify the criteria by which microscopic structures are identified. The appearance and function of neurons differ in various gray matter regions and the astrocytes display considerable individualism in the upper and lower cortical layers and in the three layers of the cerebellar cortex. Hence, nothing unusual can be ascribed to the heterogeneity that is displayed by oligodendrocytes when clustered in a group (figs. 27 28 and 29 30 and 31 47) or when situated in tissues of different composition, as gray and white matter On the basis of this view the dissimilarities between gray matter oligodendrocytes and cerebellar granule cells are neither suggestive of separate cell entities nor evidence of dissimilarities in function. The two cell types are distinguished by their differences in the stainability and in the submicroscopic composition of their cytoplasm (Palay McGee-Russell Gordon and Grillo '62) in the prominence of their nuclear membranes and in the degree of

the homogeneity in chromatin content and size of their nuclei. The thickness of nuclear membranes, when viewed with the compound microscope seems in a given animal to depend on size of nucleus which as proposed for oligodendrocytes may be a reflection of varied functional conditions (Cammermeyer '60d) The variation in size within a cluster of oligodendrocyte nuclei is indicative of functional heterogeneity which must be expected of a juxta vascular cell complex if it should be able to adjust the blood flow to neurons effici ently and rapidly according to their need. In order to fulfill such a task the cell complex must be capable of coordinating stimuli of various origin with varied actions on blood vessels for which different as yet unknown receptors and effectors would be required (Cammermeyer '60g) As participants in such an intricate mechanism some oligodendrocytes may be allied to contractile elements and others to ner vous elements (compare Lumsden and Pomerat, 51 and Scheibel and Scheibel '58 respectively) Among the myriads of granule cells which number 960 per Pur kinje cell (Fox and Barnard, '57) some y collaborate with scattered oligodendrocytes identified by the appearance of their silver impregnated cytoplasm and processes (Schroeder '35) The homogeneity of cerebellar granule cell nuclei can be associated with peculiarities in function and metabolism of the cerebellar cortex (compare Cammermeyer and Swank, '51)

Recent studies with refined silver techniques have clarified several problems concerned with the structure of the cerebellar cortex (Carrea Reissig and Mettler 47; Scheibel and Scheibel, '54 Fox and Barnard, '57 Rasmussen, '57; Fox, 59 Brodal and Grant, '62) still many details are unknown with respect to both localization (Jansen and Brodal, '58) and submicroscopic organization (Gray '61) While interests have centered on nervous circuits and manner of synapsis the possibility has been ignored that the blood vessels may be intimately connected with neurons and granule cells and integrated in nervous functions. *I am not prepared to discuss* whether such integration could utilize circuits already known to exist or whether it would depend on new ones. Also present concepts about connections and functions of oligodendrocytes are too meager to permit one to propose any mode of action. Should the hypothesis about the intrinsic blood flow control mechanism prove correct, then one may speculate as to whether *in all regions a stimulus may not simul*taneously reach a group of neurons and the juxtavascular cell complexes over wider areas thereby these complexes by their action on the various capillary channels, may permit adjustment of blood flow conforming to need of involved neurons Since the cerebellar cortex has been so thoroughly studied it will perhaps be most suitable for discerning the mechanism by which blood flow is controlled this may then form a basis for understanding the functional role of oligodendrocytes.

SUMMARY

The chromatin arrangement in nuclei of gray matter oligodendrocyte and cerebellar granule cell nuclei, compared in 19 animal species, (1) is the same in a given animal (2) remains constant for several animals of the same species (3) varies simultaneously with species (4) is retained although decreased in amount with aging and (5) is unaltered by changes in behavior induced for a short or long period. The nuclei are surrounded by a rim of cytoplasm devoid of PAS-stained material. Both types of nuclei tend to (1) cluster along blood vessels, (2) follow intervascular strands of connective tissue fibers, (3) surround astrocytes, (4) pack so closely that membranes seem to abut each other and (5) nuclear membranes seem to contact the basement membrane of blood vessels

A proposal is made that the two cell types have in common a function which may be associated with intrinsic blood flow control as recently set forth for oligodendrocytes. The mechanism of such a func tion must await clarification of the organization and connections of juxtavascular cell groups throughout the central nervous system.

ACKNOWLEDGMENT

The author is pleased to acknowledge the meticulous preparation of histologic material by Miss I. Mercado and Miss E. Pin-

nell and photographic material by Mr E. Moodhe (Laboratory of Neuroanatomical Sciences) and the constructive criticism by Mrs. M. Johnson and Mrs. J Phelps during writing of the manuscript.

LITERATURE CITED

Anderson, F D., I. Meadows and M. M. Chambers 1961 On the presence of the nucleus marginalis (Hoffmann) in the mammalian spinal cord. Program 74th Session Am. Assoc. Anat., Chicago, Illinois, March 21–24, p. 6.

Brodal, A., and G. Grant 1962 Morphology and temporal course of degeneration in cerebellar mossy fibers following transection of spinocerebellar tracts in the cat. Exp. Neur., 5 67–87

Brodal, A., and B. Rexed 1953 Spinal afferents to the lateral cervical nucleus in the cat. An experimental study J Comp. Neur 98 179–212.

Cammermeyer, J 1958 Difficulties in interpreting neuropathology of neuroglia cells. Discussion. In Biology of Neuroglia, W F Windle, ed. Charles C Thomas, Springfield, Illinois, pp 61–62, 223–227

——— 1960a Discussion. J Neuropath. Exp. Neur 19: 170–171

——— 1960b A comparative study of inter vascular connective tissue strands in the central nervous system. J Comp. Neur., *114* 189–208.

——— 1960c A new concept about oligodendrocytes' function intrinsic control of capillary blood flow Proc. 35th Ann. Congr Pan-American Medical Assoc., Mexico City May 2–11 p. 192.

——— 1960d Reappraisal of the perivascular distribution of oligodendrocytes. Am. J Anat., *106* 197–231.

——— 1960e Differences in shape and size of neuroglial nuclei in the spinal cord due to individual regional and technical variations. Acta Anat. (Basel) 40: 149–177

——— 1960f The post mortem origin and mechanism of neuronal hyperchromatosis and nuclear pyknosis. Exp. Neur., 2: 379–405.

——— 1960g The distribution of oligodendrocytes in cerebral gray and white matter of several mammals. Am. J Anat., *107* 107–127

——— 1960h Is the perivascular oligodendrocyte another element controlling the blood supply to neurons? Angiology *11* 508–517

——— 1961 The importance of avoiding "dark" neurons in experimental neuropathology Acta Neuropath., *1* 245–270.

——— 1962a An evaluation of the significance of the "dark" neuron. Ergebn. Anat. Entwicklungsgesch., *36* 1–61

——— 1962b Two mammalian Purkinje neuron types. In Livre Jubilaire Docteur Ludo van Bogaert, Acta Med. Belg., Bruxelles.

——— 1963a Cytological manifestations of aging in rabbit and chinchilla brains. J Gerontol. (in press)

——— 1963b Peripheral chromatolysis after mouse facial nerve transection. Acta Neuropath., 2: 213–230.

Cammermeyer J and R. L. Swank 1951 The effect of anaesthetics and picrotoxin on the tissue phosphatases in the cerebellum and olivary nucleus of the dog. Acta Pharmacol. et Toxicol., 7 65–82.

Carrea, R. M. E., M. Reissig and F A. Mettler 1947 The climbing fibers of the simian and feline cerebellum. Experimental inquiry into their origin by lesions of the inferior olives and deep cerebellar nuclei. J Comp Neur., 87 321–365.

Duncan, D. 1953 On the incidence and locations of nerve cells in the spinal white matter of two species of primates, man and the cynomolgus monkey Ibid., *99* 103–115.

Fox, C. A. 1959 The intermediate cells of Lugaro in the cerebellar cortex of the monkey Ibid., *112*: 39–53.

Fox, C. A., and J W Barnard 1957 A quantitative study of the Purkinje cell dendritic branchlets and their relationship to afferent fibres. J Anat., *91* 299–313.

Gray E. G. 1961 The granule cells, mossy synapses and Purkinje spine synapses of the cerebellum light and electron microscope observations. Ibid., *95* 345–356.

Jansen, J and A. Brodal 1958 Das Kleinhirn. In Nervensystem, Handbuch der mikroskopischen Anatomie des Menschen, W v Möllendorff und W Bargmann, eds. Springer Verlag, Berlin-Göttingen-Heidelberg, Ergänz. Bd. 4/1 8. Teil.

Kamimura, T 1933 Die Verteilung der Neuroglia im menschlichen und tierischen Rückenmark. Folia Psychiat. Neur. Jap., *1* 86–99

Kappers, C. U A., G. C. Huber and E. C. Crosby 1936 The Comparative Anatomy of the Nervous System of Vertebrates, Including Man. The Macmillan Co., New York, Vol. 1.

Koenig, H., and K. Barron 1962 Morphologic and enzymic alterations of reacting glia in an experimental demyelinating lesion. Anat. Rec *142* 249.

Kreyssig, F 1885 Über die Beschaffenheit des Rückenmarks bei Kaninchen und Hunden nach Phosphor und Arsenikversorgung nebst Untersuchungen über die normale Structur desselben. Virchow' Arch. Path. Anat., *102*: 286–296.

Kryspin-Exner W 1943 Beiträge zur Morphologie der Glia im Nissl-Bilde Z. Anat. Entwicklungsgesch *112* 389–416.

Levi, G. 1897 Ricerche citologiche comparate sulla cellula nervosa dei vertebrati. Riv Pat. Nerv Ment., 2 193–225.

Lumsden, C. E. 1958 Histological and histochemical aspects of normal neuroglia cells. In Biology of Neuroglia, W F Windle, ed. Charles C Thomas, Springfield, Illinois.

Lumsden, C. E., and C. M. Pomerat 1951 Normal oligodendrocytes in tissue culture. A preliminary report on the pulsatile glial cells in tissue culture from the corpus callosum of the normal adult rat brain. Exp. Cell Res., 2: 103–114

Olszewski, J 1947 Zur Morphologie und Entwicklung des Arbeitskerns unter besonderer Berücksichtigung des Nervenzellkerns. Biol. Zbl., 66 285–304.

Palay S. L., S. M. McGee-Russell, S. Gordon and M. A. Grillo 1962 Fixation of neural tissues for electron microscopy by perfusion with solutions of osmium tetroxide. J Cell. Biol., 12: 385–410.

Pannese, E. 1958 Sulla picnosi fisiologica e sui caratteri del nucleo dei gliociti dell uomo. Sist. Nerv 10 124–133.

Penfield, W and W Cone 1926 Acute swelling of oligodendroglia. A specific type of neuroglia change. Arch. Neur Psychiat., 16 131–153

Rasmussen, G. L. 1957 Selective silver impregnation of synaptic endings. In New Research Techniques of Neuroanatomy W F Windle, ed. Charles C Thomas, Springfield, Illinois.

Rexed, B and A. Brodal 1951 The nucleus cervicalis lateralis. A spino-cerebellar relay nucleus. J Neurophysiol., 14 399–407

Roback, H. N and H. J Scherer 1935 Über die feinere Morphologie des frühkindlichen Gehirns unter besonderer Berücksichtigung der Gliaentwicklung. Virchow' Arch. Path. Anat., 294 365–413.

Scheibel, M. E., and A. B. Scheibel 1954 Observations on the intracortical relations of the climbing fibers of the cerebellum. A Golgi study J Comp. Neur 101 733–763

——— 1958 Neurons and neuroglia cells as seen with the light microscope. In Biology of Neuroglia, W F Windle, ed. Charles C Thomas, Springfield, Illinois.

Schroeder A. H 1935 Gliarchitektonik des Zentralnervensystem. In Anatomie, W Spielmeyer ed. Handbuch der Neurologie, O. Bumke und O. Foerster eds. Julius Springer Berlin, Band 1

Smart, I. 1961 The subependymal layer of the mouse brain and its cell production as shown by radioautography after thymidine-H³ injection. J Comp. Neur 116 325–347

Smart, I., and C. P Leblond 1961 Evidence for division and transformations of neuroglia cells in the mouse brain, as derived from radioautography after injection of thymidine-H³ Ibid., 116 349–367

Terranova, R., F Vanni and R. Spiezzi 1962 Permeability of the neuronal membrane to the psychotropic drugs. IV Int. Kongr. Neuropath., H. Jacob, ed. Stuttgart, Georg Thieme (Thema 1) Vol. 1 pp. 233–238.

Weber A. 1959 Microneurones dans la substance blanche de la moelle épinière chez des mammifères. Schweiz. Arch. Neur Neurochir. Psychiat., 84: 222.

Weil, A. 1926 The form of the anterior horn cells of vertebrates. Trans. Amer Neur Assoc., 52: 547–558.

ADDENDUM

Two additional animal species were studied after acceptance of this paper for publication. In the weasel (Weal-082962C) the gray matter oligodendrocyte nuclei and cerebellar granule cell nuclei were distinguished by a prominent central basophil mass and several large-sized *peripheral basophil bodies, as characteristic of type 2*, and in the three-toed sloth (Slo3-030563C) by an intricate basophil network to which number of small basophil granules are attached, as characteristic of type 3. These observations are in agreement with previous conclusions (compare p. 120) It is of interest that the nuclear chromatin was more conspicuous in the weasel than in the larger representatives of the genus Mustela studied here

PLATES

Abbreviations (Plates 1–6)

a, astrocyte nucleus
d, delta nucleus in intervascular strand of connective tissue fibers
e, endothelial nucleus
G, Golgi type II neuron
m, microglia cell nucleus
n, neuron
o, oligodendrocyte nucleus
s, intervascular strand of connective tissue fibers
t, twigs of perivascular connective tissue fibers
v blood vessel
x, perivascular macrophage (?)

General explanation of figures

Most of the microscopic sections are PASG-stained, while the section for figure 3 is Mallory PTAH and for figure 96 is Feulgen stained. The linear magnification is × 2,500 throughout, except for × 760 in figures 91 and 92 and × 95 in figures 93–95.

PLATE 1

EXPLANATION OF FIGURES

Types of nuclei in cerebellar granule cell layer and brain stem of cat (C1 101559C)

1	Golgi type II neuron.
2	Astrocyte nucleus.
3	Astrocyte nucleus and glia fibers.
4	Microglia cell nucleus.
5 and 6	Endothelial nucleus.
7	Histiocyte nucleus.
8 to 14	"Delta" nucleus.
15	Macrophage (?)
16	Oligodendrocyte.
17 to 19	Oligodendrocyte nucleus in floor of fourth ventricle.


G
h
a
a
2
m
v
C
v
v
6
v
h
7
s
d
v
s
d
v
9
s
d
v
10
s
d
v
s
d
v
d
v
11
d
v
12
v
13
14
x
15
v
16
17
18
19

PLATE 2

EXPLANATION OF FIGURES

Gray matter oligodendrocytes in various regions of mulatta macaque (MI 121158C)

20	Fifth cortical layer of motor cortex.
21	Hippocampal H2 region.
22	Thalamic reticular nucleus.
23	Caudate nucleus.
24	Floor of fourth ventricle
25	Gray matter of pons.
26	Dentate nucleus, near "blue" neuron.
27	Gray matter bridges between caudate nucleus and putamen.
28 and 29	Reticular formation, next to "pink" neuron.
30 and 31	Ambiguous nucleus, next to "pink" motor neuron.
32	Spinal cord C7 next to "pink" motor neuron.
33	Spinal cord C7 next to "blue" motor neuron.
34	Spinal cord T12, next to "pink" motor neuron.
35	Spinal cord T12, next to "blue" motor neuron.
36	Intermedio-lateral substance of spinal cord T12, next to blood vessel to "pink" neuron.

20 21 22 23 24 25 26 27 28 29 30 31 32 33 34 35 36

PLATE 3

EXPLANATION OF FIGURES

White matter oligodendrocytes and cerebellar granule cells in various regions of mulatta macaque (MI 121158C)

37 and 38 Optic tract.

39 Fimbria.

40 Alveus over hippocampal H2 region.

41 Corpus callosum.

42 Subjacent to motor cortex

43 Centrum ovale.

44 Cortico-spinal tract of pons.

45 Lateral funicle of spinal cord C7

46 Lateral funicle of spinal cord C7 microglia cell nucleus (?)

47 Internal capsule.

48 Lateral funicle of spinal cord C7

49 Lateral funicle of spinal cord T12.

50 Anterior funicle of spinal cord T12.

51 Cerebellar hemisphere, white matter

52 Vermis white matter

53 Lobulus simplex.

54 Bottom of fissura prima.

55 Top of crus I.

56 Around bottom of secondary sulcus crus I.

57 Vermis.

58 Floccul s

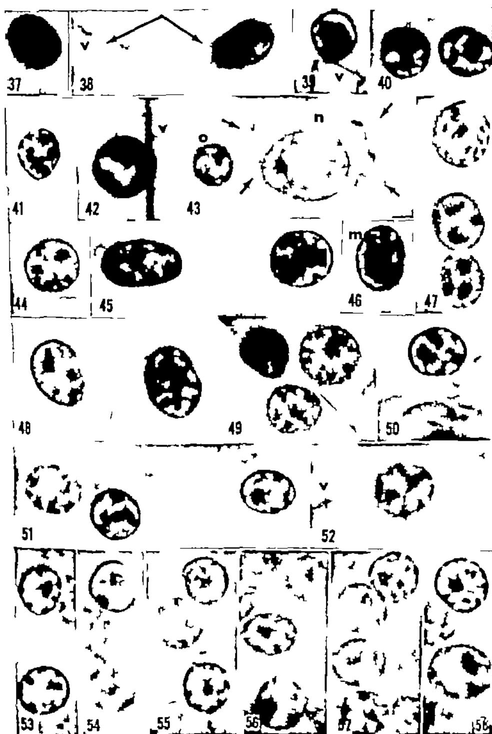

37
38
v
39
40
41
42
43
o
n
44
45
46
m
47
48
49
50
51
52
53
54
55
56
57
58

PLATE 4

EXPLANATION OF FIGURES

59 I reticular formation oligodendrocyte (?) cat, eight days old, (C4-061359C)

60 In floor of fourth ventricle, oligodendrocyte (?) cat, 33 days old (C3-061259C)

61 In floor of fourth ventricle, oligodendrocyte nucleus cat, 144 d ys old (C1 101559C)

62 and 63 In brain stem immature perivascular cells, same section in figure 59

64 From cerebellar granule cell layer inner same section in figure 59

65 Ibid, same section i figure 60

66 Ibid, same section in figure 61

67 Floor of fourth ventricl oligodendrocyt nucleus, rabbit 38 days old (Ra4-040561C)

68 Ibid, rabbit, 70 d ys old (Ra1-050561C)

69 Ibid, rabbit, 185 days old (Ra1-021061C)

70 Ibid, rabbit, 344 days old (Ra4-040461C)

71 Ibid rabbit 658 days old (Ra1-040461C)

72 Ibid, rabbit 929 days old (Ra2 122057C)

73 From cerebellar granule cell l yer same section in figure 67

74 Ibid same section in figure 68

75 Ibid, same section in figure 69

76 Ibid, same section in figure 70.

77 Ibid same section in figure 71

78 Ibid same section i figure 72.

79 In floor f fourth ventricle, oligodendrocyte ucleus, pigeon ten months old (P1-000861C)

80 Ibid, pigeon, one nd one-half years old (P3-000861C)

81 Ibid pigeon six years old (P2-120258C)

82 Ibid dog four and three-fourth years old (D1-031159C)

83 Ibid, dog, fifteen nd one-third years old (D1-081701C)

84 From cerebell granule cell layer same section in figure 79

85 Ibid same section in figure 80

86 Ibid, same section in figure 81

87 Ibid, same section i figure 82

88 Ibid, same section in figure 83

89 Ibid astrocyte with intensely PAS-stained juxtanuclea m sive inclusion body indicated by arrow same section i figures 83 and 88

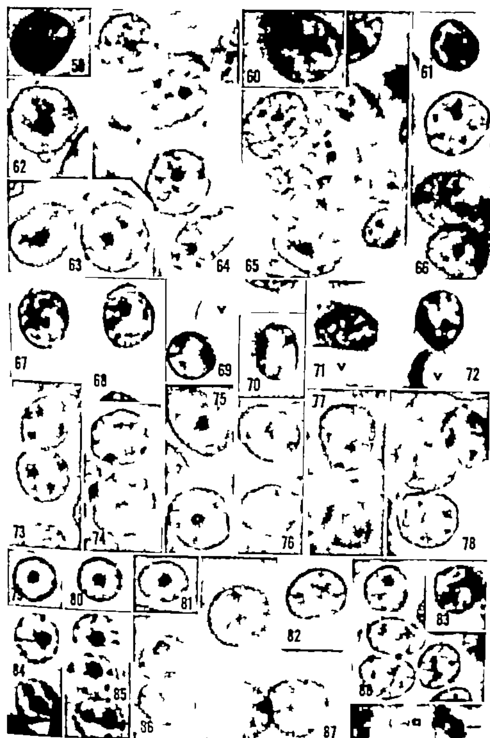

58
60
61
62
63
64
65
66
67
68
69
70
71
72
73
74
75
76
77
78
79
80
81
82
83
84
85
86
87
88

PLATE 5

EXPLANATION O FIGURES

90	In ventro-lateral funicle of spinal cord T12, neuron in longitudinal section mulatta macaque (MI 1211560)
91 and 92	In brain stem, cat (C1 101559C)
93 t 95	Cerebellum, ibid.
96	From cerebellar granule cell layer ibid.
97 and 98	In floor of fourth ventricle, oligodendrocyte nuclei, guinea pig (GP2 112558C)
99 and 100	From cerebellar granule cell layer top of leaflet and bottom of fissure respectively ibid.
101	Vacuoles in nuclear chromatin, print developed with high degree of contrast, same as figure 100
102	I cochlear nucleus, gra ule cell nucleus ibid.

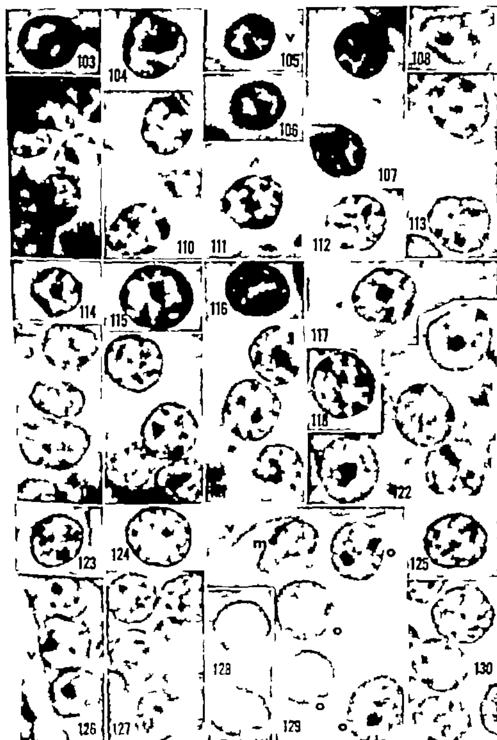

90
91
92
93
94
95
96
97
98
99
100
101
102

PLATE 6

EXPLANATION OF FIGURES

Floor of fourth ventricle and cerebellar cortex in various species.

103	Oligodendrocyte nucleus, mouse (M 1-010459C)
104	Ibid hamster (Ham2-121758C)
105 and 106	Ibid, rat (R5-011361CuC)
107	Ibid, raccoon (Rac1-032659C)
108	Ibid, woodchuck (Woc1-090801C)
109	Granule cell nuclei, same section in figure 103.
110	Ibid same section in figure 104
111	Ibid same section in figures 105 and 106.
112	Ibid, same section in figure 107
113	Ibid same section in figure 108
114	*Oligodendrocyt nucleus, mink (Mink1 103101C)*
115	Ibid opossum (OpV 1-020557C)
116	Ibid, cynomolgu macaque (M1-092358C)
117 and 118	Ibid, two-toed sloth (Sl 1 112801C)
119	Granule cell nuclei, same section in figure 114
120	Ibid same section i figure 115
121	*Ibid same section in figure 116.*
122	Ibid same section in figures 117 and 118.
123	Oligodendrocyte nucleus ferret (Fer2 110301C)
124	Ibid hinchill (Chin2-092358C)
125	Ibid squirrel monkey (SqM1-040460C)
126	Granule cell uclei, same section in figure 123.
127	Ibid same section in figure 124
1.8	Ibid sk nk (Skk1-030901C)
129	Oligodendrocyte nuclei ame section in figure 128
130	Granule cell nuclei, same section in figure 123


103
104
105
106
107
108
110
111
112
113
114
115
116
117
118
122
123
124
125
126
127
128
129
130

The Cardiac Plexus in Man[1]

NICHOLAS JAMES MIZERES
Department of Anatomy Wayne State University College of Medicine Detroit, Michigan

Senac (1749) stated that Fallopius was the first to describe the cardiac plexus. Senac also presented the views of Willis, Vieussens Lancisi, Winslow Walther Lieutand, and Haller He described "superficial" and deep" or superior and "inferior" cardiac plexuses. Murray (1772) considered a great cardiac plexus between the aorta and pulmonary trunk and a superficial" cardiac plexus in relation to the arch of the aorta. Valentin (1843) described a superior plexus around the brachiocephalic and carotid arteries and the arch of the aorta, and an "inferior plexus within the pericardium related to the arterial and venous parts of the heart. Soulié ('04) described a superficial cardiac plexus behind the aorta and pulmonary trunk and a deep cardiac plexus behind the aorta and in front of the trachea. Perman ('24) described two parts of the cardiac plexus as passing anterior and posterior to the transverse pericardial sinus. Hovelacque ('27) abandoned the concept of a deep and superficial cardiac plexus and related the plexus to the arterial and venous ends of the heart. Tinel ('37) also related it to the arterial and venous ends of the heart and stated that the deep cardiac plexus lies behind the aorta and in front of the tracheal bifurcation. Licata ('54) in his account of the embryonic heart, used the terms truncoconal cardiac plexus and sinoatrial cardiac plexus. None of these authors illustrated a plexus at the level of the tracheal bifurcation. Investigation of a number of texts (Boyd, '56; Durward, '53 Goss '59 Grant, '58 Hafferl, '53; Hollinshead '56; Hovelacque, '27; Johnston and Whillis, '54; Kuntz, '53 Larsell, '53 Mitchell, '56; Piersol, '23; White et al. '52 and Woodburne, '61) revealed variable interpretations and descriptions of the cardiac plexus. The description of the nerves contributing to the cardiac plexus also varied with each text or author. The purpose of this study is to offer a new and more logical description of the cardiac nerves and plexus in man.

MATERIALS AND METHODS

The trunks of 21 fetuses and newborns, five infants ranging from one to three years, and ten adults were dissected for this study Three of the fetuses were embalmed. However in these specimens, the fine nerve filaments were easily torn when the connective tissue was teased away during dissection. The remaining fetuses and newborns and all of the infants and adults were embalmed. In three of the embalmed fetuses, the arteries were injected with latex. This facilitated the dissection of vessels but not nerves. Much of the dissection of the cardiac plexuses was carried out under observation with a dissecting microscope.

OBSERVATIONS AND DESCRIPTION

The cardiac plexus

Dissection consistently revealed that the cardiac plexus lay on the anterior and posterior walls of the pulmonary trunk at its bifurcation and consisted of subsidiary plexuses to the great vessels and walls of the heart. These subsidiary plexuses may be named the right and left pulmonary the right and left atrial the right and left coronary and the plexus on the arch of the aorta. In view of these findings and proposed pattern of terminology the present concept of the pulmonary plexuses must be revised. The pulmonary plexuses are usually described as consisting of anterior and posterior parts in the region of

[1] Supported by U. S. Public Health Grant H-3436 and Michigan Heart Association Grant.

the hilus of the lung. However these parts are inseparable from the adventitial plexuses at the origin of the pulmonary arteries. The pulmonary plexuses should therefore be considered as being formed by cardiac nerves at the origins of the right and left pulmonary arteries, and continuing *in the adventitia of these vessels* to the hilus of the lung, where each plexus also receives both anteriorly and posteriorly branches of the vagus nerves and thoracic sympathetic trunks. The right and left pulmonary plexuses as they course in the adventitia of the pulmonary arteries send extensions to the wall of the *heart under the epicardium.*

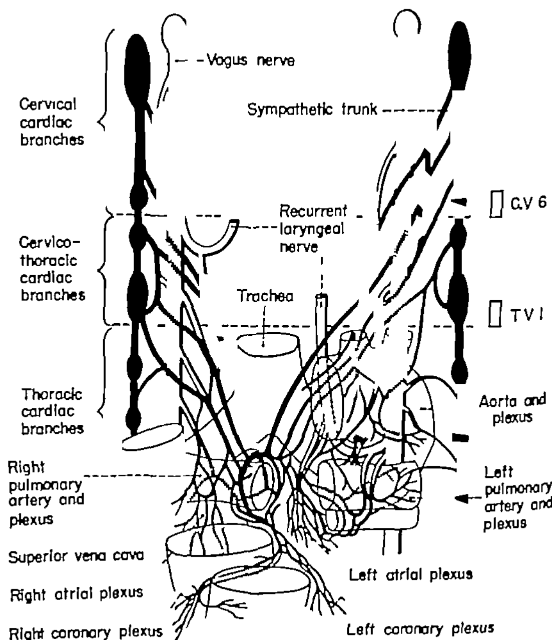


Fig 1 A diagram of the proposed terminology and description of the cardiac plexus and nerves.

The right atrial plexus, an extension of the right pulmonary plexus courses between the superior vena cava and ascending aorta and into the posterior wall of the right atrium (fig 1) *The left atrial plexus*, an extension of the left pulmonary plexus, courses directly into the left posterior atrial wall, and sends filaments into both posterior walls of both ventricles (fig 1) The right and left coronary plexuses receive filaments from the plexus on the arch of the aorta but are formed mainly from extensions of the right pulmonary plexus (fig. 1) Both coronary plexuses also send filaments to the anterior surface of the walls of both ventricles. The plexus on the arch of the aorta (fig 1) sends filaments which course in the wall of the pulmonary trunk to the right and left coronary plexuses. Occasionally a ganglion (ganglion of Wrisberg) was observed in the plexus of the arch of the aorta, or associated with one of the cervical cardiac branches lying between the arch of the aorta and pulmonary trunk (fig 4A) Soulié ('04) considered it in the deep plexus. Grossly it was not observable as a constant ganglion in this study

The cardiac branches of the sympathetic trunk

The cervical cardiac branches The cervical cardiac branches, which vary from one to three in number arise from any part of the cervical sympathetic trunk, including the superior and middle cervical ganglia, down through the level of the lower border of the sixth cervical vertebra (fig. 1) Those which arise from the right trunk join and course posterior to the common carotid artery Before this conjoined nerve reaches the aorta it fuses with one or two cervicothoracic cardiac branches, and with the cervical and at least one of the cervicothoracic cardiac branches of the vagus nerve. Then *as a single or some*times double nerve it courses between the aorta and right bronchus. Upon reaching the adventitia of the right pulmonary artery it forms a major part of both pulmonary plexuses (fig. 1) Sometimes a right cervical cardiac branch after uniting with a cervical cardiac branch of the vagus, may course anterior to the arch of the aorta and join the pulmonary and coronary plexuses directly (fig 4B) The right cervical cardiac branches together with small branches from the vagus and phrenic nerves send filaments into the thymus.

The branches which arise from the left cervical sympathetic trunk are usually interconnected before descending behind the left common carotid artery As a group of filaments they course between the aorta and left bronchus to enter the left and right pulmonary plexuses. Usually a cervical branch *fuses with the left cervical* cardiac branch of the vagus and as a single nerve courses anterior to the aorta, contributing to the plexus on the aorta and *sending a contribution to the coronary* plexuses (figs. 1 4)

The cervicothoracic cardiac branches The right cervicothoracic cardiac branches, *two or three in number arise from* the seventh, eighth and first thoracic levels of the sympathetic trunk, in relation to the seventh cervical and first thoracic vertebrae (fig. 1) They usually arise from the ansa subclavia and cervicothoracic (stellate) ganglion and sometimes from the vertebral ganglion. Before reaching the right bronchus they fuse with the cervical sympathetic group and with the cervicothoracic branches of the vagus nerve. They course as several filaments between the aorta and right bronchus and contribute to the right pulmonary plexus and sometimes directly to the right coronary plexus Often these cervicothoracic cardiac branches send filaments which fuse with the trunk of the thoracic vagus.

The left cervicothoracic cardiac branches arise from the corresponding vertebral levels of the left sympathetic trunk. They course between the aorta and left bronchus and contribute to the left pulmonary plexus (fig. 1) A few filaments course anterior to the aorta and contribute to the plexus of *the arch of* the aorta (fig. 1) The left cervicothoracic branches usually do not join any of the cervicothoracic branches of the vagus nerve

The thoracic cardiac branches. The right thoracic cardiac branches arise from the sympathetic trunk below the level of the lower border of the first thoracic vertebra and above the levels of the fourth

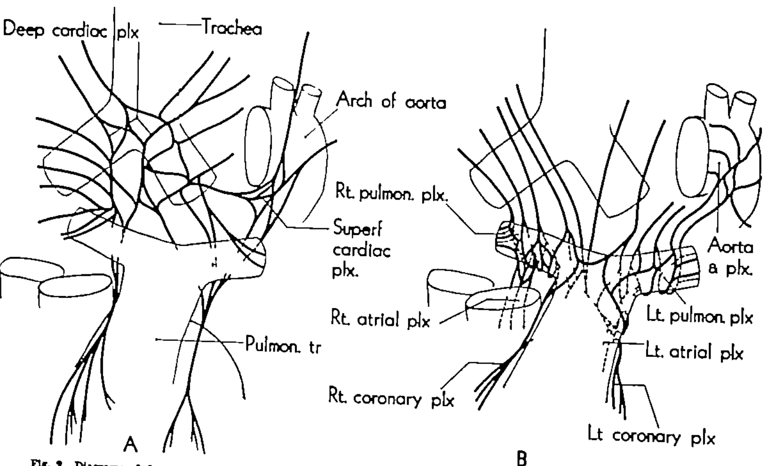


Fig. 2 Diagrams of the present concept and the proposed description of the cardiac plexus. Diagram A shows the deep cardiac plexus in front of the tracheal bifurcation. Diagram B bows the cardiac plexus beginning on the adventitia of the pulmonary trunk at its bifurcation.

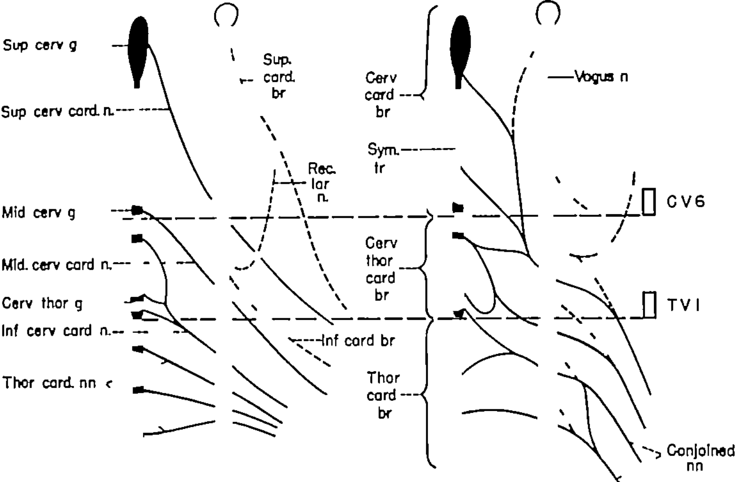


Fig. 3 Diagrams of the present concept and the proposed terminology of the cardiac branches. Diagram A shows the present concept of the cardiac nerves and diagram B the proposed terminology Note that in diagram A the thoracic cardiac branches f the vagus are not named.

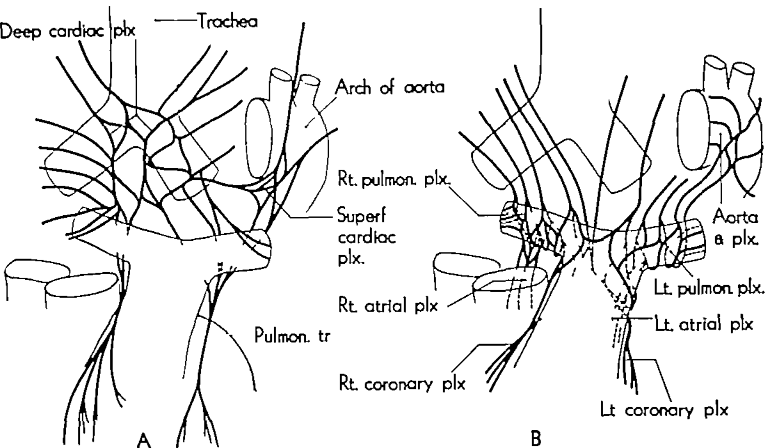


Fig. 2 Diagrams of the present concept and the proposed description of the cardiac plexus. Diagram A shows the deep cardiac plexus in front of the tracheal bifurcation. Diagram B bows the cardiac plexus beginning on the adventitia of the pulmonary trunk at its bifurcation.

or fifth thoracic vertebra. They vary from one to three in number and usually fuse immediately with at least one of the cervicothoracic cardiac branches of the sympathetic trunk and with one of the thoracic cardiac branches of the vagus nerve. They contribute directly to the right pulmonary and atrial plexuses (fig 1)

The left thoracic cardiac branches arise from the corresponding vertebral levels of the sympathetic trunk. In contrast to the right group they do not fuse immediately with other cardiac branches. They vary from two to four in number and send fine filaments into the plexus on the arch of the aorta, directly into the thoracic vagal trunk, and also to the left pulmonary and atrial plexuses (fig 1)

The cardiac branches of the vagus nerve

The cervical cardiac branches The cervical cardiac branches arise from any part of the cervical part of the vagus as far inferiorly as the lower border of the sixth cervical vertebra. In a few specimens, no cervical cardiac branches were found. In most of the specimens, the vagus nerve gives off a single branch which usually fuses with the cervical cardiac branches of the sympathetic trunk. The right cervical cardiac branch usually fuses with a right cervical cardiac branch of the sympathetic trunk, coursing posterior to the aorta and entering the pulmonary plexuses. The left cervical cardiac branch usually receives a contribution from a left cervical cardiac branch of the sympathetic trunk, and, as a single filament, descends anterior to the carotid sheath and to the arch of the aorta, contributing to the plexus on the arch of the aorta and to the coronary plexuses (fig 1) Sometimes, both the right and left cervical branches course anterior to the arch of the aorta, contributing to the plexus on the arch of the aorta and to the coronary plexuses (fig. 4B)

The cervicothoracic cardiac branches The right cervicothoracic cardiac branches arise from the right recurrent laryngeal nerve near its origin and from the vagal trunk at the levels of the seventh cervical and first thoracic vertebrae (fig. 1) Near their origins they usually join the right cervical and cervicothoracic cardiac branches of the sympathetic trunk. They thus course as conjoined nerves before reaching the right pulmonary plexus The left cervicothoracic cardiac branches, one or two in number arise from the left vagal trunk at the level of the seventh cervical and first thoracic vertebrae. They usually course anterior to the arch of the aorta, contributing to the plexus on the arch of the aorta and left atrial plexus (fig. 1)

The thoracic cardiac branches The right thoracic cardiac branches arise from the thoracic vagal trunk between the level of the lower border of the first thoracic vertebra and the pulmonary hilus. They vary from two to four in number and join the cervicothoracic or thoracic cardiac branches of the sympathetic trunk before coursing anterior to the right bronchus After joining the right pulmonary plexus, filaments of these branches can easily be followed into the right atrial plexus (fig 1) The left thoracic cardiac branches arise from the left recurrent laryngeal nerve and from the vagal trunk just below the origin of the left recurrent nerve One group of filaments which arises from the left recurrent laryngeal nerve as it courses posterior to the arch of the aorta, joins the left atrial plexus directly (fig. 1) The other group of nerves at first courses anteriorly to join the left pulmonary plexus and then courses posteriorly in the fold of the left superior caval vein (fold of Marshall) to reach the left atrial plexus (fig. 1). For this reason Worobiew ('28) named this fold the "plica nervina atrii sinistri. Although no sympathetic cardiac branches join the left thoracic cardiac branches these nerves may conceivably carry sympathetic fibers since the left thoracic cardiac branches of the sympathetic trunk send filaments directly into the trunk of the thoracic vagus (fig. 1)

The thoracic cardiac branches have not been emphasized in most texts. But the author ('35 '37 '38) has shown that in the dog the thoracic cardiac branches of the vagus nerve fuse with some thoracic sympathetic cardiac branches and thereby carry not only the majority of the cardio-

inhibitory fibers but also many cardioaccelerator fibers.

DISCUSSION

The sympathetic and vagal cardiac branches of the same side usually fuse before they reach the heart and great vessels (figs. 1 and 4) There are few if any plexiform connections between the nerves of the right and left sides before these nerves reach the heart and great vessels. Thus, a definite plexus at the level of the tracheal bifurcation was not observed in any of the 36 specimens dissected. Instead, true plexuses were observed only after the nerves reached the adventitia of the great vessels or penetrated the pericardium to reach the wall of the heart under the epicardium (fig 1) The deep and superficial cardiac plexuses are not separate groups located at the level of the tracheal bifurcation, behind, or in front of or in the concavity of the arch of the aorta. Instead the deep cardiac plexus is the plexus on the wall of the pulmonary arteries whereas the superficial cardiac plexus is the anterior part of the plexus on the arch of the aorta (fig. 2) Mitchell ('56) also suggests that the superficial and deep cardiac plexuses are created only by artificial dissection In addition the Nomina Anatomica ('61) lists only a cardiac plexus.

The usual pattern, as stated in texts, that *the superficial cardiac plexus receives* the left superior cervical sympathetic and the inferior cardiac branch of the vagus while the deep plexus receives all the rest of the cardiac nerves was found in only two of the 36 specimens studied. It was also observed that the cervical cardiac nerves were more variable than the thoracic nerves. In many instances the so-called superior cardiac branch of the vagus was absent (fig. 4) In addition the course and origin of the cervical cardiac nerves and occasionally lower branches were extremely variable on both sides arising from any part of the vagus nerve and cervical sympathetic trunk, and coursing anterior or posterior to the arch of the aorta (fig. 1) It was also noted that many of the cardiac nerves before reaching the tracheal bifurcation or the great vessels fused or were connected with other cardiac nerves of the same side. The identity of each of these cardiac nerves was therefore lost. On the basis of the observations in this study it seems necessary to abandon the present terminology and description of the cardiac nerves (superior middle and inferior) since no constant pattern could be formulated from these 36 dissections.

A major problem in formulating a new terminology is deciding which of several possible criteria for naming the branches is the most logical and useful. The nerves could be named, for example according to the numbered cervical spinal nerves, according to the ganglia of the sympathetic trunk, or according to the vertebral levels of the sympathetic trunk. However the number of cardiac nerves does not correspond to the number of the cervical spinal nerves Nor do the rami communicantes to these nerves help in identification of the cardiac branches because they carry postganglionic fibers to the corresponding spinal nerves and are not related to the number of cardiac branches. Although the present terminology (Nomina Anatomica) relates the description of cardiac branches to the ganglia of the sympathetic trunk cardiac nerves arise from any part of the sympathetic trunk (fig. 1) The middle cervical and vertebral ganglia may be absent. When present, they may be fused and are often related to the inferior thyroid and vertebral arteries respectively (Wrete, '59) A cervicothoracic ganglion (Nomina Anatomica term) is present more often than an inferior cervical and first thoracic ganglion (Jamieson, Smith and Anson, '52; Wrete '59) Additional confusion results from the fact that in the Nomina Anatomica, the cervical sympathetic cardiac branches are named *nerves* whereas the vagal cardiac branches are named *branches* Finally no thoracic cardiac branches of the vagus nerve are listed (Nomina Anatomica '61) Furthermore the cardiac branch of the cervicothoracic ganglion is named the inferior cervical cardiac nerve although if the principles of the Nomina Anatomica were followed, it would be named cervicothoracic cardiac nerve or branch *The presence of the* cervicothoracic ganglion makes it difficult if not impossible to determine grossly the

TABLE 1

In the left hand column the terms are listed according to the Nomina Anatomica ('61). In the right hand column the proposed terms are listed.

Nomina Anatomica, 1961	Proposed terminology
Superior cervical cardiac nerve of the superior cervical ganglion	Cervical cardiac branches of the sympathetic trunk
Middle cervical cardiac nerve of the middle cervical ganglion	Cervical cardiac branches of the sympathetic trunk
Inferior cervical cardiac nerve of the cervicothoracic ganglion	Cervicothoracic cardiac branches of the sympathetic trunk
Thoracic cardiac nerves of the sympathetic trunk	Thoracic cardiac branches of the sympathetic trunk
Superior cardiac branches of the vagus nerve	Cervical cardiac branches of the vagus nerve
Inferior cardiac branches of the vagus nerve	Cervicothoracic cardiac branches of the vagus nerve
N term listed	Thoracic cardiac branches of the vagus nerve.

inferior limit of the cervical sympathetic trunk and thereby to name a branch of the ganglion cervical or "thoracic. In view of the considerations and difficulties described above it was obvious that the nerves should be named according to the vertebral level of origin. It also seemed desirable to make the proposed terminology more uniform by using the term *branches* for those from the sympathetic trunk and ganglia, giving, for example cardiac *branches* of the sympathetic trunk. A comparison of the two terminologies of the cardiac nerves is depicted in table 1 and illustrated in figure 3

According to Mitchell ('56) cardiac nerves arising inferior to the stellate ganglion were known to Swan in 1830 Ionescu and Enachescu ('58) and Kuntz and Morehouse ('30) studied these thoracic cardiac branches in fetuses and adult cadavers. None of these authors were able to find nerves arising inferior to the fourth thoracic ganglion and reaching the cardiac plexus. Kuntz and Morehouse ('30) state that the nerves from the fifth and sixth thoracic ganglia could be traced toward the aorta. Their illustration depicts a deep cardiac plexus on the wall of the descending thoracic aorta. It is quite possible that this cardiac plexus may have been mistaken for the plexus on the thoracic aorta which received contributions for all parts of the thoracic sympathetic trunk. Saccomanno ('43) who reported no original dissection of human material misinterprets Kuntz and Morehouse and states that cardiac nerves arise from the sixth and seventh thoracic ganglia. In the majority of the specimens in the present study cardiac branches were found arising from the thoracic sympathetic trunk only as far inferiorly as the fourth or fifth thoracic ganglion. This does not preclude the possibility of cardiac sympathetic fibers emerging from the spinal cord inferior to this level and ascending within the thoracic sympathetic trunk.

SUMMARY AND CONCLUSIONS

A thorough dissection of 38 specimens revealed the necessity of a reanalysis of the cardiac plexus and nerves. It is suggested that the following description and terminology (fig 1) be considered. Since most of the cardiac nerves fuse or join with each other before reaching the heart and great vessels the naming of the cardiac nerves should be based upon their vertebral level of origin from the sympathetic trunk or vagus nerve. The cervical (vagal and sympathetic) cardiac branches are limited inferiorly by the lower border of the sixth cervical veterbra, the cervicothoracic (vagal and sympathetic) cardiac branches by the lower border of the first thoracic vertebra, and the nerves arising below the level of the first thoracic vertebra and above the fourth or fifth thoracic vertebra as thoracic (vagal and sympathetic) cardiac branches.

In this study no thoracic cardiac branches of the sympathetic trunk were observed to arise inferior to the fourth or fifth thoracic level of the sympathetic trunk.

The terms superficial" and deep cardiac plexus should be abandoned since these two plexuses are created only by artificial dissection The cardiac plexus is described as lying on the adventitial wall of the pulmonary trunk at its bifurcation and consists of subsidiary plexuses named the right and left pulmonary right and left coronary right and left atrial and the plexus on the arch of the aorta. The plexus on the arch of the aorta is formed mainly by the left cervical and cervicothoracic cardiac branches. The right and left pulmonary plexuses are formed by the cervical the cervicothoracic, and thoracic cardiac branches of both sides. At the hilus of each lung the pulmonary plexuses receive both anteriorly and posteriorly branches of the vagus nerve and sympathetic trunk. The coronary plexuses are formed mainly by extensions of the right pulmonary plexus with some contributions from the left pulmonary and the plexus on the arch of the aorta. The coronary plexuses may also receive direct contributions from the cervical cardiac branches and usually send filaments into the anterior ventricular walls. The right and left atrial plexuses are formed mainly by extensions of the pulmonary plexuses with direct contributions from the thoracic cardiac branches. The left atrial plexus also sends filaments into the posterior ventricular walls. All these plexuses are interconnected. The ganglion of Wrisberg was not observed as a constant ganglion in this study

ACKNOWLEDGMENT

The author wishes to thank Drs. E. Gardner and F Morin for their valuable criticism and advice.

LITERATURE CITED

Boyd, J D 1956 Textbook of Human Anatomy Ed. by W J Hamilton. MacMillan and Co. Ltd., London. 910–911.

Durward, A. 1953 In Cunningham's Textbook of Anatomy Ed. by J C. Brash. 10th ed. Oxford University Press, London, 1139–1140.

Goss C. M. 1959 In Gray's Anatomy of the Human Body 27th ed. Lea and Febiger Philadelphia, 1063–1064.

Grant, J C. B. 1958 A Method of Anatomy 6th ed. Williams and Wilkins Co., Baltimore, 675–676.

Hafferl, A. 1953 Lehrbuch der Topographischen Anatomie. Springerverlag, Berlin, 333–334.

Hollinshead, W H. 1956 Anatomy for Surgeons Vol. 2. The Thorax, Abdomen and Pelvis. Paul B Hoeber Inc., New York. Chap. 1, 119–123

Hovelacque, A. 1927 Anatomi des Nerfs Craniens et Rachidiens et du Systeme Grand Sympathique chez l'homme. Paris. Chap. IV 707–709.

Ionescu, D., and M. Enachescu 1928 Untersuchungen bei Säugetieren und beim Menschen über die aus dem Brustgrenzstrang des Sympathicus unterhalb des Ganglion stellatum entspringenen Herznerven. Ztschr f. Anat., 85 476–478.

Jamieson, R. W D B. Smith and B. J Anson 1952 Quart. Bull. Northw Univ Med. Sch., 216 219

Johnston, T B., and J Whillis 1954 In Gray's Anatomy Descriptive and Applied. 31st ed. Longmans, Green and Co., London New York, Toronto, 1200–1201

Kuntz, A. 1953 The Autonomic Nervous System. 4th ed. Lea and Febiger Philadelphia. Chap. VII, 135–136.

Kuntz, A., and A. Morehouse 1930 Thoracic sympathetic cardiac nerves in man. Arch. of Surgery 20: 607–613.

Larsell, O 1953 In Morris Human Anatomy. 11th ed. Ed. by J P Schaeffer The Blakiston Co., New York and Toronto. Section VIII, 1204–1205

Lauth, E. A. 1835 Nouveau manuel de l'Anatomie. 2nd ed. Levrault, Paris.

Licata, R. H. 1954 The human embryonic heart in the ninth week. Am. J Anat., 94 96–105, 114–116.

Mitchell, G. A. G. 1956 Cardiovascular Innervation. E. and S. Livingstone Ltd., Edinburgh and London. Chap. VIII, 196–238

Mizeres, N J 1955 Isolation of the cardioinhibitory branches of the right vagus nerve in the dog. Anat. Rec., 123 437–445.

——— 1957 The course of the left cardioinhibitory fibers in the dog. Ibid., 127 109–115.

——— 1958 The origin and course of the cardioaccelerator fibers in the dog. Ibid 132 261 279.

Murray A. 1772 Observations anatomicae de infundibulo cerebri et variationibus quibusdam in parte cervicali nerve intercostalis. Upsaliae Scriptores nour. min. sci., II 18–23

Nomina Anatomica 1961 Revised by the International Anatomical Nomenclature Committee appointed by the Fifth International Con-

gress of Anatomists held at Oxford in 1950, and approved by the Sixth and Seventh International Congresses of Anatomists, held in Paris, 1955 and New York, 1960. 2nd ed. Excerpta Medica Foundation, Amsterdam, London, Milan, New York. 63 65–66.

Perman, E. 1924 Anatomische Untersuchung über die Herznerven bei den hoheren Säugetieren und bei Menschen. Ztschr. f. Anat., Abt. I, LXXI 382–457

Piersol, G. A. 1923 Human Anatomy 8th ed. J. B. Lippincott Co., Philadelphia and London, 1367 1369.

Saccomanno, G. 1943 The components of the upper thoracic sympathetic nerves. J Comp. Neur., 79: 355–378.

Senac, J B. 1749 *Traité de la structure du coeur de son action et de ses maladies.* Paris, J Vincent, 116–138.

Soulié A. 1904 Les nerf rachidiens. In Traité d'Anatomie Humaine. Poirer et Charpy Ed. Paris, Masson et cie, Tome Troisieme, 1197–1202.

Tinel, J 1937 Le Systeme Nerveaux Vegetatif Paris, Masson, 226–231

Valentin, G. G. 1843 Traité de Neurologie. Traduction Jourdan. A Paris, 447–448.

White, J C., R. H. Smithwick and F A. Simeone 1952 The Autonomic Nervous System, Anatomy Physiology and Surgical Application. 3rd ed. MacMillan Co., New York. Chap. III, 41–43.

Woodburne, R. T 1961 Essentials of Human Anatomy 2nd ed. Oxford Univ Press, New York. Chap. V 343–344.

Worobiew Von W 1928 Plica nervina atrii *sinistri.* Ztschr. f. Anat., *86* 511–516.

Wrete, M. 1959 The Anatomy of the Sympathetic Trunks in Man. J Anat., 93: 448–459

Influence of Certain Purines and Pyrimidines on the Development of the Down Feather[1]

CHARLES W GIBLEY JR.,[2] AND HOWARD L. HAMILTON[3]
Department of Zoology and Entomology Iowa State University Ames, Iowa

Previous work on the localization of biochemical substances in the developing down feather has revealed a gradient pattern of alkaline phosphatase and its close association with ribonucleic acid in regions of morphogenesis and differentiation (Koning and Hamilton, '54) The evidence suggested that these two substances were interrelated in the formation of proteins, in particular keratin, for the construction of the feather In further investigations on feathers grown in tissue culture, Hamilton and Koning ('56) utilized beryllium which competes with magnesium for the Mg-activated phosphatases and thereby blocks their action. It was found that inactivation of the phosphatase of the pulp curtailed the synthesis of RNA in the epidermis. The authors proposed that this shortage of ribonucleic acid limits the synthesis of proteins and thus precludes further morphogenesis.

Fabiny ('59) obtained similar results with the developing down feather using Versene and β-2-thienylalanine (β-2 T) Versene chelates metallic ions needed by alkaline phosphatase for its activity Inactivation of the enzyme when Versene was added to the feather system markedly affected the synthesis and presence of RNA in the overlying epidermis. He concluded that the resulting decrease of ribonucleic acid limited the synthesis of proteins and inhibited morphogenesis. Beta 2-thienylalanine specifically inhibits the epidermal component. When added to the culture β-2 T caused an abnormal distribution of RNA within the epidermal cells of the inhibited feather It was suggested that β-2 T acts either by (a) preventing the release of RNA from the nucleolus to the cytoplasm or (b) antagonizing the utilization of RNA during the synthesis of peptides and proteins.

It would be of interest to grow the feather in the presence of certain compounds structually related to the purine and pyrimidine bases which are integral parts of the ribonucleic acid molecule. The experiments reported here were undertaken to test the effects of the growth-promoting substance, orotic acid, and the purine and pyrimidine analogs, isoguanine sulfate 8-azaguanine, thiouracil, and 2-amino-4-hydroxy-6-methylpyrimidine, with the hope that the results might further clarify the relationship of RNA and alkaline phosphatase and their role in organogenesis.

MATERIALS AND METHODS

Pieces of skin were removed under sterile conditions from the backs of New Hampshire Red chick embryos between the stages of 29 + and 33 + (6–8 days Hamburger and Hamilton, '51) Pairs of nearly identical pieces of tissue about 1 mm square were obtained in the following manner a strip of dorsal skin about 2 mm wide was isolated by cutting along either side of the mid-dorsal line from the region of the shoulder to the base of the tail, undermining the skin with a needle and severing the strip at its two ends. This piece of tissue was then cut several times at right angles to its length and each rectangular piece was divided into bilateral halves along the mid-dorsal line. Each embryo yielded eight such bilateral pairs. One member of each pair was placed in a tissue culture of the hanging-drop type consisting of one drop of heparinized

[1] This investigation was supported in part by research grant, [illegible], from the Division of Research Grants and Fellowships, National Institutes of Health, U. S. Public Health Service, and by the Industrial Science Research Institute of Iowa State University

[2] Present address Department of Biology Villanova University Villanova, Pennsylvania.

[3] Present address Department of Biology University of Virginia, Charlottesville, Virginia.

chicken plasma, one drop of embryonic extract, and one drop of Pannett-Compton saline solution. The corresponding half was placed in a similar mixture containing one drop of the test solution in place of the saline solution. The numbers of drops of Pannett-Compton solution and of test solution were varied to obtain a variety of final concentrations Cultures were incubated at 37 C for five or six days examined microscopically and treated according to the histochemical procedures described below

The embryonic extract was prepared by passing nine- or ten-day-old chick embryos through a 5-ml syringe, diluting the tissue with twice its volume of Pannett-Compton solution and centrifuging to remove tissue debris. The slightly opalescent supernatant was used in making the cultures.

The test solution was prepared by weighing the required amount of the chemical in a test tube diluting to the desired concentration with Pannett-Compton solution, and sterilizing the resulting solution by passing it through a Seitz filter into a previously-sterilized test tube. Or[illegible] acid, thiouracil, and 2-amino-4-hydroxy-6-methylpyrimidine required heating to near boiling to bring them into solution. Isoguanine sulfate and 8-azaguanine were dissolved in several drops of 0 3N KOH and an equivalent amount of 0.3N HCl was added to neutralize the mixture. Sterile Pannett-Compton solution was then added until the desired concentration was reached. The pH of the saline controls was adjusted to that of the test solution with 0 3N KOH when necessary

Cultures to be stained for alkaline phosphatase by the Gomori method were fixed in cold acetone overnight. After washing with water the control and treated cultures were placed in a substrate mixture containing 25 ml of distilled water and the following amounts of 2% solutions: 10 ml sodium barbital, 10 ml sodium glycerophosphate 4 ml calcium chloride, and 1 ml magnesium sulfate The cultures were incubated in the substrate at 37 C for 45 minutes. They were then washed with distilled water treated with 2% cobalt chloride washed again, and treated with a dilute solution of ammonium hydrosulfide to develop the precipitate of cobalt sulfide at the sites of enzymatic activity

Cultures to be examined histologically were fixed in acetic-alcohol, embedded in bayberry wax paraffin sectioned at 7 μ, stained in 0 025% toluidine blue in 5% ethyl alcohol, and destained in tertiary butyl alcohol. Prior to staining, some sections were treated with ribonuclease to localize ribonucleic acid in the tissue.

RESULTS

The concentrations of the chemicals in the cultures were varied between 3333 μg/ml and 62.5 μg/ml to ascertain the lowest concentration which would affect the development of feathers The results are summarized in table 1 Thiouracil and 2 amino 4 hydroxy 6 methylpyrimidine produced no significant effects except at very high concentrations which were probably toxic.

Orotic acid. The optimal concentration for arresting feather growth in most of the explants was 333 μg/ml. When present, the feathers were smaller and less numerous than in controls. The alkaline phosphatase reaction was markedly affected by the addition of orotic acid to the cultures. The enzyme was either absent from the explant or present diffusely not localized in feather loci (fig 2) In contrast, the control culture showed good feather growth and a strong phosphatase reaction in the pulp immediately below the growing epidermal tip (fig 1) Lower concentrations of orotic acid were added to see if growth of feathers would be stimulated. The control and treated cultures showed about equal growth and intensity of the phosphatase reaction (figs. 1 3)

Serial sections of feathers inhibited by orotic acid were stained with toluidine blue in order to check on the production or distribution of ribonucleic acid. Normally ribonucleic acid occurs in heavy concentration within the cytoplasm of those epidermal cells which lie next to the phosphatase-active pulp and particularly against the basement membrane. The nucleoli usually two per nucleus are small and spherical or ovoid (fig. 6) Ordinarily they stain homogeneously In

TABLE 1

Effect of purines and pyrimidines on growth of feathers

Chemical	Concentration in μg/ml	Number of embryos	Average diameter of control culture	Average diameter of treated culture	Total number of cultures	Number of cultures showing: Reduction in size and number of feathers	Complete absence of feathers	Better growth of feathers	No difference	Per cent inhibition of feathers
Orotic acid	1666	3	4.8	3.6	13	4	9			100
	833	2	4.5	3.7	6	1	5			100
	500	5	5.0	4.4	35	2	33			100
	400	2	3.7	3.5	4	2	2			100
	333	28	4.9	4.6	160	55	67	20	18	76
	266	3	4.8	4.5	14	4		4	6	28
	166	4	4.6	4.4	18	8		8	2	44
	125	4	4.7	4.4	23	5	7	2	9	52
	83.3	4	4.5	4.3	22	6	3	3	10	41
Thiouracil	3333	3	4.8	4.4	12	2	4	1	5	50
	2500	4	3.8	2.7	19	8	10		1	95
	1666	7	4.5	4.1	53	11	26	4	12	70
	666	1	3.9	3.4	3		2		1	66
	333	7	4.8	4.9	44	9	9	8	18	41
2-Amino-4 hydroxy-6-methyl-pyrimidine	1666	10	4.3	3.3	45	15	12	4	14	61
	833	7	4.5	3.5	47	7	19	3	18	55
	666	3	4.6	4.3	17	4		4	9	23
	500	2	4.3	4.1	16	5		6	5	31
	333	2	4.6	4.4	19	1		8	10	0.05
Isoguanine sulfate	1666	2	4.1	4.2	8	2	6			100
	833	6	4.7	3.2	34	5	26	1	2	91
	333	21	4.7	4.4	132	28	75	8	21	78
	166	10	4.4	4.8	72	23	15	7	27	53
8-Azaguanine	1000	4	4.6	2.0	16		16			100
	333	8	4.8	4.1	45	15	24	1	5	86
	166	16	5.0	4.8	100	26	42	4	18	66
	83	4	5.4	5.3	29	5		0	18	17

feathers inhibited by orotic acid the ribonucleic acid, although localized in the epidermis, is more diffuse than in the control Most striking are the multiple *nucleoli of different sizes within the* feather and giant-sized nucleoli outside the feather area. One peculiarity is the attachment of the nucleoli in a string or "chain" form. Another is the appearance of vacuolated or doughnut-shaped nucleoli (fig. 7)

Thiouracil. In contrast to orotic acid, thiouracil had no significant inhibitory effect on feather development at a concentration of 333 μg/ml. Higher concentrations did produce some inhibition but were probably toxic. Cultures stained for alkaline phosphatase showed little effect of thiouracil on the enzyme within the bounds of the original explant, except possibly to intensify the reaction. However there was a tremendous build-up of phosphatase in the peripheral fibroblasts (figs. 12 13)

Several possibilities existed that this strong reaction might be a histochemical artifact (1) thiouracil might bind phos- as calcium normally does, thus giving a false positive reaction (2) thiouracil might release sulfide groups to combine with cobalt and give a precipitate; (3) thiouracil might activate the enzyme directly Three tests were made to check the validity of these possibilities (a) calcium was omitted from the substrate mixture; (b) notice was taken of the time of CoS precipitation during the staining reaction (c) control cultures were immersed in a thiouracil solution (2.5 mg/ml) before fixation, to test for a direct effect on phosphatase. No reaction appeared either in the absence of calcium or in the control cultures immersed in thiouracil before fixation. In addition during the normal staining for phosphatase the black precipitate of cobalt sulfide did not appear until ammonium hydrosulfide was added.

Additional tests were run to determine if the reaction in the presence of thiouracil was truly due to enzymatic action and whether it was specifically caused by thiouracil acting on living cells (1) fixed cultures were placed in hot water for three minutes (6 pairs at 60 C 6 at 85 C; 6 at 100 C) in order to destroy the enzyme (2) uracil (2.5 mg/ml) was added simultaneously with thiouracil (2.5 mg/ml) at the time the cultures were made, to see whether the effects of thiouracil would be nullified (7 pairs) the rationale being that if thiouracil is antagonistic to uracil, the latter should countervail the effects of thiouracil In neither of these experiments was any reaction obtained in the fibroblasts except for a faint positive test in tissues heated at 60 C (due to incomplete destruction of the enzyme) It was concluded that the strong positive test in fibroblasts was a specific effect of thiouracil during development rather than an effect on the staining reaction.

There was no difference noted in the content of ribonucleic acid in control and thiouracil-treated cultures.

8-Azaguanine Concentrations of 333 and 166 μg/ml were the most effective in causing an inhibition of development in feathers. Lower concentrations had no effect.

The intensity of the reaction for phosphatase was at least as strong as in the controls, if not darker At 333 μg/ml, 8-azaguanine disturbed the pattern of phosphatase at the base of the feather and was responsible for the appearance of black splotches throughout the original explant. Fibroblasts in the zone of outgrowth were black in the treated cultures, but not in the controls. The great majority of treated cultures in a concentration of 166 μg/ml showed a very dark reaction which practically obscured any structure within the epidermal part of the explant (figs. 10 11) Fibroblasts stained very strongly in the zone of outgrowth. Their nucleoli were non-reactive. All cells seemed much more sharply delineated in the treated culture

Sections stained for RNA showed the greatest effect at the nucleolar level. The controls had small nucleoli usually two in number (fig. 21) Treated cultures had enlarged nucleoli and frequently contained only one per nucleus (fig 22) The intensity of the reaction was so much increased over the controls that it could be seen grossly

Isoguanine sulfate Concentrations varying from 1 666 μg/ml to 833 μg/ml pre-

vented feather germs from forming in most instances. In a few cases the effect was to reduce the number of feather loci. The phosphatase reaction within the explant was very diffuse (figs. 8 9) In the outlying tissue the fibroblasts were often blackened, but the reaction was not as extensive as that produced by thiouracil.

Lower concentrations (333 to 166 μg/ml) produced smaller and abnormally-shaped feathers which showed a more diffuse and somewhat darker reaction for phosphatase. The original explant was nearly all black (figs. 4, 5) Peripheral fibroblasts were no different from controls

Sections stained with toluidine blue showed that isoguanine sulfate inhibited further specialization within the feather area. Basophilia due to degenerating cells was present, frequently concentrated in the incipient feather loci. There was also a reduction in the number of basophilic cells. The stain was homogeneous never localized within a specific region. The most striking result was the stratified condition of the epithelium, with the nuclei parallel to the surface (fig. 15) Another unusual condition was the presence of large spherical melanoblasts embedded deep in the epidermal part of the feather (fig. 18)

2 amino- 4 hydroxy- 6-methylpyrimidine produced no effect on the histology of the feathers in any of the concentrations used.

Higher concentrations did cause a significant change in the alkaline phosphatase reaction. At 1 666 μg/ml there was a reduction in the extent of the reactive areas and a fusion of the gradients of adjoining feathers (figs. 19 20) In some cases, the treated feathers also showed a splotching of the phosphatase reaction (figs. 16 17) At 833 μg/ml a similar merging of feather areas was noted. There was also a tendency toward smaller size. The intensity of the phosphatase reaction did not change at this concentration. Lower levels (666 to 333 μg/ml) caused no reduction of enzymatic activity but there was a spreading or branching of the reactive areas.

In sections stained for RNA, there was no significant effect, except an increase in the amount of degenerative basophilia in the feather germs of cultures containing high concentrations of the chemical. This was probably a toxic effect.

DISCUSSION

Orotic acid. There is considerable evidence from the literature that orotic acid is a precursor of nucleic acid pyrimidines. Wright, et al. ('51) stated that ureidosuccinic acid is an acyclic biological precursor of the pyrimidine ring. Lieberman and Kornberg ('53 '54, '55) found that orotic acid could be converted to ureidosuccinic acid via dihydro-orotate. This metabolic pathway of the incorporation of orotic acid with nucleic acid pyrimidines has received support from Reichard and Lagerkvist ('53) Cooper Wu and Wilson ('55) and Reynolds, Lieberman and Kornberg ('55) There is recent evidence for the entry of orotic acid into uridine-5' phosphate (Hurlbert and Potter '54 Lieberman and Kornberg, '55 Crawford, Kornberg, and Simms, '57) Uridine-5 phosphate is a uridine nucleotide and could be an intermediate in the incorporation of orotic acid with RNA (Herbert, Potter and Hecht, '57)

Further evidence for the entry of orotic acid into the formation of nucleic acid pyrimidines is found in the work of a number of earlier investigators. Bergstrom, et al. ('49) showed that injected orotic acid was utilized in the biosynthesis of both uracil and cytosine. Buchanan and Wilson ('53) noted that orotic acid is a normal precursor of thymine. Orotic acid will replace uridine in promoting optimal early growth in *Streptococcus* (Hoffmann and Pavcek, '51)

Contrary to expectation orotic acid did not stimulate growth of feathers in any of our experiments. Instead, growth of the whole culture was retarded, and feathers were inhibited even at the lowest concentration (table 1) It does not seem probable that the lack of growth was due to toxicity at the lowest levels used. Other possibilities are that orotic acid diverted synthesis toward a kind of RNA not utilizable by the feather or that it substituted, in an indirect way for some necessary component in the chain of synthesis of RNA.

PLATE 1

EXPLANATION OF FIGURES

1 Control explant of skin from the back of an embryo of stage 30. Note the intense reaction for phosphatase in the pulp of each feather, immediately below the growing epidermal tip. × 70.

2 The corresponding bilateral half of the piece of tissue shown in figure 1, grown in the presence of orotic acid (333 μg/ml of mixed culture medium). Growth of feathers is inhibited and the phosphatase reaction is diffuse. × 70.

3 Explant of a piece of tissue adjacent to those shown in figures 1 and 2, grown in the presence of orotic acid (166 μg/ml). The feathers are normal in appearance and in the localization of phosphatase. × 70.

4 Control explant of skin from an embryo of stage 31 showing normal feathers and an intense phosphatase reaction within the feather germs. × 70.

5 The corresponding bilateral half of the piece of tissue shown in figure 4 grown in the presence of isoguanine sulfate (333 μg/ml). Note the absence of feather germs and the homogeneous distribution of the phosphatase reaction. × 70.

6 Part of cross section of feather in control culture of skin from an embryo of stage 30. Sectioned at 7 μ and stained with toluidine blue. The nucleoli, which usually number two per nucleus, are small and ovoid. × 1,890.

7 Part of cross section of a feather from the corresponding bilateral half of the piece of skin shown in figure 6, grown in the presence of orotic acid (333 μg/ml). Note the vacuolated or "doughnut-shaped" nucleolus. × 1,890.

vented feather germs from forming in most instances. In a few cases, the effect was to reduce the number of feather loci. The phosphatase reaction within the explant was very diffuse (figs. 8 9) In the outlying tissue the fibroblasts were often blackened, but the reaction was not as extensive as that produced by thiouracil.

Lower concentrations (333 to 166 µg/ml) produced smaller and abnormally shaped feathers which showed a more diffuse and somewhat darker reaction for phosphatase. The original explant was nearly all black (figs. 4 5) Peripheral fibroblasts were no different from controls.

Sections stained with *toluidine blue* showed that isoguanine sulfate inhibited further specialization within the feather area. Basophilia due to degenerating cells was present, frequently concentrated in the incipient feather loci. There was also a reduction in the number of basophilic cells. The stain was homogeneous never localized within a specific region. The most striking result was the stratified condition of the epithelium, with the nuclei parallel to the surface (fig. 15) Another unusual condition was the presence of large spherical melanoblasts embedded deep in the epidermal part of the feather (fig. 18)

2 amino- 4 hydroxy- 6-methylpyrimidine produced no effect on the histology of the feathers in any of the concentrations used.

Higher concentrations did cause a significant change in the alkaline phosphatase reaction. At 1,666 µg/ml there was a reduction in the extent of the reactive areas and a fusion of the gradients of adjoining feathers (figs. 19 20) In some cases, the treated feathers also showed a splotching of the phosphatase reaction (figs. 16 17) At 833 µg/ml a similar merging of feather areas was noted. There was also a tendency toward smaller size. The intensity of the phosphatase reaction did not change at this concentration. Lower levels (666 to 333 µg/ml) caused no reduction of enzymatic activity but there was a spreading or branching of the reactive areas.

In sections stained for RNA, there was no significant effect, except an increase in the amount of degenerative basophilia in the feather germs of cultures containing high concentrations of the chemical. This was probably a toxic effect.

DISCUSSION

Orotic acid. There is considerable evidence from the literature that orotic acid is a precursor of nucleic acid pyrimidines. Wright, et al. ('51) stated that ureidosuccinic acid is an acyclic biological precursor of the pyrimidine ring. Lieberman and Kornberg ('53 '54 '55) found that orotic acid could be converted to ureidosuccinic acid via dihydro-orotate. This metabolic pathway of the incorporation of orotic acid with nucleic acid pyrimidines has received support from Reichard and Lagerkvist ('53) Cooper Wu, and Wilson ('55) and Reynolds, Lieberman and Kornberg ('55) There is recent evidence for the entry of orotic acid into uridine-5' phosphate (Hurlbert and Potter '54 Lieberman and Kornberg '55; Crawford, Kornberg, and Simms, '57) Uridine-5' phosphate is a uridine nucleotide and could be an intermediate in the incorporation of orotic acid with RNA (Herbert Potter and Hecht, '57)

Further evidence for the entry of orotic acid into the formation of nucleic acid pyrimidines is found in the work of a number of earlier investigators. Bergstrom et al. ('49) showed that injected orotic acid was utilized in the biosynthesis of both uracil and cytosine. Buchanan and Wilson ('53) noted that orotic acid is a normal precursor of thymine. Orotic acid will replace uridine in promoting optimal early growth in *Streptococcus* (Hoffmann and Pavcek, '51)

Contrary to expectation, orotic acid did not stimulate growth of feathers in any of our experiments. Instead, growth of the whole culture was retarded, and feathers were inhibited even at the lowest concentration (table 1) It does not seem probable that the lack of growth was due to toxicity at the lowest levels used. Other possibilities are that orotic acid diverted synthesis toward a kind of RNA not utilizable by the feather or that it substituted, in an indirect way for some necessary component in the chain of synthesis of RNA.

PLATE 1

EXPLANATION OF FIGURES

1 Control explant of skin from the back of an embryo of stage 30–. Note the intense reaction for phosphatase in the pulp of each feather immediately below the growing epidermal tip. × 70.

2 The corresponding bilateral half of the piece of tissue shown in figure 1 grown in the presence of orotic acid (333 μg/ml of mixed culture medium). Growth of feathers is inhibited and the phosphatase reaction is diffuse. × 70.

3 Explant of a piece of tissue adjacent to those shown in figures 1 and 2, grown in the presence of orotic acid (100 μg/ml). The feathers are normal in appearance and in the localization of phosphatase. × 70.

4 Control explant of skin from an embryo of stage 31 showing normal feathers and an intense phosphatase reaction within the feather germs. × 70.

5 The corresponding bilateral half of the piece of tissue shown in figure 4 grown in the presence of isoguanine sulfate (333 μg/ml). Note the absence of feather germs and the homogeneous distribution of the phosphatase reaction. × 70.

6 Part of a cross section of feather in a control culture of skin from an embryo of stage 30. Sectioned at 7 μ and stained with toluidine blue. The nucleoli, which usually number two per nucleus, are small and ovoid. × 1,890.

7 Part of cross section of a feather from the corresponding bilateral half of the piece of skin shown in figure 6, grown in the presence of orotic acid (333 g/ml). Note the vacuolated or "doughnut-shaped" nucleolus. × 1,890.

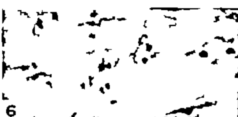

1


4


2


5


3


6


7

PLATE 2

EXPLANATION OF FIGURES

8 Control explant of skin from the back of an embryo of stage 32, stained for alkaline phosphatase. Note the strong reaction for phosphatase in the pulp of the feather × 70.

9 The corresponding bilateral half of the piece of tissue shown in figure 8 grown in the presence of isoguanine sulfate (1,666 µg/ml) There is reduction in the number of feather loci nd diffuse distribution of the reaction for alkaline phosphatase. × 70

10 Control explant of skin from the back of an embryo f stage 31 showing the normal distribution of phosphatase. × 70

11 The corresponding bilateral half of the piece of skin shown in figure 10, grown in the presence of 8-azaguanine (166 µg/ml) The phosphatase reaction is very dark and practically obscures any structure within the epidermal part of the explant. Not the darkly stained fibroblasts in the zone of outgrowth. × 70.

12 Control explant of skin from the back of an embryo of stage 33 showing the strong reaction for phosphatase within the feather germs. Note the absence of reaction in the peripheral fibroblasts. × 70

13 The corresponding bil teral half of the piece of tissue shown in fig ure 12, grown in the presence of thiouracil (2,500 µg/ml) The reaction within the original explant (left side) is essentially normal However there is tremendous build-up of phosphatase in the peripheral fibroblasts. × 70.





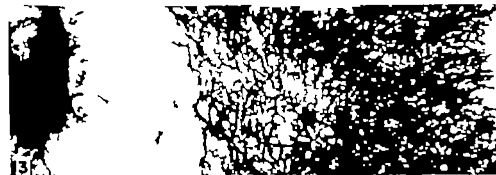



PLATE 3

EXPLANATION OF FIGURES

14 Sagittal section f feather from explanted skin of an embryo of stage 31 Sectioned at 7 μ and stained with toluidine blue. Note the heavy concentration of ribonucleic acid in the epidermal region of the feather especially in the cells which lie next to the pulp × 320.

15 Sagittal section of a feather from the corresponding bilateral half of the piece of skin shown in figure 14 grown in the presence of isoguanine sulfate (333 μg/ml) Note the stratified condition of the epithelium with the nuclei parallel to the surface. Compare with figure 14 × 320.

16 Control explant from the back of an embryo of stage 32 showing normal feather growth and reaction for phosphatase. × 70.

17 The corresponding bilateral half of the piece of skin shown in figure 16, grown in the presence of 2-amino-4-hydroxy-6-methylpyrimidine (1,666 μg/ml) The reaction for phosphatase is very splotchy within the epidermal explant. × 70.

18 Cross section of feather from the same explant as figure 15. Note the solid epidermal rod, the large spherical melanoblasts embedded in it, and the absence of barb ridges and mesodermal pulp. × 500.

19 Control explant of skin from the back of an embryo of stage 31 showing a normal reaction for phosphatase and normal feather growth. × 70.

20 The corresponding bilateral half of the piece of tissue shown in figure 19 grown in the presence of 2-amino-4-hydroxy-6-methylpyrimidine (1,666 μg/ml) Note the merging f the phosphatase gradients of adjoining feather areas. × 70.

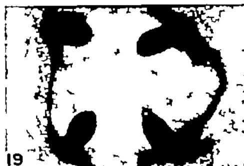
21 Part of a cross section of a feather in control culture of skin from an embryo of stage 32 Sectioned at 7 μ and tained with toluidine blue. The nucleoli are small and usually two in number × 1,890

22 Part of cross section of a feather from the corresponding bilateral half of the piece of skin shown in figure 21 grown in the presence of 8-azaguanine (333 g/ml) The nucleoli are large and frequently single. × 1,890.


14


18

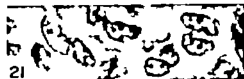

15


19


16


20


17


21


22

is essentially the same as that observed in the human embryos. However in the critical areas the absence of a nerve could not be as definitely established as in the serial sections stained specifically for nerve fibers. One always wonders if a small nerve has been broken or overlooked in the dissection For this reason the data on this material are not included.

A nerve was considered to be cutaneous only when its fibers could be traced through the deep fascia and into the subcutaneous tissue of the skin In the younger embryos where a layer of fascia had not yet differentiated a nerve was considered to be cutaneous when it pierced the myotome and entered the loose mesenchyme under the skin. No significant differences were observed between right and left sides Photomicrographs of typical embryo sections are shown in figures 1 and 2. According to Streeter ('08) primary neurons forming peripheral nerves are well established by the end of the first month of human development. The youngest embryo used in this study was about six weeks of age

OBSERVATIONS

The distribution of the cutaneous branches of the dorsal (primary) rami of the upper spinal nerves was studied on both sides in ten rabbit embryos. This makes a total of 20 spinal nerves studied at each level from cervical 1 (C1) through thoracic 1 (T1)

Figure 3 is a composite diagram illustrating the distribution of the cutaneous branches of the dorsal rami of the cervical nerves of a 20 mm rabbit embryo These cutaneous nerves are shown as if they emanate from a single spinal nerve and are projected in a single plane This diagram gives a somewhat distorted picture, but it illustrates that each cervical cutaneous branch beginning with C1 and continuing through C8 is a little more dorsally placed than the nerve above In this embryo a cutaneous branch was present for each cervical level bilaterally with the exception of C3 which communicated with C4 This communication is shown by a dotted line between C3 and 4 With the exception of the presence of the cutaneous branches of C1 this diagram illustrates the general pattern of the distribution of the cutaneous branches found in the rabbits studied

Figure 4 is a table showing the presence or absence of cutaneous branches of the dorsal rami of spinal nerves C1 through T1 on both sides of the ten rabbits studied. Cutaneous branches of the dorsal rami were lacking at the level of C1 in all but one of the rabbit embryos. In this one embryo cutaneous branches of C1 were pres-

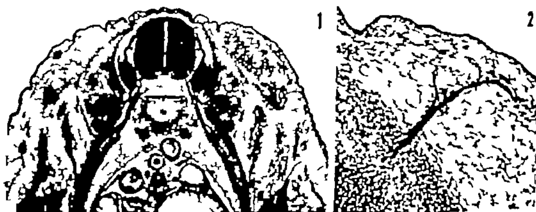


Fig. 1 A photomicrograph of transverse section of 15 mm rabbit embryo (no 89 section 6-5-7) showing the branching pattern of typical spinal nerve. Bodian method. × 20

Fig. 2 A photomicrograph of 15 mm rabbit embryo (no 91 section 7-4-7) howing cutaneous branch of dorsal ramus. It is seen extending from the dense mesoderm of myotome into the loose mesenchyme of the skin. Bodian method. × 85

Abbreviations

a, anastomotic connection between branches of two adjacent dorsal rami
b, anastomosis of two cutaneous nerves arising from two adjacent dorsal rami
ant. arch. 1st cerv. vert., anterior arch of first cervical vertebrae
c, cervical
d. r. ganglion, dorsal root ganglion
lat. br., lateral branch
maxillary proc., maxillary process
med. br., medial branch
obl. cap. sup. obliquus capitis superior
rect. cap. post. maj. et min., rectus capitis posterior major and minor
semisp. cap., semispinalis capitis
sp. cord, spinal cord
splen. cap., splenius capitis
sp. XI, spinal accessory nerve
symp. tr. gang., sympathetic trunk ganglion
T thoracic
trapez., trapezius
ven. r., ventral root

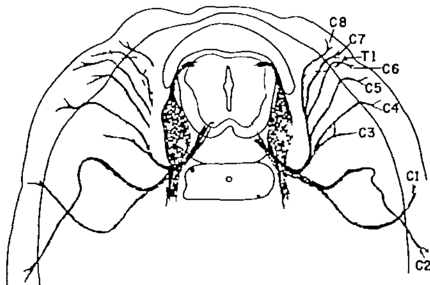


Fig. 3 A composite diagram of 20 mm rabbit embryo (no. 14 slides 6–11) illustrating the distribution of the cutaneous branches of the dorsal rami of the cervical nerves. These cutaneous branches are shown as if they emanate from single spinal nerve and are projected in single plane. Bodian method. × 25.

ent bilaterally (fig 3) The cutaneous branches of C2, 4 5 6 and 7 were present in all cases. Cutaneous branches of C3 were lacking in 14 of the 20 cases and of these, ten had a branch communicating with the next lower spinal nerve It is of interest to note that all of the cutaneous branches of C3 occurred in the three youngest rabbits. Cutaneous branches were lacking at the level of C8 in three cases and at T1 in 1 case. A 10 mm rabbit embryo (no 29) was particularly favorable for this study because the plane of the sections was such that it was possible to follow the complete course of some nerves in a very few sections. The sections were also somewhat oblique, making it possible to observe one spinal level on the right side and the next lower level on the left (figs. 5 and 6)

Fifteen human embryos were studied on both sides making a total of 30 nerves observed at each spinal level. The human embryo which came the closest to having a cutaneous branch from each dorsal ramus (C1 through T1) was number 67 Each of these levels were projected and carefully drawn. The drawings of only three levels are included here (figs. 7 8 and 9) This human embryo had cutaneous branches from dorsal rami of the first cervical spinal nerve on both sides (fig 7)

Embryo No	Crown Rump Length	Rabbit Spinal Nerves C1	2	3	4	5	6	7	8	T1
5	mm. 9	○ ○	+ +	+ +	+ +	+ +	+ +	+ +	○ +	○ +
29	10	○ ○	+ +	+ +	+ +	+ +	+ +	+ +	+ +	+ +
32	10	○ ○	+ +	+ +	+ +	+ +	+ +	+ +	○ ○	+ +
54	17	○ ○	+ +	○ ○	+ +	+ +	+ +	+ +	+ +	+ +
59	17	○ ○	+ +	⊖ ⊖	+ +	+ +	+ +	+ +	+ +	+ +
55	18	○ ○	+ +	○ ⊖	+ +	+ +	+ +	+ +	+ +	+ +
63	18	○ ○	+ +	⊖ ⊖	+ +	+ +	+ +	+ +	+ +	+ +
18	18	○ ○	+ +	⊖ ○	+ +	+ +	+ +	+ +	+ +	+ +
14	20	+ +	+ +	⊖ ⊖	+ +	+ +	+ +	+ +	+ +	+ +
19	20	○ ○	+ +	⊖ ⊖	+ +	+ +	+ +	+ +	+ +	+ +

+ Spinal nerve possessing a cutaneous branch from its dorsal ramus

⊖ Spinal nerve lacking a cutaneous branch from its dorsal ramus but communicating with a lower spinal nerve which has a cutaneous branch

○ Spinal nerve lacking both a cutaneous branch and a communication with another spinal nerve

Fig. 4 This table shows the distribution of cutaneous branches of the cervical and first thoracic nerves in ten rabbit embryos.

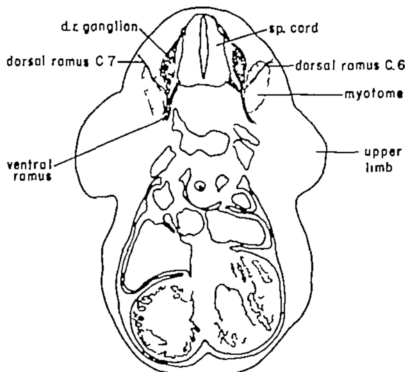


Fig. 5 A composite diagram of transverse sections (slightly oblique) of 10 mm rabbit embryo (no. 29 right section 7-2-11 and left section 8-1-4) Bodian method. × 25.

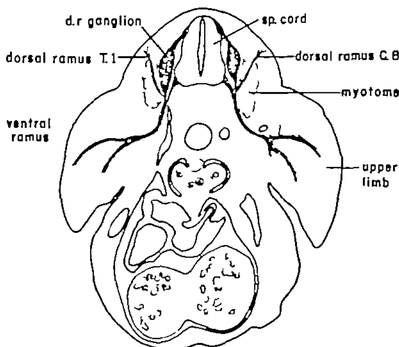


Fig. 6 Another composite diagram similar to figure 5 of the same 10 mm rabbit embryo at slightly lower level (no. 29 right section 8-1 15 and left section 8-2-14) Bodian method. × 25.

rect. cap post
maj. et min.
trapez.
sp cord
semisp
cap.
sp. XI
ven. r.
d. r ganglion
obl cap. sup
splen. cap.
ant. arch
1st cerv vert
odontoid process

Fig. 7 A composite diagram of transverse sections of 28 mm human embryo (no. 67 slides 23-24) at the level of the first cervical nerves. Bodian method. × 20.

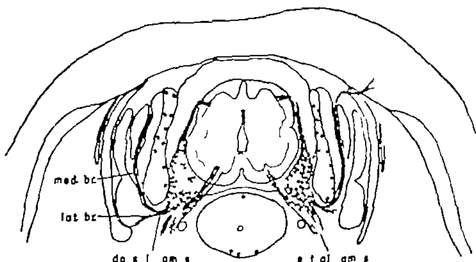


Fig. 8 A composite diagram of transverse sections of a 28 mm human embryo (no. 67 slides 31-32) t the level of the sixth cervical nerves. Bodian method. × 20.

The dorsal ramus broke up into several small bundles which supplied the muscle masses which will constitute the rectus capitis posterior major and minor and the semispinalis capitis muscle. It continued through the muscle bundles which form the obliquus capitis superior which it supplied, and gave branches to the semispinalis capitis and splenius capitis muscles. One bundle pierced the splenius

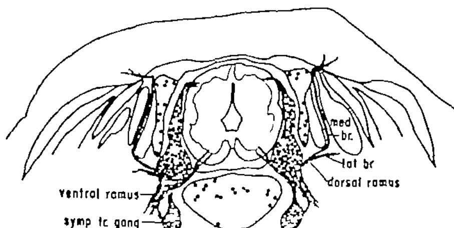


Fig. 9 A composite diagram of transverse sections of a 28 mm human embryo (no. 67 slides 33–37) at the level of the first thoracic nerve. Bodian method. × 20.

capitis muscle and continued into the subcutaneous tissue of the skin. A cutaneous branch of C1 was observed on one side in human embryo H-1194 The plane of the sections of this embryo was not favorable for a complete analysis of the cervical nerves and observations on this embryo are not included in these data.

In almost all of the human embryos studied (fig. 10) there were cutaneous branches of the dorsal rami of C2 3 and 4 with but one exception at the level of C4 in embryo number 246. In this case there was a well-developed communicating branch with C5 Cutaneous branches at the level of C5 were present in 22 of the 30 cases.

The dorsal rami of cervical nerves six, seven and eight were characterized more by the absence of cutaneous branches than by their presence (fig. 10) Cervical six had cutaneous branches in only two cases, C7 in only five cases and C8 in only six of the cases observed for each of these levels. However the dorsal rami of the first thoracic nerves had cutaneous branches in 28 of the 30 cases.

It is usually said that the dorsal ramus of C1 does not divide into medial and lateral branches (Cunningham, '31 and others) It should be noted that the cutaneous branches from the dorsal rami of C1 in this embryo (no. 67 fig. 7) arose from the most laterally placed bundles of this nerve. All of the other cutaneous nerves observed (C2–T1) arose from the medial branches of the dorsal rami with one exception, that being at the first thoracic level on one side of human embryo number 48.

In making these observations we noted branches connecting one spinal nerve with another Some of these occurred deep among the muscles and could not be traced to cutaneous areas (fig. 11 a) The ultimate destination of the fibers in these communicating branches could not be determined. These are indicated in the tables by a circle containing a dash (figs. 4 and 10)

A second type of communication was where a branch from each of two spinal nerves joined to form a single nerve bundle which proceeded directly into the subcutaneous tissue of the skin (fig. 11 b) In such cases both levels were recorded as having a cutaneous branch. This was found once between C7 and C8; and four times between C8 and T1

Our observations on the distribution of the cutaneous branches of the dorsal rami of spinal nerves C1 through T1 in rabbit and human embryos are summarized in figure 12. The variance between the distribution pattern of rabbit and human embryos is apparent. In the rabbit, cutaneous branches of C1 and C3 are absent in the majority of the cases with only an occasional branch missing at the levels of

Embryo No	Crown Rump Length	Human Spinal Nerves C1	2	3	4	5	6	7	8	T1
179	mm 12	⊖ / ⊖	+ / +	+ / +	+ / +	+ / +	+ / O	O / O	O / O	+ / +
175	15	⊖ / ⊖	+ / +	+ / +	+ / +	O / +	O / O	O / O	O / O	+ / +
232	15	⊖ / ⊖	+ / +	+ / +	+ / +	+ / O	O / O	O / O	O / O	+ / +
140	16	⊖ / ⊖	+ / +	+ / +	+ / +	+ / +	O / O	O / +	O / +	+ / +
48	17	⊖ / ⊖	+ / +	+ / +	+ / +	+ / +	O / O	O / O	O / O	+ / +
180	20	O / O	+ / +	+ / +	+ / +	O / +	O / O	+ / O	+ / +	+ / +
31	22	⊖ / ⊖	+ / +	+ / +	+ / +	O / +	O / O	+ / ⊖	O / +	O / +
104	23	⊖ / ⊖	+ / +	+ / +	+ / +	+ / +	O / O	O / O	O / O	+ / +
246	24	O / O	+ / +	+ / +	+ / ⊖	+ / +	O / O	O / O	O / O	+ / +
218	25	⊖ / ⊖	+ / +	+ / +	+ / +	O / +	O / O	O / O	O / +	+ / O
67	28	+ / +	+ / +	+ / +	+ / +	+ / +	⊖ / +	+ / +	⊖ / ⊖	+ / +
27	29	O / O	+ / +	+ / +	+ / +	O / O	O / O	O / O	O / O	+ / +
174	30	O / O	+ / +	+ / +	+ / +	+ / +	O / O	O / O	O / O	+ / +
219	34	⊖ / ⊖	+ / +	+ / +	+ / +	+ / +	O / O	O / O	O / +	+ / +
197	35	O / ⊖	+ / +	+ / +	+ / +	O / +	O / O	O / O	⊖ / ⊖	+ / +

Fig. 10 This table shows the distribution of cutaneous branches from the dorsal rami of the cervical and first thoracic nerves in 15 human embryos. For explanation of symbols, see figure 4.

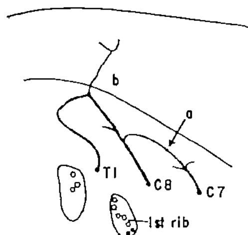


Fig. 11 A diagram showing two types of communications between the dorsal rami of adjacent spinal nerves. See page 175 for explanation.

C8 and T1. In the human embryos, C1 6 7 and 8 failed to have cutaneous branches in the majority of cases Only a few were missing at the levels of C4, 5 and T1

DISCUSSION

The pattern of dermatomes has been studied by a number of investigators. Sherrington (40) isolated single nerve roots in Macacus rhesus by cutting several nerve roots above and below the nerve in question and determined the remaining areas of sensitivity The dermatome areas of the monkey were thought to be comparable to those in man. Bolk (1898 1899) and Johnston ('09) based their findings on the dissection of human bodies. Head and Campbell ('00) based their findings on the pattern of skin lesions in patients with herpes zoster in which a single spinal nerve was involved. Foerster ('33) employed essentially the same methods as *those used by Sherrington in defining der*matome patterns in man. By cutting nerve roots above and below the nerve in question he plotted the remaining areas of sensitivity He also used a method to stimulate vasodilation which produced patterns similar but not identical to the areas

Spinal Nerves with Cutaneous Branches from Dorsal Rami

Total Number of Spinal Nerves

30 25 20 15 10 5

Maximum 29 28 22 6 5 2 2

Max 19 17 6 2

2C – 1 – 10 – 5

C1 2 3 4 5 6 7 8 T1
Human Spinal Nerves

C1 2 3 4 5 6 7 8 T1
Rabbit Spinal Nerves

Fig. 12 A table showing the distribution of th cutaneous branches of the dorsal rami of the cervical and first thoracic nerves in human and rabbit embryos.

of herpetic eruption described by Head and Campbell ('00)

The presence of a gap in the sequence of dermatomes in the lower cervical levels on the posterior aspect of the trunk was recognized by Sherrington ('40) Bolk (1898 1899) Johnston ('09) Haymaker and Woodhall ('53 chart modified from Foerster '33) and Head and Campbell ('00)

The dermatome charts of Edinger ('04) Dejerine ('14) and Keegan and Garrett ('48) show a cutaneous distribution of each of the dorsal rami of the lower cervical nerves.

Keegan and Garrett found that even when a single posterior nerve root is interrupted, that a diminution of sensitivity could be demonstrated in a dermatome. They plotted the areas of diminished sensitivity by the use of a light pin scratch. According to their findings, the dermatomes of the upper limbs from cervical 5 to thoracic 1 extend as a series of bands from the mid-dorsal line of the trunk into the limbs.

According to Hamilton, Boyd and Mossman ('52) *each myotome of human embryos* between the fifth and sixth week (7–8 mm) becomes divided by a longitudinal constriction into a dorsal portion (epimere) which receives dorsal rami, and a ventro-lateral portion (hypomere) *which receives ventral rami.*

In figures 5 and 6 a groove marks the boundary between the limb bud and the dorsal body wall in a 10 mm rabbit embryo. Figure 13 is a drawing of a 6.3 mm human embryo The groove (dorsolateral line) indicating the boundary between the dorsal body wall and the ventrolateral body wall with the limb buds is clearly shown. The skin of the dorsal body wall receives its innervation mainly through the dorsal rami, and the skin of the limb buds and ventrolateral body wall mainly through the ventral rami.

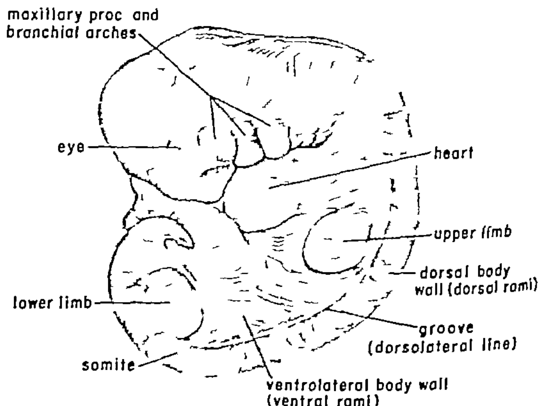


Fig. 13 A 6.3 mm human embryo. × 15. (After Blechschmidt, S. Karger A. G. Basel, Switzerland, '61)

Cunningham ('51 fig. 953) and Last ('59 fig 18) suggest that the body wall may be divided into three longitudinal strips, i.e. dorsal, lateral and ventral. The former was thought to be supplied by the dorsal rami and the latter two by the ventral rami. The border between the skin areas supplied by the dorsal and ventral rami has been referred to as the dorsolateral *line* (Ariëns Kappers Huber and Crosby ('36) This line is said to extend from the head to the upper side of the os coccyx. It was also recognized by Bolk (1898 1899) and Dejerine ('14)

It is our opinion that the groove shown in figure 13 approximates the future dorsolateral line. According to Last ('59) the limb buds grow out of the lateral strip and are supplied by the lateral branches of the ventral rami.

Herringham (1886) Bolk (1898 1899) Sherrington (40) and others have proposed theories to explain the gap in the sequence of cutaneous branches from the dorsal rami of the lower cervical nerves. The most widely accepted of these theories (Haymaker and Woodhall, '53) postulates that during development certain dermatomes migrate with the result that C5 6 and 7 occupy the preaxial part of the limb while dermatomes C8 T1 and 2 occupy the postaxial portion. Such a migration of dermatomes would explain how C4 (5) comes to lie adjacent to T1 (2) in the dorsal part of the trunk. However the dorsal rami of the cervical spinal nerves are not concerned with the innervation of the limbs and we can see no reason to assume that the skin supplied by these nerves has migrated into the limbs during development.

Last ('59) has defined an axial line as the line of junction of two dermatomes supplied by discontinuous spinal levels. Since there is no gap in the lower dorsal cervical dermatomes in the rabbit, there would be no dorsal axial line in relation to the upper limb. Keegan and Garrett (48) failing to find a gap in the lower dorsal cervical dermatomes in man question the presence of a dorsal axial line.

In a preliminary report (Pearson and Bass '61) the opinion was expressed that the cutaneous branches from the dorsal rami could be demonstrated for all of the cervical nerves in some human embryos. Our conclusions made at that time were based mainly on one human embryo (no. 67) and our series of rabbit embryos. A re-examination of this human embryo has subsequently demonstrated that certain levels which apparently had cutaneous branches simply had a communication with an adjacent spinal nerve (fig. 11) *The study of the human embryos in our* series was not completed at that time and we were misled by the preponderance of evidence collected from our studies on rabbit embryos.

The variance between the pattern of dermatomes in the rabbit and man illustrates that care should be taken in carrying over an observation made in one animal form to another The rabbit probably represents more closely the segmental dermatome pattern one would expect to find in most vertebrates.

SUMMARY

The concept that the only cervical nerves having cutaneous branches from their dorsal rami are C2, 3 4 and 5 (6) has been recently questioned by Keegan and Garrett ('48) These authors postulate that dermatomes C5 to T1 extend as a series of bands from the mid-dorsal line into the limbs.

Independent cutaneous branches of dorsal rami were studied in 10 rabbits and 15 human embryos. Since the nerves were studied bilaterally a total of 20 rabbit and 30 human spinal nerves were observed for each level.

In rabbits, cutaneous branches from the dorsal rami of C2, 4 5 6 and 7 could be *demonstrated in all cases. Cervical 8 had* cutaneous branches in 17 cases and T1 in 19 Cervical 1 and 3 failed to have cutaneous branches in the majority

In human embryos C2 and 3 had cutaneous branches in all cases, and C4 in all but one Cutaneous branches of C5 were present in 22 instances. Cervical 1 and 6 each had cutaneous branches in 2, C7 in 5 C8 in 6 and T1 in 28 cases. Communicating branches were noted

The distribution of cutaneous nerves in the rabbit support the pattern suggested by Keegan and Garrett (48) however the pattern in human embryos seems to sup-

port the older dermatome charts showing a gap in lower cervical levels.

LITERATURE CITED

Ariëns Kappers, C. U G. C. Huber and E. C. Crosby 1936 The comparative anatomy of the nervous system of vertebrates including man. The Macmillan Co., New York.

Blechschmidt, E. 1961 The stages of human development before birth. W B Saunders Co., Philadelphia, London.

Bodian, D 1936 A new method for staining nerve fibers and nerve endings in mounted paraffin sections. Anat. Rec., 65 89–97

Bolk, L. 1898, 1899 Die Segmentaldifferenzierung des menschlichen Rumpfes und seiner Extremitäten, I Morphol. Jahrb., 25 465–543; II Ibid., 26 91–211; III Ibid., 27 630–711; IV Ibid., 28 105–146, Quoted from Keegan and Garrett (48)

Cunningham, D J 1951 Cunningham's textbook of anatomy ninth edition J C. Brash, editor Oxford Univ Press, London.

Dejerine, J 1914 Sémiologie des Affections du Système Nerveux. Masson et Cie, Paris.

Edinger L. 1904 Neue Darstellung der Segmentinnervation des menschlichen Körpers, Zeitschrift Für Klinische Medicin., 53 53–57

Foerster O. 1933 The dermatomes in man. Brain, 56 1–39

Hamilton W J J D Boyd and H W Mossman 1952 Human embryology Second edition, W Heffer & Sons, Ltd., Cambridge.

H W and B Woodhall 1953 Peripheral nerve injuries. W B. Saunders Co., Philadelphia and London.

Head, H., and A. W Campbell 1900 The pathology of herpes zoster and its bearing on sensory localisation. Brain 23 353–523.

Herrick, C. J 1899 The cranial and first spinal nerves of menidia. J Comp. Neur., 9 153–455.

Herringham, W P 1886 The minute anatomy of the brachial plexus. Proc. Roy Soc. London, 41 423–441

Huber, J F 1936 Nerve roots and nuclear groups in the spinal cord of the pigeon. J. Comp. Neur 65 43–91

Johnston, H. M. 1909 The cutaneous branches of the posterior primary divisions of the spinal nerves, and their distribution in the skin. J. Anat. and Physiol., 43 80–92.

Keegan, J J and F D Garrett 1948 The segmental distribution of the cutaneous nerves in the limbs of man. Anat. Rec., 102: 409–437

Last, R. J 1959 Anatomy regional and applied. Little Brown and Co., Boston.

Pearson, A. A., and J J Bass 1961 Cutaneous branches of the posterior primary rami of the cervical nerves. Anat. Rec., 139: 263.

Pearson, A. A., and S. L. O'Neill 1946 A silver-gelatin method for staining nerve fibers. Anat. Rec., 95 297–301

Sherrington, C S 1940 Selected writings of Sir Charles Sherrington. Compiled and edited by D. Denny Brown. Paul B Hoeber Inc., New York.

Streeter G. L. 1908 The peripheral nervous system in the huma embryo t the end of the first month. Am. J Anat., 8 285–301

Placentation and Fetal Membranes of the Central American Noctilionid Bat *Noctilio labialis minor*[1]

JOHN WALBERG ANDERSON[2] AND WILLIAM A. WIMSATT[3]
Department of Anatomy University of Wisconsin, Madison, Wisconsin, and Department of Zoology Cornell University Ithaca, New York

As emphasized by Mossman ('37 '53) the fetal membranes represent one of the most conservative, and hence most ideal organ systems for the determination of phylogenetic interrelationships of recent mammals. While discrete interspecific or intergeneric differences are seldom noted, similarities in the fetal membranes between orders or between families may demonstrate relationships in these major groups. Considerable interest therefore attaches to the elucidation of fetal membrane structure in major groups of mammals not previously studied. The structure of the fetal membranes and placenta has been described in only nine of the seventeen families of bats currently recognized (cf Wimsatt, 54 for literature) Similarities and dissimilarities in the structure of the membranes in the nine families, and the possible interrelationships they reflect, point up the need for information concerning the as yet undescribed families of bats

It has been our good fortune to obtain a graded series of pregnant uteri of *Noctilio labialis minor* of the family Noctilionidae. We have been able to find no previous account of the structure of the fetal membranes and placenta of a representative of this family and it is therefore the purpose of this paper to provide one. As might be expected, this noctilionid bat displays peculiarities of fetal membrane and placental structure not previously recorded in the nine families described to date These involve especially the orientation of the implantation site and of the embryonic disc, the nature of the yolk-sac placenta the transitory existence of a chorioamniotic placenta, and certain structural features of the chorioallantoic placental membrane. Although in most other respects the developmental history of the fetal membranes of *Noctilio* follows the general chiropteran pattern, in a few instances it may indicate relationships not reflected in the current taxonomic groupings.

MATERIALS AND METHODS

Most of the bats used in this study were collected over a period of ten years by Dr Harold Trapido of the Gorgas Memorial Laboratory Juan Mina, Panama. They were obtained from sites along the Chagres River We should like to acknowledge our great debt to Dr Trapido for his continued and enthusiastic aid in making these collections. We are also indebted to Dr Herbert C. Clark, former Director of the Gorgas Laboratory for permitting use of the Laboratory's facilities, and for bearing expenses in the procurement of the material.

Some of the bats were caught alive; but it was necessary to obtain some by shooting them and fixing the tissues immediately upon retrieving the animals. Usually the entire uterus was removed and immersed in the fixative but at times the fetus was removed to allow for more rapid penetration of the fixative. In one series the live bats were brought to Ithaca and were fixed by injection of the fluid into the fetal membrane cavities following which the entire uterus was immersed in the fixative

As information became available from study of the earlier specimens obtained, it was possible to plan the collection dates to illuminate critical stages of develop-

[1] A part of the material presented in this paper was reported at the 50th Annual Meeting of the American Society of Zoologists in Boston, Massachusetts, December 1953 (Anderson and Wimsatt, '53).
[2] Supported by National Institutes of Health, grant H-[illegible].
[3] Supported by National Science Foundation grant G-[illegible].

ment, and serial sections now in our possession from this source date from December through May and July

A recent visit to the Chicago Natural History Museum, through the courtesy of Dr Joseph Moore has yielded the reproductive tracts of several specimens of *Noctilio* which had been collected in September 1933 Although the fixation is not appropriate for cytological detail, nonetheless it has been possible to ascertain several important points from this material. These uteri were further fixed in Bouin's fluid, then treated as the others The specimens in our collection now total over seventy

A wide variety of fixatives was used on the material from Dr Trapido including 10% formalin, Bouin's fluid absolute alcohol formalin, absolute alcohol picric acid-formalin, and Helly's Rossman's and Maximow's fluids. In addition selected specimens were fixed in cold acetone for demonstration of alkaline phosphatase.

Serial sections were cut at 8 and 10 μ and stained in various ways. Harris' hematoxylin and eosin, Azan, Masson and Heidenhain's iron hematoxylin procedures were used most commonly Occasional sections were stained with the periodic acid Schiff procedure (McManus 48 Hotchkiss, 48) particularly for the study of Reichert's and similar membranes Other methods employed were: eosin and methylene blue to show cytoplasmic basophilia; and Gomori's (41) technic for alkaline phosphatase using fructose 1 6-diphosphate and sodium β-glycerophosphate as substrates

OBSERVATIONS AND DISCUSSION

Reproductive cycle Although we have made no direct observations on breeding activity it can be assumed that breeding takes place in late November and December since a specimen obtained on December 6 (fig. 5) shows a newly implanted blastocyst. A second specimen taken on that date has a well developed corpus luteum in one ovary and clumped sperm in the uterine tubes but careful search of the entire series has not revealed an ovum or blastocyst. No tubal ova were observed in any of our specimens. Considerable variation in development of the embryos at each collection date indicates that the breeding season extends at least a week or two. Only a single embryo has been found in any female.

Specimens taken in early April were in an advanced stage of pregnancy and Dr. Trapido reports that he found females suckling young during the third week in May Thus parturition occurs in late April or early May Several of our specimens taken from December through April were not pregnant, nor were any of our May July or September specimens.

In this regard *Noctilio* resembles most of the other microchiroptera, its breeding season being annual and of relatively short duration. The length of gestation compares with that of the other bats for which data are available with the exception of the Vespertilionidae, which normally have a gestation period of only 40–60 days (Wimsatt, 45a) The single young observed in all of our pregnant specimens also fits the pattern set by all other microchiroptera which have been studied (cf Wimsatt and Trapido '52) with the exception once again, of the Vespertilionidae.

Gross morphology of the female reproductive tract. Figure 1 depicts the reproductive tract (without the vagina) of a mature bat collected in early July The uterine horns are equal in size and the separation between the horns continues internally well down into the body; but eventually the two horns unite, and there is a single cervix. The ligamentum teres of the uterus is prominent. A rather long tortuous oviduct is continuous with the ovarian bursa, as is shown in figures 1 and 3 An ostium connects the cavity of the bursa and the peritoneal cavity as has been described for the mouse by Wimsatt and Waldo (45)

Microscopic anatomy of the ovary Figure 3 illustrates the ovary in early pregnancy and will serve as a basis for description. The prominent, highly vascular corpus luteum is the only one in this ovary and there is none in the other Occasionally a corpus can be found in each ovary but one is then much larger In every case in our material, the single corpus or the larger one is in the ovary attached to the pregnant horn. Atretic fol

licles including vesicular follicles, can be seen through most of the year being quite numerous in later stages of pregnancy

It is interesting to note that there are prominent corpora lutea in the ovaries of mature bats collected during July Intensive search of serial sections of oviducts and uteri of these specimens has revealed no ova or blastocysts, nor were any sperm detected. The corpora lutea were well-developed, appearing similar to the corpora lutea of pregnancy The interpretation of this phenomenon would require more complete data. It is possible that the July corpora are the result of a post partum ovulation, but this is usually followed by fertilization, if not immediate implantation, and these specimens were collected two months after parturition. It is possible that luteal material persists for some time after parturition, in a way analogous to that of the porcupine (Mossman and Judas, 49) but not for as long a time. In our September specimens one ovary of each animal contained a corpus albicans and numerous secondary follicles many undergoing atresia. Sometime between July and September then the persistent luteal material degenerates.

The uterus. The non-pregnant uterus of *Noctilio* is bicornuate and symmetrical in the May July and September specimens (fig. 1) A striking feature is the presence of a ridge of endometrium running the length of each uterine horn. This ridge was found in all non-pregnant females. It is lateral and antimesometrial, as can be seen in figure 2. Although this particular section is of a uterus in the breeding season, it is similar to the situation found at other times of the year

The progestational response of the uterus is relatively slight; the epithelium is low columnar and the glands remain few and simple. This is in sharp contrast to the situation in *Desmodus* (Wimsatt, '54) and *Myotis* (Wimsatt, 44) in which the progestational response is much more marked.

It should be noted that, in contrast to the uterus in females collected in July and September the non-pregnant uterus in December is definitely asymmetrical. The uterine horn opposite to the one shown in figure 2 is smaller shows less overall endometrial thickness and vascularity and has a much less marked ridge.

Decidual reaction. The decidual reaction is a prominent feature of the earliest pregnant specimens in our collection (fig. 5) The cells are typical, with light staining, vacuolated cytoplasm, containing glycogen (fig. 4) Many mitoses were also found, as well as multinucleate giant cells. Both deciduae basalis and parietalis are formed, but no decidua capsularis develops, as will be explained below

The decidua parietalis, never prominent (figs. 12 and 14) is thinned out at an early stage by the expanding conceptus its definitive condition is shown in figure 16 The decidua basalis also is reduced as a result of the invasion of the trophoblast and in late stages of gestation there is little decidua and the glycogen is lost.

Implantation. The earliest implanting specimen is shown in figure 5. It will be noted that the embryonic mass is almost completely surrounded by the decidua basalis and invading trophoblast. A marked expansion of the yolk sac, however has resulted in an excentric, rather than interstitial implantation, preventing formation of a decidua capsularis.

As a result of the massive decidua formation on the implantation ridge, the presumptive placenta is, from the beginning attached over a limited area. The bilaminar omphalopleure expands into the submarginal sulcus (fig. 11)

The orientation of the embryonic disc is evidently dependent upon the orientation of the ridge which forms a constant feature of the uterus, for the disc is lateral and antimesometrial at this stage The surrounding placenta remains in this lateral position after the embryo retreats into the exocoelom, and is to be found here in our latest stages. It should be noted that the orientation is not directly lateral tending more toward the antimesometrial pole.

Regarding the depth of implantation *Noctilio* resembles both *Myotis* and *Desmodus* (Wimsatt, 44 '54) since they also show a more superficial implantation and no decidua capsularis. With respect to the orientation of the embryonic mass *Noctilio* fits in well with its taxonomic grouping, since the more primitive bats

show an orientation either mesometrial or tending in that direction whereas the next higher family of bats (Megadermatidae) shows an antimesometrial orientation (Gopalakrishna, '50)

Amnion. Although the process of amniogenesis could not be followed in detail in our material, there seems little doubt that it results from cavitation rather than folding. As has already been seen shortly after implantation the inner cell mass is surrounded almost completely by the trophoblast and decidua basalis. In our earliest stages showing an amniotic cavity (fig 6) the embryonic disc has been separated from the trophoblast, except at the edges and forms a boundary between amniotic and yolk-sac cavities. In a somewhat later stage (fig. 7) the embryo can be seen sinking into the exocoelom, "dragging the amnion with it. Throughout gestation the amnion remains simple showing little connective tissue in addition to the ill defined squamous ectodermal epithelium (fig. 16)

It should be noted here that the presence of the amnion, embedded in the substance of the developing placental disc, and in intimate contact with the chorionic mesoderm indicates the great possibility that there is exchange of metabolites and wastes between the closely apposed maternal vessels and the amniotic cavity Indeed it is difficult to imagine that the embryo would survive in the face of an avascular chorion, without some such mechanism. Such a relationship as is shown in figure 6 may be termed a "chorio-amniotic placenta.

Allantois The development of the allantois is not well illustrated in our material, closely seriated stages being lacking In figure 11 an unusual feature of the allantoic development in *Noctilio* is illustrated. Here it can be seen that, although the allantoic mesoderm, including the vessels occupies a large part of the exocoelom, the allantoic cavity is small. The great expansion of the allantoic mesoderm is probably caused by the normal accumulation of extracellular fluid In all of our later stages the allantois is represented by a narrow duct within the umbilical cord (fig. 20) The stalk is invested with a smooth muscle sheath and in the definitive condition, is accompanied by two umbilical arteries and a single vein. Here, again, *Noctilio* follows the general chiropteran pattern, differing significantly only from *Hipposideros* (Gopalakrishna, '58) and the Vespertilionidae (Wimsatt, 45b) in which the allantois is more prominent.

Chorioallantoic placenta. As mentioned above the chorioallantoic placenta begins development on the lateral and antimesometrial aspect of the uterus retaining this orientation throughout gestation. The establishment of the definitive chorioallantoic membrane closely resembles the process in *Desmodus* described by Wimsatt ('54) It will be seen from figures 5 and 6 that the trophoblast rapidly invades the endometrium having formed a considerable mass before differentiation of the embryonic disc has begun. The endometrial epithelium is lost, as is most of the connective tissue. A thin PAS-positive "interstitial membrane can be detected between trophoblast and the maternal endothelium (fig 8); if this is of fetal origin then the only remaining maternal tissue in many areas is the hypertrophied endothelium. The "interstitial membrane in bat placentas has been previously discussed (Wimsatt, '58)

The initial invasion is by a syntrophoblastic shell apparently derived from the cytotrophoblast. At the junction between the invading trophoblast and the decidua basalis darkly-staining syntrophoblastic masses can be distinguished for some time (figs. 7 and 12)

Before the syntrophoblastic invasion is complete cytotrophoblastic villi invade the syntrophoblastic shell. Whereas the syntrophoblastic cytoplasm is basophilic, that of the cytotrophoblast is not. In contrast to the presence of a PAS-positive membrane which separates the syntrophoblast from the maternal endothelium, none appears between the two layers of trophoblast. The differences in cytoplasmic basophilia of the two types of trophoblast constitute the most useful way of distinguishing the boundary between them.

The syntrophoblast is perforated at the maternal side of the disc by tongues of cytotrophoblast, which form the outermost fetal tissue in contact with the decidua basalis. Figure 10 shows this, as well as

the intensely basophilic cytoplasm of the outermost syntrophoblast, and the knots of syntrophoblastic nuclei in this area.

Soon after the invasion by the cytotrophoblast begins, and before the primitive streak can have become very active (fig. 6) there is formed a considerable amount of primary" mesoderm, which invades the placenta within the cytotrophoblastic villi, and, with the trophoblast, forms the chorion. As can be seen from the relations in figure 6 the most likely source of the primary" mesoderm would be the trophoblast. There is a PAS-positive membrane separating the cytotrophoblast and mesoderm (fig. 8) At a later stage the cytotrophoblast is reduced, the cells being very low cuboidal. In still later stages (fig. 17) the cytotrophoblast is almost entirely lost, and only the much reduced cytotrophoblastic shell remains.

With the development of the allantois, and the invasion of the chorionic placenta by the allantoic mesoderm containing the umbilical vessels the chorioallantoic placenta is formed. As in all other labyrinthine placentas, the maternal vessels pass through the substance of the discoidal placenta, breaking up into dilated capillaries which run from the fetal to the maternal surface, and there collect into veins. With the umbilical vessels doing just the opposite, a countercurrent flow is established (Mossman, '26) The maternal endothelium is considerably hypertrophied, containing as many as 6–10 nuclei surrounding one section of a single vessel. Several lobules are established by major branches of maternal vessels.

The above described conditions persist until the latest stages which we possess. The syntrophoblast and the PAS-positive membrane remain, as does the maternal endothelium. In areas where the trophoblast surrounds larger maternal vessels the PAS-positive membrane reaches prominent thickness (figs. 17 and 18) Endothelial nuclei are not as numerous as in early stages, but there are usually at least two or three nuclei around the periphery of each maternal sinusoid. Thus, in the definitive condition, the placenta is endotheliochorial. At least in late stages, the maternal endothelium shows a very strong alkaline phosphatase reaction (fig. 19) It was not possible to determine whether the enzymes were also present in the interstitial membrane or whether the precipitate there was merely a diffusion artifact.

Yolk-sac placentation. Yolk-sac placentation in *Noctilio* is characterized by the formation of at least three different placentral types. In our earliest implanting embryo the yolk sac has reached a significant size, being responsible for the excentric rather than interstitial implantation. The two layers of the bilaminar omphalopleure are separated by a prominent Reichert's membrane. The membrane is similar to that of other species, taking up the aniline blue dye of the Azan stain (fig. 16) and being intensely PAS-positive (fig. 10)

The bilaminar omphalopleure is in direct contact with the decidua parietalis It is also in contact with the placental disc, thus forming a choriovitelline placenta (figs. 5 7) In many places where the endoderm contacts the chorioallantoic placental surface finger-like projections invade the substance of the disc (fig 9) These projections are transitory and because they are not hollow they do not increase the area of the choriovitelline placenta.

With the invasion of the mesoderm the original bilaminar omphalopleure is transformed into a trilaminar omphalopleure which extends as far as the margin of the placental disc. Before the mesoderm reaches the lateral margin of the disc however vitelline vessels appear within the mesoderm, forming a second and vascular choriovitelline placenta (fig 7) The likelihood that this placenta is of greater functional significance can be inferred from the study of areas such as the one depicted in figure 13 in which the relatively thin barrier between the maternal vessels and the vitelline vessels can be seen. At this stage, the maternal vessels may very well be exchanging substances both with the vitelline vessels and with the contents of the yolk-sac cavity The mesodermal cells facing the exocoelom form a continuous epithelium which persists to late stages but remains low cuboidal (fig. 16)

The expansion of the exocoelom destroys the intimate apposition of the vitelline vessels with the surface of the disc, undoubtedly reducing or eliminating the vascular choriovitelline placenta as a functional entity. Since the parietal wall of the yolk sac persists until term, and the visceral wall becomes quite closely approximated to it in late stages (fig. 16) the yolk sac of *Noctilio* may be classified by Mossman's ('37) schema as "partially inverted." Definitively there extend from the margin of the chorioallantoic placental disc (fig. 15): the vascular splanchnopleure and the trilaminar omphalopleure which undercuts the disc and is continuous with the bilaminar omphalopleure.

Umbilical cord. The definitive umbilical cord (fig. 20) contains two umbilical arteries and one vein, the allantoic stalk surrounded by smooth muscle, and the vitelline artery and vein.

Summary of temporal sequence of placental development. It may be seen from the foregoing that six types of placental relationships develop in chronological and overlapping sequence. The functional interpretation of each of these placental relations rests solely upon morphological grounds and not upon any experimental data.

At the time of implantation the chorionic vesicle contacts the endometrium over its entire circumference. In the embryonic hemisphere the trophoblast of the bilaminar omphalopleure invades the decidua basalis and by its differentiation establishes a relationship with the endometrium which differs from that of the abembryonic hemisphere (fig. 5). In the embryonic hemisphere, the cytotrophoblast gives rise to a mantle of syntrophoblast which engulfs the more superficial capillaries of the decidua basalis. Concurrently a number of transitory finger-like projections of the omphalopleure develop extending into the presumptive placental disc (fig. 9). These projections shortly disappear, however with the expansion of the exocoelom.

In the abembryonic area, on the other hand the cytotrophoblast does not give rise to invasive syncytium and the endoderm does not form villi. The relationship is one of simple apposition of fetal and maternal tissues and is destined to persist throughout gestation.

Following amniogenesis (by cavitation) the amniotic membrane remains in intimate contact with the chorion, establishing what appears to be a chorioamniotic placental area (figs. 6 and 8) in the central region of the presumptive discoidal placenta. A chorioamniotic placenta of this sort has not previously been described.

The spread of mesoderm from the margins of the embryonic disc converts the area where the endoderm subtends the presumptive placental disc into a trilaminar omphalopleure (a non vascular choriovitelline placenta). Eventually this region becomes vascularized by vitelline vessels, forming the vascular choriovitelline placenta.

The subsequent development of the exocoelom drastically modifies the above relationships (fig. 7). The enlargement and extension of the exocoelom separates the amnion from the chorion in the central area, thereby abolishing the chorioamniotic placental area. The lateral expansion of the exocoelom results in the formation of a free vascular splanchnopleure disrupting the vascular choriovitelline placenta. This process extends over a period of time however and is not completed for some weeks.

During this period, allantoic vessels infiltrate the chorionic disc converting it into the chorioallantoic placenta. Throughout the rest of gestation, two major placental types persist: the definitive chorioallantoic placenta, and the extensive, "partially inverted" yolk-sac placenta.

SUMMARY AND CONCLUSIONS

The reproductive tracts of over 70 female specimens of *Noctilio labialis minor* have been examined, from collections made during the months of December through May and in July and September. It is concluded that breeding takes place in late November or early December, parturition in late April or early May. There was but a single young in each of the pregnant specimens, and usually a single corpus luteum but occasionally one corpus was found in each ovary.

The uterus is bicornuate and symmetrical in July and September showing an

endometrial ridge extending along the lateral and antimesometrial wall of each horn. In non-pregnant December specimens, one horn is larger than the other Implantation apparently is oriented by the ridge, and, although the embryonic mass becomes mostly surrounded by the developing decidua basalis no decidua capsularis is formed. The expanding bilaminar omphalopleure contacts the uterine wall on all sides, and, from our earliest stage undercuts the decidua basalis. At early stages, villi of the choriovitelline placenta penetrate into the developing trophoblastic mass but these disappear with the subsequent expansion of the exocoelom. This latter process also divides the yolk sac into visceral and parietal portions, and, in later stages, the yolk sac is partially inverted.

Amniogenesis appears to be by cavitation and since the amnion remains in intimate contact with the chorionic placenta, a chorioamniotic placenta is formed. As the exocoelom expands this placental relationship is destroyed.

The allantois is of significant size only early in gestation, being shortly reduced to a rudiment. In late stages, the allantoic duct persists with a very narrow epithelium-lined lumen, surrounded by a sheath of smooth muscle The definitive umbilical cord contains, in addition, two umbilical arteries and one vein, and one vitelline artery and vein.

The chorioallantoic placenta is formed in much the same way as has been described in *Desmodus* the original syntrophoblastic shell being invaded successively by cytotrophoblast and by umbilical vessels. The definitive placenta is lateral to antimesometrial, discoidal and labyrinthine endotheliochorial. A total of six different placental areas have been found at various stages of gestation

ACKNOWLEDGMENT

It is a pleasure to acknowledge the skill of Mrs. Patricia ·ecliger in making the diagram of th f t l membranes.

LITERATURE CITED

Anderson, J W and W A. Wimsatt 1953 The fetal membranes and placentation of the tropical American noctilionid bat, Dirias albiventer minor. Anat. Rec., 117 573–574

Gomori, G. 1941 The distribution of phosphatase in normal organs and tissues. J Cell. and Comp. Physiol., 17 71–83.

Gopalakrishna, M. 1950 Studies on the embryology of Microchiroptera, Part VI. Structure of the Placenta in the Indian vampire bat, *Lyroderma lyra lyra* (Geoffroy)—(Megadermatidae) Proc. Nat. Inst. Sci. India, 16 93–98.

——— 1958 Foetal membranes in some Indian Microchiroptera. J Morph 102 157–197

Hotchkiss, R. D. 1948 A microchemical reaction resulting in the staining of polysaccharide in fixed tissue preparations. Arch. Biochem., 16 131–141

McManus, J F A. 1946 Histological demonstration of mucin after periodic acid. Nature, 158 202.

Mossman, H. W 1926 The rabbit placenta and the problem of placental transmission. Am. J Anat., 37 433–497

——— 1937 Comparative morphogenesis of the fetal membranes. Carnegie Contrib. Embryol., 26 129–246.

——— 1953 The genital system and the fetal membranes as criteria for mammalian phylogeny and taxonomy J Mamm., 34 289–298.

Mossman, H. W and I. Judas 1949 Accessory corpora lutea, lutein cell origin, and the ovarian cycle in the Canadian porcupine. Am. J Anat., 85: 1–39.

Wimsatt, W A. 1944 An analysis of implantation in the bat, Myotis lucifugus lucifugus. Ibid., 74: 355–411.

——— 1945a Notes on breeding behavior pregnancy and parturition in some vespertilionid bats of the eastern United States. J Mammal 26 23–33.

——— 1945b The placentation of vesper tilionid bat, Myotis lucifugus lucifugus. Am. J Anat 77 1–51

——— 1954 The fetal membranes and placentation of the tropical American vampire bat, Desmodus rotundus murinus. Acta Anat., 32: 285–341.

——— 1958 The allantoic placental barrier in chiroptera new concept of its organization and histochemistry Ibid., 21 141–186.

Wimsatt, W A., and H. Trapido 1952 Reproduction and the female reproductive cycle in the tropical American vampire bat, Desmodus rotundus murinus Am J A t 91 415–446.

Wimsatt, W A., and C H l 1945 The normal occurrence n ——ening in the bursa ovarii of t rs Rec 93 4 –57

PLATE 1

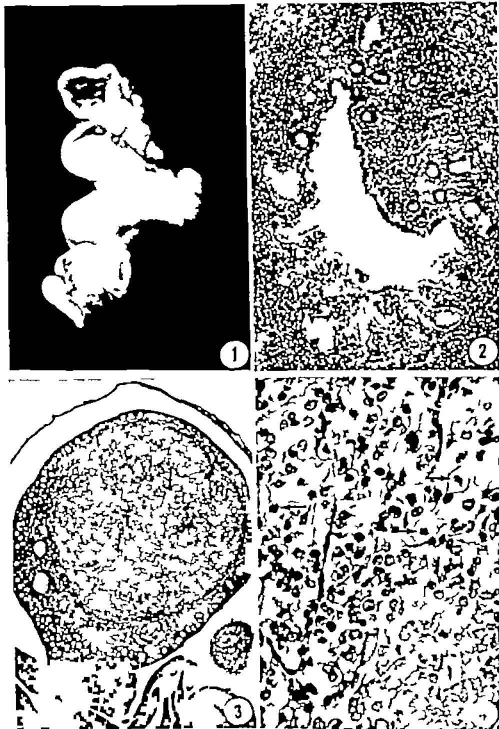
EXPLANATION OF FIGURES

1 Uterus of mature specimen of Noctilio collected in July. Note particularly the symmetry of the cornua, the coiled uterine tube and the filmy bursa ovarii surrounding the ovary.

2 Section of uterus of a December specimen in the estrus phase. The mesometrium is toward the bottom of the figure indicating that the "implantation ridge" is both antimesometrial and lateral. The gland development in this species is not very great, and the uterine stroma is very highly cellular. Masson stain, × 110.

3 Ovary of a pregnant specimen, taken shortly after implantation (cf. fig. 5). Note the atretic follicles, the large number of primary follicles in the hilus, and the bursa ovarii. Hematoxylin and eosin × 55.

4 The decidual reaction in early pregnancy. This area is in the decidua basalis, which is the only decidua which develops to any significant degree. The large, light, vacuolated cells give evidence that this is typical decidual reaction. Note the mitotic figures (arrows). Hematoxylin and eosin. × 360.


1
2
3

Abbreviations (Plates 2 7)

The areas of potential physiological exchange between mother and fetus are indicated by the double-ended arrows.

AC, Amniotic cavity	PE, Parietal endoderm
AL, Allantois	RM, Reichert' membrane
CT Cytotrophoblast	ST Syntrophoblast
DB Decidua basalis	VE, Visceral endoderm
EM, Embryonic mass	VV Vitelline vessel
EX, Exocoelom	YC, Yolk-sac cavity
MV Maternal vessel	

PLATE 2

EXPLAN TION OF FIGURES

5 Implanting embryo, collected December 6. It appears that the re stricted lumen of the yolk-sac cavity is artifactual, resulting from the collapse of the bilaminar omphalopleure during histological processing. The extent of the trophoblastic invasion can be learly seen, owing to the contrast between the more basophilic fetal tissue nd the more lightly staining decidua basalis. Note the still relatively poorly developed glands. Hematoxylin and eosin, × 90.

6 Embryonic disc, amniotic cavity and developing placenta of speci men collected January 13. Judging by the relatively undifferentiated state of the disc (note primitive pit) it seems most likely that the extraembryonic mesoderm which is invading the trophoblast, produc ing the chorion, has not come from the spread of gastrul ted mesoderm but has rather formed from trophoblast. Since the amnion has not yet separated from the chorion, and since there re ma y maternal vessels in close proximity to the amniotic surf ce there is the possibility of chorioamniotic placental relationship. The are at top center is shown in higher powe in figure 8. PAS and hematoxylin × 130.

DB

YC

5

YC

AC

MV

6

PLATE 3

EXPLANATION OF FIGURE

7 Semidiagrammatic view of specimen collected February 4. At this stage the expanding yolk-sac cavity undercuts the placental disc being bounded laterally by the persistent bilaminar omphalopleure. The embryo is moving away from the placental disc owing to the expansion of the exocoelom. By this process the chorioamniotic and the choriovitelline relationships are destroyed. Cytotrophoblast stippled. Syntrophoblast and Reichert membrane, both heavy line. The mesodermal area within the placental disc has been left white. Thus, an extensive labyrinth of trophoblast and maternal vessel has been built up before any significant vascularization of the disc takes place. × 35.

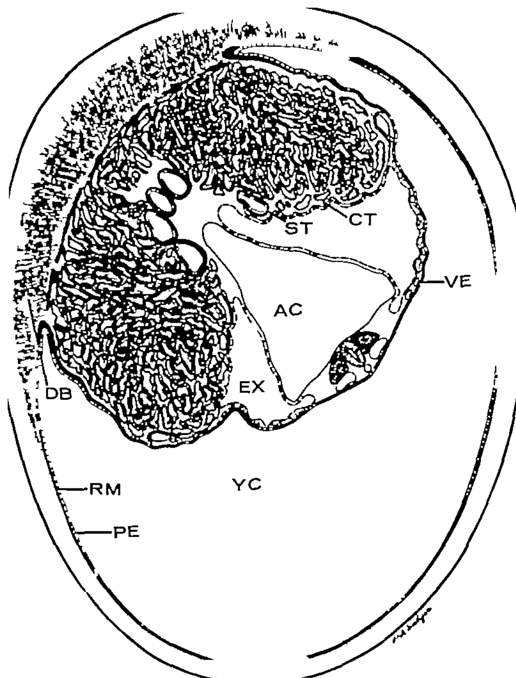

ST
CT
VE
AC
EX
DB
RM
YC
PE

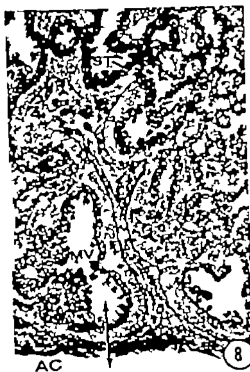
PLATE 4

EXPLANATION OF FIGURES

8 Higher power view of area indicated in figure 6, showing the invading "tongue" of mesoderm, the PAS-positive membrane separating it from the cytotrophoblast, the more basophilic syntrophoblast (not clearly separated from the cytotrophoblast) and the PAS-positive membrane separating the syntrophoblast from the maternal endothelium. The amniotic cavity is at the bottom of the figure. PAS and hematoxylin, × 270.

9 High power view of specimen collected December 15 showing how two "villi" of endoderm have invaded into the substance of the placental disc. The maternal vessels have collapsed completely in fixation, but they are in close proximity to the vitelline cavity (arrow). Hematoxylin and eosin, × 310.

10 Junctional zone between decidua basalis and decidua parietalis, showing also the zone of contact between the placental labyrinth and the decidua basalis. The cytoplasmic basophilia of the syntrophoblast can be seen; the large clear nuclei with prominent nucleoli lying beyond the edge of syntrophoblast, are those of cytotrophoblast. Note that the decidual reaction is now much diminished. Also to be seen are the uterine gland and the intense PAS-positivity of Reichert's membrane. PAS and hematoxylin, × 300





MV
YC
10

PLATE 6

EXPLANATION OF FIGURES

14 Uterine wall of specimen shown in figure 11 The parietal endoderm is on the extreme right, in contact with the vitelline cavity Under lying this is Reichert's membrane, and this, in turn is in contact with cells which may be either trophoblast or decidua, or both. Im mediately subtending thi layer can be seen several blood vessels. The exchange of materials between these vessels and the vitelline cavity is postulated. × 430.

15 Low power view of placental disc of specimen collected April 4 The visceral wall of the yolk sac has pulled free of its ttachment to the margin of the placental disc. Note that the placental disc is undercut, and is lined in this rea by the persistent trilaminar omphalopleure. Figures 16, 17 and 20 are also taken from this specimen. Masson stain, × 60.

16 Photomicrograph of specimen shown in figure 15 showing from left fetus, amnion, visceral yolk sac, and parietal yolk sac in intimate contact with the uterine wall. The persistence of Reichert' membrane may be noted, well a the m ternal vessel immediately underlying it. With the expansion of the embryo, nd the resulting pposition of parietal and visceral walls of the yolk sac (partial inversion) the vitelline vessel are brought very near the maternal vessels, and the potential for maternal-fetal interchange i more obvious. Azs stain × 430.

YC
EX
AC
YC
14
15
PE
RM
VE
EX
AC
YC
16

Development of Leydig Cells in the Normal Human Testis

A CYTOLOGICAL CYTOCHEMICAL AND QUANTITATIVE STUDY[1]

ROBERTO E. MANCINI, OSCAR VILAR, JUAN CARLOS LAVIERI, JUAN A. ANDRADA AND JUAN J HEINRICH
Instituto de Anatomía General y Embriología, Facultad de Ciencias Médicas Buenos Aires, Argentina

Various authors have studied the histology of the human testis and postulated that Leydig cells are derived from fibroblasts in the fetus (Bouin and Ancel, '03 Stieve, '27; Esaki, '28 Gillman, 48) and also at puberty (Charny et al., '52; Sniffen '52 Albert et al. '53) Although cytological features of human Leydig cells have been studied the precise characterization of the different cell types and their quantitative variation during the development of the human testes have not been fully accomplished. Cytochemical observations have been restricted to lipids and cholesterol in the mature cells (Pollock, 42 Montagna and Hamilton, '51 Mancini et al. '52) but investigations of these and other substances *as well as enzymes, during the* development of Leydig cells have not been performed

In order to add more information on these subjects the following investigation was carried out (a) cytological, cytochemical and enzymatic study of the different types of fibroblasts and Leydig cells of the intertubular spaces in the normal human testis and (b) study of the quantitative, absolute and relative variations of these *cell types and of their interrelationships in order to establish the precursors, develop*ment and fate of Leydig cells.

MATERIAL AND METHODS

Sixty-six cases were studied, distributed by age as shown in table 1 Most of the material was obtained by biopsy according to the technique of Charny and Meranze (42) but fresh necropsy material was also used when microscopic observations showed it to be free from alterations as judged by comparison with the

TABLE 1

Source of human testicular material and distribution according to age

Group	Age	Number of cases
Embryo	*2 to 4 months*	4
Fetus	6 to 8 months	3
Lactant	Up to 60 days	8
Infancy I	Up to 4 years	8
Infancy II	4 years to puberty	11
Puberty I	variable	8
Puberty II	variable	6
Puberty III	variable	4
Adult	post pubertal	14

biopsy material. Cytochemical techniques could only be applied to fresh material obtained by biopsy

The tissue was immediately divided into five parts and fixed as follows: (a) in Bouin's solution for general morphology glycogen, nucleoproteins mucopolysaccharides and glycoproteins (b) in 10% calcium formaldehyde for lipids, cholesterol esters and silver impregnation; (c) in acetone at 0 C for enzymes; and (d) in a special reagent for ascorbic acid (Deane and Morse, 48) Fresh frozen sections were also used for enzymes.

For general morphology the following staining techniques were used hemateineosin, Heidenhain-azan stain and del Rio Hortega's panoptic silver impregnation. The histochemical methods applied were (a) 0 055% toluidine blue at pH 3.5 and Alcian blue controlled by incubation in hyaluronidase (30 T.R.U per cm) at 37 C for 3 and 12 hours for mucopolysaccharides; (b) 0.055% toluidine blue at pH 4 7 controlled by incubation in ribonu

[1] This work was supported by The Population Council, Inc., New York.

clease (Nutritional Biochemical Co. 1 mg per cm³) at 37 C for 30 and 60 minutes for nucleoproteins (c) the periodic acid-Schiff technique controlled by incubation in Taka-diastase (Parke Davis 0 5%) at 37 C for 60 minutes and in methanol-chloroform for two hours for glycogen, glycoproteins and glycolipids and (d) Sudan IV and Sudan black B for lipids and digitonin for cholesterol. Enzymes were analyzed cytochemically according to the following methods alkaline phosphatase (Gomori, '52; Manheimer and Seligman 49); acid phosphatase (Gomori, '52); 5-nucleotidase (Pearse and Reiss, '52); glucose-6-phosphatase (Wachstein and Meisel, '56)- phosphorylase (Takeuchi, '58) phosphamidase (Gomori 49) esterases (Nachlas and Seligman, 49); lipase (Gomori, '50); leucyl-aminopeptidase (Burstone and Folk, '56) cytochrome oxidase (Nachlas et al. '58); succinic dehydrogenase (Pearson '58) and 3-β-ol-dehydrogenase (Wattenberg, '58 Levy et al. '59; Niemi and Ikonen '61) To check the specificity of these enzymes, similar sections were in- for identical periods in control of the same composition minus the specific substrates. Inhibitors were also used as follows malonic acid disodium salt (3 7 mg per ml) for succinic dehydrogenase sodium azide (0 005 M) for cytochrome oxidase sodium fluoride (0 01 M) for acid phosphatase and esterase; versene (0 01 M) for leucyl-aminopeptidase potassium cyanide (0 01 M) for alkaline phosphatase.

To simplify the quantitative study cases from fetal life to adulthood were grouped by age. Since there appeared to be little *correlation between the age of the individ*ual and either the appearance or duration of puberty (Greulich et al. 42) it was considered advisable to separate the puberal cases into three subgroups The first group included those specimens from individuals in whom there were clinical signs of puberty (pubic and axillary hair change in voice etc.) indicative of circulating androgens but in whom there were no histological signs of spermatogenesis The second group comprised those cases where in addition to the clinical signs of puberty histological examination showed evidence of the initiation of spermatogenesis and the presence of spermatocytes. The third group included individuals in whom puberty was not clinically complete but histological study revealed spermatogenesis. Serial sections of biopsies were used for cell counts 200 intertubular cells were counted at random in all specimens and the number of all cell types was calculated in any age group on the basis of an average per 200 cells. The average for each cell type was compared at different ages and the significance of these variations statistically determined.

RESULTS

The morphological and cytochemical picture of the different intertubular cellular types (figbroblasts Leydig cells) will be described first and then the cell counts and the cell transformations from fibroblasts to Leydig cells.

Cellular types

Different types of cells, with special distributions according to age were seen in the intertubular spaces and were designated as types A, B C and D of a cell known as fibroblast-like cell"; fetal and adult Leydig cells and degenerating cells. This cellular subdivision was better revealed by panoptic silver impregnation than with other staining techniques especially in the case of fibroblasts. Due to the lack of counterstaining when cytochemical reactions were applied, the localization of reactive substances in the different cell types was possible using phase contrast microscopy or by running an identical section submitted to staining techniques When sections were incubated in control media to determine the specificity of the results for enzymes the reactions were sharply depressed or eliminated.

Fibroblasts

Fibroblast A resembled the juvenile fibroblast of the mesenchyme It had a round nucleus with pale chromatin and a small nucleolus. The scarce cytoplasm showed numerous branches which contacted those of similar neighboring cells (figs. 1 7) Basophilia, due to the presence of ribonucleoproteins was present in the cytoplasm but reactions for lipids, PAS-positive substances mucopolysaccharides, ascorbic

acid and enzymes were negative. *Fibroblast B* had a round or elongated shape with fewer and shorter branches than fibroblast A. The nucleus showed a thin membrane, fine chromatin granules and a small nucleolus (figs. 1 8) Except for a weak basophilia around the nucleus the rest of the histochemical reactions applied gave negative results. *Fibroblast C* presented a nucleus with a thicker membrane and coarser chromatin than that of fibroblast B and a nucleolus which was sometimes surrounded by a clear vesicle. The cytoplasm was finely granular around the nucleus and showed very thick branches (figs. 4 9 10) Some of these cells in addition to a perinuclear basophilia, revealed a slight positive reaction for lipids and ascorbic acid. *Fibroblast D* was similar to fibrocytes of connective tissue proper Two morphological varieties were seen which appeared to be transitional stages between them; both were characterized by spindle shape. Variety D1 contained a pale nucleus, chromatin in fine granules and often a small nucleolus. Variety D2 presented an elongated nucleus with compact chromatin (fig. 2)

Leydig cells

Three main types of *fetal Leydig cells* were observed. The first one (F.L.C.I) was small and possessed a well delimited cytoplasm and a nucleus with fine chromatin and a small nucleolus (figs. 1 11) The cytoplasm was faintly eosinophilic and frequently numerous granules and a perinuclear area of moderate basophilia were seen. The second type (F C.L.II) was larger and polyhedral. The nucleus had thick chromatin and prominent nucleolus. The cytoplasm, which was weakly eosinophilic contained small perinuclear granules. Some vacuoles were located at the periphery of the cell (figs. 2, 12) A faint basophilia and droplets of lipids and cholesterol were present throughout the cytoplasm. PAS-positive granules resistant to ptyalin and methanolchloroform were occasionally seen, but pigment and crystals were never found. The third type (F.L.C III) was the largest of this series. It presented a somewhat pyknotic and displaced nucleus, loss of granules and eosinophilia in the cytoplasm while vacuoles at the periphery appeared increased in size and number (figs. 2, 13) Basophilia was reduced and only weak reactions for lipids and cholesterol were present.

There were also different types of *adult Leydig cells*. The first type (A.L.C.I) had a polygonal or round shape. When compared with fibroblastic C it was larger the cytoplasm was finely granular and eosinophilic (figs. 5 15) the nucleus was frequently small with a thick membrane, abundant chromatin and a large nucleolus. Fine droplets of lipids were frequently present in the cytoplasm. The perinuclear basophilia and reactions for cholesterol, cytochrome oxidase, succinic dehydrogenase leucyl-aminopeptidase lipase esterase, 3-β-ol-dehydrogenase and ascorbic acid were moderately positive. Alkaline and acid phosphatase, 5-nucleotidase, phosphamidase glucose-6-phosphatase and phosphorylase reactions were negative. The second type (A.L.C.II) was a polyhedral and larger cell. The cytoplasm was less eosinophilic and showed small peripheral vacuoles; the nucleus had a thick membrane and one or two nucleoli (figs. 6 16) Reactions for lipids and cholesterol were intensely positive basophilic staining and the reaction for ascorbic acid appeared weaker and enzyme content was the same as that demonstrated in Leydig cell I (figs. 19 to 30) Pigment, crystals and PAS-positive granules resistant to diastase and methanol-chloroform were sometimes present in these cells. The third type (A.L.C.III) was the largest; it sometimes had a pyknotic nucleus or more frequently shrinkage of the nuclear membrane and partially or fully vacuolated cytoplasm (figs. 6 17) It contained lipids but the rest of the cytochemical reactions were only slightly positive or negative.

Degenerating cells

The size and shape of degenerating cells were variable Nuclei were pyknotic and the cytoplasm fully vacuolated (figs. 3 18) Only moderate positive reactions for lipids and ascorbic acid were occasionally seen. They had neither crystals nor pigment. Between fibroblast C, the fetal and adult Leydig cells and the degenerating cell, various transitional cellular types were observed (fig 14) These cells were

tivity in tissues of intact and hypophysectomized rats. Endocr 65 932–943.

McEnery W B., and W O. Nelson 1951 Cytochemical studies of the testes of rats. Anat. Rec., 109 324–332.

Mancini, R. E., R. Narbaitz and J C. Lavieri 1960 Origin and development of the germinative epithelium and Sertoli cells in the human testis Cytological, cytochemical and quantitative study Ibid., 136. 477–490.

Mancini, R. E., J. Nolazco and F A. de la Balze 1952 Histochemical study of normal adult human testes. Ibid., 114 127–147

Manheimer, L. H., and A. M. Seligman 1949 Improvement in the method for the histochemical demonstration of the alkaline phosphatase and its use in a study of normal and neoplastic tissue. J. Nat. Cancer Inst., 9 181–199.

Montagna, W., and J B. Hamilton 1951 Histological studies of human testes. I. The distribution of lipids. Anat. Rec., 109 635–659

Nachlas, M. M., and A. M. Seligman 1949 Histochemical demonstration of esterase. J. Nat. Canc. Inst., 9: 415–425.

Nachlas, M. M., D T Crawford, T P Goldstein and A. M. Seligman 1958 The histochemical demonstration of cytochrome-oxidase with a new reagent for the Nadi reaction. J Histochem. Cytochem., 6 445–456.

Niemi, M., and M. Ikonen 1961 Steroid 3-β-ol-dehydrogenase activity in fetal Leydig cells. Nature, 189 592–593.

Pearse, A. G. E., and J. L. Reis 1952 The histochemical demonstration of a specific phosphatase (5-nucleotidase) Biochem. J 50: 534–536.

Pearson, B J 1958 Improvement in the histochemical localization of succinodehydrogenase by use of nitroneotetrazolium chloride. J Histochem. Cytochem., 6: 112–121.

Pollock, W F 1942 Histochemical studies of the interstitial cells of the testis. Anat. Rec., 84: 23–27

Roosen-Runge, E. C., and D. Anderson 1959 The development of the interstitial cells in the testis of the albino rat. Acta Anat., 37 125–137

Samuels, L. T., M. L. Helmreich, M. B. Lasater and H. Reich 1951 An enzyme in endocrine tissues which oxidizes Δ-5-3-hydroxysteroids to α-β unsaturated ketones. Science, 113. 490–491.

Sniffen, R. C. 1952 Histology of the normal and abnormal testis at puberty Ann. N. Y Acad. Sci., 55 609–618.

Stieve, H. 1927 Die Entwicklung der Keimzellen und der Zwischenzellen in der Hodenanlage des Menschen. Ein Beitrag zur Keimbahnfrage. Z. mikr.-anat. Forsch., 10: 225–285.

——— 1930 Harn- und Geschlechtsapparat. II. Teil. Männliche Genitalorgane. In v Möllendorff Hb. mikr. Anat. d. Menschen., VII, edited Springer Berlin.

Takeuchi, T 1958 Histochemical demonstration of branching enzyme (amylo-1 4-1 6-transglucosidase) in animal tissues. J Histochem. Cytochem., 6: 208–216.

Tillinger, K. G. 1957 Testicular morphology Acta Endocrinol., suppl. 30, 24: 27–38.

Verne, J. 1953 Les estérases des cellules interstitielles du testicule. Ann. d'endocrinologie., 14 747–750.

Vilar O., M. I. Perez del Cerro and R. E. Mancini 1962 The Sertoli cell as a "bridge cell" between the basal membrane and the germinal cell. Histochemical and electronmicroscopical observations. Exp. Cell Res., 27 158–161

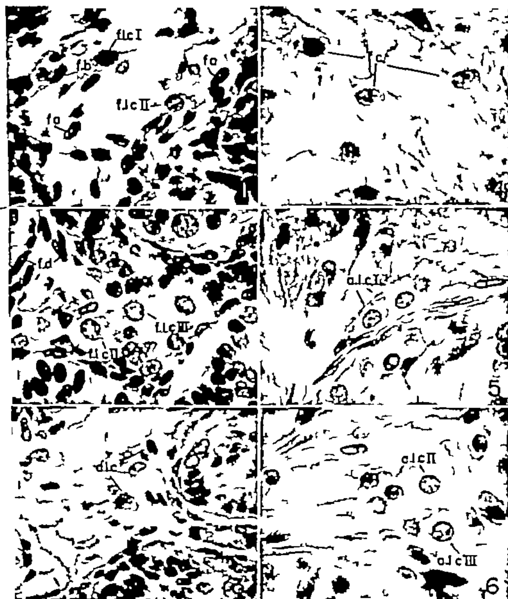
Wachstein, M., and E. Meisel 1956 On the histochemical demonstration of glucose-6-phosphatase. J Histochem. Cytochem., 4: 592–601.

Wattenberg, L. W 1958 Microscopic histochemical demonstration of steroid-3-β-ol-dehydrogenase in tissue sections. Ibid., 6 225–232.

Williams, R. G. 1950 Study of living interstitial cells and pieces of seminiferous tubules in autogenous grafts of testis. Am. J Anat., 86: 343–370.

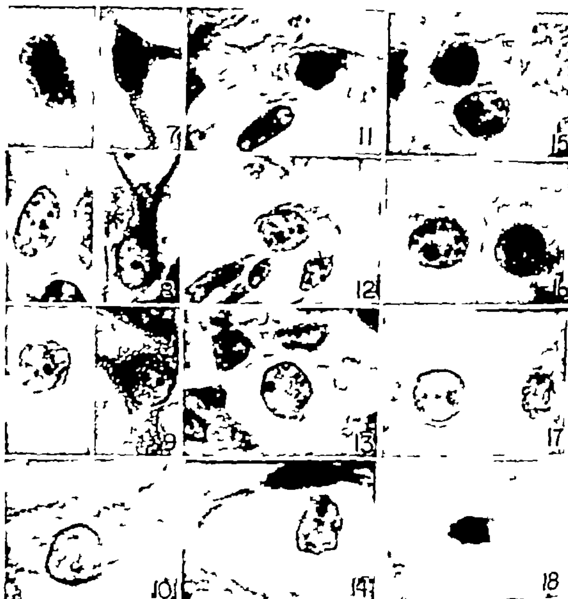
Yamauchi, S. 1955 Histo-and endocrinological studies on interstitial cells in rat testes. Post-natal development of interstitial tissue in the testis. Acta. Anat. nipponica., 30: 377–385.

Roberto E. Mancini, Oscar Vilar, Juan Carlos Lavieri, Juan A. Andrada and Juan J. Heinrich



Cell popul tion of intertubular spaces f the tes I fetal and pubertal ages Various types of fibroblasts Leydig cells are seen H d E 930.

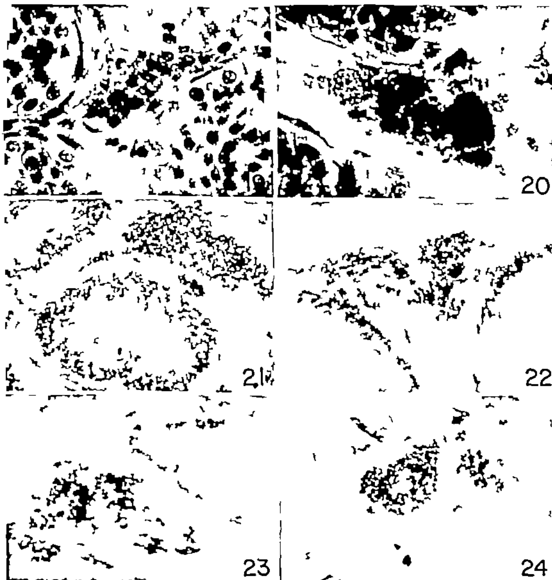
1 Fetal period (third month) Fibroblasts A f) B (f b) and Leydig cells type I and II (f l f f l II)
2 Fetal period xth month) Leydig cells II and III (f.l II f l III) surrounded by fibroblasts D (f d) A the op and at the bottom seminiferous tubules are seen
3 Fetal period (month) Different types f degenerating L dig cells (d.l)
4 First phase of pub Fibroblasts C (f.c)
5 Second phase of pu Leydig cells I (l I) in the vicinity f seminiferous tubule
6 Third phase of puberty g ell II and III (a.l.c.II a.l II) Also few fibroblasts D and seminiferous tubules hown.



Different types of fibroblasts and Leydig cells. H. and E. stain. × 2[illegible]

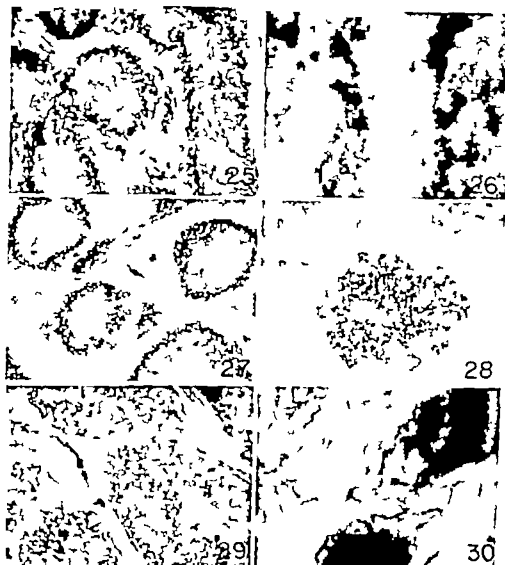
7 Fetal period (second month) Fibroblast A (left) At right the same cell seen with panoptic silver impregnation of del Rio Hortega.
8 Fetal period (second month) Fibroblast B (left) At right the same cell as seen with panoptic silver impregnation of del Rio Hortega
9 First phase of puberty Fibroblast C (left) At right the same cell seen with panoptic silver impregnation of del Rio Hortega.
10 First phase of puberty Fibroblast C Transitional stage to Leydig cell I.
11 Fetal period (second month) Leydig cell I.
12 Fetal period (sixth month) Leydig cell II.
13 Fetal period (eighth month) Leydig cell III.
14 Fetal period (eighth month) Degenerating Leydig cell, early stage
15 Second phase of puberty Leydig cell I.
16 Second phase of puberty Leydig cell II.
17 Third phase of puberty Leydig cell III.
18 Third phase of puberty Degenerating Leydig cell, advanced stage.

Roberto E. Mancini, Oscar Vilar, Juan Carlos Lavieri, Juan A. Andrada and Juan J. Heinrich



Histochemical techniques.

19 Second phase of puberty. Ascorbic acid in testis. Positive reaction (as fine granules) in the cytoplasm of Leydig cells. Counterstaining with hematoxylin. × 400.
20 Second phase of puberty. Lipids in testis. Positive reaction in Leydig cells. Sudan IV counterstaining with hematoxylin. × 420.
21 Second phase of puberty. Leucyl-aminopeptidase in testis. Positive reaction in small group of Leydig cell and also in germinal cells of tubules. × 220.
22 Same preceding higher magnification showing positive leucyl-aminopeptidase in group of Leydig cells. 400
23 Third phase of puberty. 3 β-ol dehydrogenase in testis. Positive reaction in clump of Leydig cells and negative in germinal cell of seminiferous tubule. × 1.0
24 Same preceding one at higher magnification, showing cell with positive reaction in the cytoplasm. × 1 100



Histochemical techniques.

25 Third phase of puberty. Cytochrome oxidase in testis. Positive reaction in groups of Leydig cells as well as in germinal cells of t bules. × 220.

26 Same as preceding showing group of Leydig cells between two tubules; higher magnific tion. × 1,200.

*7 Third phase of puberty. Succinicdehydrogenase in testis. Positive reaction in groups of Leydig cells as well as in germinal cells f tubules. × 220.

28 Same as preceding showing group of Leydig cells t higher magnific tion. × 1,200.

29 Second phase of puberty. Esterases in testis. Positive reaction in groups of Leydig cells and negative in germinal cells. × 375.

30 Same as preceding howing group of Leydig cell t higher magnification. × 1,500.

A Correlated Histochemical and Biochemical Study of Glycogen Storage in the Rat Placenta[1]

HELEN A. PADYKULA AND DOROTHY RICHARDSON
Department of Anatomy, Harvard Medical School, Boston, Massachusetts and the Department of Zoology, Connecticut College, New London, Connecticut

Since Claude Bernard suggested in 1859 that the placenta may perform the glycogenic function before the fetal liver has acquired this capacity, considerable attention has been given to localizing this important metabolic reserve. Bernard's observation that the decline in placental glycogen correlates in time with the onset of glycogen storage in the fetal liver has been verified histochemically and biochemically in several species (*rabbit*, Lochhead and Cramer, '08; Tuchmann-Duplessis and Bortolami, '54; *guinea pig*, DuBois and Ducommun, '55; *rat*, Padykula, '58b; *human*, Villee, '53). Despite this general agreement, the full significance of placental glycogen remains to be demonstrated.

Bernard's correlation was made on the basis of studies on the guinea pig and rabbit placentas. In the rabbit, glycogen is localized exclusively in the maternal placenta; the fetal placenta, including the yolk sac, is devoid of glycogen (Davies, '56). However, in the human and rat placentas glycogen storage is widespread, occurring in various maternal and fetal components (*human*, Wislocki and Padykula, '61; *rat*, Goldmann, '12; Krehbiel, '37; Bridgman, '48a and b; Wislocki and Padykula, '53; Padykula, '58b; Bulmer and Dickson, '60). In the human fetal placenta glycogen is abundant only early in gestation, and it begins to disappear after eight weeks. Glucose secretion is a property of the human fetal placenta *in vitro* only during this early period of gestation (Villee, '53; Hagerman et al., '59). It was assumed that glucose-6-phosphatase activity was present only in the early human placenta and was responsible for this release of glucose *in vitro*.

In this report, an attempt has been made to relate the histochemical and cytochemical localizations and fluctuations in amount to the quantitative changes in the glycogen level of the rat placental membranes. Some ultrastructural localizations of glycogen in the visceral endoderm and spongiotrophoblast are also presented. To discover which of the glycogen storage regions of the rat placenta might participate in glucose secretion, glucose-6-phosphatase activity has been localized histochemically. The present results emphasize the striking quantitative importance of glycogen storage in the spongiotrophoblast and also suggest that only the decidua and labyrinthine trophoblast in the rat placenta secrete glucose into the fetal blood.

MATERIAL AND METHODS

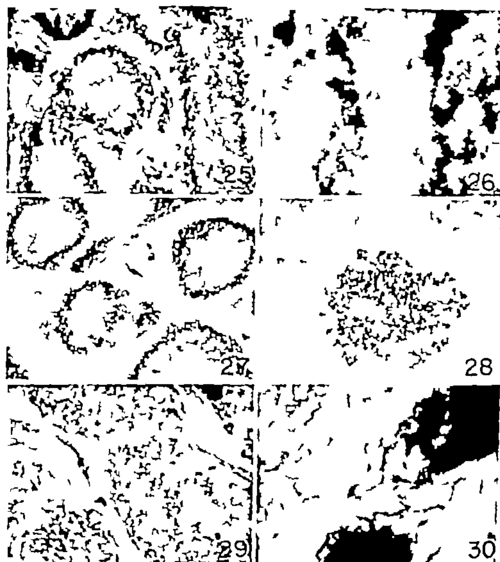
The placental membranes of albino rats were studied principally between 13 days and term (23 days). The first day of gestation was designated as that of the morning on which spermatozoa were found in the vagina. For both histochemical and biochemical studies, the animals were killed with chloroform.

Some histochemical and biochemical determinations also were made on placentas from rats which had been injected with trypan blue. These rats were given 1 ml of 1% trypan blue subcutaneously on the seventh, eighth and ninth days of gestation. Such exposure to this teratogenic agent results in 60% abnormal fetuses (Wilson, '55). These experimental animals were autopsied on the eighteenth day

[1] Supported by U S P H S grants [illegible]

[2] Research Career Development Award from the United States Public Health Service.

[3] National Science Foundation, Science Faculty Fellow, [illegible]



Histochemical techniques

25 Third phase of puberty. Cytochrome oxidase in testis. Positive reaction in groups of Leydig cell as well as in germinal cells of tubules. × 220.

26 Same preceding showing group of Leydig cells between two tubules; higher m g nific tion. 1,200.

27 Third ph se of puberty. Succinicdehydrogenase in testis. Positive reaction in groups of Leydig cells as well as in germinal cells of tubules. × 220.

28 Same as preceding showing group of Leydig cells t higher magnification. × 1,200.

29 Second phase of puberty. Esterases in testis. Positive reaction in groups f Leydig cells and negative in germinal cells. × 375.

30 Same a preceding bowing group of Leydig cells t higher magnification. × 1,500.

ded according to the technique for electron microscopy Visceral yolk sacs were fixed in 1% osmium tetroxide and embedded in methacrylate (15% methyl 85% butyl) Sections (2 μ thick) were cut according to standard procedures on a Porter Blum ultramicrotome mounted on glass slides in a drop of 10% acetone dried on a hot plate, and subjected to the periodic acid Schiff procedure The principal histochemical limitation of this osmicated material resides in the fact that malt diastase or salivary amylase is unreactive toward glycogen preserved in this manner Specific identification of glycogen in these circumstances is dependent on simultaneous study of the same sites in paraffin sections and/or identification of characteristic glycogen particles by lead staining of ultrathin sections (Watson '58; Revel et al., '60) Some ultrastructural observations of glycogen storage in the visceral endoderm and spongiotrophoblast were made using ultrathin sections of similarly osmicated material. These thin sections were stained with lead hydroxide and then examined in an RCA-EMU 3E electron microscope

(2) *Glucose-6-phosphatase* activity was preserved by freezing half of a placenta at − 20 C Thawed, dried, chemically untreated cryostat sections (10–15 μ) were incubated in a medium composed of tris buffer (pH 6 7) glucose-6-phosphate (G-6-P) and lead nitrate (Wachstein and Meisel, '56) The relatively low placental phosphatase activity toward G-6-P required one to two hours incubation to obtain an adequate staining reaction. Glycerophosphate and adenosine triphosphate were also used as substrate under these conditions. Maternal liver was usually incubated along with the sections of placenta to serve as the standard for comparison.

Biochemical determination of glycogen Isolated placental discs and visceral yolk sacs were used for quantitative determinations of glycogen levels between 13 and 21 days. The placental disc can be easily separated from the maternal tissue by blunt dissection especially late in gestation The separation occurs at the junction of the giant cells with the decidua thus the isolated disc is composed of giant cells, spongiotrophoblast, and labyrinth permeated with fetal and maternal blood (text fig 1) Each visceral yolk sac can be severed at the point of its circular attachment to the antimesometrial or fetal surface of the chorio-allantoic disc

Approximately 200–1000 mg of disc were digested in 5 ml of 35% KOH. This was later diluted to 10 ml, and the glycogen was isolated from 2 ml aliquots. Since the visceral yolk sac is a thin, delicate membrane approximately 20-300 mg were digested in only 1 ml of 35% KOH The glycogen was then isolated from this total volume of 1 ml. Glycogen was separated and purified by alcoholic precipitation over a period of one hour after acid hydrolysis, the resulting glucose was measured by the Nelson-Somogyi reagents (Nelson, 44 Somogyi, '52) The measure was expressed in terms of mg glycogen/100 mg wet weight tissue. The glycogen level of the maternal liver served as a standard for comparison with placental levels this hepatic glycogen usually comprised about 5% of the wet weight, as determined by this procedure.

RESULTS

I *General histophysiological description of the rat placenta between 13 days and term*

A brief histophysiological description of the components of the chorioallantoic placenta and the inverted yolk sac placenta is included here for convenience in interpreting the histochemical-biochemical results presented in this paper Detailed cytological and histological descriptions may be found in the following publications Duval 1891 Everett '35 Krehbiel '37 Mossman '37 Bridgman, 48 a and b Holmes and Davies 48 Amoroso '5_ Wislocki and Padykula, '53; Wislocki and Dempsey '55 Padykula '58a, Anderson, '59 Schiebler and Knoop '59 Bulmer and Dickson, '60

By the thirteenth day the chorio-allantoic placent [illegible] clearly differentiated and the trophoblast of the ectoplacental cone and lami[illegible] has given rise to three closely related regions of the placental disc (text fig 1) The *labyrinthine trophoblast* is arranged [illegible] the form of numerous branching and [illegible]nastomosing cords or plates and [illegible] to the maternal blood in a hem-

ochorial relationship (Wislocki and Dempsey '35) The resultant extensive surface *provides the major site of physiological* transfer between the maternal and fetal bloodstreams The mesometrial surface of the labyrinth is capped by the *spongiotrophoblast* which is an epithelial mass of cytotrophoblast permeated by sinuses which contain maternal blood. The function of this trophoblastic region is unknown except for its prominent role in glycogen storage The outer surface of the spongiotrophoblast is continuous with a loose meshwork of *giant cells* which lie in close association with the maternal decidua. These giant trophoblastic cells are phagocytes in part (Alden 48) and recently were identified as the probable sites of steroid synthesis in the rat placenta by Deane and her associates ('61). The ultrastructure of these three trophoblastic derivatives has been recently delineated in an important paper by Schiebler and Knoop ('59)

The inverted yolk sac placenta of the rat is composed also of three distinct histological derivatives (text fig 1) (1) an *inner visceral wall (visceral splanchnopleure)* (2) the outer parietal wall (bilaminar omphalopleure) and (3) the endodermal sinuses Before the sixteenth day the outer non-vascular *parietal wall* is closely adherent to the decidua capsularis and it is composed of parietal endodermal cells resting on the thick basement membrane of Reichert. One portion of the parietal wall clothes the fetal surface of the chorio-allantoic disc (see diagram in Anderson '59) After the sixteenth day most of the parietal wall disappears except for that attached to the fetal surface of the disc which is continuous with a coiled remnant of Reichert's membrane (text fig 1) After this architectural change the yolk sac cavity and uterine cavity become confluent. The *visceral splanchnopleure* near its attachment to the placental disc is enlarged through the formation of ridges (or villi) which become taller and more branched as gestation proceeds. This highly vascularized layer is an early site of fetal hematopoiesis. In the visceral endoderm many of the cytological and cytochemical properties of an actively absorbing epithelium can be observed (Wislocki and Dempsey '35 Padykula, '58) The phagocytic properties of the visceral endoderm have long been recognized (Goldmann 12; Everett, '35; Luse 57) Recently Brambell and his associates (48 '56 '57) have demonstrated that in the rabbit and rat maternal antibodies are transferred exclusively through the visceral endoderm Thus, in these species passive immunity is imparted prenatally through the mediation of the ancient yolk sac membrane The *endodermal sinuses* are invaginations composed of both parietal and visceral layers of the yolk sac which accompany the branching umbilical vessels into the placental disc (Duval 1891 Amoroso, '52; Wislocki and Padykula '53) These peculiar derivatives of the yolk sac are best developed after the fifteenth day and may perform an absorptive function (Duval 1891; Brambell and Halliday '56 Padykula '58)

II. *Histochemical sequences in glycogen storage during gestation*

Although some of the localizations described below have been reported in part in previous publications (Bridgman 48 a and b Wislocki and Padykula, '53 Bulmer and Dickson '60) many new localizations and observations are added here to the existing literature A review of histochemistry of the rat placenta is needed for interpretation of the quantitative results reported in this paper A comparison of the distribution of glycogen and glucose-6-phosphatase also necessitates this histochemical review

A Decidua The completion of implantation at eight days shows the blastocyst in a decidua rich in glycogen especially in the lateral mesometrial regions (fig 1) In early placental differentiation (13 days) the decidua basalis forms a thick layer rich in glycogen (fig 2) As gestation proceeds the fetal chorioallantoic disc enlarges progressively and the decidual layer becomes thinner with a steady loss of its glycogen (figs 5 and 6) However the decidua stores some glycogen for as long as it lasts

B Giant cells Glycogen occurs in the cytoplasm of the giant cells in rather small

but variable amounts throughout gestation. An interesting nuclear-cytoplasmic *relationship concerning glycogen* has been reported by Schiebler and Knoop ('59) in the 21 day rat placenta. The nuclear membrane of the giant cells shows numerous invaginations, and thus portions of the cytoplasm seem to extend deep into the nucleus. Such apparent nuclear inclusions may contain lipid and glycogen (Schiebler and Knoop, '59) In this study such nuclear glycogen was observed in giant cells as early as 18 days, and this phenomenon is illustrated in figure 17

C. *Spongiotrophoblast.* At implantation, the fetal trophoblast possesses a striking amount of glycogen (fig. 1) This primitive trophoblast gives rise to three closely related regions of the placental disc: labyrinth, spongiotrophoblast, and giant cells. In early placental differentiation (10–13 days) the spongiotrophoblast has a massive store of glycogen (fig. 2) whereas the giant cells have only small deposits and the labyrinthine trophoblast has none. At this time the spongiotrophoblast has a relatively compact, epithelial appearance and almost every cell contains some glycogen. Between 13 and 15 days, glycogen storage as determined histochemically is at a peak in the spongiotrophoblast. At 15 days individual glycogen-rich, binucleate cells make a conspicuous appearance in tissue spaces or lacunae within the trophoblast (figs. 3 and 5) Some glycogen-bearing cells of the spongiotrophoblast have lost their close epithelial association and become highly specialized free cells in tissue spaces or lacunae (figs. 5 and 21) These specialized cells are typically binucleate, and the nuclei have a central position. The organelles are relatively sparse and most of the cytoplasm is packed with glycogen. These distinctive cells are located in tissue spaces containing a fluid material which is acidophilic and has also a glycoprotein or mucoprotein component which is revealed by the periodic acid-Schiff reaction. Although the relationship of these tissue spaces to the maternal blood channels is not established, a communication is suggested since electron microscopic examination reveals that red blood cells occur in these spaces together with the specialized glycogen cells.

Later it will be demonstrated that these free glycogen cells represent a large per centage of the glycogen of the chorioallantoic disc. Electronmicrographs of the spongiotrophoblast at 17 days show that glycogen particles occupy most of the cytoplasm and that the cytoplasmic organelles are sparse in these binucleate cells (figs. 19 and 20) The nuclei occupy a fairly central position in each cell, and a small paranuclear or internuclear region of glycogen-free cytoplasm contains most of the Golgi apparatus, elements of a granulated endoplasmic reticulum, and a few mitochondria (figs. 20 and 21) The Golgi apparatus is principally in the form of tiny vesicles the granulated endoplasmic reticulum is lamellar in form and shows considerable parallel orientation of its elements (fig. 19) The remainder of the cytoplasm is packed with glycogen particles except that occasional mitochondria and strands of endoplasmic reticulum course through it. Immediately beneath the plasma membrane there is a thin band of superficial cytoplasm or ectoplasm which contains mitochondria and small smooth-surfaced vesicles.

The number of these highly specialized glycogen bearers decreases markedly between 15 and 18 days (compare figs 5 and 6) During this period a compact epithelial mass of cytotrophoblast appears in this region containing very little glycogen (fig 6) and with intense cytoplasmic basophilia. Near term (21 days) only occasional glycogen cells persist, and there is an overall depletion of glycogen from the spongiotrophoblast (fig. 7) However in the labyrinth at this late date, islands *of cytotrophoblast conspicuously rich in* glycogen may occur both near and far from the spongiotrophoblast (fig. 7). These glycogen-rich islands appear to be structurally similar to those of the spongiotrophoblast.

D *Labyrinth.* The trophoblast of the labyrinth initiates glycogen storage soon after mid-gestation, i.e on the fourteenth day (fig. 9) Between 14 and 18 days, storage becomes more widespread, and the peak occurs near 18 days (fig. 10) This rise in labyrinthine glycogen is unrecognized or masked in the quantitative

measurement of glycogen in the fetal disc (text fig. 2) From 18 days to term there is a progressive reduction in the amount of labyrinthine glycogen.

E. Yolk sac. At 14 days gestation, the *visceral wall* of the yolk sac initiates glycogen storage. The steady increase in this splanchnopleuric glycogen between 14 and 18 days has been observed by several investigators (Bridgman, 48; Wislocki and Padykula, '53; Bulmer and Dickson, '60) After 18 days, there is a progressive loss of glycogen from this membrane. Although the visceral endoderm is the principal site of glycogen storage the mesenchymal cells which lie between the endoderm and the vitelline vessels can also synthesize glycogen. It is generally lacking from the mesothelium.

In the visceral endodermal cell, glycogen storage occurs typically in a subnuclear position and occasionally occupies most of the subnuclear cytoplasm (figs. 11 and 12) Some cells of the visceral layer also have a large deposit which is immediately supranuclear Although large masses of glycogen (5-10 μ in diameter) are characteristic, smaller accumulations of granules in addition, occur in the most active cells.

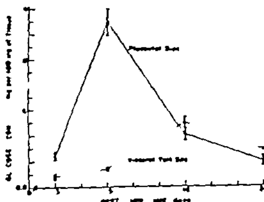


Fig. 2 Glycogen was extracted from isolated placental discs and visceral yolk sacs by KOH digestion and alcoholic precipitation (one hour) After acid hydrolysis of the glycogen, the resulting glucose was measured with the Nelson-Somogyi reagents. The results are expressed in terms of mg glycogen/100 mg tissue wet weight. The standard error is indicated by the vertical bars at each point. Each point on this graph represents the mean of determinations made on at least ten individual discs or yolk sacs.

In electronmicrographs the glycogen mass is composed of small particles about 300 A in diameter which are readily stained with lead hydroxide or lead acetate (figs. 17 and 18) Mitochondria (fig. 18) or smooth-surfaced tubules or vesicles (fig. 17) may be partially or completely surrounded by glycogen particles. Smaller aggregates of particles may occur at various sites throughout the cytoplasmic matrix.

Glycogen was observed in the *parietal endoderm* at 15 days although the cycle of deposition and release in this tissue layer has not been studied. The epithelial components of the endodermal sinuses do not participate in glycogen storage.

F Uterine smooth muscle The glycogen store of the uterine muscle increases steadily between 13 and 21 days. Near term, when both maternal and fetal placental components have lost most of their carbohydrate reserve the uterine muscle retains an abundant supply (fig. 15) This accumulation in smooth muscle may represent an energy reserve needed at parturition. In the guinea pig there is a similar accumulation of glycogen in the uterine muscle late in gestation (DuBois and Ducommun, '35)

G Metrial gland. The complexities of glycogen storage in this maternal region remain to be elucidated. The characteristic metrial gland cells with their specific granulation (Wislocki et al., '57) also have glycogen deposits (fig. 4) Between 15 and 18 days there is an intermingling of glycogen storage cells in the spongiotrophoblast, decidual sinuses (fig. 4) and around the central artery (fig. 3)

III. *Correlation of biochemical determination of glycogen with histochemical sequences*

Between 13 and 15 days, there is a large increase in the glycogen content of the placental *disc* (0.23% to 1.3%) (see text fig. 2) This six fold increase during a two day period represents principally the rapid accumulation in the spongiotrophoblast (figs. 2, 3 5) The specialized glycogen storage cells appear in great numbers during this period. Between 15 and 18 days the amount of glycogen/unit wet weight declines from maximal storage to

0.4%. Thus, in this three day interval, the total glycogen content is reduced to one-third. This terminal decline in rat placental glycogen was also measured by Corey ('33). When this three day period is viewed histochemically it is characterized by a steady loss of glycogen from the spongiotrophoblast (figs. 5 and 6) and by increased deposition to a maximum in the labyrinth (figs. 9 and 10). In the quantitative measurement the rise in the diffusely arranged labyrinthine trophoblast is completely masked by the changes in the spongiotrophoblast and the loss of glycogen from the latter dominates the quantitative result. From these comparisons it may be concluded that the glycogen cells of the spongiotrophoblast represent a large proportion of the glycogen stored in the placental disc. The maximal amount of placental glycogen is comparable in magnitude to that stored in adult rat skeletal muscle but is generally lower than that of adult liver.

In the *visceral yolk sac*, storage of glycogen is first perceptible histochemically around the fourteenth day. Between 13 and 15 days a slight rise in the measurable glycogen is recognized in the biochemical analysis (text fig. 2). During the next three days, the rise to maximal storage at 18 days (0.5%) can be equally well discerned in the biochemical and histochemical measures. As has been pointed out previously, the visceral endoderm is the principal site of storage although mesenchymal cells which intervene between the visceral endoderm and the vitelline vessels also synthesize glycogen. The ultrastructural relationships within the visceral endoderm during maximal storage may be observed in figures 17 and 18. Between 18 and 21 days, there is a progressive loss of glycogen. However, at 21 days an appreciable amount of glycogen can still be detected histochemically with glycogen storage occurring only in certain epithelial cells.

IV. *Glucose-6-phosphatase activity of the placental membranes*

To determine whether glucose secretion may occur in any of these glycogenic regions, glucose-6-phosphatase activity was localized histochemically. It was found that glucose-6-phosphate can be dephosphorylated principally by two of the glycogenic placental regions: the maternal decidua and the labyrinthine trophoblast. In the earlier placenta, i.e., at 13 days, glucose-6-phosphatase activity is localized primarily in the decidua (fig. 13). As gestation proceeds, the decidual activity wanes while glucose-6-phosphatase activity appears and increases in the labyrinthine trophoblast (fig. 8). The labyrinthine phosphatase activity which first becomes perceptible near 13 days increases to a high level by 19 days.

The blood spaces in the spongiotrophoblast are lined by trophoblastic cells which resemble in enzymic activity those which line the maternal blood spaces of the labyrinth. At 19 days these particular lining cells of the spongiotrophoblast resemble the labyrinthine cells in their capacity to dephosphorylate glucose-6-phosphate. It was difficult to determine with certainty whether the highly specialized glycogen cells possess this enzyme which in the adult liver is known to be exclusively a microsomal enzyme (de Duve and Barthet, '54). Since the ergastoplasm of these cells is sparse (see figs. 19 and 20) it follows that it might be difficult to detect accumulation of reaction product originating at such small sites. At 19 days there was a suggestion of glucose-6-phosphatase activity in an internuclear position where organelles are congregated in a glycogen-free cytoplasm; however this activity was demonstrable only in sections which had been incubated for three hours and which showed evidence of diffusion of reaction products.

The visceral wall of the yolk sac between 13 and 21 days of gestation lacks glucose-6-phosphatase activity under the conditions of this histochemical test.

Placental glucose-6-phosphatase activity is always lower than that of adult liver. Initial biochemical comparisons indicate that the decidual activity is approximately 25% that of adult liver and the labyrinthine activity is about 10% that of adult liver. This low level of activity prompted an examination of the separateness of this enzyme in the labyrinth since other phosphatases might be splitting glucose-6-phosphate. It is well known that the brush

border of the labyrinthine trophoblast is rich in alkaline phosphatase Cytological examination of glucose-6-phosphatase preparations indicated a cytoplasmic localization with no brush border activity; this difference in localizations eliminates the possibility of interference by alkaline phosphatase at pH 6 7 When glycerophosphate is subsituted for glucose-6-phosphate an identical histochemical and cytochemical pattern is obtained and this appears consistent with the known affinity of hepatic glucose-6-phosphatase for glycerophosphate (Beaufay and De Duve '54) However with ATP a different pattern of localization is obtained Cytological and histological differences in localization suggest that this enzyme is distinctive and separate from alkaline phosphatase acid phosphatase and ATPase

The uterine smooth muscle cells have a similar type of phosphatase activity demonstrable at pH 6 7 which becomes manifest during the last week of gestation (fig. 16) Both glucose-6-phosphate and glycerophosphate are hydrolyzed by this enzymic activity which is located in the cytoplasm at the nuclear poles and also at the periphery of the muscle cells The cellular outlines are brought out clearly by this reaction product This latter localization at the surface may be obtained also with ATP and thus it is not clear whether this site is occupied by one or more phosphatases

V Glycogen content of the visceral yolk sac after trypan blue uptake

After the injection of trypan blue into a pregnant rat on the seventh eighth and ninth days of gestation this dye is taken up principally by the visceral endoderm. Gross examination of placental membranes on the eighteenth day reveals an intensely blue visceral yolk sac while the remaining placental structures retain their natural color Cytological examination of the visceral endoderm shows that the trypan blue has been aggregated in the supranuclear cytoplasm of these absorptive cells. With the electron microscope it is evident that the dye particles are segregated within membrane limited vacuoles of varying density

Since trypan blue administered at the time of implantation is a potent teratogenic agent it seemed worthwhile to determine whether the load of foreign material stored in the visceral endoderm influenced its ability to accumulate glycogen. Histochemical and biochemical measurements were made on visceral yolk sacs of normal-appearing fetuses on the eighteenth day which is usually the point of maximal accumulation The trypan blue-laden membranes had accumulated glycogen which amounted to 0.5% glycogen by wet weight which corresponds to the normal collective mean. Thus there was no change in the glycogen content of yolk sac membranes of normal-appearing fetuses However deviations from the normal value were observed in instances of gross fetal abnormalities but the validity of these deviations is questionable since the abnormal fetuses were often dead

DISCUSSION

Placenta as a fetal liver In Claude Bernard's (1859) study of placental glycogen he reported that he was unsuccessful in finding glycogen in any part of the placentas of cow and sheep However when he examined the placentas of the rabbit and guinea pig he found that glycogen was abundant in cells which were située principalement entre la portion maternelle et la portion foetale du placenta. He further observed that this group of cells après s'être développée elle m'a paru s'atrophier à mesure que le foetus approche du moment de sa naissance. This led him to suggest that the placenta performs the hepatic glycogenic function until the fetal liver has developed the capacity to synthesize this carbohydrate reserve

From Claude Bernard's observations one may interpret that this glycogen was localized in the decidua basalis which wanes with the expansion of the fetal placenta. Glycogen storage in the early stages of gestation is a characteristic of the rodent and primate placentas; however ungulates do not store placental glycogen (Dancis '60) In the human and rat placentas glycogen continues to be demonstrable in the relatively few decidual cells which survive until term The significance

of decidual glycogen to the fetus is problematic, since glucose secretion into the surrounding maternal blood vessels could hardly benefit the fetus directly It has long been thought that the decidual cells may form a pabulum on which the early embryo can feed through the mediation of the trophoblast. Boyd ('59) has also suggested that, in the early human placenta before fetal circulation has been established, glycogen might be taken up in particulate form. In this report a third possibility presents itself since glucose-6-phosphatase activity was demonstrated in the decidual cells of the rat placenta. This observation suggests that glucose secretion by the decidual cells is a distinct possibility the glucose liberated might be absorbed locally by nearby trophoblastic cells. Since some degradation of decidual cells is observed at the maternal-fetal junction of the rat, it seems likely that decidual stores may be available to the fetus in various forms.

The essential transport functions of the placenta, along with its endocrine activity have long been appreciated. As biochemical knowledge of the placenta has expanded, it has become clear that this temporary organ has some of the biochemical characteristics of the adult liver lung, kidney small intestine and endocrine glands (Villee '60) To dissociate a hepatic function from all the others is a distinct challenge and histochemical evidence may be crucial for the separation. In exploring the possibility of temporary hepatic function by the placenta it is necessary to establish a role in glucose secretion as well as in glycogen storage. In the adult liver glycogen storage is clearly related to its role in glucose secretion or regulation of blood glucose. The high level of glucose-6-phosphatase activity in the ergastoplasm of the hepatic cells mediates the secretion of glucose into the extracellular phase. This relatively specific phosphatase is localized in the membrane of the granulated endoplasmic reticulum (Palade and Siekevitz, '58) and Siekevitz ('59) has made the interesting suggestion that hydrolysis of glucose-6-phosphate at this membrane may result in the secretion of glucose into the cavities of the endoplasmic reticulum. The secreted glucose would then be in a potentially extracellular compartment, according to some interpretations of cellular ultrastructure (Siekevitz, '59)

Glucose-6-phosphatase has a relatively limited distribution in the mammalian body It has been demonstrated biochemically and histochemically (Chiquoine, '55) in the liver kidney small intestine, and rectum, but it is absent from skeletal muscle as well as from most tissues and organs However recent studies indicate that this enzyme may have a more extensive distribution, since it may also be present in the salivary gland (Raggi et al. '60) pancreatic islets (Lazarus '59) and epididymis (Allen, '61) Of the three well established loci of glucose-6-phosphatase the liver has the highest activity; the renal enzyme has 74% of the activity found in the liver (Weber '61) and the intestinal enzyme shows only 20% of the hepatic activity (Spencer and Knox, '60)

The first report of possible glucose-6-phosphatase activity in the placenta was made by Villee in 1953 who observed that the early human fetal placenta incubated *in vitro* releases glucose into the medium. It was suggested that this release is effected through the activity of placental glucose-6-phosphatase although no attempt was made to isolate or characterize the enzyme. In a later report Hagerman Roux, and Villee ('59) using whole homogenates of human term placenta found no phosphatase activity toward glucose-6-phosphate or fructose-6-phosphate at pH 6 4 although rapid splitting of these substrates occurred at pH 9 0 These results suggest the lack of a specific glucose-6-phosphatase in the human placenta at term. However to establish the existence of glucose-6-phosphatase in the human placenta, a more detailed biochemical and histochemical study is needed.

In the present investigation of the rat placenta the cytochemical and histochemical evidence indicates that a specific glucose-6-phosphatase activity is demonstrable in the decidual cells and labyrinthine trophoblast. The localizations and sequences of activity during gestation differ from that of alkaline phosphatase, acid phosphatase, and ATPase (Padykula '58) By both histochemical and biochemical

measures the glucose-6-phosphatase activity of the decidua and labyrinth is low in comparison to the adult liver and is more comparable in level of activity to that of the small intestine. The coincidence in the development of glucose-6-phosphatase activity in the labyrinthine trophoblast with the onset of glycogen storage in this placental component may have functional significance. This coincidence between 14 and 18 days suggests that utilization of glycogen might occur during this period of steady accumulation of glycogen stores in the labyrinth. Later during the period of glycogen loss from the labyrinth (18 days to term) the glucose-6-phosphatase activity is heightened and *there are also indications of a steady increase* in activity until term. Thus it is possible that glucose secretion may occur steadily during the glycogen phase of the labyrinthine trophoblast. These relationships differ significantly from those in the fetal liver of the rat. In the developing liver glycogen deposition commences late in gestation (around the seventeenth day in the rat) and continues to a maximum *at term however there is no glucose-6-*phosphatase in the prenatal liver (*guinea pig* Nemeth '54 *rat*. Padykula, unpublished observations) This enzyme makes its first appearance in the liver early in the first postnatal day when glycogen utilization occurs to provide an energy supply for the newborn during the strenuous first hours after birth. The presence of glucose-6-phosphatase in the decidua and laby*rinthine trophoblast and its complete ab*sence from the prenatal liver adds a measure of support to Bernard's hypothesis of hepatic function by the placenta. In addition, the absence of glucose-6-phosphatase from the prenatal liver actually eliminates the possibility of glucose secretion by the fetal liver This enzymic comparison suggests that the placenta may function in terms of glucose secretion as *a fetal liver throughout* gestation.

The close morphological relationship of the labyrinthine trophoblast with the fetal blood vessels provides a direct route for secreted glucose to reach the fetus. However as Dancis ('61) has pointed out, it is difficult to understand the need for placental glycogen stores since the glucose of the maternal blood is presumably available for transport across the hemochorial barrier at all times. The labyrinthine glycogen store declines at about the time the fetal liver first begins to deposit glycogen, and it is conceivable that this placental glycogen may represent a food reserve to be called upon should maternal blood glucose decline precariously Although it is generally assumed that placental glycogen stores are very difficult to deplete (Huggett and Hammond, '52) systematic experiments should be performed on a laboratory rodent which will challenge the stability of the glycogen in the various placental components. Experiments with placental glycogen labeled with isotope *are needed to determine the degree of* turnover and also to trace the fate of such labeled glycogen. Another possible function of labyrinthine glycogen which must be considered is that this carbohydrate reserve may have an intrinsic role within the trophoblastic epithelium during its great expansion in the last third of gestation. The possible significance of epithelial glycogen is discussed in the next paragraphs.

Glycogen in differentiating epithelia. Deposits of glycogen have been identified histochemically in many differentiating epithelia of the fetus and adult. In stratified squamous epithelia of the adult, glycogen occurs in some non-keratinized epithelia, but is absent from the skin (Wislocki et al., '51; Weinmann et al. '59) Although the exact function of the glycogen deposits in these adult epithelia *is unknown, Bullough ('52) indicated that* the energy supply for mitosis in the mouse epidermis is derived from glycogen, glucose and its derivatives. If epithelial glycogen is related to the mitotic rate of the epithelium then glycogen storage should be a common phenomenon during some phase in the growth and differentiation of epithelial surfaces. A good example in support of this concept can be found in the differentiation of the airways of the mammalian lung (Sorokin et al., '58) In the earliest stages of lung formation glycogen occurs in the primitive respiratory epithelium. As the secondary bronchi emerge they are rich in glycogen whereas glycogen disappears from the primary (or older) bronchi. As expansion of the airway pro-

ceeds through terminal bud formation, glycogen leaves the older parts of the airway and the terminal buds are always the richest in this substance. Thus there is a wave-like deposition of glycogen in the budding portions of the lung which are also the loci of intense mitotic activity The differentiating pulmonary epithelium offers this striking example of rapid growth in a glycogen rich membrane.

There is a distinct period of glycogen accumulation in the visceral endoderm of the yolk sac between 15 and 18 days. Maximal accumulation is reached near the eighteenth day and thereafter glycogen is steadily depleted until term. The absence of glucose-6-phosphatase from this membrane suggests that the glycogen serves an intrinsic function. Between 15 days and term there is a fifty fold increase in the weight of the visceral wall (Padykula and Wilson, '60) The exact growth mechanism is not clear since a recent measure of mitotic rate indicates that there is a steady decline in mitotic activity between 14 and 18 days (1.5% to 0 8%) (Jones, '61) These preliminary results suggest that hypertrophy plays an important role in the later expansion of this membrane since increase in weight continues despite a decline in mitotic rate. There is also some experimental evidence which supports the concept that the glycogen serves an intrinsic function in the visceral endoderm. Sorokin and Padykula ('60) explanted bits of 13 day old visceral wall to the conditions of organ culture. Glycogen deposition in the explants occurred on schedule near the fifteenth day; it accumulated steadily though more slowly to form a broad peak between 20 and 25 days, and thereafter depletion occurred. Thus there was a mimicking of the *in vivo* pattern of glycogen deposition and release. Furthermore, glycogen-free membranes explanted near term (20 days) were capable of glycogenesis. This suggests that the terminal loss of glycogen which occurs *in vivo* may be related to a lack of substrates or appropriate hormonal factors or to other extrinsic factors.

There is also a strong likelihood that this glycogen may be an energy reserve for the transport functions of this vascular splanchnopleure Brambell ('57) reported a steady increase in the rate of transfer of maternal antibodies by the rat yolk sac between 17 days and term. Although the transport of antibodies and other serum proteins by the visceral endoderm is most likely accomplished by pinocytosis, it is possible that the energy requirements of this uptake may be similar to that of phagocytosis. Karnovsky ('62) has reviewed the evidence which indicates that phagocytosis in neutrophils is dependent on the energy derived from glycolysis. It is important to recall at this point that the visceral endoderm is also a highly phagocytic epithelium which will ingest and segregate colloidal substances, such as trypan blue or colloidal gold. Thus the visceral endoderm participates both in pinocytosis and phagocytosis two cell functions which may have an identical basis (Holter '59) Although various temporal sequences have suggested a fetal liver function for the yolk sac glycogen (McKay et al., '55; Padykula, '58b) it seems necessary from the above considerations to have a broader view of the possible significance of yolk sac glycogen.

Problems related to glycogen storage in the spongiotrophoblast. Histochemical evidence suggests that the functions of this placental tissue may be manifold. It is assumed that the spongiotrophoblast is gradually converted to vascularized labyrinth as gestation proceeds, although in the rat some spongiotrophoblast persists until term in the form of a highly basophilic epithelial tissue (Schiebler and Knoop '59) In these respects this layer is comparable to the peripheral cytotrophoblast of the human placenta which may be the site of production of chorionic gonadotropin (Wislocki and Padykula, '61) The glycogen storage function of the spongiotrophoblast has long been known, and the results of this investigation emphasize that a large proportion of the glycogen of the placental disc is stored by the highly specialized glycogen cells.

The histological organization of the spongiotrophoblast has not yet been adequately described, and its interesting differentiation has been incompletely analyzed. The principal cells of this layer the cytotrophoblasts, are held in a loose epithelial association by desmosomes (Schei

bler and Knoop '59) At 21 days these cells form a network with rather wide meshes, and the specialized glycogen cells occur within the meshes or tissue spaces (Schiebler and Knoop '59) From Schiebler and Knoop's observations at 21 days and our observations at 17 days with the electron microscope there emerges the possibility that maternal blood may directly bathe these cytotrophoblasts by percolating throughout the epithelial meshwork. The coexistence of glycogen cells and red blood cells in the tissue spaces suggests this epithelio-vascular relationship. This leads us to a consideration of the nature of the blood supply to this region of the placental disc. The spongiotrophoblast is not vascularized by fetal blood vessels, but instead is permeated with maternal blood (Holmes and Davies '48) Arterial maternal blood is conveyed to the disc through a large central placental artery which as it penetrates the disc, gives off small branches to the spongiotrophoblast before proceeding to the labyrinth (Boe, '50 Young '56). However the main blood suppy to the spongiotrophoblast is venous. Venous blood which drains from the region of physiological transfer in the labyrinth enters into venous sinusoids in the spongiotrophoblast which are lined by flattened trophoblasts which resemble histochemically those which line the maternal blood spaces in the labyrinth. The relationship of the venous sinusoids to the tissue spaces previously mentioned has not been delineated but there is reason to believe that communication may be possible since erythrocytes occur in the tissue spaces. Despite our incomplete knowledge of the precise vascular pathway it seems clear that this region is served mainly by maternal blood, and that products of this trophoblastic layer would most likely enter the maternal circulation. This fact makes the significance of the glycogen cells more difficult to understand since their direct association is with the maternal blood rather than with the fetal blood.

Preliminary ultrastructural observations suggest that these glycogen cells arise from the epithelial cytotrophoblasts. As they deposit large stores of glycogen they lose most of their epithelial moorings and become more individualized in a tissue space However histological study of the fetal-maternal junction shows a wide distribution of such specialized storage cells which reside on both sides of this border (figs 3 and 4) and this fact has led several investigators to believe that these glycogen cells may also be maternal in origin (see Bridgman, 48 for a review of this literature)

The cytotrophoblasts have a well developed ergastoplasm or granulated endoplasmic reticulum which is in the form of highly oriented cisternae (Schelbler and Knoop '59) This elaborate machinery for protein synthesis indicates that these cells are most likely producing protein for export. As mentioned earlier these cells bear some resemblance by their histological relationships and high content of cytoplasmic ribonucleoprotein to the peripheral cytotrophoblasts of the human placenta, and may be the site of production of chorionic gonadotropin (Wislocki and Padykula '61)

SUMMARY

The various maternal and fetal components of the chorio-allantoic and inverted yolk sac placentas of the albino rat have different patterns of glycogen storage and glucose-6-phosphatase activity A histophysiological review of the rat placenta is included for convenience in interpreting the histochemical and biochemical results. The importance of comparing quantitative determinations with histochemical localizations in this heterogeneous organ is illustrated. Claude Bernard's hypothesis (1859) that the placenta may function as a fetal liver is tested by histochemical comparisons.

The decidua which is rich in glycogen also possesses glucose-6-phosphatase activity; this suggests that in the first half of gestation glucose secretion may occur in this part of the maternal placenta

The major sites of fetal glycogen deposition in the chorio-allantoic disc are the spongiotrophoblast and labyrinth. The spongiotrophoblast increases its glycogen store steadily from implantation to 15 days. Highly specialized glycogen storage cells arise during this period and some of their ultrastructural characteristics are

described here. Glycogen first appears in the labyrinthine trophoblast at 14 days and is most abundant at 18 days. From these two peaks, storage is curtailed as term is approached. Small amounts of glycogen occur in the giant cells throughout gestation. The placental disc can be easily separated from the decidua, and consists of labyrinth, spongiotrophoblast, and giant cells. Quantitative measurement of the glycogen content of such isolated discs indicates that maximal storage occurs near 15 days (1.3% wet weight) this reflects chiefly the glycogen of the spongiotrophoblast. By 18 days glycogen content drops to 0 5% ; when viewed histochemically this three day period is char acterized by loss from the spongiotrophoblast and by steady accumulation in the widespread labyrinthine trophoblast. The changes in the spongiotrophoblast dominate the quantitative results and the labyrinthine rise is masked. These results emphasize that a large proportion of the glycogen of the placental disc is stored by the highly specialized glycogen cells.

Glucose-6-phosphatase activity of the disc is localized mainly in the labyrinthine trophoblast glucose secretion may occur in this fetal layer during the last half of gestation. Thus there are two placental regions, the decidua and the labyrinthine trophoblast, which may be involved in glucose secretion at different times during gestation. Glucose-6-phosphatase activity of both the decidua and labyrinthine trophoblast is always low when compared with that of the maternal liver The spongiotrophoblast is generally free of this enzymic activity except for the trophoblastic lining of the venous sinusoids which are active.

In the visceral yolk sac glycogen stor age occurs between 14 days to term, with the maximum (0 5%) occurring at 18 days. There is good correlation between the histochemical and biochemical measures. Cytological aspects of glycogen stor age in the visceral endoderm are described. Some observations on glycogen storage in the visceral yolk sac after the uptake of trypan blue are presented.

Glycogen accumulates steadily in the uterine smooth muscle and becomes most abundant at parturition. The smooth muscle cells can hydrolyze glucose-6-phosphate quite readily during the last week of gestation.

ACKNOWLEDGMENTS

We wish to acknowledge the expert and generous assistance of Miss Eileen Hall in the histochemical and biochemical techniques and of Mr Leo Talbert in the photographic work.

LITERATURE CITED

Alden, W H. 1948 Implantation of the rat. III. Origin and development of primary trophoblast giant cells. Amer J Anat., 83 143–182.

Allen, J M. 1961 The histochemistry of glucose-6-phosphatase in the epididymis of the mouse. J Histochem. Cytochem., 9 681–689

Amoroso, E. C. 1952 Placentation. In Mar shall Physiology of Reproduction 3rd ed., Ed. A. S. Parkes. Longmans, Green and Company New York, Vol. 2 127–311.

Anderson, J W 1959 The placental barrier to gamma-globulins in the rat. Am. J Anat., 104 403–430.

Beaufay H., and C. De Duve 1954 Le système hexose-phosphatasique. IV Spécificité de la glucose-6-phosphatase. Bull. Soc. Chim. Biol., 36 1525–1537

Bernard, Claude 1859 Recherches sur l'origine de la glycogénie dans la vie embryonnaire; nouvelle fonction du placenta. Comptes Rendus des Seances et Memoires de la Societe de Biologie, Tome premier de la troisieme serie.

Bøe, Finn 1950a Studies on placental circulation in rats. I. Vascular pattern illustrated by experiments with Indian ink. Acta endocrinol., 5 356–358.

——— 1950b Studies on placental circulation in rats. II. Vascular pattern illustrated by corrosion preparations. Ibid 5 369–375.

Boyd, J D 1959 Some aspects of the relationship between mother and child. Ulster Medical Journal, 28 35–46.

Brambell, F W R., W A. Hemmings and W T Rowlands 1948 The passage of antibodies from the maternal circulation into the embryo in rabbits. Proc. Roy Soc., London, ser B 135 390–403.

Brambell, F W R., and R. Halliday 1956 The route by which passive immunity is transmitted from mother to foetus in the rat. Ibid., 145 170–185

Brambell, F W R 1957 The development of fetal immunity Macy Foundation Conferences on Gestation 4 143– 01

Bridgman J 1948 A morphological study of the developme f h placenta f the ra I A ou levelopment f the pl cen e I lorph 83 61–85

——— A morphological study of the d w f he ra II. A l stud f the de l ac placent f at 5–223

Bulmer D and A. D. Dickson 1960 Observations on carbohydrate materials in the rat placenta. J Anat., 94 46–58.
Bullough, W S. 1952 The energy relations of mitotic activity Biol. Rev., 27 133–168.
Chiquoine A. D. 1955 Further studies on the histochemistry of glucose-6-phosphatase. J Histochem. Cytochem., 3 471–478.
Corey E. L. 1955 Growth and glycogen content in the fetal liver and placenta. Amer J Physiol., 112. 263–267
Dancis, J 1960 Placental function and fetal nutrition. In The Placenta and Fetal Membranes Ed. C. A. Villee. The Williams & Wilkins Company Baltimore, pp 85–89
Davies, J 1956 Histochemistry of the rabbit placenta. J Anat., 90 135–142.
Deane H. W B. L. R bin E. C. Driks, B. L. Lobel and G. Leipsner 1962 Trophoblastic giant cell in placentas of rats and mice and their probable role in steroid-hormone production. Endo., 70 407–419
De Duve C., and J Berthet 1953 The use of differential centrifugation in the study of tissue enzymes. Internat. Rev Cytol 3 225–275.
DuBois, A. M and S. Ducommun 1955 Developpement et teneur en glycogène du placenta de cobay Revue Suisse de Zoologie 62 119–136
Duval M. 1892 La Placenta des Rongeurs Ed. Felix Alcan. Paris Ancienne Librairie Germer Baillière et Cie.
E erett J W 1935 Morphological and physiological studies of the placenta of the albino rat J Exper Zool., 70 243–285.
Goldmann, E E 191 Neue U tersuchungen übe die äussere und innere Sekretion des gesunden nd kranken Organism im Lichte der "Vitalen Färbung Tübigen verlag des H La ppachen.
Graumann, W 1958 Untersuchungen zum cytochemischen Glykogennachweis. II Chemische Fixation uf Pikrinsäurebasis. H stochemie 1 97 108
Grillo, T A. I. 1959 A contribution to the tudy of the fix tion of glycogen in embryonic tissues Ibid 1 311 314
H german, D D J Rou and C. A. Villee 1959 Studies of the mechanism of fructose production by human placenta. J Physiol 146 98–104.
Holmes R. P and D V Davies 1948 The scular p ttern of the placenta nd its development in the rat. J Obst Gynaec Brit Emp., 55 583–607
Holter H 1959 Pinocytosis. Interna Rev Cytol., VIII 481 504
Huggett A. St. G nd J Hammond 1952 Physiology of the placenta. In Marshall' Physiology of Reproduction. 3rd ed Ed. A. S Parkes Longmans, Green and Company New York, Vol. 2 312–397
Jones, L. A. 1961 A study of the formation of the placenta in the rat. Thesi presented to the Faculty of Connecticut College New London, Connecticut
Karnovsky M. L. 1962 Met bolic basi of phagocytic activity Physiol. Rev 42 142 168
Krebbiel, R. H. 1937 Cytological studies of the decidual reaction in the rat during early pregnancy and in the production of deciduomata. Physiol. Zool., 10 212–234
Lazarus, S S. 1959 Acid and glucose-6-phosphatase activity of pancreatic cells fter cortisone and sulfonylureas. Proc Soc Exp Biol. Med., 102: 303–306.
Lochhead J and W Cramer 1908 The glycogenic changes in the placenta and the foetus of the pregnant rabbit contribution to the chemistry of growth. Proc. Roy Soc London, ser B 80 263–284
Luse S. A. 1957 The morphological manifestation of uptake of materials by the yolk sac of the pregnant rabbit. Macy Foundation Conferences on Gestation 4 115–142.
McKay D G., E. C. Adams, A. T Hertig and S. Danziger 1955a Histochemical horizon in human embryos. I. Five millimeter embryo-Streeter horizon XIII. Anat. Rec., 122 125–151.
——— 1955b Histochemical horizons in human embryos. II. Six and seven millimeter embryos-Streeter horizon XIV Ibid., 126 433–463.
Mossman, H W 1937 Comparative morphogenesis of the foetal membranes nd accessory uterine structures. Contr Embryol., Carnegie Inst., Washington 26 129–246.
Nelson, N 1944 A photometric adaptation f the Somogyi method for the determination of glucose. J Biol Chem., 153 375–380
Nemeth A. M. 1954 Glucose-6-phosphatase in the liver of the fetal guinea pig. Ibid 208 773–776.
Padyk la, H A. 1958a A histochemical and quantitativ study of enzymes of the rat placenta J Anat. 92 118–129.
——— 1958b Histochemistry of the rat' placenta. I Environmental Influence on Prenatal Development, Ed Beatrice Mintz University of Chicago Press, Chicago, pp 34–38
Padykula, H. A., and T H. Wilson 1960 Differentiation of bsorptive capacity in the isceral yolk sac of the rat. Anat. Rec 136 254
Palade G E., and P Siekevitz 1956 Liver microsomes. An integr ted morphologic l and biochemical tudy J Biophys Biochem Cytol 2 1 1 200.
Pearse A G. E 1960 Histocheml try Theoretical and Applied. Little Brown and Company Boston.
Rezzi, F D S Kronf ld and M Kleiber 1960 Glucose-6-phosphat se activity in arious sheep tissues. Proc Soc Exp Biol Med 105 485–486
Res l, J P L. Napolitano nd D W F wcett 1960 Identific tion of glycogen in lectron micrograph of thin tissue section J Biophys. Biochem Cytol 8 573–589
Richardson, K C L. J rett nd E H Fink 1960 Embedding in epoxy resin for ultra thin sectioning in lectron microscopy Stain Tech 3 313–323
Schiebler T H nd A Knoop 1959 H tochemische und Electronenmikroskopische Un-

tersuchungen an der Rattenplazenta. Ztschr Zellforsch 50 494–532.

Seekevitz, P 1959 On the meaning of intracellular structure for metabolic regulation. In Regulation of Cell Metabolism. Ciba Foundation Symposium, Churchill, London, pp. 17–49

Somogyi, M. 1952 Notes on sugar determination. J Biol. Chem., 195 19–23.

Sorokin, S., H. A. Padykula and E. Herman 1959 Comparative histochemical patterns in developing mammalian lungs. Dev Biol., 1 125–151

Sorokin, S., and H. A. Padykula 1960 Differentiation of visceral yolk sac in vitro. Anat. Rec., 136 348.

Spencer R. D., and W W Knox 1960 Comparative enzyme apparatus of the gut mucosa. Fed. Proc., 19 886–897

Swigart, R. H., C. E. Wagner and W B Atkinson 1960 The preservation of glycogen in fixed tissue and tissue sections. J Histochem. Cytochem., 8 74–75.

Tuchmann-Duplessis, H., and R. Bartolami 1954 Les constituants histochimiques de allantoplacenta d lapin. Bull. Micro. Appl., 4: 73–83.

Villee, C. A 1953 Regulation of blood glucose in the human fetus. J Appl. Physiol., 5 437–444

——— 1960 Biochemical aspects. In The Placenta and Fetal Membranes. Ed. C. A. Villee. The Williams & Wilkins Company Baltimore 100–108.

Wachstein M., and E. Meisel 1956 On the histochemical demonstration of glucose-6-phosphatase. J Histochem. Cytochem., 4: 592.

W tson, M. L. 1958 Staining of tissue sections for electron microscopy with heavy metals. II. Application of solutions containing lead and barium. J Biophys. Biochem. Cytol., 4: 727–730.

Weber G. 1961 Kidney enzymes of gluconeogenesis, glycogenesis, glycolysis, and direct oxidation. Proc. Soc. Exp Biol. Med., 108 631–634

Weinmann, J J Meyer D Mardfin and M. Weiss 1959 Occurrence and role of glycogen in the epithelium of the alveolar mucosa and of the attached gingiva. Am. J Anat., 104 381–402.

Wilson, J G 1955 Teratogenic activity of several azo dyes chemically related to trypan blue. Anat. Rec., 123 313–334.

Wislocki, G. B., and E. W Dempsey 1955 Electron microscopy of the placenta of the rat. Ibid 123 33–63.

Wislocki, G. B., D W Fawcett and E. W Dempsey 1951 Staining of stratified squamous epithelium of mucous membranes and skin of man and monkey by the periodic-acid-Schiff method. Ibid., 110 359–376.

Wislocki, G B and H. A. Padykula 1953 Reichert membrane and the yolk sac of the rat investigated by histochemical means. Am. J Anat 92 117–152.

——— 1961 Histochemistry and electron microscopy of the placenta. Chap. 15. In Sex and Internal Secretions, 3rd ed. Ed. William C. Young, The Williams and Wilkins Company Baltimore.

Wislocki, G B L. P Weiss, M. H. Burgos and R. A. Ellis 1957 The cytology histochemistry and electron microscopy of the granular cells of the metrial gland of the gravid rat. J Anat., 91 130–140.

Young, A. 1956 The vascular architecture of the rat uterus during pregnancy Trans. Roy Soc. Edinburgh, 63 167–183.

PLATE 1

EXPLANATION OF FIGURES

Figures 1–4 are photomicrograph of periodic acid-Schiff (PAS) preparation of Rossman fixed paraffin sections of the rat placenta.

8 days

1 At this arly tage fetal placental glycogen is located hiefly in the ectoplace tal cone (EC) Maternal decidual glycogen is bundant especially in the "lateral wings of the decidua (D) which c be seen in the right and left margins of this photograph. × 110.

13 days

2 The principal site f glycogen storage in the fetal placenta t 13 days is the spongiotrophoblast which is the dark band stretching acros the lower half of the photograph. Below thi rich deposit of glycogen, the unreactive labyrinth (L) and visceral yolk sac (Y) be seen Abov the spongiotrophobla t, the thick band of decidua (D) is moderately rich in glycogen. The PAS reactivity in the upper right corner is loc ted in the metrial gland (M) × 30

15 days

3 Glycogen storage continues t high level i the spongiotrophoblast (S) while it curtailed in the decidu (D) In the region of the central rtery (right center f the photogr ph) curiou swarm f glycogen cell spans the fetal-maternal junction extendi g from the metrial gland hrough the decidua and pongiotrophoblast 30.

18 days

4 Glycogen storage ll bound i lacu ae of the pongiotrophobla t (S) in the decidua nd around the wall of the blood vessels in metrial gland (M) 30


1
2
L
3
L
D
4
a
s
D

PLATE 2

EXPLANATION OF FIGURES

Figures 5–8 are illustrations of the *placental disc* and are enlarged 110 ×

15 days, Rossman fixative PAS reaction

5 During this period of maximal storage in the spongiotrophoblast most of the cells in this region are storing glycogen. Glycogen packed cells occur principally in lacunae or tissue spaces. Relatively delicate particles of glycogen are located in the cytoplasm of the giant cells (G). An island of decidual cells (D) rich in glycogen, can be seen at the upper margin of the photograph. In the labyrinth (L) glycogen storage has begun, and the particles are sparsely distributed at this time.

18 days, Rossman's fixative PAS reaction

6 Compare with figure 5 to observe the decline which occurs in the glycogen storage of the spongiotrophoblast and the increased deposition in the labyrinthine trophoblast (L) between 15 and 18 days. In the spongiotrophoblast, the glycogen-laden cells occur in lacunae; in the epithelial mass of cytotrophoblast, some cells contain small deposits of glycogen. Decidual (D) glycogen is less abundant.

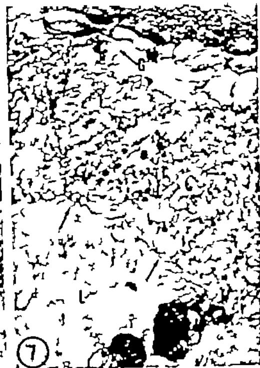
21 days Rossman fixative PAS reaction

7 The two arrows indicate the line of junction between the spongiotrophoblast and labyrinth (L); glycogen storage has declined sharply since 18 days (fig. 6) in both these fetal zones. Isolated pockets of glycogen-rich cytotrophoblast often occur in the labyrinth (see lower margin of photograph) at this late stage in gestation. The giant cells (G) shown here are depleted. Some glycogen still persists in the decidua.

17 days glucose-6-phosphatase activity 10 cryostat section nuclei stained with carmine

8 The junction of the spongiotrophoblast and labyrinth runs across the lower center of the photograph. A cluster of glycogen cells in a lacuna of the spongiotrophoblast is starred. Note that glucose-6-phosphatase activity is localized in the labyrinth (L) and that the spongiotrophoblast including the glycogen cells, is quite free of this enzymic activity. Compare with figure 6 which illustrates the amount and distribution of glycogen in these placental regions at a comparable time in gestation.


O
G
L
5


G
L
7


6


8

PLATE 3

EXPLANATION OF FIGURES

9 Fourteen days labyrinth, Rossman's fixative PAS reaction.

10 Eighteen days, labyrinth Rossman fixative PAS reaction.
The localization of glycogen within the elongated strands of labyrinthine trophoblast is illustrated here especially in figure 10 Comparison of these two photographs reveals the rise which occurs in the glycogen level of the labyrinth between 14 and 18 days. Figure 10 represents the peak storage in this region. This rise in the glycogen content of the labyrinth is completely masked in the quantitative determinations made on the isolated discs (see text fig. 2) × 500

11 Seventeen days, villous visceral splanchnopleure, fixation in buffered OsO_4 (pH 7 7) 2 µ methacrylate section, PAS reaction.
In this placental membrane glycogen is stored mainly in the visceral endoderm. Glycogen deposits here are black; the cell nuclei are light (or unstained) and the cytoplasm has low overall PAS reactivity (grey) Note that most of the glycogen is stored in a subnuclear position in these cells. The mesothelium (m) does not store glycogen. Occasional mesenchymal cells which intervene between the visceral endoderm and vitelline vessels ( ) may contain glycogen. The cytological distribution of glycogen in the visceral endoderm can be seen in figure 12. × 325.

12 Seventeen days, visceral endoderm, fixed in buffered OsO_4 (pH 7 7) methacrylate section, PAS reaction.
An unstained nucleus (n) can be recognized in each columnar endodermal cell. Although dark masses of subnuclear glycogen occur commonly dense supranuclear deposits are also conspicuous in several of these cells. Glycogen may be stored in most of the cytoplasm, except in the specialized superficial cytoplasm which consist of microvilli and canaliculi. Note especially the heavily laden cell in the center of the photograph × 1,000.







PLATE 4

EXPLANATION OF FIGURES

13 Placental disc (13 days gestation) glucose-6-phosphatase activity 10 µ cryostat section, nuclei stained with carmine.
At this earlier stage in gestation, glucose-6-phosphatase activity is localized in the decidua (D) exclusively with none in the fetal pla centa. The rrow points to the nucleus of a giant cell to indicate the region of the fetal-maternal junction. The labyrinth (L) is unreactive t this stage but later develops this enzymic activity (see fig. 8) × 30.

14 Giant cell t 18 days gestation, periodic acid-Schiff (PAS) nd hem-toxylin The dark granules (g) in the ucleus are deposits of gly cogen and, according to the ultrastructural findings of Schiebler and Knoop ('50) these deposits are act ally located in fine invaginations of the cytoplasm into the nucleus. Thus, their intranuclear position is pparent rather tha real. Large irregula masses of mucopoly saccharide (mp) other than glycogen seem to be located in the cyto-plasm, but m y be various manifestations of the surface coat of mucopolysaccharide × 500.

15 Uterine wall and portion of the pl cental disc (21 days) Rossman fixation, paraffin section, PAS reaction.
Near term the fetal placental glycogen (§ L) is gre tly depleted and the m ternal decid has declined along with it glycogen tore In the terine wall (U) near term the principal glycogen reserve is localized in the terine smooth muscle (indicated by arrows). × 30.

16 Uterine wall (17 days) glycero-phosph tase activity (pH 6.7) 10 µ cryostat section, ucle! stained with carmine
The terine smooth muscle cell have phosph tase activity toward both glycerophosph te and glucose-6-phosphate (t pH 6.7) duri g the last week of gestation. In this photograph the uterine epithelium occurs in the upper field, the reactive smooth muscle cells stretch across the center and the serosa surface is toward the bottom. × 115


13


mp
g
14


l
15



PLATE 5

EXPLAN TION OF FIGURES

17 Visceral endoderm at 1 days, supranuclear cytoplasm, electron micrograph, lead hydroxide staining.
Glycogen particles heavily stained with lead, form large irregular ggreg tion within the supranuclear cytoplasm. This ggregation is fairly homogeneous, except for a few small vesicles (arrow) which are surrounded by glycogen particles. The mass of glycogen occurs in cytoplasm which is richly packed with organelles. Numerou profiles of granulated endoplasmic reticulum (er) are evident. Ribosomes also occur free in the cytoplasm In addition t the mitochondria two large vacuoles ( ) occur in this sample f the cytoplasm. × 21 400.

18 Visceral endoderm t 19 days, basal cytoplasm electron micrograph lead hydroxide staining.
Accum lations of glycogen particles in the basal cytoplasm of two endodermal cells are ill trated here The basal surfaces of these cell can be traced by following the basement membrane (b) The lateral cell surfaces have points of firm attachment which are marked by desmosomes (d) There are frequent wide expansions of the intercellular spaces (X) and the content of the intercellular material is preserved in the form of fine precipitate Portions of two nuclei (n) are shown d in the nucleus to the left, uclea pores (p) are shown in tangential section through the nuclear envelope
Glycogen particles occupy wide area of the basal cytoplasm. The actual expanse of this storage site can be better appreciated i the light micrographs of the visceral endoderm shown in figures 11 and 12 In this electronmicrograph the glycogen particles are ggregated for the most part into masses with irregular outlines. In the cell t the left the glycogen particles partially surround three mitochondria In that same cell, profiles of the cisternae of the gra ular endoplasmic reticulum occu beside the glycogen depot, and the cisternae are arranged longitudinally and are somewhat parallel to ach other Tiny smooth-surfaced vesicles are present, especially near the plasma membranes. × 18,200

17

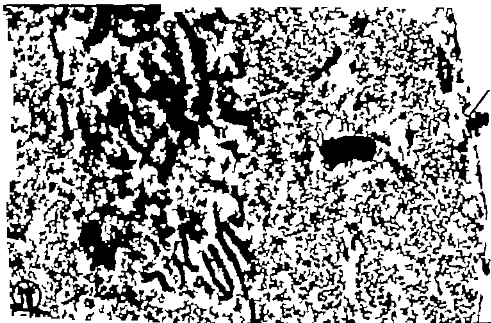
18

PLATE 5

EXPLAN TION O FIGURES

17 Visceral endoderm t 17 days, supranuclea cytoplasm, electron micrograph lead hydroxide staining.
Glycogen particles heavily stained with lead, form large irregular aggregation within the supranuclear cytoplasm. This aggregation is fairly homogeneous, except for few small vesicles (arrow) which are surrounded by glycogen particles. The mass of glycogen occurs in cytoplasm which is richly packed with organelles. Numerous profiles of granulated endopl smic reticulum (er) are evident. Ribosomes also occur free in the cytoplasm. In addition to the mitochondri two large vacuoles (v) occur in this sample of the cytoplasm. × 21 400.

18 Visceral endoderm at 19 days, basal cytoplasm, electron micrograph, lead hydroxide staining.
Accumulations of glycogen particles in the basal cytoplasm of two endodermal cells are illustrated here The basal surfaces of these cell can be traced by following the basement membrane (b) The lateral cell surfaces have point of firm ttachment which are marked by desmosomes (d) There are frequent wide expansions of the intercellular spaces (X) and the content of the intercellular material is preserved in the form of fine precipit te Portions of two nuclei (n) re shown, and in the nucleus to the left nuclear pores (p) are shown in tangential section through the ucle r envelope
Glycogen particles occupy wide rea of the basal cytoplasm. The actual expanse of thi storage site can be better appreciated in the light micrographs of the visceral endoderm shown in figures 11 nd 12 In thi electronmicrograph the glycogen particles are aggreg ted for the most part into masses with irregul outlines. In the cell to the left, the glycogen particles partially surround three mitochondria. I that same cell, profiles of the cisternae of the granula endoplasmic reticulum occur beside the glycogen depot, and the ci ternae are arranged longitudinally and are somewhat parallel to each other Tiny smooth-surfaced esicles are present, especially near the pl sma membranes. × 18,200.







The Development of the Clitorine Urethra and the Distal Vagina in *Dipodomys*[1]

E. W. PFEIFFER
Department of Zoology, Montana State University, Missoula, Montana

The external genitalia of the female rodent, *Dipodomys* include a penis-like clitoris with a urethra conducting urine to its tip (Pfeiffer '60) In this respect, the female *Dipodomys* resembles certain insectivores (Godet, '50) and primates (Wood-Jones, 14b) This condition is also found occasionally in new born humans (Reilly et al., '58) and is known as phallic urethra. Phallic urethra has been induced experimentally in primates (Wells and Van Hagenen, '54) and in rats (Green, et al., '39) However in the abnormal human and in the experimental animal, the vagina is usually absent or so malformed as to be non-functional.

Although the developmental anatomy of the reproductive tracts of the experimental forms has been investigated there are few reports of the manner in which both a functional vagina and a phallic urethra develop in those mammalian species which exhibit this characteristic. To my knowledge, the European mole *Talpa* is the only species whose normally pseudohermaphroditic external genitalia have been studied developmentally (Wood-Jones 14a; Godet, op. cit.) In the hope that such comparative studies may contribute to further understanding of mammalian developmental anatomy a description of the embryonic origin and development of the clitorine urethra, distal vagina, and bulbovestibular glands of *Dipodomys* is presented in this report. Possible factors in the development of female pseudohermaphroditism in *Dipodomys* are discussed.

METHODS AND MATERIALS

The urogenital tracts of 41 prenatal and two newborn specimens of *Dipodomys* were serially sectioned at 10 to 15 μ in the transverse sagittal or frontal planes and stained with hematoxylin and eosin after treatment in the usual manner Table 1 gives pertinent data on these specimens. In addition to crown-rump measurements certain features of the abdominal organs are briefly described to indicate further the state of development of the specimens. The state of differentiation of the gonads has been assessed by applying the criteria of Gilman ('48) The descriptions assume that the fetus or embryo is in the upright posture with the clitoris pointing forward (fig. 1) Therefore the tip of the clitoris is anterior the base posterior the surface which is continuous with the infra-umbilical abdominal wall is superior (ventral in the adult) whereas that which is continuous with the perineum is inferior (dorsal in the adult)

According to Anthony ('28) there are only very slight anatomical differences between the species of *Dipodomys* used in this study The only significant difference that I have observed involves morphological changes of the clitorine urethra of *D ordii* during the sex cycle (Pfeiffer op cit.) These changes were not observed in other species, and the significance of this observation will be pointed out below

Reconstructions were made by projecting the sections proportionally enlarged onto sheets of blotting paper whose thicknesses were 18 and 42 times that of the actual sections. The enlarged images of the epithelia of the structures to be reconstructed were cut out of blotting paper glued consecutively together painted and photographed.

[1] This investigation was supported in part by grants from the National Science Foundation and the National Institutes of Health.

TABLE 1
Data on specimens studied

Species and specimen identification	No. of males	No. of females	C-R length	Blotting paper reconstructions	Graphic reconstructing
			mm		
D ordii; Fnm	3-indifferent		6–7		
B-Utah	1-indifferent		6–7		
D merriami; Arizona-1	2 indifferent		6–7		
D agilis; California 11	3-indifferent		6–7		
D. merriami; Arizona-9	2-indifferent		10		
D. ordii; Dnm	2	1	11 12		
D. ordii; A-Utah		1	13–15		
K-Utah		1	13–15		
Anm		2	13–15		
D. merriami; Nevada-1	1	1	13–15		
Arizona-11	1	1	13–15		
Arizona 12	1	2	13–15		
D. merriami; California-12	1	1	21		
D. merriami; Arizona-4		2	24		
D. ordii L-Utah		1	24–27		
Enm	1	1	21–27		
D merriami; Arizona-2		2	24–27		
Arizona-10		2	24–27		
Arizona 12		1	24–27		
D ordii C-Utah		2	33		
Bnm	2	1	33		
D ordii; Cnm		2	Newborn		

DESCRIPTION

Indifferent embryos In the 6–7 mm embryo there is a small genital tubercle and the urorectal fold is beginning to divide the cloaca into primitive rectum or dorsal cloacal remnant Bengmark and Forsberg '59) and urogenital sinus or ventral cloacal remnant (fig. 1) The anterior wall of the urogenital sinus portion of the cloaca forms a lamella which meets a *thickening and infolding of the ectoderm* to form the cloacal membrane (figs. 5 6) This membrane is called the cloacal septum by Hall ('36) in her studies of the urogenital sinus of the mouse

The gonads at this stage are small masses of condensed mesenchyme and thickened celomic epithelium (Gilman's indifferent stage no 1) medial to the well developed mesonephros Metanephric buds are approaching the metanephrogenic tissue

In 10 mm embryos of *D merriami* the genital tubercle is now a phallus with a shallow groove on its inferior surface This groove appears to have been formed by infolding of ectoderm to form a solid median urethral plate continuous proximally with the cloacal membrane (fig 6) The ectodermal ingrowth of the cloacal membrane first appears inferior to the hind gut at the junction of the latter *with the almost completely divided cloaca* (fig. 7) Distally the plate extends to within about 150 μ from the tip of the phallus The superior proximal part of the plate is penetrated by the hollow pars phallica of the urogenital sinus. The gonads show sex cords continuous with the celomic epithelium (Gilman's stage no. 1) The Mullerian ducts are present along the cephalic end of the Wolffian ducts. Collecting ducts are budding from the primitive pelvis of the metanephros

Female embryos. In 13 mm and 14 mm embryos there is a groove beginning posteriorly at the anus and extending anteriorly onto the under-surface of the phallus (fig. 8) Posteriorly this groove is the *anlage of the perineal or anourethral* raphe, which is present in adult females and anteriorly it is the anlage of the primitive urethral groove of Glenister ('54) Near the junction of the urogenital sinus with the proximal urethral plate (the cloacal membrane), the anlagen of the bulbovestibular glands are seen as epithelial buds (figs. 9 11) They are apparently derived from the ectodermal ingrowth of the urethral plate in the manner described by Barnstein and Mossman ('38) and are posterior to the tubular phallic portion of the urogenital sinus which protrudes into the urethral plate. The gonads are similar to those of 11 mm embryos, but the Müllerian ducts have now reached the urogenital sinus. Bowman's capsules are forming in the metanephros.

In 15 mm embryos there are well developed urethral folds lateral to a urethral groove. The urogenital ostium leads into the urogenital sinus as the latter joins the proximal urethral plate and there are two spaces separated by a thin sheet of cells (figs. 12, 13) *Superiorly is the lumen of* the urethral plate formed by dissolution of the central cells (the secondary urethral groove of Glenister) and inferiorly there is the urogenital ostium covered by a membrane and this ostium is continuous distally with the primitive urethral groove formed by downgrowth of the urethral folds. It seems probable that endodermal cells move distally along the urethral plate and that ectodermal cells move proximally into the urogenital sinus. There are no prostate or seminal gland anlagen in either sex at this stage. In both sexes the Müllerian ducts are fusing as they enter the urogenital sinus and well developed Wolffian ducts are present lateral to the Müllerian ducts. There are glomeruli and Bowman's capsules in the metanephroi The ovaries are in Gilman's stage of sexual differentiation and growth stage 2.

In the 21 mm female embryo of *D merriami*, preputial folds are developing on the glans and associated with them is the urethra of the glans clitorides extending to the tip of the phallus which appears to be the distal end of the urethral plate with the ingrowth of surface ectoderm ending at the terminal pit, (fig. 14) The urethra of the glans is not canalized as is the proximal urethral plate whose lumen has been formed by dissolution of the central cells. The thin strand of cells shown in figure 13 which separates the secondary urethral groove from the urogenital ostium has disappeared although the membrane covering the ostium remains.

Hypertrophied epidermal cells continuous with the epidermis of the inferior surface of the phallus and perineum extend into the urogenital sinus to meet the endodermal cells which line the proximal urogenital sinus. Proximal to the origin of the bulbovestibular gland anlagen, the urogenital sinus is partly divided by the urethro-vaginal fold into an inferior vaginal part, which is penetrated by the fused ends of the Müllerian ducts and by the degenerating Wolffian ducts, and a superior urethral part (fig 2) The urethro- vaginal folds originating at Muller's tubercle as lateral folds of the sinus wall, appear to grow as described in the rat by Bengmark and Forsberg (op. cit.) and probably are continuous with the urethral folds. There appears to be a short sinus upgrowth similar to that described in the human by Bulmer ('57) as follows "The enlargement of the sinus behind the urethro-vaginal folds also forms the root of the short sinus upgrowth, projecting dorsally and cranially from the sinus to meet the caudal end of the Müllerian epithelium.

In the 24–27 mm (figs. 3 15 16 17) embryos the urethro-vaginal folds almost separate the urogenital sinus and its ostium into an urethra and the distal end of the vagina.

At the base of the phallus a midline anourethral raphe, representing the vestige of the cloacal membrane connects the anal canal with the urogenital ostium into which leads the wide and shallow urethral groove The ostium and its urethral and vaginal parts and the anal canal are lined by a hypertrophied and hyperplastic stratified squamous epithelium. The ducts of the bulbovestibular glands arise from the vaginal portion of the uro-

genital ostium and the glands are tubular branched structures lateral to the rectum and apparently derived from the ectoderm of the urogenital ostium (fig. 16). The proximal region of the urethral folds joins the urethro-vaginal folds. At the point of urethro-vaginal separation the vagina is a solid cord of ectoderm which extends cephalad for a short distance. At the proximal end of this cord centrally located large clear cells similar to those described by Raynaud in the mouse and probably derived from the endodermal urogenital sinus are seen (figs. 15 17). These are penetrated proximally by the fused Müllerian ducts. There does not appear to be any degeneration of Müllerian duct tissue at this point as has been described in some other forms (Bulmer '57; Bengmark and Forsberg '59) At the level of the intermingling of endodermal and ectodermal tissue in the vagina there is a cul de-sac which arises from the urethra and extends for a short distance cephalad (fig 17) This sac represents the proximal end of the urethral plate (now the clitorine urethra) at its junction with the former urogenital sinus now the membranous urethra The gonads are still in Gilman's Stage 2 but there are large numbers of degenerating primitive sex cells

In 35 mm fetuses (near term) fusion of the urethro-vaginal folds has moved distally completely separating the urogenital sinus and its ostium into vagina and urethra (fig. 18) The lumen of the latter has a thin strand of cells which separates the former primitive and secondary grooves. Distal to the point of fusion of folds the primitive urethral groove is shallow and wide and dissolution of the central cells of the urethral plate is forming a lumen (fig 21) As a result of the complete separation of the distal end of the urogenital sinus into vagina and urethra, the bulbovestibular gland ducts at this and later stages arise from the vaginal epithelium which is clearly continuous with the epidermis of the skin (fig 18) The bulbovestibular glands are coiled, branched, tubular encapsulated outgrowths of the ducts lateral to the rectum They are not as well developed as in the male fetus of the same age and there is no indication of any other sex accessory organs homologous to those present in male fetuses. The fused distal ends of the Müllerian ducts penetrate the urogenital sinus portion of the vagina as in the previous stage so that cells from the ectodermal ingrowth from the endodermal urogenital sinus and from the Müllerian duct mesoderm are intermingled (fig. 19) The gonads remain in Gilman's Stage 2 and exhibit many apparently degenerating sex cells.

In newborn females the urethral folds are fused almost to the tip of the clitoris (fig. 20) The urogenital sinus is completely separated into the urethra, vagina, and vulva. The epidermis of the vulva and perineal region does not show as much hypertrophy and hyperplasia as does that of the prenatal fetuses. The other structures are as in the 35 mm fetuses.

The labio-scrotal swellings are not involved in the development of the structures here considered, because they develop lateral and posterior to the perineal region between the anus and the tail. In breeding males the testes lie in separate scrotal sacs lateral and posterior to the anus which is the position found in the Cheiroptera (Wood Jones 14b)

DISCUSSION AND CONCLUSIONS

The primordium of the urethral plate in *Dipodomys* appears to be derived in the very early stages from the cloacal membrane which extends anteriorly onto the inferior surface of the genital tubercle As the genital tubercle enlarges into a phallus, there is an ingrowth of ectoderm from the inferior surface of the phallus which forms a median lamina, the urethral plate continuous proximally with the ectodermal ingrowth of the cloacal membrane Sinus endoderm is undoubtedly incorporated into the proximal superior part of the urethral plate but it is impossible with the techniques employed to determine the extent to which endodermal tissue moves distally along the urethral plate However the clitorine urethral epithelium of the adult *D ordii* reacts to certain sex hormones (Pfeiffer '60) while that of the other species of *Dipodomys* does not (unpublished observations) although the gross anatomical relationships are the same in

all species. A possible explanation of this phenomenon is that in female *D. ordii* the ectodermal elements predominate, producing a very reactive clitorine urethral epithelium and that in the other species there is sufficient endoderm to suppress the reactivity. This explanation appears consistent with Zuckerman's ('50) views on the histogenetic potency of the cloacal region. The ectodermal elements are reactive since in no species of *Dipodomys* is there any reactivity in that part of the female urethra known to be endodermal only. The female *Dipodomys* never develops any prostate gland or related structure derived from urethral endoderm as occurs in certain mammals.

The clitorine urethra in *Dipodomys* appears to be formed by four processes. There is first an ingrowth of ectoderm along the undersurface of the phallus beginning at the cloacal membrane. Secondly there is a downgrowth of lateral mesenchymal folds, the urethral folds, to form a primitive urethral groove. Thirdly some of the central cells of the ectodermal ingrowth now undergo dissolution proximally producing a secondary urethral groove in the roof of the primitive groove. If dissolution is incomplete a lumen may be produced in the superior urethral plate. Finally fusion of urethral folds begins at the urogenital ostium and proceeds distally so that the clitorine urethral epithelium is derived from surface ectoderm. The urogenital sinus meets the urethral plate to form the membranous urethra, and this junction is clearly indicated in both embryos and adult females by a cul-de-sac which is the proximal end of the urethral plate. In *D. ordii* this cul-de-sac and the clitorine urethra are reactive to ovarian and possibly other steroid hormones while the membranous urethra is not.

The urogenital sinus is divided into a ventral urethra and a dorsal vagina by ingrowth and fusion of the lateral sinus walls to form a urethro-vaginal fold in a manner similar to that described in the mouse (Raynaud, '42) and in the rat (Bengmark and Forsberg, '59) except that partition of the urogenital sinus is incomplete in these species (fig. 4).

The lateral ingrowths which form the urethro-vaginal folds are continued onto the under surface of the phallus as the urethral folds so that the urethra of urogenital sinus origin is continuous with that of urethral plate origin. Therefore, the factor(s) which causes masculinization of the clitoris and stimulates the fetal bulbovestibular glands of *Dipodomys* nevertheless permits feminization of the urogenital sinus by complete partition of the sinus into vagina and urethra while in the intersexes of Wells and Van Wagenen ('54) and of Greene, Burrill, and Ivy ('39) the exogenous androgens not only masculinized the clitoris, but also the urogenital sinus by suppressing its partition.

The fused distal ends of the Müllerian ducts move caudally with the urethro-vaginal fold and almost reach the ectodermal vulva. There does not appear to be a replacement of Müllerian duct cells by urogenital sinus cells and the distal vagina is therefore derived from ectoderm of the cloacal membrane, a small portion of the endodermal urogenital sinus and the mesoderm of the Müllerian ducts.

The bulbovestibular glands appear to arise from the ectoderm of the urethral plate as described by Barnstein and Mossman. They are displaced from the urethra in the female by the splitting of the distal urogenital sinus into urethral and vaginal parts in the manner just described. They, therefore, arise in the newborn females from the vaginal epithelium. Although the bulbovestibular glands in the newborn females are almost as well developed as in the newborn male, in the adult females only the two ducts remain. The significance of this observation is discussed below.

Since there is no vestibule or common chamber derived from urogenital sinus tissue into which both membranous urethra and vagina open, as is found in the human female, the bulbovestibular glands of *Dipodomys* should be referred to as bulbo-vaginal glands.

This study favors the view of Barnstein and Mossman which postulates an ectodermal origin of the urethral plate and bulbo-urethral glands in the male red squirrel. This view is consistent with the phylogeny of the vertebrate copulatory organ (Wood Jones, '14b) and of the bulbo-ure-

genital ostium and the glands are tubular branched structures lateral to the rectum and apparently derived from the ectoderm of the urogenital ostium (fig 16) The proximal region of the urethral folds joins the urethro-vaginal folds. At the point of urethro-vaginal separation the vagina is a solid cord of ectoderm which extends cephalad for a short distance. At the proximal end of this cord centrally located large clear cells similar to those described by Raynaud in the mouse and probably derived from the endodermal urogenital sinus are seen (figs. 15 17) These are penetrated proximally by the fused Müllerian ducts. There does not appear to be any degeneration of Müllerian duct tissue at this point as has been described in some other forms (Bulmer '57; Bengmark and Forsberg '59) At the level of the intermingling of endodermal and ectodermal tissue in the vagina there is a cul de-sac which arises from the urethra and extends for a short distance cephalad (fig 17) This sac represents the proximal end of the urethral plate (now the clitorine urethra) at its junction with the former urogenital sinus now the membranous urethra. The gonads are still in Gilman's Stage 2 but there are large numbers of degenerating primitive sex cells.

In 35 mm fetuses (near term) fusion of the urethro-vaginal folds has moved distally completely separating the urogenital sinus and its ostium into vagina and urethra (fig 18) The lumen of the latter has a thin strand of cells which separates the former primitive and secondary grooves. Distal to the point of fusion of folds the primitive urethral groove is shallow and wide and dissolution of the central cells of the urethral plate is forming a lumen (fig 21) As a result of the complete separation of the distal end of the urogenital sinus into vagina and urethra, the bulbovestibular gland ducts at this and later stages arise from the vaginal epithelium which is clearly continuous with the epidermis of the skin (fig 18) The bulbovestibular glands are coiled branched tubular encapsulated outgrowths of the ducts lateral to the rectum They are not as well developed as in the male fetus of the same age and there is no indication of any other sex accessory organs homologous to those present in male fetuses The fused distal ends of the Müllerian ducts penetrate the urogenital sinus portion of the vagina as in the previous stage so that cells from the ectodermal ingrowth from the endodermal urogenital sinus and from the Müllerian duct mesoderm are intermingled (fig. 19) The gonads remain in Gilman's Stage 2 and exhibit many apparently degenerating sex cells.

In newborn females the urethral folds are fused *almost to the tip of the clitoris* (fig 20) The urogenital sinus is completely separated into the urethra vagina and vulva. The epidermis of the vulva and perineal region does not show as much hypertrophy and hyperplasia as does that of the prenatal fetuses. The other structures are as in the 35 mm fetuses.

The labio-scrotal swellings are not involved in the development of the structures here considered because they develop lateral and posterior to the perineal region between the anus and the tail. In breeding males the testes lie in separate scrotal sacs lateral and posterior to the anus which is the position found in the Cheiroptera (Wood-Jones 14b)

DISCUSSION AND CONCLUSIONS

The primordium of the urethral plate in *Dipodomys* appears to be derived in the very early stages from the cloacal membrane which extends anteriorly onto the inferior surface of the genital tubercle As the genital tubercle enlarges into a phallus, there is an ingrowth of ectoderm from the inferior surface of the phallus which forms a median lamina the urethral plate continuous proximally with the ectodermal ingrowth of the cloacal membrane. Sinus endoderm is undoubtedly incorporated into the proximal superior part of the urethral plate but it is impossible with the techniques employed to determine the extent to which endodermal tissue moves distally along the urethral plate However the clitorine urethral epithelium of the adult *D ordii* reacts to certain sex hormones (Pfeiffer '60) while that of the other species of *Dipodomys* does not (unpublished observations) although the gross anatomical relationships are the same in

administration of progesterone during pregnancy Proc. Staff Meetings Mayo Clinic, 33 200-203.
Jones, H. W and W W Scott 1958 Hermaphroditism Genital Anomalies and Related Endocrine Disorders. Williams and Wilkins Co., Baltimore.
Pfeiffer E. W 1960 Cyclic changes in the morphology of the clitoris and vulva of *Dipodomys*. J Mammal., *41* 43-48.
Raynaud, A. 1942 Recherches embryologiques et histologiques sur la differenciation sexuelle normale de la souris. Supplement xxix Bull. Biol. de France et de Belgique.
Reilly W A., F Hinman, D K Pickering and *G. T Crane* 1958 *Phallic urethra in female* pseudohermaphroditism. A.M.A.J Dis. Children., 95 9-17
Wells, L. J and G van Wagenen 1954 Androgen-induced female pseudohermaphroditism in the monkey (*Macaca mulatta*) anatomy of the reproductive organs. Contr. Embryol. Carneg. Inst., 35 95-106.
Wood-Jones, F 1914a Some phases in the reproductive history of the female mole, (Talpa europea) Proc. Zool. Soc. Lond., 191-216.
——— 1914b The morphology of the external genitalia of the mammals. Lancet, *186* pt. 2, 1099-1103.
Zuckerman, S. 1950 The histogenetic potency of the cloacal region. Arch. d'anat. micros. et de morph. exper *39: 608-617*

Abbreviations (Plates 1-4)

A, anus
GT genital tubercle
AR, anourethral raphe
BV bulbovestibular glands
C, cloaca
CC, corpus cavernosum clitoris
CM, cloacal membrane
CW cloacal wall
CLU clitorine urethra
END endodermal cells
ECTC, ectodermal cells
FU fusion of the urethro-vaginal folds
FUF fusion of the urethral folds
GT genital tubercle
GU, urethra of the *glans clitorides*
H, hind gut
IE, ingrowth of surface ectoderm
LUP lumen of the urethral plate
M, membrane covering the urogenital ostium
MD, Müllerian ducts
METD metanephric duct
MU membranous urethra
PF preputial fold
PPH, pars phallica of the urogenital sinus
R, rectum
S, cul-de-sac formed by the proximal end of the urethral plate t its junction with the membranous urethra
UF urethral folds
UG, primitive urethral groove
UGS, urogenital sinus
UP urethral plate
UM, umbilicus
UV urethro-vaginal fold
UGO ostium of urogenital sinus
WD, Wolffian duct

PLATE 1

EXPLANATION O FIGURES

1 Schematic lateral view of the cloaca and related structures I a 6 mm embryo based on a graphic reconstruction of s gittal sections. The ectoderm of the loacal membrane is heavily stippled, the endoderm i cross-hatched. The oblique line indicates the level of the section shown in figure 6. × 60.

2 Graphic reconstruction of sagittal sections through the clitoris, urogenital sinus, and the lower end of the uterovaginal canal of a 21 mm embryo. The urethrovaginal fold i beginning to divide the urogenital sinus into superior urethra and inferior vagina. The Wolffian ducts are regressing. The probable germ layer origins are indicated in figure 1 — Müllerian and Wolffian duct epithelium is black.

3 Graphic reconstruction of sagittal sections through the clitoris, urogenital sinus, nd the lower end of the uterovaginal anal of a 26 mm embryo. The urethro vaginal fold has almost completely divided the urogenital sinus into a superior urethra and inferior vagina. × 18.

4 Sagittal section of the posterior part of the genital tract of female newborn mouse (Mus) drawn from a photomicrograph by Raynand (op. cit.) Probable germ layers are as indicated in figure 2. The cross-hatched area consists of the cellules claires of Raynaud. The urethro-vaginal fold does not separate completely the urogenital sinus into urethral and ginal parts as it does in *Dipodomys*. × 32.

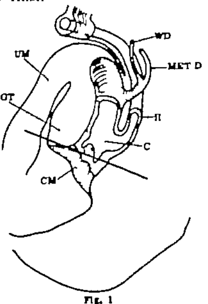


Fig. 1

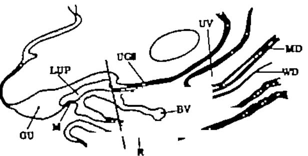


Fig. 2

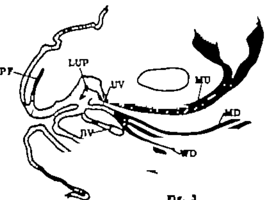


Fig. 3

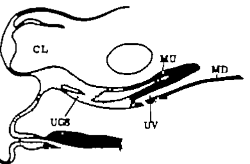


Fig. 4

PLATE 2

EXPLANATION O FIGURES

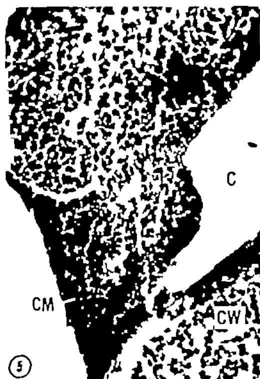
5 Sagittal section through the cloacal region of 6 mm embryo. The thickened anterior wall of the cloaca joins the ingrowth of surface ectoderm to form the cloacal membrane. × 30.

6 Frontal section through the loacal region of a 6 mm embryo as indicated in 1 The double anterior cloacal w ll meets ingrowth from the surface epithelium to form the cloacal membrane × 200.

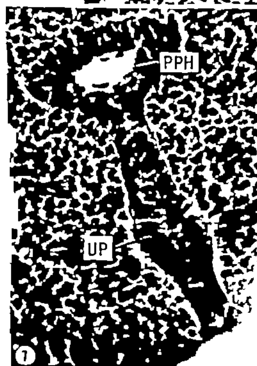
7 Transverse section of the urethral pl te of a 10 mm embryo showing the pars phallica of the urogenital sinus t its most distal penetration f the urethral plate × 220.

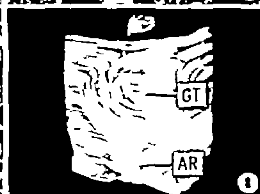
8 Anterior iew f reconstruction of the genital t bercle and related area of a 13 mm female embryo. The anourethral raphe marks the line of ingrowth of surfac ectoderm to form the cloacal membrane and urethral plate

9 Lateral iew of the model hown in 8 with the left side partially cut w y X marks the most nterior and inferior point of penetration of the pars phallica of the urogenital sinus. The line t the left indicates the level of the section illustrated in 10 nd the line t the right corresponds to 11


C
CM
CW
5


C
END
IE
6


PPH
UP
7


GT
AR
8

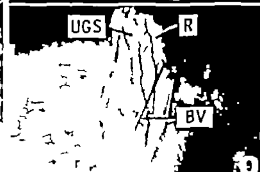

UGS
R
BV
9

PLATE 4

EXPLAN TION OF FIGURES

16 Trans erse section through the urogenital sinus of a 34 mm female embryo t the point of origin of the bulbo-vestibular gland ducts. Urethro-vaginal fold are separating the urogenital sin int a superior urethral part and inferior vaginal part. The pproxi- m te lev l of the section is indicated in figure 2. × 63.

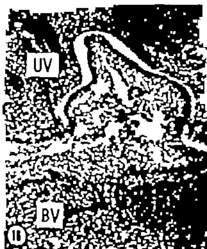
17 Sagittal section through the posterior reproductive tract of a 26 mm embryo. The urethro- aginal fold has almost completely divided the urogenital sinus into superior urethra and inferior vagin The cul-de-sac t the junction of the membranous nd clitorine urethra l clearly seen. 47

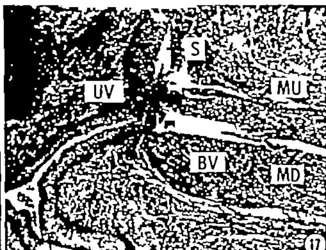
18 Transverse section through the vagina and clitorine urethra of a 35 mm fetus. The point of fusion of the rethro-vaginal folds is distal to th t in 16 so that the bulbo-vestibular gland ducts arise from the vaginal epithelium rather than the urogenital sinus epitheli m s in 16. × 70.

19 Transverse section of the vagina of the 35 mm fetus. The fused Mulleria ducts penetrate the solid cord of ectodermal and endoder mal cell of the distal vagina. × 110.

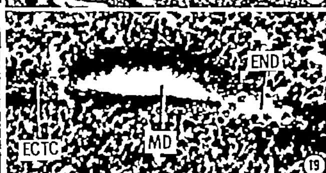
20 Transverse section through the clitoris of newborn female t th most distal point of fusion of the urethral folds. × 30

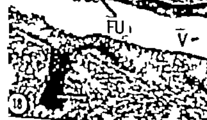
21 Transverse section of the clitoris of 35 mm fet s. The rethral fold re widely separated and the urethral plate has acq ired lu- men by dissolution of central cells to form the secondary urethral groov × 30


UV
BV
16

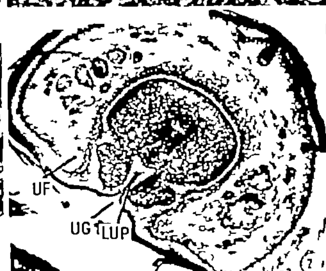

S
UV
MU
BV
MD
17


LUP


END
ECTC
MD
19


FU
V
18


FUF
20


UF
UG
LUP

Staining Properties of Hyaline Cartilage[1]

JAMES L. CONKLIN
Department of Anatomy The University of Michigan Medical School, Ann Arbor Michigan

Despite numerous attempts to develop and evalute specific methods for the histochemical demonstration of mucopolysaccharides, definitive information is not readily available This is in spite of the notable contributions of Hale (46); Steedman ('50); Gomori ('50) Kramer and Windrum ('54); Mowry ('56 '58); Spicer ('60); Belanger and Migicovsky ('61) and Goldstein ('62) to mention only a few

With few exceptions (Joel et al. '56; Warren and Spicer '61) histochemical specificity has been determined by applying the method to a variety of tissue mucopolysaccharides. While this approach is appropriate for establishing differences between tissues, it usually provides little useful information about the method itself This is not surprising since the chemical and physical properties of both the methods and mucopolysaccharides are obscure and the material stained may vary from tissue to tissue.

An alternative approach (Davies, '52 Braden, '55 Pal and Schubert, '61; Spicer and Jarrels '61) has been to employ spot" or test tube methods in which purified mucopolysaccharides are utilized as the test material. The most obvious objection to this type of analysis is the assumption that the test material and the material *in situ* will exhibit similar properties. The artificiality of such an *in vitro* system renders such data open to question unless confirmed by other methods.

The more useful approach to an under standing of histochemical procedures is the direct approach, i.e. the demonstration of tissue components by the application of the method to the material *in situ*. In order to do this it is necessary that (1) the material to be examined is preserved and (2) that it is preserved in as unaltered a condition as possible. Therefore fixation should be a primary consideration when methods are to be evaluated since consistent results cannot be obtained if the tissue components are inadequately preserved.

Cetyl pyridinium chloride-formalin has been demonstrated to provide excellent preservation of acid mucopolysaccharide (Williams and Jackson, '56 Conklin, '63) Utilizing this fixative, the acid mucopolysaccharides of hyaline cartilage have been examined by histochemical methods. The excellent preservation of cartilage ground substance has in turn afforded a means of evaluating the specificity of the methods, the results of which are reported here.

MATERIALS AND METHODS

Adult monkey and adult rat tracheal cartilage served as the test material for the evaluation of the histochemical procedures. Tissue samples were fixed in 10% neutral formalin containing 8% cetyl pyridinium chloride and by freeze substitution in 10% acrolein in absolute alcohol for seven days at −70 C. Tissues fixed in the formalin derivative were washed dehydrated in graded alcohols, cleared in cedarwood oil and paraffin embedded. Tissues fixed by freeze substitution were brought to −40 C for six hours, to 4 C for six hours, transferred to three changes of methanol for 12 hours each at 4 C transferred to chloroform at 4 C for two hours brought to room temperature in a second change of chloroform and paraffin embedded.

Tissue sections were stained by the following procedures

1 Colloidal iron (Mowry's modification '58) followed by counterstaining in 1% Bismarck brown Y Cert. no. NN 11 in 1% acetic acid for one minute.

[1] Supported by U.S.P.H.S. grant no. RG-[illegible] and The University of Michigan Cancer Research Project 36.

2. 0 1% alcian blue 8GX (lot no. 130P Allied Chemical Co.) in 3% acetic acid (final pH 2.0) for 30 minutes.

3. 0 01% azure A, Cert. no. NAz 17 brought to pH 2.0 and 4 0 with hydrochloric acid for 15 minutes.

4 Periodic acid-Schiff (Mowry's modification of the Hotchkiss procedure 58)

5 Aldehyde fuchsin (Gomori '50) (pH 1.5) without prior oxidation.

6. 0 05% methylene blue, Cert. no NA 23 in 0 1 M citric acid phosphate buffer pH 5 6.

7 Two per cent light green, SF Cert. no. NL 19 in 1% acetic acid.

Tissues stained with azure A were dehydrated in acetone. After all other methods the tissues were dehydrated in alcohols, cleared in xylene and mounted in HSR. The several staining procedures were applied singly and in various combinations (table 1) in order to demonstrate regional differences in the cartilage matrix.

An indication of the specificity of the various methods was obtained by treating the sections with acid methylation (0 3 cm³ concentrated HCl in 40 cm³ methanol at 60 C for three hours) deesterification 1% KOH in 80% alcohol at 25 C for 20 minutes) acid methylation followed by deesterification and sulfation (diethyl ether and concentrated sulfuric acid 1:1 for five minutes) prior to staining.

For descriptive purposes the cartilage matrix was divided into five zones. These have been designated as the capsular territorial, interterritorial (divided into amorphous and granular) and subperichondrial matrices.

RESULTS

Cetyl pyridinium chloride-formalin proved to be an excellent fixative for the preservation of cartilage mucopolysaccharides but was a poor cellular fixative at the concentration employed. Acrolein freeze-substitution gave comparable preservation of the ground substance and also resulted in excellent preservation of the various cell types (fig. 1) Since the primary objective of the study was the comparison of methods the staining characteristics to be reported are based only on cetyl pyridinium chloride-formalin fixation. The effect of acrolein fixation with the introduction of aldehydes on the various methods remains to be established The only methods applied to acrolein fixed tissues were combined colloidal iron and Bismarck brown procedures. The staining which resulted was essentially the same as that observed after cetyl pyridinium chloride-formalin fixation (figs. 5 and 6)

When the several histochemical procedures were applied to hyaline cartilage distinct zones were demonstrated within the cartilage matrix (table 1) The capsule of the lacuna exhibited certain staining characteristics distinct from the territorial matrix. In addition, the interterritorial matrix was divisible into two areas a zone adjacent to the territorial matrix, completely lacking in structure was designated as the amorphous matrix (fig. 6) An area containing granular material located at the junction of adjacent amorphous areas was designated as the granular matrix (figs. 2 and 5) Finally the staining properties of the subperichondrial matrix (fig. 8) are described. The staining properties of the various zones and the effect of blockade procedures are summarized in table 1 The intensity of each reaction has been arbitrarily ranked from + to ++++

In the untreated sections, the lacunar capsule differs from other regions by being PAS and light green negative. However this zone becomes PAS and light green positive when methylation or demethylation sequences are employed prior to staining (fig 7) The territorial and granular interterritorial matrices are alike in untreated sections but differ in the treated sections by the more intense light green staining in the territorial matrix after demethylation. The most marked difference between the two areas is the gamma metachromasia exhibited by the granular matrix (fig. 2) This is in contrast to the milder beta metachromasia of the territorial matrix.

The amorphous interterritorial matrix is the most distinctive zone since it is the only region which exhibits an affinity for Bismarck brown in the untreated sections (fig 6)

The subperichondrial matrix is characterized by being the most intensely stained by the PAS reaction and exhibiting the

TABLE 1

The staining properties of hyaline cartilage

	Untreated	Methylation	Methylation deesterification	Deesterification	Sulfation
Lacunar capsule:					
Alcian blue	+++	—	—	+++	++
Colloidal iron	+++	—	—	+++	+
Aldehyde fuchsin	+++	—	—	+++	++++
Azure A (2.0)	β++	—	—	0+	0+++
Azure A (4.0)	β+	—	—	0+	0+++
Bismarck brown	—	—	—	—	++
PAS	—	+	+	+++	—
Light green	—	++	++	++	—
Territorial matrix:					
Alcian blue	+++	—	—	+++	+
Colloidal iron	+++	—	—	+	±
Aldehyde fuchsin	+++	—	—	—	++
Azure A (2.0)	β+++	—	β+	0+	0+++
Azure A (4.0)	β++	—	β+	0+	0+++
Bismarck brown	—	—	—	—	++++
PAS	++	+++	++	+	—
Light green	++	++	++	+++	—
Interterritorial matrix (amorphous):					
Alcian blue	+	—	—	++	+
Colloidal iron	—	—	—	—	±
Aldehyde fuchsin	+++	—	—	—	++
Azure A (2.0)	0+	—	—	0++	β++++
Azure A (4.0)	0++	—	—	0+	β+++
Bismarck brown	+++	—	—	—	++++
PAS	+	++	+	+	—
Light green	+	++	+	++	—
Interterritorial matrix (granular):					
Alcian blue	+++	—	—	++	+
Colloidal iron	+++	—	—	++	+
Aldehyde fuchsin	+++	—	—	++	++
Azure A (2.0)	γ++++	—	—	γ++	β++++
Azure A (4.0)	γ+++	—	—	γ+	β++++
Bismarck brown	—	—	—	—	++++
PAS	+	++	+	+	—
Light green	+	++	+	—	—
Subperichondrial matrix:					
Alcian blue	+	—	—	++	+
Colloidal iron	—	—	—	—	±
Aldehyde fuchsin	+	—	—	—	+
Azure A (2.0)	—	—	—	—	0+
Azure A (4.0)	0±	—	—	—	0+
Bismarck brown	—	—	—	—	+++
PAS	+++	++	+++	++	—
Light green	++	++	+	++	—

PAS, periodic acid Schiff; β, beta metachromasia; γ, gamma metachromasia; 0, orthochromasia; — indicates the absence of staining. 2.0, pH 2.0; 4.0, pH 4.0. The intensity of each stain has been arbitrarily ranked from to ++++.

least affinity for azure A. Neither the subperichondrial matrix nor the amorphous interterritorial matrix are stained by colloidal iron.

Of the blockade methods, the methylation procedure consistently inhibited staining by alcian blue, colloidal iron, aldehyde fuchsin, Bismarck brown and azure A. With the exception of the staining of the territorial matrix, this inhibition was not reversed by demethylation. The sulfation procedure was consistent in inhibiting staining by PAS and light green. It reduced the intensity of alcian blue and

colloidal iron staining, intesified or introduced Bismarck brown affinity and reduced staining by aldehyde fuchsin. The effect of sulfation on azure A staining was to reduce or inhibit metachromasia except in the amorphous matrix where meta chromasia was produced.

The effect of demethylation alone is somewhat obscure since this procedure ex hibited more regional variation than the other types of treatment. Demethylation intensified the PAS reaction and light green affinity of the capsule but either had no effect or reduced this staining in other areas. This treatment was without pronounced effect on the alcian blue or col loidal iron procedures although it did appear to intensify the alcian blue staining of the amorphous and subperichondrial matrices. Metachromatic staining by azure A was consistently reduced while aldehyde fuchsin staining was either inhibited (ter ritorial and amorphous matrices) or re duced (granular matrix)

DISCUSSION

In considering the specificity of the vari- methods it is helpful to know the iden tity of the material demonstrated The mucopolysaccharides of adult hyaline car tilage are chondroitin, chondroitin sulfates A and C and keratosulfate (Muir '61; Partridge et al. '61) Thus the groups which are present and may be involved in the staining reactions are carboxyl and sulfate groups and vicinal hydroxyls. Ace tylated amines are also present but there is as yet no evidence to suggest their par ticipation in the staining process.

As demonstrated previously (Conklin '63) azure A at pH 2.0 does not stain ma terial which is lacking in strongly acidic groups. Therefore azure A staining is in dicative of the presence of either sulfate or phosphate groups. The fact that there is a regional difference (figs 2 and 3) in the staining which occurs with azure A i.e orthochromasia vs. metachromasia is probably due to a difference in either the nature or concentration of sulfate groups. It has been demonstrated that the occur rence of metachromatic staining is dependent upon the presence of a high molecular weight chromotrope (Schubert and Hamerman '56) Methylation and a methylation-deesterification sequence consist ently inhibited staining with azure A. This is in agreement with the concept that sulfate esters are methanolyzed and subsequently removed by the latter treatment (Spicer and Lillie 59) It should be noted however that all methods except PAS and light green were also inhibited by this treatment. The inability to restore staining of certain methods after methylation oc curs only in certain highly sulfated tissues such as cartilage and cornea (Spicer '60) and in these tissues methylation-deesterifi cation cannot be employed to distinguish between carboxyl and sulfate groups. The fact that deesterification alone reduced the degree of metachromatic staining would indicate that this treatment resulted in the partial deesterification of sulfate esters and that azure A (pH 2.0) is indeed specific for strongly acidic groups. Sulfation of cartilage prior to staining with azure A had a curious effect in that the introduction of sulfate groups produced metachromasia in areas which were previously orthochromatic and decreased metachromasia in previously metachromatic areas. This alteration of staining properties could be due to a requirement for ether optimal concentration or optimal stereochemical relationship of anionic groups in order for maximal metachromasia to occur Since some staining with azure A (pH 2.0) occurred throughout the cartilage matrix (fig. 2) sulfate groups must also be present throughout. The greatest concentration of sulfates appears to be in the granular inter territorial matrix since this is where the most pronounced metachromasia occurs. The subperichondrial matrix seems to contain the fewest sulfate groups as indicated by the weakness of azure A staining. Azure A at pH 4 0 exhibits less specificity (fig. 3) since the amorphous interterritorial matrix is also stained by this method. However the distribution of gamma metachromasia is the same as with azure A at pH 2 0.

It is of interest that the subperichondrial matrix exhibits the most prominent PAS staining. This finding is in agreement with the concept that adjacent acidic groups may prevent the demonstration of aldehydes produced by the periodate oxidation

of vicinal hydroxyls (Spicer '61) The fact that sulfates may interfere with the PAS reaction is further supported by the observation that sulfation completely inhibited the PAS reaction in all areas of cartilage and that methylation-deesterification induced PAS staining in the lacunar capsule. The distribution of light green staining was quite similar to the location of the PAS positive material. Since both methods will stain collagenous fibers, it is possible that they are demonstrating the same material.

The concept that aldehyde fuchsin, when employed without oxidation, is specific for sulfate groups was suggested by Scott and Clayton ('53) and supported by Sulkin ('60) although Spicer ('60) has observed that sialic acid-containing and non-sulphated mucins exhibit a weak affinity for aldehyde fuchsin. In the present study rather equivocal results were obtained with aldehyde fuchsin. The fact that all areas of the cartilage except the subperichondrial matrix (fig. 8) exhibited a strong affinity for the stain would indicate that sulfate groups are involved in the staining reaction. This is further supported by the fact that deesterification reduced aldehyde fuchsin staining with the exception of that in the lacunar capsule. However sulfation reduced aldehyde fuchsin staining in all areas with the exception of the lacunar capsule where staining was enhanced. While this leaves the nature of aldehyde fuchsin staining unsettled, it does point up the fact that the lacunar capsule is distinctive in its response to this pretreatment.

The amorphous interterritorial matrix also displays a distinctive staining characteristic in that it is the only area which is Bismarck brown positive in untreated sections (fig. 6) Staining is inhibited by deesterification and occurs in previously negative areas after sulfation. This would indicate that the stain is demonstrating sulfate groups. However these groups must differ from those in other areas since except for the subperichondrial matrix, this area has the least affinity for azure A. It is of interest that developing hyaline cartilage does not stain with Bismarck brown but there is an increasing affinity for the stain with increasing age of the cartilage (unpublished observation) It should also be noted that Bismarck brown staining is pronounced only after fixation with either formalin-sodium acetate formalin-cetyl pyridinium chloride or acrolein.

While it has been suggested that the alcian blue and colloidal iron procedures stain the same substances (Pearse, '60) their behavior in the staining of cartilage is not the same. Both methods will stain mucopolysaccharide which contains only carboxyl groups (Conklin, '63) Spicer ('60) has suggested that alcian blue may also stain certain sulfate groups while Belanger and Migicovsky ('61) maintain that colloidal iron will demonstrate unbound sulfate groups. The observation that neither method is positive after methylation-deesterification does not argue for the role of sulfates in these reactions since as previously noted this method is not discriminatory in sulfate-rich areas. Deesterification was either without effect on alcian blue staining (lacunar capsule and territorial matrix) enhanced the staining (amorphous and subperichondrial matrices) or reduced the staining (granular matrix) Colloidal iron staining was either unaffected by this treatment (lacunar capsule) or reduced (territorial and granular matrices) In untreated sections some alcian blue staining occurred in the amorphous and subperichondrial matrices while the colloidal iron reaction was negative in these areas. All of the above observations would indicate that both methods will demonstrate sulfate groups, in addition to carboxyl groups. The fact that deesterification reduced the colloidal iron staining in certain areas (fig 10) would support Belanger and Migicovsky's concept that the method may be demonstrating unbound sulfate esters. The occurrence of variable staining with both methods after sulfation would suggest that some degree of stereospecificity of sulfate groups may be involved. Goldstein ('62) on the other hand, has suggested that the specificity of these methods may be a function of the size of the dye particle and the density of the cartilage matrix. The distribution of staining in the present study would not support this concept.

PLATE 1

EXPLANATION OF FIGURES

All figures are of hyaline cartilage. × 125.

1 Hyaline cartilage fixed by acrolein freeze-substitution and stained with colloidal iron and Bismarck brown. Contrast with figure 6 which is cetyl pyridinium chloride fixed and stained with the same methods.

2 Azure A pH 2.0. Note the staining of the lacunar capsule, territorial matrix, and granular interterritorial matrix (arrow) Only the latter zone exhibits gamma metachromasia. Photographed through a Zeiss interference green filter

3 Azure A pH 4.0 The staining is more diffuse at this pH and also occurs in the amorphous interterritorial matrix (upper half of figure) Photographed as figure 2.

4 Alcian blue The lacunar capsule territorial matrix, and granular interterritorial matrix are stained. Photographed through a W tten no. 22 filter

5 Colloidal iron and Bismarck brown. The distribution of colloidal iron is the same as alcian blue (fig. 4) Photographed as figure 4

6 Colloidal iron and Bismarck brown. A portion of the Bismarck brown stained amorphous interterritorial matrix is visible (arrow) Photographed through a no. 25 Wratten filter

7 Hyaline cartilage treated by methylation and stained by the PAS reaction. The lightly stained lacunar capsule (arrow) may be distinguished from the territorial matrix. Interference green filter

8 Aldehyde fuchsin. Note the intense staining of all areas except the subperichondrial matrix (arrow)

9 Hyaline cartilage treated by deesterification and stained with Alcia blue Note the general staining throughout the matrix. No. 22 Wratten filter

10 Hyaline cartilage treated by deesterification and stained with colloidal iron. Staining is most prominent in the lacunar capsule No. 22 Wratten filter


2
3
4
5
6
8
9
10

PLATE 1

EXPLANATION OF FIGURES

All figures are of hyaline cartilage. × 125

1 Hyaline cartilage fixed by acrolein freeze-substitution and stained with colloidal iron and Bismarck brown. Contrast with figure 6 which is cetyl pyridinium chloride fixed and stained with the same methods.

2 Azure A, pH 2.0. Note the staining of the lacunar capsule territorial matrix, and granular interterritorial matrix (arrow) Only the latter zone exhibits gamma metachromasia. Photographed through a Zeiss interference green filter

3 Azure A, pH 4.0. The staining is more diffuse t this pH and also occurs in the amorphous interterritorial matrix (upper half of figure) Photographed as figure 2.

4 Alcian blue. The lacunar capsule, territorial matrix and granular interterritorial matrix are stained. Photographed through W atten no. 22 filter

5 Colloidal iron and Bismarck brown. The distribution of colloidal iron is the same as alcian blue (fig. 4) Photographed as figure 4

6 Colloidal iron and Bismarck brown. A portion of the Bismarck brown stained amorphous interterritorial matrix is visible (arrow) Photographed through a no. 25 Wratten filter

7 Hyaline cartilage treated by methylation and stained by the PAS reaction. The lightly stained lacunar capsule (arrow) may be distinguished from the territorial matrix. Interference green filter

8 Aldehyde fuchsin. Note the intense staining of all areas except the subperichondrial matrix (arrow)

9 Hyaline cartilage treated by deesterification and stained with Alcin blue. Note the general staining throughout the matrix. No. 22 Wratten filter

10 Hyaline cartilage treated by deesterification and stained with colloidal iron. Staining i most prominent in the lacunar capsule No. 22 Wratten filter

Histology and Fine Structure of the Avascular and Vascular Yolk-sac Placentae and the Obplacental Giant Cells in the Rabbit[1]

JORGEN FALCK LARSEN[2,3]
Department of Anatomy Washington University School of Medicine
St. Louis, Missouri

The yolk-sac placenta possibly is the most primitive form of placentation. It is the only means of transfer between the mother and the fetus in the opossum (Hill, '18) and in other marsupials it is believed to be of more importance than the chorio-allantoic placenta (Amoroso '52) A type of yolk-sac placenta is found also in Elasmobranchii (Steno 1673; Müller 1840) and in Teleostei (Turner '33)

The rabbit forms two kinds of yolk-sac placentae the chorio-vitelline placenta or the non-vascular type and the inverted yolk-sac placenta (Amoroso '52) In the rabbit the yolk-sac consists of a visceral part which is vascular and a parietal part or "bilaminar omphalopleure which lacks mesenchymal elements. The border between the two parts is marked by a vessel, the sinus terminalis.

The chorio-vitelline placenta is formed by the attachment of the bilaminar omphalopleure to the uterine epithelium of the antimesometrial side This yolk-sac placenta degenerates during the eleventh and twelfth day of pregnancy and by its disappearance the luminal surface of the visceral part of the yolk sac becomes exposed to the regenerated uterine epithelium of the antimesometrial side

The changes at the antimesometrial side of the uterus and the non-vascular yolk sac placenta are briefly described in the monographs by Duval (1889) and Chipman ('03) but are mentioned in more detail by Minot (1889) Maximow (1898) and Amoroso ('52) In the light of the recent investigations on the yolk-sac of the rabbit showing the importance of this organ in the transport of macromolecules (Brambell et al. '51; Luse '58 and Davies '59) it was believed to be of value to repeat the early investigations of the yolk-sac placentae in the rabbit and use the electron microscope to study some of the problems connected with the morphology and function of these structures.

MATERIAL AND METHODS

Tissue was obtained from the antimesometrial uterine mucosa and the yolk-sac of rabbits on the seventh, eighth ninth tenth, eleventh, twelfth fourteenth seventeenth eighteenth, twenty-first twenty fifth and twenty-eight day of pregnancy For observation in the light microscope the tissue was fixed in Bouin's solution embedded in paraffin, sectioned on a Spencer microtome and stained with hematoxylin and eosin, by the Periodic Acid-Schiff (PAS) method or with methylene blue.

For electron microscopy the tissue was first fixed *in situ* by replacing the fetal fluids with 1% osmic acid in White's saline ('54) The fixative was injected through the uterine wall and after ten minutes the uterus was opened selected areas were then cut into pieces of less than 1 mm in diameter and placed in fresh fixative for one hour It was found difficult to obtain satisfactory fixation of the non-vascular yolk-sac placenta because the delicate tissue becomes easily detached from the uterine mucosa. Pre-embedding larger pieces of the tissue in agar before it was cut into the smaller pieces helped in preserving the relationship of the structures. This method, however changed

[1] This investigation was supported in part by grants RG-3784 and RG-840 from the United States Public Health Service and by the Josiah Macy J Foundation.

[2] International Postdoctoral Research Fellow of the National Institutes of Health grant no. FFG-168).

[3] A supplementary grant for travel and living expenses was supplied by the Danish State (Statens almindelige Videnskabsfond).

implantation site (Falck Larsen, '61). A row of vacuoles marked the place of fusion and in places homogenous electron dense material was found at the same site. This material probably corresponds with the PAS-positive and metachromatic substance found in the light microscope. It was confirmed by the electron microscope that the ectoderm formed a syncytium after the contact with the uterine symplasma. The ectodermal nuclei were large and ovoid with an irregular surface and contained one or two skein-like nucleoli resembling the nuclei of the trophoblastic epithelium at the implantation site (Falck Larsen '61). The ectodermal tissue seemed to be degenerating shortly after the fusion with the uterine epithelium as the cytoplasm became granular without any ergastoplasmic channels. This change however may be caused by inadequate fixation which proved to be very difficult for this particular tissue. The basal plasma membrane of the ectodermal syncytium was very irregular and processes of the syncytium was observed projecting into the space between ectoderm and endoderm (fig. 5). A discontinuous basement membrane was found which did not seem to follow the processes but was penetrated by them. The presence of mononuclear cells in the ectoderm was confirmed by the electron microscope. These cells were spindle-shaped with nuclei resembling those of the syncytial ectoderm. Their cell membranes were irregular and the membranes of adjacent cells had interlocking projections.

The cytoplasm of the uterine symplasma was also poor in ergastoplasm. It contained numerous mitochondria and many uniform granular inclusions (fig. 6). The basal plasma membrane possessed many microvilli-like projections often forming a network in the subepithelial stroma separating the uterine epithelium from the submucous vessels. The nuclei of the symplasma were smaller than those of the ectoderm (fig. 5) and were round or ovoid with dense nuclei. During the eleventh and twelfth day th[illegible] degeneration was accompanied by de[illegible]crease of electron density and by di[illegible]integration of nuclei and nucleoli. Va[illegible]oles appeared in the basal part of the symplasma.

The inverted yolk-sac placenta (figs. 7, 9 and 10)

Following the degeneration of the endoderm and ectoderm of the non-vascular yolk-sac placenta the inner surface of the yolk-sac became exposed to the material in the uterine lumen. The inverted yolk sac is kept in contact with the antimesometrial uterine epithelium by the tension of the fluid in the amnion and extra-embryonic coelom. That this is a considerable pressure may be understood from the fact that the yolk-sac becomes herniated from the uterine cavity if a minor incision is made in the wall of the uterus.

The fetal component of the inverted yolk-sac placenta consists of the visceral yolk-sac epithelium and the underlying vitelline vessels, the maternal component comprises the antimesometrial uterine epithelium and its submucous vessels. The yolk-sac epithelium appeared in the electron microscope as tall cuboidal cells each with one nucleus containing one or two skein-like nucleoli (fig. 9). In some of the nuclei fat inclusions were found. The surface possessed many irregular microvilli and immediately beneath it many vacuoles indicative of pinocytosis were found. The cytoplasm was rich in ergastoplasm and contained numerous inclusions of different size, shape and electron density. Some of the inclusions were fat droplets and others may have been altered red blood cells. Most, however, consisted of a granular substance enclosed by a membrane which was incomplete in some cases so that the material in the inclusions seemed to merge with the surrounded cytoplasm. The cell membranes were slightly irregular and intercellular spaces were found. The cells had a basement membrane and they were connected at th[illegible] surface with desmosomes. Th[illegible]he yolk sac lay close to the b[illegible]membrane of the epithelium but [illegible]laces separated from it by proc[illegible] [illegible]esenchymal cells (fig. 9). [illegible]pithelium facing the yolk [illegible] of tall columnar [illegible] were ovoid and [illegible] containing one or

two dense nucleoli. The surface possessed many slender and regular microvilli. Desmosomes were found between adjacent cells. The supranuclear part of the cytoplasm contained small vacuoles and many inclusions most of which were small compared with the inclusions found in the epithelium of the yolk sac. The inclusions were electron dense solid ring shaped or granular surrounded by distinct membranes. In the supranuclear part of the cells a well developed Golgi apparatus was observed perhaps indicative of a secretory polarity The basal part of the cells was occupied by dilated ergastoplasmic channels containing a slightly electron dense material. The mitochondria were few and most of them were situated in the luminal cytoplasm.

The obplacental giant cells (figs. 3 7 8 11 and 14)

The giant cells were seen first on the ninth day of pregnancy in the areas of invasion by the ectoderm (fig. 3) At this stage they were about 20–30 μ in diameter; most of them were globular but spindle-shaped cells were also observed In the early stages they were found only in the outermost part of the submucosa. The cells had one or more nuclei with conspicuous nucleoli and basophilic inclusions. The cytoplasm stained faintly with hematoxylin and gave positive PAS reaction which was unaltered by previous treatment with saliva

The cells increased in number and size during the following week and were most numerous on the seventeenth and eighteenth day of pregnancy At this stage they were found throughout the uterine mucosa except in the area of the chorio-allantoic placenta. Most of the giant cells were found in submucosa often in such close relation to the vessel that they gave the impression of being a part of the lining (fig 8) At this stage the cells were very large some of them more than 100 Most of the cells appeared mononuclear but many had two or more nuclei in which strongly basophilic bodies were found The cytoplasm contained no glycogen but reacted positive by the PAS-reaction after pretreatment with saliva A strongly PAS-positive [illegible] was observed around the cells. The giant cells decreased in size and number during the following week and at full term no giant cells could be observed.

In the electron microscope the nuclei were found to contain intranuclear inclusions (fig 11) These inclusions were solid or consisted of granular material arranged in groups or islands surrounded by membranes. The cytoplasm was rich in ergastoplasm but in this respect varied from one area to another within a single cell and from cell to cell. Many channels and vacuoles of the Golgi apparatus were observed Cytoplasmic inclusions were numerous especially at the periphery of the cytoplasm (fig 13) Most of these inclusions consisted of granular electron dense material often surrounded by a membrane Others were strongly electron dense laminar bodies, reminiscent of myelin figures. A few fat inclusions were also found Mitochondria of nondescript shape were scattered The cell membrane was complicated (fig 13) and often infolded into the cytoplasm in the form of channels which may be intracellular canaliculi.

The giant cells were not found to be part of the lining of a vessel in any section. In the electron microscope it was always possible to find narrow processes of endothelial cells between the lumen and the cell membrane of the giant cells As mentioned above the ergastoplasm varied from one cell to another but it was not possible to classify them into types, and there was no characteristic difference between the cells in the submucosa and in the muscular layer A cytoplasmic continuity between giant cells and smooth muscle cells was not found in the electron microscope. In some cases, however the smooth muscle cells were found in close contact with the folded membrane of a giant cell (fig 14)

DISCUSSION

The importance of the non vascular yolk-sac placenta in the early days of pregnancy in the rabbit is difficult to evaluate in the present state of our knowledge It is the only anatomical contact between the fetus and the mother during the seventh day The absence of vessels in the

bilaminar omphalopleur is compensated for by the extensive surface of the absorbing ectoderm in contact with the uterine symplasma at more than half the circumference of the uterus. The projections of the syncytial ectoderm and those of the uterine symplasma also increase the area of transfer The debris resulting from the degenerating of the non-vascular yolk-sac placenta is potentially available to the fetus by absorption through the visceral yolk-sac epithelium (fig 7)

The ultrastructure of the uterine epithelium facing the inverted yolk-sac suggests that the former is very active in producing material which may be released into the uterine lumen to be resorbed by the yolk-sac epithelium. The electron microscopy of the visceral yolk-sac has not been described in detail since such a description already has been given by Luse ('58) She found that the yolk-sac epithelium was very active in uptake of materials, and that colloidal gold, erythrocytes and fat were absorbed if placed into the uterine lumen. In the present investigation fat inclusions were found in the nuclei of the yolk-sac epithelium. Luse ('58) found intra-nuclear carbon particles after injection of indian ink into the uterine lumen. The resorption of proteins was shown by Davies ('59) using the fluorescent antibody method.

The origin of the giant cells has been a matter of much discussion and has been reviewed by Amoroso ('52). Duval (1889) Minot (1889) and Chipman ('03) believed that the cells arose from the uterine epithelium, while Maximow (1898) claimed that they came from the perivascular cells in submucosa and muscularis. Davies and Halmi ('53) suggested that some of the cells were myogenic It has not been possible to support this view by electron microscopic findings, and the observations tend rather to confirm the theory of Hammond ('17) and Sansom ('27) who claimed that their origin was the invading ectoderm. The failure of such authorities as Duval (1889) Minot (1889) and Chipman ('03) to mention the invasion by the ectoderm in the obplacental area may be explained by the difficulty in fixing the antimesometrial structures.

The functions of the giant cells are unknown The cells are phagocytic and contain inclusions some of which probably are red blood cells. The ergastoplasm is highly developed in some of the cells suggesting a production of unknown substances perhaps proteolytic enzymes or hormones A striking feature is the limited life time of these cells which disappear before the last week of pregnancy in contrast to the giant cells of some rodents in which they may be seen also after the end of the pregnancy (Amoroso '52)

SUMMARY

The non-vascular yolk-sac placenta, the inverted yolk-sac placenta and the obplacental giant cells are described. Electron microscopic studies show that a fusion of the cytoplasm of the ectoderm and that of the uterine epithelium takes place, as at the implantation site.

The ultrastructure of the antimesometrial uterine epithelium suggests that it is very active in the production and secretion of materials that may be absorbed later by the inverted yolk-sac.

It is suggested that ectodermal cells invading the submucosa of the antimesometrial side may be the origin of the obplacental giant cells. These cells are phagocytic and some have highly developed ergastoplasmic elements possibly indicating the production of an unknown secretory substance. Nuclear inclusions were observed in the giant cells.

ACKNOWLEDGMENTS

I wish to express my thanks to Dr E. W Dempsey for making available to me the facilities of his department and for many helpful suggestions during the investigation. Dr Jack Davies has given valuable help in progress of the work and in the preparation of the manuscript.

The skillful technical assistance of Mrs Susan Philpott Mrs. Lizzie Benzing and Mr Paul Myers and also the assistance of Mr M. W Rhoades in the preparation of the light micrographs are acknowledged.

two dense nucleoli The surface possessed many slender and regular microvilli. Desmosomes were found between adjacent cells. The supranuclear part of the cytoplasm contained small vacuoles and many inclusions most of which were small compared with the inclusions found in the epithelium of the yolk sac. The inclusions were electron dense solid ring shaped or granular surrounded by distinct membranes. In the supranuclear part of the cells a well developed Golgi apparatus was observed perhaps indicative of a secretory polarity The basal part of the cells was occupied by dilated ergastoplasmic channels containing a slightly electron dense material. The mitochondria were few and most of them were situated in the luminal cytoplasm

The obplacental giant cells (figs 3 7 8 11 and 14)

The giant cells were seen first on the ninth day of pregnancy in the areas of invasion by the ectoderm (fig 3) At this stage they were about 20–30 μ in diameter most of them were globular but spindle-shaped cells were also observed In the early stages they were found only in the outermost part of the submucosa. The cells had one or more nuclei with conspicuous nucleoli and basophilic inclusions. The cytoplasm stained faintly with hematoxylin and gave positive PAS reaction which was unaltered by previous treatment with saliva

The cells increased in number and size during the following week and were most numerous on the seventeenth and eighteenth day of pregnancy At this stage they were found throughout the uterine mucosa except in the area of the chorio-allantoic placenta Most of the giant cells were found in submucosa often in such close relation to the vessel that they gave the impression of being a part of the lining (fig 8) At this stage the cells were very large some of them more than 100 Most of the cells appeared mononuclear but many had two or more nuclei in which strongly basophilic bodies were found The cytoplasm contained no glycogen but reacted positive by the PAS-reaction after pretreatment with saliva A strongly PAS-positive border was observed around the cells. The giant cells decreased in size and number during the following week and at full term no giant cells could be observed

In the electron microscope the nuclei were found to contain intranuclear inclusions (fig 11) These inclusions were solid or consisted of granular material arranged in groups or islands surrounded by membranes. The cytoplasm was rich in ergastoplasm but in this respect varied from one area to another within a single cell and from cell to cell. Many channels and vacuoles of the Golgi apparatus were observed. Cytoplasmic inclusions were numerous especially at the periphery of the cytoplasm (fig 13) Most of these inclusions consisted of granular electron dense material often surrounded by a membrane Others were strongly electron dense laminar bodies, reminiscent of myelin figures. A few fat inclusions were also found. Mitochondria of nondescript shape were scattered The cell membrane was complicated (fig. 13) and often infolded into the cytoplasm in the form of channels which may be intracellular canaliculi.

The giant cells were not found to be part of the lining of a vessel in any section. In the electron microscope it was always possible to find narrow processes of endothelial cells between the lumen and the cell membrane of the giant cells As mentioned above the ergastoplasm varied from one cell to another but it was not possible to classify them into types and there was no characteristic difference between the cells in the submucosa and in the muscular layer A cytoplasmic continuity between giant cells and smooth muscle cells was not found in the electron microscope In some cases however the smooth muscle cells were found in close contact with the folded membrane of a giant cell (fig 14)

DISCUSSION

The importance of the non-vascular yolk-sac placenta in the early days of pregnancy in the rabbit is difficult to evaluate in the present state of our knowledge It is the only anatomical contact between the fetus and the mother during the seventh day The absence of vessel in the

PLATE 1









PLATE 2

EXPLANATION OF FIGURES

Electron micrographs of the non-vascular yolk-sac placenta.

5 Area similar to the one indicated by square in figure 1. The ectoderm has many basal processes (P) in relation to a discontinuous basal membrane (BM) The line of fusion between the cytoplasm of the ectoderm and the uterine "symplasma" is indicated by arrows. Vacuoles (V) are found on the ectodermal side of the zone of fusion. The ectodermal nucleus (NE) is larger and more irregular than those of the "symplasma" and it contains a skein-like nucleolus. 3,500.

6 Basal part of the uterine "symplasma" (US) containing inclusion (I) The cell membrane has many microvilli-like processes (P) Vacuoles (V) seemingly in the stroma are formed between the "symplasma" and the underlying capillary (C) NC Nucleus of capillary 5,000.


51
V
US
V
C
C

PLATE 3

EXPLAN TION OF FIGURES

7 Light micrograph of the inverted yolk-sac placenta on the seventeenth day of pregnancy The epithelium of the inverted yolk sac (YS) faces the uterine epithelium from which it is separated by the uterine lumen (UL) Debris (D) of the degenerated non-vascular yolk-sac placenta is found in the lumen. The terine epithelium has been restored forming columnar epithelium and obplacental giant *cells are found in submucosa (GS) as well s in the inner layer of* muscularis (GM) H. and E., × 100

8 Light micrograph of obplacental giant cells on the ighteenth day of pregnancy Some of the cells (GV) seem to be part of the lining of the essels, while others (GM) seem to have cytoplasmic continuity with smooth muscle cells. UL Uterine lumen. YS Yolk sac H and E × 100.


YS
D
UL
GS
GM
7
UL
GV
GM
5

PLATE 4

EXPLANATION OF FIGURES

Electron micrographs of the inverted yolk-sac placenta.

9 Visceral yolk-sac on the fourteenth day of pregnancy Many inclusions are found of which some are f t droplet (F) others are composed by granular material with an open (I) or complete (I) surrounding membrane. Solid electron dense inclusions may be engulfed red blood cells (I_2) A fetal nucleated blood cell (FB) is seen in vessel (VY) in the yolk sac. A process of fetal mesenchymal cell (FM) separates the vessel from the basement membrane of the epithelium. D Desmosomes. IF Tonofibrils. M Mitochondria. NY Nucleus of a epithelial cell. UL Uterine lumen. × 4,000.

10 Antimesometrial uterine epithelium on the eighteenth day of pregnancy The surface ha microvilli which ppea very regular compared with those on the surface f the yolk-sac epithelium. The supranuclear part of the cell contains Golgi membranes (G) and many inclusions (I) The basal part is occupied by dilated ergastoplasmic channels (E) Connective tissue (CT) separates the epithelium from the underlying vessel (VE) M Mitochondria. NU Nucleus of epithelial cell. × 10,000.

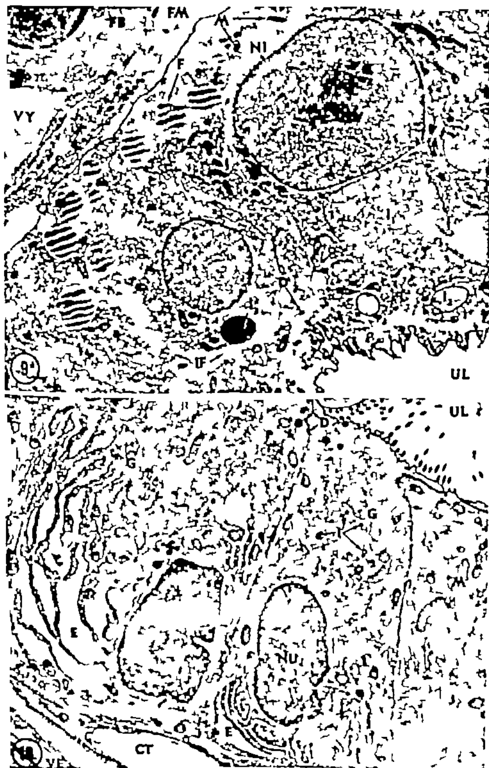

FM
FB
A
NI
F
VY
IF
UL
9
UL
D
G
E
NU
CT
VE
10

PLATE 5

EXPLANATION OF FIGURES

Electron micrograph of parts of obplacental giant cell

11 Part of nucleus of giant cell. CG Cytoplasm of giant cell. N Nucleolus. NU Nuclea inclusions. × 3,000.

12 Cytoplasm of giant cell. CM Cell membrane. E Ergastoplasmic channel. I Incl sion. M Mitochondria. × 25 000.

13 Cytoplasmic inclusions in giant cell. I Fat droplet. I Electron dense laminar inclusions. I_1 Granular material surrounded by membrane I Larger and more lectron dense granules. I Solid, electron dense incl sions The cell membrane shows complic ted folding (CM) × 6,000.

14 Smooth muscle cell (MC) in contact with the cell membrane of giant cell CG Cytoplasm of giant cell. NM Nucleu of smooth muscle cell × 3,000.


N
7c
12
11
14
MC
NM

Identification of and Observations on Epinephrine and Norepinephrine Containing Cells in the Adrenal Medulla[1]

JOE G. WOOD
Department of Anatomy The University of Texas Medical Branch, Galveston, Texas

According to Bennett (41) Vulpian in 1858 was the first to call attention to the unusual properties of the adrenal medulla. This work was followed by a progressive series of physiological, chemical and finally histochemical studies which have led to our present knowledge regarding the two adrenal medullary hormones, epinephrine and norepinephrine.

Chemical identification and subsequent synthesis of the two catecholamines, epinephrine and norepinephrine stimulated not only further research on their physiological and pharmacological properties, but aroused interest in the associated histology and histochemistry and resulted in efforts to identify two distinct types of medullary cells. Such attempts include electron microscope studies directed towards correlating submicroscopic structure with the more gross histochemical determinations. Until very recently studies of this nature have done little to provide a definite correlation between the types of cells seen with the electron microscope and the two catecholamines.

Consequently there is still need for a definitive cytological study of the adrenal medulla which accomplishes a correlation between cell types and the functional state of the cells in relation to the amounts of norepinephrine and epinephrine present. A study with the light microscope would serve as a starting point in correlating observations with the electron microscope and further histochemical studies. It is hoped that a successful method for differential staining of the catecholamines in the adrenal medulla will lead to techniques sufficiently refined that they can be used to identify these compounds in the central and autonomic nervous systems.

REVIEW OF THE LITERATURE

Vulpian observed in 1856 that in the suprarenal medullary tissue there was a substance which on oxidation produced characteristic color reactions. Henle in 1865 found that subjecting the adrenal medulla to chromic acid or to potassium dichromate produced a dark brown coloration of the adrenal medullary cells which he termed the "chromaffin reaction since the characteristic color was believed to be due to the formation of a chrome salt with the products of oxidation of the medullary tissue.

This brownish color was eventually thought to be the result of the oxidation of the contents of the adrenal medullary tissue and not due to the formation of the chrome salts as believed by Henle, but the term "chromaffin was so well entrenched in the literature that any effort at a later change in terminology was met with anything but success (Bennett 41 Coupland, '54)

One of the compounds responsible for this reaction was isolated by both Aldrich and Takamine in '01 and Abel ('02) gave the description for the proper method for purification. Synthesis of epinephrine was accomplished by Stolz in '04 and the identification of the oxidation product as adrenochrome was achieved in '37 by Green and Richter. The nature of this oxidation product was further studied by Harley Mason in 48. Recently there has been

[1] This investigation was supported by U.S.P.H.S. Anatomy Training Grant 2G-[illegible](C1) and represents in part portions of a dissertation submitted to the Graduate Faculty of the University of Texas on March [illegible], 19[illegible] as partial fulfillment of the requirements for the degree of Doctor of Philosophy.

Present address: Department of Anatomy University of Arkansas Medical Center Little Rock, Arkansas.

some discussion regarding the amount of chrome salt present in the adrenal medullary tissue following oxidation with the chromates. The evidence indicates that whether or not the chrome is responsible for the dark coloration there is indeed a considerable amount of it present in the adrenal medulla following oxidation with potassium dichromate (Hale '58) Coupland ('54) indicates that chrome deposits are actually present and certain staining reactions which occur readily in dichromate fixed material do not occur in tissue fixed by other means.

In 49 Euler and Hamberg (49b) and *Bergstrom, Euler and Hamberg established* the presence of norepinephrine in the suprarenal gland. In that same year Euler and Hamberg identified noradrenochrome and noted the significant fact that the rates of oxidation of epinephrine and nor epinephrine were different depending on the pH of the oxidizing solution (49a) This made it possible to study the relative amounts of both catecholamines in various tissues. (Eade '58 Goodall, '51; Hökfelt, 1 Van Arman, '50; West and Hunter)

The history of the cytological and histological studies up until the middle of the twentieth century is best summarized by Bennett (41) This contribution gives an excellent coverage of the literature and ideas up until the time of its publication. In addition to a detailed cytological description of the adrenal medulla of the cat, Bennett discussed the nature of the chromaffin reaction in relation to the one known neurohumor of the time epinephrine.

Bänder ('50) reported a staining technique *whereby he observed a different* coloration of two kinds of cells in the adrenal medulla. Although Bänder distinguished these two differently staining cells in a number of animals he was unable to do so in the rat which was definitely known to have both epinephrine and nor epinephrine in its adrenal medulla. The same worker in '54 published additional work, but was still unable to differentiate two adrenomedullary cell types in the rat. Bänder was of the opinion that if two cells were to secrete two different compounds a difference must exist in their colloidal chemistry therefore one should be able to develop a suitable staining procedure to distinguish between the two cell types.

Bänder's techniques included observations with the light and phase microscope on tissue stained by a variety of methods. Hematoxylin and eosin staining of formol-dichromate fixed material produced light appearing cells with large coarse granules and darker appearing cells with a more homogenous cytoplasm. Bänder described two sizes of cells for each cell type thus cells which were concerned with each catecholamine were found to exist in large as well as small varieties. He ascribed this *size difference to the functional state of the* cell and further hypothesized that the cells with the large granules were concerned with norepinephrine production while those with the homogeneous cytoplasm belonged to the epinephrine producing group Destaining was a critical factor in this procedure and as has been pointed out recently (Eränkö and Palkama '59) the procedure is not readily reproducible.

In '52 Eränkö reported on the fluorescent reaction in adrenal medullary tissue. He postulated that this reaction might be related to epinephrine and norepinephrine. Later Eränkö utilized the fluorescent technique in a number of animals to establish that the fluorescing islets of cells actually possessed a relation to norepinephrine ('55a-c)

Hillarp and Hökfelt ('53) gave evidence as to the location of epinephrine and nor epinephrine in separate adrenal medullary cells with the use of the potassium iodate method for locating islets of norepinephrine containing cells. They found that potassium iodate produced a precipitate *with norepinephrine but not with epi*nephrine and that hydroxytyramine and dihydroxyphenylalanine (dopa) reacted with potassium iodate in much the same manner as did norepinephrine. They did not consider it practical to attempt the chromaffin reaction with potassium dichromate at a pH of four since it was noted that in *in vitro* studies of granules at a pH of less than five the catecholamines were found split off from the storage granules. It was also noted that no evidence was present indicating a cytological differentiation of the two cell types of the

adrenal medulla in relation to epinephrine and norepinephrine. Hillarp Hökfelt and Nilson ('54) performed a detailed cytological study and demonstrated granules in chromaffin cells in both the fixed and live state. These granules in both instances were less than 1 μ in diameter. Such granules remained within the cells after the cells had been depleted of the catechol amine content by the administration of insulin.

Eränkö ('55b, '55c) presented statistical evidence from a number of laboratory animals indicating that the fluorescing islets corresponded to the chemical data indicating the presence of norepinephrine.

Hillarp and Hökfelt ('55) again used the iodate method and found as before that it was positive not only for norepinephrine but for the related compounds hydroxytyramine and dopa as well. These same investigators stated, as did Falk and Hillarp ('59) that the pigments formed during the dichromate fixation of adrenal medullary cells were soluble and lost during paraffin embedding. The chromate dichromate fixation of Hillarp and Hökfelt indicated the presence of both the epinephrine and norepinephrine containing cells but sections with this method were 10–20 μ thick and precluded detailed cytological study. A comparison of the iodate and fluorescent methods revealed that both methods singled out the same cellular areas of the adrenal medulla and that the fluorescent method was the more sensitive and specific of the two (Eränkö '55d).

West gives an excellent summary of the chemical, histochemical and physiological work in regard to the adrenomedullary catecholamines in his '55 review.

Another approach to the problem of cell type identification was presented by Klein and Kracht in '57 when they attempted to identify the epinephrine and norepinephrine secreting cells of the adrenal medulla in paraffin sections. They pointed out the limitations of thick frozen sections and the need for more detailed cytological identification. The techniques were similar to those employed by Bänder and depended on critical destaining under the microscope in order to obtain the desired cell coloration. Like Bänder these two workers demonstrated two types of medullary cells on the basis of granularity and staining, but also like Bänder's technique the procedure was difficult and, as indicated by later attempts, not consistent in that it is not positive for norepinephrine in the rat (Eränkö and Palkama, '59).

The administration of drugs and their subsequent effect on the catecholamine content of the adrenal medulla has been a topic of study for many years. Camanni, Lozana and Molinatti ('58) found that specific doses of reserpine would selectively deplete the rat adrenal medulla of norepinephrine. Eränkö and Hopsu ('58) obtained similar results and presented chemical data which verified the histochemical results. Camanni and Molinatti ('58) showed a selective depletion of norepinephrine from the adrenal gland of the Syrian hamster by reserpine and this drug has been used by a number of other workers studying the catecholamine content of the adrenal medulla (Coupland, '58, '59; Mirkin, '61; Zbinden and Studer, '58).

Electron microscopy of the adrenomedullary tissue has been carried out by a few workers but these have been at variance as to their findings in regard to the identification of epinephrine and norepinephrine cells (deRobertis and Ferreira, '57a,b; Eränkö and Hänninen, '60; Lever, '55; Sjöstrand and Wetzstein, '56). Recently, following a preliminary report of the present study (Wood, '62) and utilizing the information contained herein, electron microscopy was carried out utilizing the technique of differential fixation of the adrenal medullary cells (Yates, Wood and Duncan, '62). This same electron microscopic study utilized conventional methods of fixation and two types of adrenomedullary cells were identified on the basis of granule size.

MATERIALS AND METHODS

Animals and Techniques. The animals used in these experiments were 8 cats, 3 rabbits, 5 chickens, 5 Chinese hamsters, 7 Syrian hamsters, 11 mice and 52 rats. Of these 5 cats and 14 rats were fixed by perfusion via the left ventricle. The adrenals from the remaining animals were sliced and fixed by immersion in the appropriate fixative. The animals which were not killed by the perfusion method

were either decapitated or had their necks broken and the adrenals were removed immediately

Three of the histochemical procedures employed were the iodate method of Hillarp and Hökfelt ('53) the potassium chromate-dichromate method of Hillarp and Hökfelt ('55) and the fluorescent method of Eränkö ('52) These methods use sections cut on the freezing microtome at 10–20 µ. The sections were mounted on glass slides, and studied in the pre scribed manner

Two additional fixatives used were Orth s according to Lillie (48) and a new fixative developed during the course of the investigation. This new fixative consists of a solution of 2.5% potassium dichromate and 1% sodium sulfate (anhy drous) in an M/5 acetate buffer at a pH of 4 1 At the time of fixation a 10% formaldehyde solution was added in a ratio of one part of formaldehyde of ten parts of the dichromate solution. The pH of the resulting fixative was then carefully adjusted to 4 0–4.2. Fixation was for 24 followed by rinsing overnight in The tissue was dehydrated in alcohols, cleared in xylene and embedded in Tissumat. Sections were cut at 2–5 µ on a rotary microtome and mounted on glass slides.

The mounted paraffin sections were deparaffinized in xylene, carried through two changes each of 100% 95% and 70% alcohols to water where they remained in the last change of water for 30 minutes. Following the last change in water the sections were stained rinsed in distilled water differentiated in 95% alcohol and carried through two changes each of absolute alcohol, xylene and covered with glass coverslips and permount. The stains employed were the modified Giemsa method according to Pearse ('60) and a newly developed stain with the following composition:

1% aqueous eosin yellow
0.5% aqueous anilin blue
M/5 cetate buffer at pH 4

These constituents were mixed in a 1:1 1 ratio and the pH of the staining solution was adjusted to 4 0 Staining time was 15 minutes after which the sections were differentiated dehydrated, cleared and covered as described above.

The animals used in this part of the study were 3 rabbits 5 chickens 5 Chinese hamsters 5 Syrian hamsters 8 cats, 11 mice and 37 rats. As mentioned earlier these animals were either perfused while under the influence of anesthesia or were rapidly decapitated with the exception of the rabbits and one cat which were killed by a blow on the back of the neck with an iron rod.

Adrenal slices were placed in Orth s and the new fixative while adjacent slices from the same gland were placed in the potassium iodate solution. The initial sections from both pieces of tissue were then studied in order to determine the pattern of cell type distribution. The potassium iodate method was used initially for locating the norepinephrine containing elements of the adrenal medulla. Paraffin sections were studied for distribution and cytological characteristics of the different cell types

Reserpine administration. The animals which received reserpine were two Syrian hamsters weighing 125 and 135 gm and 15 rats which weighed between 250 and 300 gm. All animals received subcutaneous injections of the drug and were sacrificed 24 hours following the last injection. In cases where multiple injections were given, injections were administered 24 hours apart. The two hamsters received single injections of 4 mg/kg reserpine. Six rats were given 0.25 mg four received 0.5 mg, one received 1 12 mg and another 1.25 mg of the drug in single doses. Three rats received eight daily injections of 1.25 mg reserpine.

RESULTS

The results of potassium iodate fixation of adrenal medullary tissue of the rat is shown in figure 9 The dark iodate positive islets of the norepinephrine secreting cells are scattered throughout the medullary area. The epinephrine secreting elements are represented by the clear areas of the medulla in this type of preparation. As can be seen in figure 5 the brown pigment formed in the norepinephrine containing cells upon treatment with potassium iodate is located at the periphery of

the medullary area and immediately adjacent to the cortex in the Syrian hamster. This location was consistent in this animal regardless of the plane of section unless the section happened to include only a peripheral area of the medulla resulting in an appearance of all cells being of the norepinephrine type. Iodate positive islets were also found in the mouse where they occupied a larger medullary area than in either the rat or the Syrian hamster. Iodate positive material in the cat was in more of a continuous pattern than in islets. Medullary tissue in this animal showed alternating layers of iodate positive and negative tissue. The chicken showed scattered cellular areas of iodate positive material throughout the adrenal gland and there was no characteristic pattern of distribution because in this animal, the cortical and medullary areas are interspersed with one another. No iodate positive reaction was present in the rabbit and no yellow staining norepinephrine cells were seen. In all these preparations sections were of the order of 10–20 μ in thickness and detailed cytologic study was not possible. The potassium chromate-dichromate method of Hillarp and Hökfelt ('55) when applied to the rat adrenal produced a reversal of the picture obtained by the potassium iodate method. Thus, the chromate-dichromate treated adrenal medulla showed relatively dark staining cells interspersed with islets of lightly stained cells. The dark cells correspond to the epinephrine containing or iodate negative cells and the lightly staining cells were identified as the iodate positive or norepinephrine containing cells. Again, the thick sections necessary with this method precluded detailed study of the different cell types. The cells which were observed to fluoresce with ultraviolet illumination following formalin fixation correspond to the norepinephrine containing cells distinguished previously.

Fixation of the tissue in Orth's fluid and subsequent staining with the eosin-anilin blue stain presented two differently staining cell types in the adrenal medulla. One type which dominated the medullary area in the rat was of brownish-purple color while the other medullary chromaffin cells were yellow. Both types of cells possessed a granular cytoplasm. Fixation with Orth's fluid produced extremely hard material and poor penetration of the fixative was evidenced by increasing numbers of poorly fixed cells which occurred as sections were made deeper within the block of tissue. The use of 10% formaldehyde in place of the full strength commercial product made the tissue less hard and penetration was somewhat better; however, both fixatives were observed to change in pH during fixation, from 3.98 to 4.50 in 24 hours. Dissolving of the constituents of the fixative in the M/5 acetate buffer instead of distilled water and the subsequent adjusting of the pH of the fixative to 3.9 gave good penetration but some diminishing of color intensity of the medullary cells. A fixative with a pH of 4.0 to 4.2 gave optimal results. The use of the 10% formaldehyde in this buffered fixative was preferred to the use of full strength formaldehyde which in most cases gave deeper coloration but undesirable hardness to the tissue.

Differential staining with the eosin-anilin blue mixture was dependent on the ionization of the anilin blue component, thus the dye solution was buffered to a pH of four which is approximately that of the 0.5% solution of anilin blue. Eosin still maintains its staining properties at this pH and anilin blue staining is at its maximum. Rinsing in distilled water, differentiating in 95% ethanol and dehydrating in absolute ethanol followed by clearing in xylene resulted in preparations which clearly illustrated the two chromaffin cell types.

Evidence for the consistency of this staining procedure is seen in figures 1, 2 and 3. The epinephrine containing cells are of a brownish-purple granular consistency while the norepinephrine cells located in their characteristic position and numbers are of a yellow color with a granular appearance. In all the animals studied the distribution pattern of the yellow staining medullary cells is consistent with that of the iodate positive cells previously mentioned. Overnight staining with the Giemsa stain produced norepinephrine containing cells staining a darker green than the epinephrine containing cells, figure 11. Twenty four hour staining with the Giemsa stain served to darken the

epinephrine cells. The eosin-anilin blue mixture was generally employed since it was found to be more sensitive and was specific for the cell types studied.

Evidence for the selective fixation of the two cell types and their contents in the Syrian hamster is shown in figures 6 7 and 8 while such fixation in the rat is illustrated by figures 10 and 13 These preparations are unstained sections from tissues which have been fixed in the buffered fixative. Both phase and ordinary light microscopy clearly indicate the darker norepinephrine cells contain large coarse granules while the granules of the epinephrine cells are not readily discernible. All such sections illustrated were cut at 3 μ.

A detailed study of eosin-anilin stained material at higher powers with the light microscope indicates specific differences in the two types of adrenal medullary cells in the rat. The epinephrine containing cells possess a granular cytoplasm of a brownish to purple color These cells appear to be aggregated into islets with the nuclei of the cells located toward the central portion of the islet. Between the nucleus and the peripheral border of the cell there is a bluish staining area indicative of the Golgi zone. The granular cytoplasm is more homogeneous than that of the norepinephrine cells and occasionally there are cells of lighter staining intensity The nuclei are generally blue to deep purple and possess one or two bright red, eccentrically located nucleoli. Occasionally one sees cells with very dense blue nuclei however these are in the minority The norepinephrine containing cells as previously mentioned possess a yellow granular cytoplasm and give the appearance of being less homogeneous in regard to the cytoplasmic structure. These yellow cells are smaller in size and the nucleus which usually stains blue seems to be located more toward the center of the cell. The one to two eccentrically placed nucleoli stain bright red as do those in the epinephrine cells. The bluish Golgi area is evident, but not to the extent as in the epinephrine cells. These yellow cells are more closely packed and lack the degree of polarity of the epinephrine cells. Also, the norepinephrine cells can be found as solitary cells within patches of epinephrine containing cells and at the periphery of the ganglion cells which themselves occur in clusters. A few of the norepinephrine cells display the dark blue, dense nuclei and occasionally there is observed a yellow cell which stains very lightly Other cells in addition to the regular ganglion cells which show few differences other than occasional vacuolization with this procedure are found scattered throughout the medullary area. Certain of these scattered cells are clearly cortical cells and others resemble neuronal elements. These last mentioned cells are considerably smaller than regular ganglion cells but possess eccentric, brightly staining nucleoli. They are further characterized by containing *cytoplasmic bodies which appear as* placques or vesicles. In general, the cytoplasm of such cells has a bluish granular appearance and is more dense than that of the ganglion cells.

The other animals studied exhibited similar differences in the cell types and the distribution differences have been noted here as well as by previous workers. The Syrian and Chinese hamsters and the chicken possess medullary cells exhibiting a mixture of brown and yellow staining properties indicating the presence of both epinephrine and norepinephrine within the same cell and the Chinese hamster is characterized by having a large number of both light and dark staining epinephrine cells. The norepinephrine cells in both types of hamsters show a greater degree of polarity than do similar cells in the rat and the incidence of both cortical cells and the neuronal appearing cells is much less in the Syrian hamster than in the rat.

Comparison of fixation by perfusion and by immersion of the freshly removed adrenal gland gave evidence that the lengthy procedure of perfusion did not warrant its extensive use in this study In some cases, fixation by the perfusion method appeared less satisfactory than with the simple immersion procedure. In a number of cases, the stress applied to the animals by anesthesia and perfusion produced a vacuolization of the medullary parenchymal cells and loss of the stainable material. This type of effect was also

noted in the cats which had been anesthetized with chloralose. The more rapid, less tedious and more reliable immersion fixation was the method principally employed.

Reserpine The six rats receiving single doses of 0.25 mg reserpine exhibited only a slight loss of yellow stainable material, while the four receiving single injections of 0 5 mg of reserpine 24 hours prior to decapitation presented adrenal medullary tissue like that shown in figures 4 12 and 14. All evidence of iodate positive material was absent when the iodate method was applied and staining of the tissue fixed in the buffered fixative indicated a loss of staining properties in the norepinephrine cells, figure 4. Close examination of these cells as in figure 4 indicates that there is still a hint of yellow staining capacity but in general most of the stainable material is absent thus leaving a bluish cast to the normally bright yellow cells. The depleted norepinephrine cells are somewhat smaller than similar cells in the control animals. Figure 4 also shows the brown epinephrine cells as relatively unaffected by this dose of reserpine. Another aspect of reserpine depletion of norepinephrine is presented in the unstained material which has been fixed in the buffered fixative. As indicated in figures 12, 14 there is a loss of granularity in the norepinephrine cells as compared to the control animals in figures 10 and 13 This loss of granularity occurs consistently in conjunction with the loss of staining properties of the norepinephrine cells following reserpine administration. The animals receiving doses of 1 12 and 1.25 mg of reserpine showed a more extreme loss of stainable material paralleled by a corresponding loss of granularity In all of these animals it is evident that the staining of norepinephrine is the first to be affected. Rats receiving eight daily injections of 1 25 mg of reserpine and the Syrian hamsters receiving single injections of 4 mg/kg of the drug show an almost complete loss of stainable material and granularity Generally there was only a slight hint of brown staining material within the cells but no yellow staining was evident upon careful study at high powers.

A study of other tissues of the animals employed was done to determine whether cells such as argentaffin cells might stain with characteristics similar to medullary cells. Sections of intestine containing argentaffin elements indicated that these cells stained with their own characteristic color This color is of a very light golden appearance and not similar to that of either of the two adrenomedullary cell types studied. The argentaffin cells also possess a finely granular cytoplasm. In the same tissue Paneth cells show large dense, dark blue staining granules. The granules in tissue eosinophiles stain with an intense, bright red color while mast cells contain a mixture of granules which are stained both blue and bright red. Sections from the pancreas present an intense red staining of the zymogen granules in the acinar areas but in this tissue as in others mentioned there is no indication of any staining similar to that of either of the two adrenomedullary cells.

DISCUSSION

The results with potassium iodate treatment presented here in the rat, mouse and cat agree quite well with those of Hillarp and Hökfelt ('53) and Eränkö ('55d) and the results in the Syrian hamster are in agreement with those obtained by Camanni and Molinatti ('58) and Eränkö ('56) The facts that no iodate positive material is seen in the adrenal medulla of the rabbit and no norepinephrine cells are present agree with both histochemical and chemical data since it has generally been accepted that the norepinephrine content of the adrenal medulla of the rabbit is practically nil (Hökfelt and McLean '50) Fluorescing islets of medullary cells in the rat were seen that corresponded to the iodate positive cells as pointed out by Eränkö ('55d) but since the iodate method was the easier to use, this was the established method employed for the detection of the norepinephrine cells.

The fact still remains however that the iodate method and its procedure of frozen sections ranging from 10–20 μ gives material which is not suitable for the study of individual medullary cells and their secretory products. Also neither the iodate nor the fluorescent methods demonstrate both

catecholamines simultaneously Thus the need for sections ranging from 2–7 μ and demonstrating both epinephrine and nor epinephrine was apparent as pointed out earlier in this paper Former workers such as Bänder ('50 '54) and Klein and Kracht ('57) attempted the use of methods involving paraffin sections but their results as pointed out by Eränkö and Palkama ('59) were not or could not be considered reliable.

A possible starting point for paraffin embedded tissue appeared to be the origi nal chromaffin reaction therefore the procedure for this reaction as outlined in Pearse ('60) was attempted and positive results were obtained. It was evident from the study of the tissue fixed in Orth s fixative that the stainability of the tissue was intense so much that detailed cytological observation was not possible due to the heavy staining with the Giemsa stain. Since some of the constituents of the Giemsa stain are salts of eosin and since eosin is an acid dye this seemed to be a possible departure in the selection of a dye for the staining of chromaffin tissue. Other components of the Giemsa stain are of a basic nature; therefore it was believed that if another acid type of dye could be found to complex with eosin then this complex of two acidic dyes might be more specific for the products of dichromate oxidation of adrenal medullary tissue and eliminate overshadowing by the basic dyes. The dye selected as the second component of the complex was anilin blue and it was reasoned that the complex of these two dyes would couple with only the oxi dation products of the catecholamines of the adrenal medulla in such a manner as *to produce a color difference between the* cell types. It was believed that there must be a high sensitivity of the staining compound if it were to detect the slight differ ences between the two dichromate oxidized catecholamines. The initial procedure of first staining the tissue with the eosin solu tion followed by subsequent immersion in anilin blue gave an indication that this line of reasoning had been correct for two two cells types were evident in most cases. However it also became evident that the procedure was not consistent for the anilin blue solution soon lost its staining proper ties When small amounts of eosin were added to the anilin blue solution all indication of staining properties of the latter disappeared and the stain took on an entirely different aspect. When the sections were carried through anilin blue prior to eosin staining the two cell types were again difficult to demonstrate. From these observations it became apparent that the desired staining did actually depend on the eosin-anilin blue complex, but the desired complex was dependent on the relative proportions of each dye in solution and this solubility might well be dependent on the ionization of the respective dyes. A study of the pH of the two dye solutions revealed the pH of the eosin to be 6 15 while that of the anilin blue was 4 00 When the anilin blue solution was buffered to the pH 4 00 with the M/5 acetate buffer addition of eosin had no apparent effect on the staining ability of the blue dye Finally a mixing of the two dye solutions gave evidence that the complex exhibited its greatest differentiating powers when it was buffered to the pH of four

The fixed tissue was found to be peculiar in that staining was erratic deeper into the tissue block. Careful examination indicated that penetration of the fixative was poor and this might have accounted for some of the previous descriptions of vari ous cell types The fact that the pH of the fixative changed in the direction of basicity during the period of fixation suggested that in all probability fixing of the outer portion of the tissue block prevented the deeper penetration of the fixative. The buffered fixative was successful when employed and quite to the contrary of the *statements of Hillarp and Hökfelt ('55)* and von Euler ('51) the use of a fixative with a pH of less than 5 0 proved to be successful. Ranges of pH studied indicated that best penetration and best fixation of tissue occurs at the 4 0 to 4.2 pH and that values higher than this result in poor fixation while lower values produce decreased staining ability It should be pointed out that the investigations of Hillarp and Hökfelt ('55) involved the use of potassium dichromate fixatives and apparently no formalin was employed It was noted during the present study that when tis-

sues were fixed in potassium dichromate solutions buffered to the pH of 4.0 or less there was certainly a loss of granularity of the cells. Thus, the ideas regarding potassium dichromate fixation which have been held for a long time cannot be doubted here; however when formaldehyde is added to the buffered dichromate fixative, the picture is entirely different and it is believed that the use of the formaldehyde is instrumental in the subsequent fixing of the tissue following the initial oxidation of the catecholamines with the potassium dichromate solution. Moreover such a technique of oxidative fixation is quite selective and readily differentiates the two types of catecholamine containing cells even when such fixation is employed alone.

The fixation and staining procedures described were instrumental in permitting a detailed study of the cells in the adrenal medulla of the animals employed. The perusal of unstained as well as stained sections contributed to an interpretation of the cell types with the Syrian hamster being most useful due to the unique localization of cell types. The larger granules which are evident in the norepinephrine cells agree with the descriptions given previously (Hillarp Hökfelt and Nilson, '54; Schuman, '57) as do the smaller granules of the epinephrine cells. In actuality the granular appearance of the epinephrine cells is such that the term granular might be considered a misnomer since granules *per se* are not actually discernible. The appearance and location of the cells in the animals employed is in agreement with other works which involved the use of frozen sections. Also the approximate area are volume occupied by the cell types in reference to one another agrees with the earlier chemical data (Goodall, '51; Hökfelt, '51 West, '55)

It is evident that a morphological difference exists between the two parenchymatous types of adrenomedullary cells when stainability granular appearance and size are considered. It is also apparent in rats which have been treated with the 0.5 mg dose of reserpine that the depleted norepinephrine cells are smaller than in the uninjected animals but marked variations in size within one cell type or the other in the same animal are not evident. The other cell types present in the adrenal medulla are either ganglion cells cortical cells or the neuronal type which has been described here. It is evident that more than two cell types are present in the adrenal medulla of most of the animals studied. In many instances small cells which usually stained like the norepinephrine medullary type are found in the position of satellite cells located in direct proximity to the ganglion cells. Occasionally epinephrine cells are also seen in this location.

A comparison of the cell types observed in this work with those seen by former workers is difficult, but there is agreement as to granule size as interpreted by Bänder ('50 '54) and Klein and Kracht ('57) Other correlations with paraffin sectioned tissue are difficult and might be due to the discrepancies pointed out by Eränkö and Palkama ('59) It is the belief here that a method which distinctly demonstrates the cell types of adrenal medullary tissue is important especially when certain comparisons can be made to recent work in electron microscopy (Yates Wood and Duncan, '62) Also the neuronal appearing elements which are found scattered through the medulla cannot be overlooked and present an interesting picture for further study

The effects of reserpine in the rat are consistent with the findings of Camanni, Losana and Molinatti ('58) Coupland ('58) and Eränkö and Hopsu ('58) but the total depletion of the catecholamines from the adrenal medulla from the Syrian hamster is contrary to the findings of Camanni and Molinatti ('58) when they stated that they were unable to produce total catecholamine depletion in this animal with the use of reserpine. Strain differences and resistance to the drug might well account for such a discrepancy The fact that loss of stainability correlates well with the changes produced in other studies indicates that the stain is specific for the material for which it is designed. The action of reserpine in its selective depletion of norepinephrine has been quantitatively studied by Eränkö and Hopsu ('58) and was used in this work as a confirmation of the loss of norepinephrine from the adrenal medulla. Also the fact that the mate-

rial prepared with the new fixative can be stained by other methods or studied unstained speaks well for a selective oxidative fixation process which might not be basically too different from the chemical method employed by Euler and Hamberg (49a)

It should be pointed out that although the technique is readily usable consistent and specific, and has proved useful in other work which will be reported shortly under a variety of conditions it is even more valuable when used in conjunction with other methods of study Further work with the electron microscope as previously mentioned is in progress as well as are certain physiological investigations. The ability to study the cells in greater detail along with the presence or absence of the secretory products is certainly an advantageous situation, and the high degree of specificity and sensitivity is showing promise in quantitative histochemical studies which are in progress.

SUMMARY

A technique has been developed which permits study of adrenal medullary tissue in 2–5 μ sections made from paraffin embedded tissue This method clearly distinguishes the epinephrine from the norepinephrine containing cells by differential fixation and staining. The two parenchymatous cell types of the adrenal medulla are identified by differences in staining ability and by visualization of characteristic cytological differences. Patterns of distribution in various species and reserpine induced alterations in the rat are in agreement with earlier works which have been presented in the literature.

The results indicate that the procedure is more specific and sensitive than earlier methods. With this technique it is obvious that there exists a morphological difference between epinephrine and norepinephrine cells on the basis of granularity and size. This study has led to the demonstration of these two cell types with the electron microscope

ACKNOWLEDGMENTS

The author wishes to thank Dr E. G Rennels who served as Supervising Professor for the dissertation and Dr C Wallace McNutt for the use of laboratory facilities and the color photographic apparatus. Special appreciation is extended to Dr Walther Hild of the Tissue Culture Laboratory for the taking of the phase photomicrographs and to Dr Donald Duncan for his invaluable advice and criticism. The author is also indebted to Mr Earl Pitsinger of the Tissue Culture Laboratory for his technical assistance.

LITERATURE CITED

Abel, J J 1902 On a simple method of preparing epinephrine and its compounds. Bull Johns Hopkins Hosp., 13 29–38.

Aldrich T B. 1901 A preliminary report on the active principle of the suprarenal gland. Am. J Physiol., 5: 457–461

Bänder A. 1950 Über zwei verschiedene chromaffine Zelltypen im Nebennierenmark und ihre Beziehung zum Adrenaline und Arterenolgehalt. Anat. Anz., 97 172–176.

——— 1954 Über zwei Chromaffine Zelltypen im Nebennierenmark und ihre Beziehung zum Vorkommen von Adrenalin und Arterenol. Arch. exper Path. u. Pharmakol., 223 140–147

Bennett, H. S. 1941 Cytological manifestations of secretion in the adrenal medulla of the cat. Am. J Anat., 69 333–382.

Bergstrom, S., U S. v Euler and U Hamberg 1949 Isolation of nor-adrenalin from the adrenal gland. Acta Chem. Scand., 3 305.

Camanni, F., O Losana and G. M. Molinatti 1958 Selective depletion of nor-adrenaline in the adrenal medulla of the rat after administration of reserpine (histochemical research). Experientia, 14 199–201

Camanni, F and G. M. Molinatti 1958 Selective depletion of noradrenalin in the adrenals of the hamster produced by reserpine. Acta Endocrinol., 29 369–374

Coupland, R. E. 1954 Observations on the chromaffin reaction. J Anat., 88 143–151.

——— 1958 The effects of insulin, reserpine and choline 2 6 xylylether bromide on the adrenal medulla and on medullary autografts in the rat. J Endocrinol., 17 191–196.

——— 1959 The catecholamine content of the adrenal medulla of the rat following reserpine induced depletion. Ibid., 18 154–161.

de Robertis, and A. V Ferreira 1957a Electron microscope study of the excretion of catechol-containing droplets in the adrenal medulla. Exper Cell Res., 12: 568–574

——— 1957b A multivesicular catechol-containing body of the adrenal medulla of the rabbit. Ibid., 12 575–581.

Eade, N R. 1958 The distribution of the catechol amines in homogenates of the bovine adrenal medulla. J Physiol., 141 183–192.

Eränkö O 1952 On the histochemistry of the rat adrenal medulla. Acta Physiol. Scand., 25 22–63.

——— 1955a Distribution of fluorescing islets adrenaline and noradrenaline in the adrenal

medulla of the cat. Acta Endocrinol., 18 180–188.

——— 1955b Fluorescing islets, adrenaline and noradrenaline in the adrenal medulla of some common laboratory animals. Ann. Med. Exp. Biol. Fenn., 33: 278–290.

——— 1955c Distribution of fluorescing islets, adrenaline and noradrenaline in the adrenal medulla of the hamster. Acta Endocrinol., 18: 174–179.

——— 1955d Histochemistry of noradrenaline in the adrenal medulla of rats and mice. Endocrinology 57 363–368.

——— 1955e Distribution of adrenaline and noradrenaline in the adrenal medulla. Nature, 175: 88–89.

——— 1956 Histochemical demonstration of noradrenaline in the adrenal medulla of the hamster. J Histochem. Cytochem., 4: 11–12.

Eränkö, O and L. Hänninen 1960 Electron microscopic observations on the adrenal medulla of the rat. Acta Pathol. Microbiol. Scand., 50 126–132.

Eränkö, O., and V Hopsu 1958 Effect of reserpine on the histochemistry and content of adrenaline and noradrenaline in the adrenal medulla of the rat and the mouse. Endocrinology 62: 15–23.

Eränkö, O., and A. Palkama 1959 Differential staining of the adrenaline and noradrenaline-containing adrenomedullary cells. Acta Pathol. Microbiol. Scand 47 357–363.

Euler U S. v 1951 Noradrenaline (arterenol) adrenal medullary hormone and chemical transmitter of adrenergic nerves. Ergebnisse der Physiol., 46 261–307.

Euler U S. v and U Hamberg 1949a Colorimetric determination of noradrenaline and adrenaline. Acta Physiol. Scand., 19: 74–84.

——— 1949b L-noradrenaline in the suprarenal medulla. Nature 163: 642–643.

Falk, B., N-A. Hillarp 1959 A note on the chromaffin reaction. J. Histochem. Cytochem., 7 149.

Goodall, M C. 1951 Studies of adrenaline and noradrenaline in mammalian heart and suprarenals. Acta Physiol. Scand 24 Supp. 85.

Green, D. E., and D. Richter 1937 Adrenaline and adrenochrome. Biochem. J 31 596–616.

Hale A. J 1958 Observations on the nature of the chromaffin reaction. J Physiol., 141 193–197.

Harley Mason, J 1948 The structure of adrenochrome and its reduction products. Experientia, 4 307–308.

Henle, J 1865 Ueber das Gewebe der Nebenniere und der Hypophyse. Zeitsch. f. rat Med., 24 143–152. (Cit. Takamine, '01)

Hillarp, N-A., and B. Hökfelt 1953 Evidence of adrenaline and noradrenaline in separate adrenal medullary cells. Acta Physiol. Scand., 30 55–68.

——— 1955 Histochemical demonstration of noradrenaline and adrenaline in the adrenal medulla J Histochem. Cytochem., 3 1–5.

Hillarp N A., B Hökfelt and B. Nilson 1954 The cytology of the adrenal medullary cell with special reference to the storage and secretion of the sympathomimetic amines. Acta Anat., 21 155–167.

Hökfelt, B. 1951 Noradrenalin and adrenalin in mammalian tissues. Acta Physiol. Scand., 25 Supp. 92.

Hökfelt, B., and J McLean 1950 The adrenaline and noradrenaline content of the suprarenal glands of the rabbit under normal conditions and after various forms of stimulation. Ibid., 21 258–270.

Klein, U and J Kracht 1957 Über Hormonbildungsstätten im Nebennierenmark. Endokrinologie, 35 259–280.

Lever J D. 1955 Electron microscopic observations on the normal and denervated adrenal medulla of the rat. Endocrinology 57 621–635.

Lillie, R. D. 1948 "Histopathologic Technique, The Blakiston Co., Philadelphia.

Mirkin, B. L. 1961 The effect of synaptic blocking gents on reserpine-induced alterations in adrenal medullary and urinary catecholamine levels. J Pharmacol. and Exper Therap., 133: 34–40.

Pearse, A. G. E. 1960 "Histochemistry Theoretical and Applied," second edition, Little Brown and Co., Boston.

Schümann, H. J 1957 The distribution of adrenaline and noradrenaline in chromaffin granules from the chicken. J Physiol., 137 318–326.

Sjöstrand, F S., and R. Wetzstein 1956 Elektronenmikroskopische Untersuchung der phäochromen (chromaffinen) Granula in den Markzellen der Nebenniere. Experientia, 12 196–199.

Stolz, F 1904 Über Adrenalin und Alkylaminoacetobenzcatechin. Ber. dtsch. chem. Ges., 37 4149–4153.

Takamine J 1901 Adrenalin the active principle of the suprarenal glands and its mode of preparation. Am. J Pharmacy 73 523–531.

Van Arman, C. G. 1950 Factors ffecting epinephrine content of adrenal glands. Amer. J Physiol., 162 411–415.

Vulpian, A. 1856 Quelques réactions propres à la substance des capsules surrénales. C. R. Acad. Sci. Paris 43 633, (cit. Bennett, 41)

West, G. B. 1955 The comparative pharmacology of the suprarenal medulla. Quart. Rev Biol., 30 116–137.

West, G. B., and R. B. Hunter 1951 Noradrenaline and the suprarenal medulla. Lancet (1) 471.

Wood, J G. 1963 Identification of and observations on noradrenalin and adrenalin containing cells in the adrenal medulla. Anat. Rec., 145: 292.

Yates, R. D., J G. Wood and D. Duncan 1962 Phase and electron microscopic observations on two cell types in the adrenal medulla of the Syrian hamster. Texas Reports on Biology and Medicine, 20 494–502.

Zbinden, G., and A. Studer 1958 Histochemische Untersuchungen über den Einfluss von Iproniazid (Marsilid) auf die durch Reserpin erzeugte Freisetzung von Adrenalin und Noradrenalin us dem Nebennierenmark. Experientia, 14 201 203.

PLATE 1

EXPLANATION OF FIGURES

1 Adrenal gland of a normal adult Syrian hamster fixed in the buffered formol-dichromate fixative, sectioned at 3 µ and stained with eosin-anilin blue. The yellow norepinephrine cells are located on the left and upper part of the picture toward the blue staining cortex while the brown staining epinephrine cells are located toward the right and lower portion of the photomicrograph. The marker in the upper left hand portion of the picture represents 200 µ.

2 Another portion of the same section as illustrated in 1 Yellow staining norepinephrine cells occupy the left hand area while the brown staining epinephrine cells are found to the right in the photomicrograph (blue filter) The marker represents 100 µ.

3 Normal rat adrenal fixed in the buffered formol-dichromate fixative and stained with the eosin-anilin blue stain. Yellow stained cells represent the norepinephrine element while the brown stained cells which have grayish cast due to the blue filter indicate the epinephrine element of the adrenal medulla. The cortex in the upper left area of the picture stains blue. The marker represents 100 µ.

4 Adrenal gland of 250 gm rat which had received 0.5 mg reserpine subcutaneously 24 hours prior to sacrifice. Tissue was fixed in the buffered formol-dichromate fixative and tained with eosin-aniline blue. There is pronounced loss of yellow staining material (arrows) from the norepinephrine containing cells. The bluish cast in these cells becomes apparent along with the loss of yellow staining properties. The epinephrine containing cells continue to stain brown. The hint of yellow color present in the norepinephrine cells indicates that small amount of this catecholamine is still present. Marker represents 100 µ.









PLATE 2

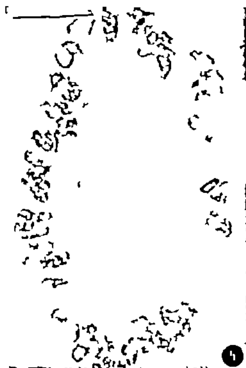
EXPLAN TION OF FIGURES

5 Adrenal gland of normal adult Syrian hamster treated with saturated potassium iodate solution and sectioned at 15 μ on the freezing microtome The dark iodate positive norepinephrine containing cells are located in their characteristic position at the periphery of the medullary area while the epinephrine containing cells in the center of the medulla remain unstained as do the cortical cells. Marker represents 300 μ.

6 Adrenal gland of normal adult Syrian hamster fixed in the buffered formol-dichromate fixative sectioned t 7 μ and mounted unstained. The darker appearing norepinephrine containing cells are located in their characteristic peripheral medullary position. Centrally situated epinephrine cells are indicated by lighter area while the cortical area shows no pigment form tion (ordinary light) Marker represents 300 μ.

7 A higher magnification of section from the sam block of tissue as illustrated in 6 but viewed with phase microscopy Norepinephrine cells located in the central area of the photomicrograph show dark coarse granules while the epinephrine cells (E) show more homogeneous cytoplasm. Cortex (C) is illustrated in the upper left portion of the picture Marker represents 70 μ.

8 The same area as depicted in 7 and photographed under the same conditions with the exception of being t higher magnification. Norepinephrine cells show larger more dense granules in contrast to the epinephrine cells (E) which exhibit more uniform, finely granular cytoplasm. Marker represents 20 μ






C
C


C
E

PLATE 3

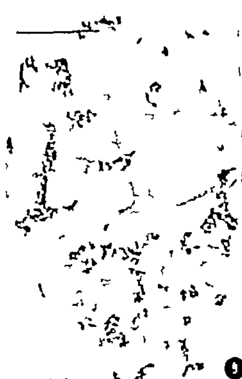
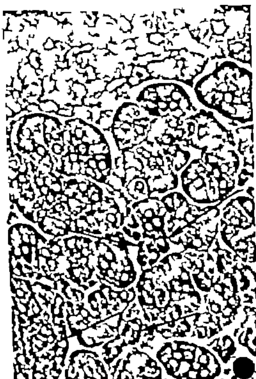
EXPLANATION O FIGURES

9 Adrenal gland of normal adult rat treated with saturated potassium iodate solution and sectioned t 15 μ on the freezing microtome. The dark islets of iodate positive cells indicate the norepinephrine containing element of the adrenal medulla while the epinephrine area and the cortical area remains unaffected by the procedure. Marker represents 200 μ.

10 Adrenal of normal adult rat fixed in the buffered formol-dichromate fixative, sectioned at 3 μ and mounted unstained. Phase microscopy reveals the cortex in the upper portion of the picture. The majority of cells present are the epinephrine containing medullary cells, but scattered islets of smaller norepinephrine cells which appear darker are indicated by the arrows. Marker represents 70 μ.

11 A section from the same block of tissue as ill strated in 10, but shown with ordinary light and after eight hours staining with the Giemsa stain. Arrows point to the islets of darker taining norepinephrine cells while the remainder of the medullary tissue stains with lighter color Marker represents 100 μ.

12 A 3 μ section from the same adrenal as illustrated in 4 but mounted unstained and viewed with phase microscopy Cortex is illustrated at the upper border nd arrows point to islets of norepinephrine cells which show partial loss of granularity due to the reserpine injection, compared with 10. Epinephrine cell appear relatively unaffected by the drug. Marker represents 70 μ.



About the N Cutaneus Brachii Lateralis Inferior

TATSUO KASAI
Department of Anatomy School of Medicine Hirosaki-University Hirosaki, Japan

By the seventh International Congress of Anatomists in '60 the n. cutaneus brachii lateralis inferior was adopted as a branch of the radial nerve and at the same time the n. cutaneus brachii lateralis, a branch of the n. axillaris, was renamed the n. cutaneus brachii lateralis superior In the B.N.A., J.N.A. and P.N.A. ('55 before the revision in '60) only the names of the n. cutaneus brachii posterior and the n. cutaneus antebrachii posterior appear as cutaneous branches of the radial nerve distributed to the skin of the arm and the forearm. As stated below since three branches are distinguishable as cutaneous branches of the radial nerve to the arm and the forearm, naming only two in the international nomenclature caused rather needless confusion in the descriptions of text-books.

The n. cutaneus brachii posterior is commonly described, in the text-books of the English-American school, as a branch running around the medial side of the long head of the triceps muscle and supplying the skin of the dorsal surface of the arm, but in those published in Germany and Japan, it is described as piercing the lateral intermuscular septum, running along the lateral side of the brachialis muscle and being distributed to the skin of the lateral surface of the arm. For verifying these accounts, the present author undertook examination of the courses of the cutaneous branches of the radial nerve in 60 arms of 32 human bodies (29 right side and 31 left-side specimens) and found that branches running the two courses above were both constant and accordingly there were at least three distinct cutaneous branches arising from the radial nerve as explicitly given in Gray's Anatomy (English Edition) and Cunningham's Anatomy as well as in the B.R. (Birmingham Revision, '33) Thus the author has been dissatisfied with the deficiency in the anatomical nomenclature, and welcomes the P.N.A. revision in '60

Since there is however no work systematically treating the origins and the courses of these three cutaneous branches of the radial nerve I wish to report on what I have studied on the relative position of these branches and the triceps muscle in the main, on the occasion of recognition of the three distinct branches in the P.N.A. revision. The precise delineation of the area of distribution of these nerve branches was outside the immediate scope of this study but as far as macroscopic dissection could reveal, the area was estimated with the accuracy possible.

OBSERVATIONS

1 The n. cutaneus brachii posterior This is the first branch of the radial nerve arising at a level of the upper border of the latissimus dorsi. It rounds the medial side of the long head of the triceps to its dorsal side and supplies the skin of the dorsal surface of the arm. It is 2–3 mm in diameter on the average at the origin. This branch runs under the deep fascia in the part where it runs around the medial side of the long head of the triceps and is accompanied by a small artery sent out by the profunda brachii artery at a point near its departure from the brachial artery

It is usually possible to find three separate cutaneous branches which course around the medial side of the arm and are distributed on the dorsal surface of the arm. The proximalmost is the n. intercostobrachialis having anastomosed with the n. cutaneus brachii medialis, the distalmost is the n. cutaneus brachii medialis and the n. cutaneus brachii posterior lies between them (fig. 1) The relative position of the three are accurately mapped out in Piersol's Human Anatomy Where they

run around the medial side of the arm, the n. cutaneus brachii posterior runs under the deep fascia and is accompanied by a small artery as described above, but the other two run above the deep fascia and are not accompanied by arteries.

Most of the authors of text-books published in Germany and Japan have over looked the existence of the n. cutaneus brachii posterior being discussed here and they have misnamed the n. cutaneus brachii lateralis inferior described in next paragraph the n. cutaneus brachii posterior As the n. cutaneus brachii posterior the cutaneous branch of the radial nerve running around the medial side of the arm is present in all of the cases an omission of this branch is apparently incorrect.

2. The n. cutaneus brachii lateralis inferior The text-books published in Germany and Japan mostly misname this branch the n. cutaneus brachii posterior This branch arises from the radial nerve at the spiral groove of the humerus, runs through the lateral intermuscular septum, at a point higher than the trunk nerve does, to the lateral side of the brachialis and is finally distributed to the skin of the lateral surface of the lower half of the arm. Its diameter at the origin measures about 2 mm. This branch was also present in every specimen without exception. In 42 (70%) of the 60 specimens it branched out singly from the radial nerve trunk, but in 18 (30%) it branched out in a common subtrunk *with the n. cutaneus antebrachii* posterior

3. The n. cutaneus antebrachii posterior This branch comes out from the radial nerve at the spiral groove then reaches the skin either through the space between the aponeuroses of the brachioradialis and of the lateral head of the triceps or through the lateral head of the triceps. We can make out three types by such courses of this branch, as follows:

Type I The branch running between the two aponeuroses above (39 specimens

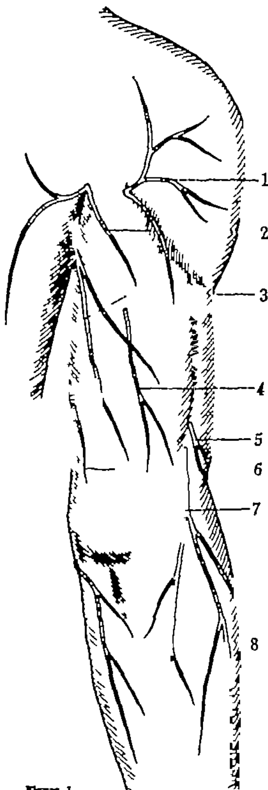


Figure 1

Fig. 1 The cutaneous nerves of the right upper limb. Posterior surface. 1 N cutaneus brachii lateralis superior; 2, Nn. intercostobrachiales; 3 N. cutaneus brachii posterior; 4 Perforating cutaneous branch of the radial nerve; 5 N cutaneus brachii lateralis inferior; 6, N cutaneu brachii medialis; 7 N. cutaneus antebrachii posterior; 8 N. cutaneus antebrachii medialis.

65%) There are two subtypes distinguishable:

(A) Arising from the trunk separately from the n. cutaneus brachii lateralis inferior (31 specimens)

(B) Arising in common with the n. cutaneus brachii lateralis inferior (eight specimens)

Type II The branch running through the lateral head of the triceps, always near the lateral intermuscular septum (nine specimens, 15%) In these cases, the branch always arises independent from the n. cutaneus brachii lateralis inferior

Type III Cases having two branches of both types above (twelve specimens, 20%) In this case, the two branches usually communicate with each other as soon as they reach the skin. Here too two subtypes are possible

(A) Type I (A) with Type II — two specimens.

(B) Type I (B) with Type II — ten specimens.

4 The perforating cutaneous branch. Besides these constantly present three branches there was a cutaneous branch, piercing the triceps muscle and being distributed to the skin of the arm, in 31 (52%) of the specimens. Of the 29 remaining cases this branch was absent in 25 specimens but in four specimens, I could confirm neither its existence nor its absence. The branch is usually thin, but sometimes nearly equaling or even exceeding the n. cutaneus brachii posterior or the n. cutaneus brachii lateralis inferior in diameter In most cases, it arises from the radial nerve together with the muscular branches to the lateral or the long head of the triceps and supplies the skin of the dorsal surface of the arm. It was found running through the lateral head of the triceps in 67% the long head in 21% and between the two heads in 12% of the cases.

5. A classification of the radial nerve by the total number of the cutaneous branches distributed to the arm and the forearm. In summary of the above findings we may distinguish three following types

Type I With three cutaneous branches (25 of 56 specimens 45%) that is,

(1) N cutaneus brachii posterior

(2) N cutaneus brachii lateralis inferior

(3) N cutaneus antebrachii posterior

Type II. With four cutaneous branches (29 specimens, 52%) that is,

(1) (2) (3) — Each of them is the same above.

(4) One perforating branch (running through the lateral head of the triceps in 20 specimens, the long head in six, and between the two heads in three)

Type III With five cutaneous branches (two specimens, 4%) that is

(1) (2) (3)

(4) Two perforating branches (in one of the specimens, both of the branches ran through the lateral head and in the other one branch ran through the long head and the other between the two heads of the triceps)

The four cases in which neither the presence nor the absence of the perforating branch could be confirmed have been excluded here. When the n. cutaneus antebrachii posterior consisted of two roots it was counted as one branch.

6. Interrelation between the lateral intermuscular septum and the radial nerve. The lateral intermuscular septum is the aponeurosis extending from the deltoid tuberosity of the humerus to the lateral epicondyle and can be divided into upper and lower portions by the defect at the spiral groove. The upper half is the portion giving rise to the lateral head of the triceps and the brachialis, and lateral head of the triceps and the brachioradialis arise from the inferior part. At the defect of the septum, the aponeurosis of the lateral head of the triceps forms a stout tendinous arch stretching over both the upper and the lower halves beneath which runs the radial nerve trunk close along the humerus. The n. cutaneus brachii lateralis inferior runs either beneath the same arch or through the upper half of the septum, to the lateral side of the brachialis. The n. cutaneus antebrachii posterior penetrates the aponeurosis of the lateral head of the triceps to come out into the skin through the space between it and the aponeurosis of the brachioradialis.

DISCUSSION

In the current text-books of anatomy the cutaneous branches of the radial

nerve mentioned above are described in four different ways as presented in table 1

Of these cases described in table 1 we may dismiss the case 1 overlooking the existence of the n. cutaneus brachii posterior The case 2–A fails in correctly interpreting the finding of the n. cutaneus brachii lateralis inferior So what remains is to adopt either case 2–B and treat the n. cutaneus brachii lateralis inferior as a subbranch of the n cutaneus antebrachii posterior or to follow case 2–C and regard these two nerves as a separate branch of the radial nerve. The present author claims that the two should be acknowledged *as utterly distinct branches on the* following grounds

(1) The n cutaneus brachii lateralis inferior is an always present constant branch and is as thick as the n cutaneus brachii posterior

(2) The n. cutaneus brachii lateralis inferior arises from the radial nerve trunk independently in more than two-thirds of the examined cases, but only in less than one-third simultaneously with the n. cutaneus antebrachii posterior *forming a* common trunk.

(3) The former runs through the middle portion of the lateral intermuscular septum in company with the radial nerve, but always on the proximal side of this nerve. The latter runs through the lower half of the lateral intermuscular septum or the lateral head of the triceps.

(4) The former supplies only the skin of the lateral surface of the lower half of the arm

SUMMARY

Seeing that there are frequent discrepancies *in the description of the cutaneous* branches of the radial nerve distributed to the arm and the forearm in the current text-books, the present author conducted anatomical examination mainly focussed on the relative position of such cutaneous branches and the triceps muscle in 60 specimens of the upper limbs of 32 human bodies.

At least three of cutaneous branches were found arising from the radial nerve

TABLE 1

The various descriptions about the cutaneous branches of the radial nerve distributed to the arm and the forearm, in the text-books of anatomy

Contents		Text-books[1]
1 The n. cutaneus brachii posterior unmentioned, and misnaming the n. cutaneus brachii lateralis inferior the n. cutaneus brachii posterior		1 Beninghoff ('50) 2. Braus ('60) 3. Corning ('22) 4 Pernkopf ('43) 5. Rauber-Kopsch ('55) 6. Sobotta ('57)
2. Mentioning the n. cut. br post. without mistake.	A. Missing the n. cut. br lat. inf., or including it in the n. cut. antebr. post.	1 Spalteholz ('59)
	B. Mentioning the n. cut. br. lat. inf. and thus admitting the existence of three different cutaneous branches of the radial nerve, but calling this a branch of the n. cut. antebr post. without giving it separate name.	*1 Gegenbaur (1696)* 2. Goss ('59) — American edition of the Gray' Anatomy 3. Sappey (1869) 4. Schaeffer ('51) 5. Testut (1897) 6. Thane (1883)
	C. Mentioning the three branches seperately under specific names.	1. Bardeleben ('06) 2. Brash ('51) 3. Johnston-Whillis ('50) — English edition of the Gray' Anatomy 4. Piersol ('18)

[1] About the book-names and the authors in complete form, see literature cited, presented at the end of this paper.

in every specimen and the discrepancies in the text-books have been caused by the adoption of only two of them in the nomenclature of the B.N.A. J.N.A. and P.N.A. (before its revision in '60) The present study has clarified the origin, the course and the area of distribution of all the three constant cutaneous branches, and also revealed the existence of the perforating cutaneous branches running through the triceps muscle in 31 (52%) of the 60 specimens.

In this study the conception of the n. cutaneus brachii lateralis inferior newly adopted in the P.N.A. is clarified and the propriety of distinguishing three different and independent cutaneous branches of the radial nerve is also demonstrated.

LITERATURE CITED

Bardeleben, K. 1906 Lehrbuch der systematischen Anatomie des Menschen. 813–815. Urban & Schwarzenberg. Berlin & Wien.

Benninghoff, A. 1950 Lehrbuch der Anatomie des Menschen. Bd. 3. Aufl. 3. 344–346. Urban & Schwarzenberg. München & Berlin.

Brash, J. C. 1951 Cunningham' Text-book of Anatomy 9 ed. 1074–1082. Oxford University Press, London.

Braus, H. 1960 Anatomie des Menschen. Bd. 3. Aufl. 2. 162–163. Springer Verlag, Berlin.

Corning, H. 1922 Lehrbuch der topographischen Anatomie. Aufl. 12–13. 648–649 München & Wiesbaden.

Gegenbaur, C. 1896 Lehrbuch der Anatomie des Menschen. Bd. 2. Aufl. 6. 497–499. Leipzig.

Goss, C. M. 1959 Gray' Anatomy 27 ed. 1029–1031. Philadelphia.

Hirasawa, K. 1931 Plexus brachialis u. d. Nerven d. oberen Extremität. Arbeiten aus d. III Abt. d. Anat. Instit. d. Kaiserlichen Univ Kyoto. Serie A. Hefte 2. 95–98.

Johnston, T B., and J Whillis 1950 Gray' Anatomy 30 ed. 1125–1133. Longmans, Green and Co., London.

Linell, E. A. 1921 The distribution of nerves in the upper limb. J. Anat., 55: 79–112.

Pernkopf, E. 1943 Topographische Anatomie des Menschen. Bd. 1. Hälfte 2. 494. Urban & Schwarzenberg, Berlin & Wien.

Piersol, G. 1916 Human Anatomy 5 ed. 1308–1314. J B. Lippincott Co., Philadelphia & London.

Rauber Kopsch. 1955 Lehrbuch und Atlas der Anatomie des Menschen. Bd. 2. Aufl. 19 513–514. Georg Thieme Verlag, Stuttgart.

Sappey C. 1889 Traité d'anatomie descriptive. Tome 3. 4 ed. 432–436. Paris.

Schaeffer, J P 1951 Morris Human Anatomy 10 ed. 1105–1107 Blakiston Co., Philadelphia.

Sobotta, J 1957 Atlas der descriptiven Anatomie des Menschen. Teil 3. Aufl. 40. 54–55. Urban & Schwarzenberg, München & Berlin.

Spalteholz-Spanner 1959 Handatlas der Anatomie des Menschen. Teil 2. Aufl. 16. 394–395. Scheltema & Holkema N. V., Amsterdam.

Testut, L. 1897 Traité d'anatomie humaine. Tome 2. 3 ed. 698–703. Paris.

Thomson, A., E. A. Schäfer and G. D. Thane 1882 Quain Element of Anatomy Vol. 1. 9 ed. 614–617 Longmans, Green and Co., London.

Fine Structure of the Reticulum and Sinuses of Lymph Nodes[1,2,3]

ROGER E. MOE
Departments of Anatomy and Surgery University of Washington, School of Medicine Seattle Washington

Studies based upon light microscopic observations of lymph nodes are hampered by limited resolving power of the instrument and by the nature of lymphoid tissue, which contains tightly packed cells of diverse sizes, shapes and appearances. Further confusion arises from the existence of numerous transitional appearances of cells, leading to difficulty in precise identification.

During the past decade the superior resolving power of the electron microscope has proved to be of value in studying lymph nodes. Since Braunsteiner et al. ('53) first employed the electron microscope for studying lymph nodes, several other electron microscopists have described the reticulum and sinuses of lymph nodes (Tanaka, '58 Fresen and Wellensiek, '58 '59; Moe, '60; Sorenson, '60 Han, '61 '62)

The present study was undertaken because our knowledge of the reticulum and sinuses is incomplete. This article describes the fine structure of the reticulum and sinuses in lymph nodes from mice as studied with the electron microscope. First, details are shown of the reticulum within the parenchyma, of the reticuloendothelial lining of the sinuses, of a perisinusoidal space and of a perisinusoidal sheath or adventitia. Next, the concept of a "reticular interstitium is brought forth. Again, electron microscopic findings are brought to bear upon a number of controversies in the literature of light microscopy Finally lymph node sinuses are compared morphologically with reticuloendothelial tissue elsewhere and with lymphatic vessels. In this report many findings of the electron microscopists mentioned above are confirmed. Numerous early light microscopic observations are also confirmed (Kölliker 1852, 1854; Brücke 1854 His 1860 1862; Frey 1861; Teichmann, 1861 von Recklinghausen, 1870 Bizzozero 1876; and others)

MATERIALS AND METHODS

Mice were selected as experimental animals since their lymph nodes are small and can be embedded whole Animals of both sexes weighing 20–28 gm were used. Deep and superficial cervical nodes were excised under pentobarbital sodium anesthesia. Mesenteric nodes were excised while the mice were unconscious after being struck on their heads during these excisions the abdominal cavity was flooded with Tyrode's solution to prevent damage from drying. Within one to three minutes after interruption of the local blood supply to each lymph node, the excised tissue was immersed for one-half to one hour in cold 1% or 2% osmic acid buffered to pH 7 4–7.5 by the method of Palade ('52) or with 0.05 M s-collidine (Bennett and Luft, '59) After dehydration in alcohol within one hour the tissue was embedded in n-butyl methacrylate or in Araldite (Luft, '61) and sectioned in the usual manner on a Servall microtome. Some of the sections were stained with lead tartrate (Millonig '61) or with uranyl acetate (Watson, '58) (The latter stain makes reticular fibrils more prominent although they can be seen in unstained sections.) Microscopy was performed with an RCA EMU 2C electron microscope fitted with a 500 μ condenser aperture, a 50 μ objective aperture with a compensated pole piece, and a specially stabilized power supply

[1] Supported by the Life Insurance Medical Research Fund G-61-45 and by Research Surgery Training Grant 2G 223, U. S. Public Health Service, National Institutes of Health.

[2] Presented in part at the VIIth International Congress of Anatomists, New York, April, 1960.

[3] Much of this work is included in thesis submitted in 1960 in partial fulfillment of requirements for the degree of Doctor of Medicine at the University of Washington, Seattle, Washington.

OBSERVATIONS

The supporting framework of lymph nodes includes a capsule with extensions called trabeculae which penetrate into the lymph node and a fibrocellular net or reticulum which spans the regions between the capsule, trabeculae and blood vessels. The cells of the reticulum are called reticular cells and reticuloendothelial cells. In this paper the terms reticular cells and "reticuloendothelial cells are used in the sense that Aschoff ('24) used them in his groups 3 and 4 In group 3 reticular cells include those mesenchymal cells which are a part of the net or reticulum within the cortical nodules and medullary cords of lymph nodes while in group 4 reticuloendothelial cells are those cells of the reticulum which line lymphatic sinuses.

Reticulum within the parenchyma

Passing among densely packed free lymphoid cells in the parenchyma are narrow curved strands of the reticulum (arrows, fig. 1) Each strand of the reticulum is composed of reticular cells and an extracellular component around which thin sheet-like processes of reticular cells are wrapped like a tube or sheath (RC figs. 2, 5)

Reticular cells are stellate and contact each other by simple cell-to-cell abutment, by overlapping, or by irregular cell junctions. At random intervals gaps are found between adjacent reticular cells (arrows fig. 3) The nuclei of the reticular cells are ovoid, with homogeneous chromatin a double nuclear membrane and nuclear pores. The cytoplasm of the reticular cells contains some tubular and ovoid mitochondria with obvious cristae, numerous vesicles of varying size, and ergastoplasm which in some cells may occupy nearly all the visible cytoplasm. One or more Golgi areas can sometimes be seen; usually multiple stacks of Golgi membranes are found concurrently with well-developed extensive ergastoplasm.

The extracellular component or core of the reticulum is a space 0 05 μ–2 μ wide penetrated at irregular intervals by reticular cell processes (c, figs. 2, 4 5) The contents of this space are what light microscopists often interpreted as a reticular fiber or sometimes simply as "reticulum" When the electron microscope is employed, many sections of the extracellular core reveal no fibers; the contents of this space appear to be amorphous with uniformly low density (c, figs. 2, 4) or to have a faint filamentous orientation (c, fig. 5) In other sections however obvious fibrils embedded in structureless ground substance can be visualized in the extracellular core of the reticulum, particularly in sections stained with uranyl acetate (f fig. 6) These fibrils vary in size from 200 A – 700 A, but are commonly about 400 A wide. Many fibrils show substructure suggesting filaments 25–35 A wide and a longitudinal periodicity of about 650 A.

At some sites in the extracellular core of the reticulum there may be a light region of very low density in the photomicrograph as if an empty space exists. In other sites a dark region may be seen. These light and dark areas seem to be partly an artefact of sectioning due to a difference in the ease with which the knife penetrates the extracellular core, frequently encountering dense tough collagenous fibrils The light areas are thought to be due to the knife cutting more thinly as if it were almost sliding over the reticular core rather than cutting through it; such areas could also be a result of non-uniform infiltration of the embedding medium into areas containing abundant mucopolysaccharides. The dark areas are thought to be sites of compression due to a snow-plow effect of the knife against the fibers.

Sinuses

General structure (figs 7–9). The lumina of lymphatic sinuses are bounded by thin flattened, greatly elongated reticuloendothelial cells. Strands of reticulum traverse the lumina much like suspension bridges. Along the reticuloendothelial lining on the side away from the lumen is a perisinusoidal space which contains variable ratios of wavy fibrils and ground substance. Between the perisinusoidal space and parenchymal cells is a sheath or adventitia of reticular cells.

Reticuloendothelial lining The cytoplasm of the reticuloendothelial cells (RE, figs. 7–9) contains many particles of un-

known identity and many vesicles of different sizes. The number of mitochondria and the quantity of ergastoplasm are not constant. In some reticuloendothelial cells the number of mitochondria seems to vary inversely with the quantity of endoplasmic reticulum. Cells containing a larger number of mitochondria may have sparse ergastoplasm and a large number of cytoplasmic vesicles other reticuloendothelial cells may show only a small number of mitochondria and have more abundant ergastoplasm. The nuclei are ovoid, with homogeneous chromatin. It may be noted that the outer nuclear membrane sometimes shows extensions or evaginations which project into the adjacent cytoplasm (x, fig. 9) Like ergastoplasm these extensions are lined on one side with Palade's particles suggesting that part of the ergastoplasm within a cell may develop from the outer nuclear membrane.

The reticuloendothelial lining has discrete cell junctions (J figs. 8 11) which reveal a fairly uniform interval of about 140 A between adjacent plasma membranes. Larger gaps approximately 0.1 µ–1.0 µ wide also exist between adjacent plasma membranes of reticuloendothelial cells (G fig. 9) making a significant discontinuity in the lining of the sinus. But these larger gaps are infrequent and do not occur at every cell junction.

Reticulum which traverses the sinus lumen. A major characteristic of lymphatic sinuses is the strands of reticulum which span the lumina like bridges. These strands of reticulum are comprised of a tube of reticuloendothelial cell processes around a reticular core (figs. 11 13) Extending into the lumen from the sinus wall (fig. 13) this tube of reticuloendothelial cells is constructed in the same fashion as a tube of reticular cells within the parenchyma, except that the tube of reticuloendothelium crossing the sinus is not usually perforated by gaps. The extracellular core looks identical to the reticular core within the parenchyma.

Perisinusoidal space External to the reticuloendothelial cells on the side away from the lumen is a perisinusoidal space 0.05 µ–1.5 µ wide (s figs. 7–9 12, 13) The perisinusoidal space contains either amorphous material or collagenous fibrils in ground substance. In some places within the perisinusoidal space there is a thin feltwork of moderately dense material like a basement membrane located along the reticuloendothelial lining; in other places the perisinusoidal space is entirely filled with diffuse material of moderate density Thus in the sense of a very thin membrane adherent to the base of endothelial or epithelial cells as seen with the electron microscope, a basement membrane is regarded as being inconstant around the sinuses of lymph nodes in mice. The perisinusoidal space is continuous with the reticular core within the parenchyma (fig. 12) and with the extracellular core of the reticulum within the sinuses (fig. 13)

Perisinusoidal reticular cell sheath Draped around the reticuloendothelial lining of the sinuses like a fish-net is an incomplete sheath of reticular cells. These cells are located along the border of the perisinusoidal space next to the parenchyma (RC, figs. 8 9) Rather large gaps often exist between the sheath cells (arrows, fig. 9) Perisinusoidal reticular sheath cells resemble reticuloendothelial cells quite closely Sometimes the perisinusoidal reticular cells contain more abundant particles of Palade or more ergastoplasm than reticuloendothelial cells (fig. 8) but this is not always so (fig. 9) Furthermore, perisinusoidal reticular cell processes sporadically join cell processes of reticuloendothelial cells and of parenchymal reticular cells, although this is infrequently seen on electron micrographs because of the thinness of the sections.

DISCUSSION

Reticular interstitium. A single integrated communicating space called the reticular interstitium courses throughout the reticulum in lymph nodes. This extensive structure comprises the extracellular portion of the entire supporting framework. That is to say the extracellular core of the reticulum within the parenchyma connects with a perivascular space located around blood vessels and with the perisinusoidal space (fig. 12) The perivascular space is intentionally disregarded in this paper since it is more appropriately described in a paper to be published subsequently The perisinusoidal

Concepts mentioned up to this point are summarized in a schematic drawing, figure 14

Comparison of lymph node sinuses with other reticuloendothelial tissue and lymphatic vessels Electron microscopic reports are available describing the sinuses of nearly every organ containing reticuloendothelial tissue, such as the hypophysis (Rinehart and Farquhar '55) adrenal cortex, (Lever '55 Luft and Hechter '57 Zelander '59 Luse, '61) liver (Fawcett, '55; Parks '56 Hampton, '58) spleen (Weiss, '57 '59 '62) and bone marrow (Weiss '61; Zamboni and Pease '61) Also lymphatic vessels have been described by Palay and Karlin ('59) and Fraley and Weiss ('61) The lymphatic vessels and the sinuses of most of the above organs have been categorized by Weiss ('61) according to a system of classification devised by Bennett et al. ('59) Supplementary comparative data may be useful.

Intercellular fenestrations which may be sparse or numerous have been found in the lining of the sinuses of lymph nodes bone marrow liver and red pulp of the spleen. Some lymphatic vessels also have intercellular fenestrations. The lining of the sinuses of the adrenal cortex and hypophysis may differ in this respect. In the adrenal cortex, Zelander ('59) and Luse ('61) showed small fenestrations which look like intracellular rather than intercellular fenestrations. On the other hand, Luft and Hechter ('57) indicated that such fenestrations may be artefactual. In the hypophysis, Rinehart and Farquhar ('55) found no fenestrations although they did state that cytoplasmic processes of pericapillary cells could pass through the endothelium.

Basement membranes are incomplete (frequently not detected) around the sinuses of lymph nodes and the red pulp of the spleen. Lymphatic vessels and sinuses of the liver and bone marrow lack basement membranes while sinuses of the adrenal cortex and hypophysis have complete and continuous basement membranes. Yet it is to be noted that a space containing ground substance and a variable number of collagenous fibrils surrounds the contraluminal side of cells lining lymphatic sinuses of all the organs mentioned above. This space is part of the extracellular compartment of the body and it is large and broad around lymphatic capillaries and bone marrow sinuses or narrow and compact around sinuses of organs such as lymph nodes the adrenal cortex, hypophysis and liver This space is not the same as a basement membrane as defined for this paper Basement membranes occupy only a part of this space as exemplified most clearly in electron micrographs of the hypophysis (Rinehart and Farquhar '55) and adrenal cortex (Zelander '59)

A substantial, but incomplete perisinusoidal cellular investment surrounds sinuses of lymph nodes the adrenal cortex and hypophysis. In contrast, lymphatic vessels, sinuses of the bone marrow and liver and apparently also the red pulp of the spleen lack such an investment.

Hence it appears that there are some differences in the electron microscopic morphology of reticuloendothelial tissue as compared in different organs, and as compared with lymphatic vessels.

SUMMARY

The reticulum within the parenchyma of lymph nodes consists of narrow strands formed by stellate reticular cells with an extracellular core of amorphous substance and collagenous fibrils both components are equally important. Gaps here and there between the reticular cells allow some communication between the reticular core and adjoining parenchymal regions.

Lymphatic sinuses are bounded by flat tended discrete reticuloendothelial cells which in essence are reticular cells serving as endothelium. Usually an interval of about 140 A exists between adjacent plasma membranes, but occasionally one finds gaps approximately 0 1 μ-1 0 μ wide through which various substances or even cells may pass. Abutting on the contraluminal side of the reticuloendothelial lining is a perisinusoidal space 0 05 μ-1.5 μ wide containing ground substance and collagenous fibrils. A basement membrane is inconstant. An incomplete or fenestrated perisinusoidal sheath of reticular cells lies between the perisinusoidal space and the parenchyma.

An important feature is a single extensive communicating structure called the reticular interstitium. It includes the perisinusoidal space, extracellular core of the reticulum, and a perivascular space; the perivascular space is not described in the present paper, however The contents of these three areas look identical and are directly continuous. The reticular interstitium is regarded as a structural support and may also serve as a distribution pathway for many substances.

In contiguity with and limiting the reticular interstitium is an integral group of cells which includes reticuloendothelial cells, perisinusoidal reticular sheath cells and parenchymal reticular cells. These are all regarded as similar cells which may vary to some extent in appearance, depending upon local functions, and with the reticular interstitium they make up the general reticulum of lymph nodes

Finally the structure of lymph node sinuses has been compared with analogous structures in other organs containing reticuloendothelial tissue and with lymphatic vessels, pointing out certain similarities and differences.

ACKNOWLEDGMENTS

The author is indebted to Dr H. Stanley Bennett, Dr John Luft, and Dr Richard Wood for valuable advice and assistance, and to Dr. Henry N Harkins, Dr Newton B Everett and Dr Lloyd M. Nyhus for providing an opportunity to complete this study

LITERATURE CITED

Aschoff L. 1924 Das reticuloendotheliale System. Ergeb. inn. Med. u. Kinderheilk., 26 1–118.

Benedetti, E. L. 1954 Ricerche sul tessuto connettivo reticolare con il microscopio elettronico. Nota II. Rilievi sulla morfologia delle fibre delle microfibrille. Rend. ist. super. sanità, Roma, 17 839–850.

Bennett, H. S., and J Luft 1959 s-Collidine as basis for buffering fixatives. J Biophys. Biochem. Cytol., 6 113–114.

Bennett, H. S., J. Luft and J Hampton 1959 Morphological classifications of vertebrate blood capillaries. Am. J Physiol., 196: 381–390.

Bizzozero, G. 1876 Beiträge zur Kenntnis des Baues der Lymphdrüsen. In Untersuchungen zur Naturlehre des Menschen und der Thiere. J Moleschott, ed. E. Roth, Giessen, Vol. XI 300–309.

Bloom, W 1938 Lymphatic tissue; lymphatic organs. In Handbook of Hematology H. Downey ed. Paul B. Hoeber Inc., New York, pp. 1428–1467

Braunsteiner H., K. Fellinger and F Pakesch 1953 Elektronenmikroskopische Untersuchung der Plasmazellen im lymphoreticulären Gewebe. Deut. Arch. klin. Med., 200: 657–663.

Brücke, E. 1854 Über die Chylusgefässe und die Resorption des Chylus. Denkschr Akad. Wiss. Wien, 6 13–136.

Downey H. 1922 The structure and origin of the lymph sinuses of mammalian lymph nodes and their relations to endothelium and reticulum. Haematologica, 3 431–468.

Drinker, C., G Wislocki and M. Field 1933 The structure of the sinuses in lymph nodes. Anat. Record, 56 261–265.

Ekholm, R., and Y Edlund 1959 Ultrastructure of the human exocrine pancreas. J Ultrastruc. Res., 2: 453–481.

Fawcett, D 1955 Observations on the cytology and electron microscopy of hepatic cells. J Nat. Cancer Inst., 15(Suppl.) 1475–1502.

——— 1958 Structural specializations of the cell surface. In Frontiers in Cytology S. Paley ed. Yale University Press, New Haven, pp. 19–41.

Fraley E., and L. Weiss 1961 An electron microscopic study of the lymphatic vessels in the penile skin of the rat. Am. J Anat., 109 85–101.

Fresen, O., and H. Wellensiek 1958 Elektronenoptische Befunde am retikulumzelligen Gewebe. Zentr allgem. Pathol. u. pathol. Anat., 97 406–407

——— 1959 Zur elektronenoptischen Struktur des Lymphknotens. In: Verhandlungen der Deutschen Gesellschaft für Pathologie, Wien, Tagung 42, pp. 353–363.

Frey H. 1861 Untersuchen über die Lymphdrüsen des Menschen und der Säugethiere. W Engelmann, Leipzig.

Hampton, J 1958 An electron microscope study of submicroscopic particles injected into the blood stream and into the bile duct. Acta Anat., 32: 262–291

Han, S. 1961 The ultrastructure of the mesenteric lymph node of the rat. Am. J Anat., 109 183–225.

——— 1962 The relationship of the fiber-associated reticular cell to reticular fibers in the lymph node and spleen of the rat. Anat. Record, 142: 238 (Abstract)

Heidenhain, M. 1911 Das Retikulum der lymphatischen Organe. In Handbuch der Anatomie des Menschen. K. von Bardeleben, ed. G. Fischer, Jena, Vol. 6 (pt. 1 sec. 2) 1054–1058.

Hellman, T 1930 Die Lymphknötchen und die Lymphknoten. In Handbuch der Mikroskopischen Anatomie des Menschen. W von Möllendorff, ed. J Springer, Berlin, Vol. VI (pt. 1) 233–396.

His, W 1860 Beiträge zur Kenntnis der zum Lymphsystem gehörigen Drüsen. Z. wiss. Zool., 10· 333–357

——— 1862 Beiträge zur Kenntnis der zum Lymphsystem gehörigen Drüsen. Ibid., 11 65–85.

EXPLANATION OF PLATES

All figures are electron micrographs of mouse lymph nodes fixed in buffered osmium tetroxide except figure 14 which is a schematic drawing based upon electron microscopic observations. The line near the figure number represents 1 μ, except in figure 1 where the line represents 5 μ.

Abbreviations (plates 1–8)

c, extracellular core of the reticulum
E, eosinophile
f collagenous fibrils
G, gap in reticuloendothelium
J cell junction
L, lymphocyte
lu, lumen of sinus
MC, medullary cord
n, nucleus
P, parenchyma
Ph, phagocyte
ps pseudopodium
RC, reticular cell
RE, reticuloendothelial cell
s, perisinusoidal space
T trabeculum
x, extension of outer nuclear membrane

PLATE 1

EXPLAN TION OF FIGURES

1 Low power electron micrograph showing very thin elongated strands of the reticulum (arrows) coursing through portion of the parenchyma of lymph node. Most of the visible cells are tightly packed lymphocytes (L) although several reticular cells (RC) are seen. Many nuclei contain one or more nucleoli, which are more dense than the surrounding chromatin. × 2,200

2 Further magnification of strand of the reticulum within the parenchyma. Overlapping reticular cell processes (RC) surround an extracellular component or core (c) which *is 0.05–0.15 μ wide at this site.* Longitudinal section. × 23,000

3 Oblique section of strand of the reticulum within the parenchyma. A gap approximately 0.6 μ wide (between arrows) separating two reticular cell processes permits an adjacent lymphocyte (L) to abut on the extracellular core (c) of the reticulum. The homogeneous nucleus (n) of the lymphocyte is surrounded by an exceedingly thin rim of cytoplasm. The top of the figure is occupied by the cytoplasm of reticular cell (RC) rich in ergastoplasm. × 21,000


RC
c
RC
c
RC
2

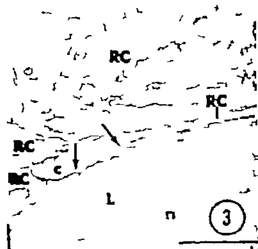

RC
RC
RC
c
RC
L
n
3

PLATE 2

EXPLANATION OF FIGURE

4 Higher magnification of longitudinal section of the reticulum. The extracellular core ( ) is penetrated by several cell processes of adjacent reticular cell (RC) Several vesicles in one of the reticula cells (arrows) suggest a transfer of material between the reticular cell and the extracellular core. Note the amorphous appearance of the reticular core ( ) × 43,000


RC
c
RC
RC
c
RC
c
RC
c
4

PLATE 3

EXPLAN TION OF FIGURES

5 Further magnification of cros section of trand of reticulum in the parenchyma shows wrapping of reticular cell processes (RC) around an extracellular core ( ) which is largely amorphous except for faint filamentou pattern. × 61,000.

6 Another region of the reticulum at similar magnification shows collagenous fibrils (f) in the extracellular core. Note that none of th fibrils suggest any intracytoplasmic continuity (Stained with uranyl acetate.) × 65,000.

RC

c

RC

RC

5

RC

RC

n

6

PLATE 4

EXPLANATION OF FIGURES

7 Lymphatic sinus. Within the lumen (lu) are parts of several free lymphocytes (L) and an eosinophile (E) The lining of the lumen is formed by narrow reticuloendothelial cells (RE) At the base of the reticuloendothelium is perisinusoidal space ( ) which in this section ppears stippled by black collagen fibrils. An incomplete sheath of perisinusoidal reticular cells (arrows) exists between the perisinusoidal space and the parenchyma (P) much like the adventitia of capillaries. (Stained with uranyl acetate.) × 11,500

8 Narrow lymphatic sinus which lies between trabeculum (Tr top of figure) and medullary cord (MC bottom of figure) The cell processes of the reticuloendothelial cells (RE) contain clumps of particles, scattered vesicles, and few mitochondria. A cell junction (J) is present between two reticuloendothelial cells in the middle of the figure. Several pseudopodia (ps) project into the lumen (lu) of the sinus some of them contain vesicles of phagocytized material. Outside the perisinusoidal space ( ) portion of several reticular sheath cells (RC) contain more particles of Palade and more ergastoplasm than the RE cells, but these differences in appearance are not constant A transected area of the reticular core ( ) is seen at the upper left corner of the figure Longitudinal section. × 17,000

PLATE 5

EXPLANATION FIGURES

9 Longitudinal section of one edge of lymphatic sinus. A gap 0.16 μ wide (G) exists in the reticuloendothelium, allowing the contents of the sinus lumen (l) to communicate with the perisinusoidal space (s) The outer nuclear membrane of the reticuloendothelial cell (RE) has projections (x) which are lined on one side with particles of Palade suggesting transition to ergastoplasm. The cytoplasm of the RE cell looks about the same as that of djacent perisinusoidal reticular sheath cells (RC). Note gap (between arrows) of 0.2 μ separating cell processes of the reticular sheath cells (RC) (Stained with lead tartrate.) × 19,000

10 A rounded phagocytic cell (Ph) lies adjacent to gap (G) of 0.4 μ in the reticuloendothelium. Such gaps might occur as phagocyte frees itself from the reticuloendothelium (RE) The light appearance inside the gap is due to the reticular core ( ) where it is exposed to the sinus lumen (lu) × 17,000.

lu
X
X
X
X
X
n
RC
RC
G
s
s
s
9


lu
Ph
G
RE
c
10

PLATE 5

EXPLAN TION OF FIGURES

9 Longitudinal section of one edge of lymphatic sinus. A gap 0.18 μ wide (G) exists in the reticuloendothelium, allowing the contents of the sinus lumen (l) to communicate with the perisinusoidal space ( ) The outer nuclear membrane of the reticuloendothelial cell (RE) has projections (x) which are lined on one side with particles of Palade suggesting transition to ergastoplasm. The cytoplasm of the RE cell looks about the same as that of adjacent perisinusoidal reticular sheath cells (RC) Note gap (between arrows) of 0.2 μ separating cell processes of the reticular sheath cells (RC) (Stained with lead tartrate) × 19,000.

10 A rounded phagocytic cell (Ph) lies adjacent to gap (G) of 0.4 μ in the reticuloendothelium. Such gaps might occur as phagocyt frees itself from the reticuloendothelium (RE) The light ppearance inside the gap is due to the reticular core ( ) where it is exposed to the sinus lumen (l) × 17,000.

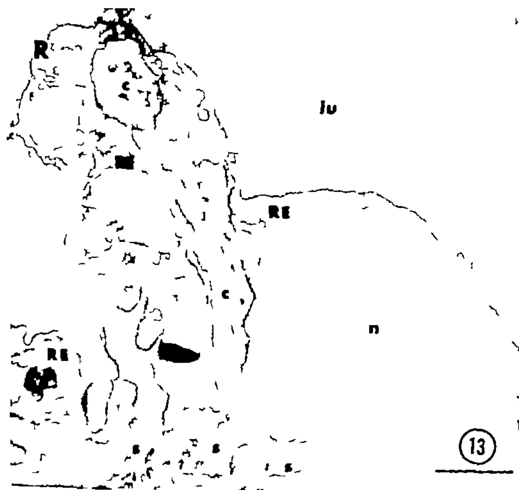


n
s
RE
lu
s
RC
s
s
s
c
RC
RC
RC
c
12

PLATE 7

EXPLAN TION OF FIGURE

13 Edge of lymphatic sinus t the base of a strand of reticulum (R) where it juts into the lumen (l) from the side of the sinus. Note tha the perisinusoidal space ( ) merges with the core ( ) of the strand of reticulum. (Stained with lead tartrate.) × 19,000


R
C
lu
RE
C
n
RE
S
S
S
13

Extracellular Studies of Uterus

I. DISAPPEARANCE OF THE DISCRETE COLLAGEN BUNDLES IN ENDOMETRIAL STROMA DURING VARIOUS REPRODUCTIVE STATES IN THE RAT

THEODORE FAINSTAT

Department of Obstetrics and Gynecology of Harvard Medical School, and The Biological Laboratories of Harvard University

In '26 a great impetus was given to thoughts concerning the dynamic roles of extracellular components of tissues in health and disease. Wolbach and Howe ('26) showed that the normal formation of collagen fibers is dependent on the presence of vitamin C. These investigations concerning tissue integrity in experimental scorbutus led to the characterization of scurvy as the inability of supportive tissues to produce and maintain extracellular substances. Since that time our knowledge of connective tissues has been extended through studies on numerous mesenchyme derivatives. An incomplete list meant to imply the scope of subjects studied from the point of view of connective tissue dynamics would include aging (Sobel, Gabay, Johnson and Hassan, '59), wound healing (Jackson, Flickinger and Dunphy, '60; White, Shetlar and Schilling, '61), collagen formation in embryonic development (Porter and Pappas, '59), the carageenin granuloma (Robertson and Sanborn, '58), muscular dystrophy (Bourne and Golarz, '59), the symphysis pubis (Talmage, '47; Hisaw and Zarrow, '50), the comb of the cockerel (Ludwig and Boas, '50), the uterus (Masters, Maze and Gilpatrick, '57; Malbenco, '60) and vascular aging (Boucek, Noble and Woessner, '59).

The focus of orientation in the study reported here is based on the endometrium as essentially a mesenchyme derivative. In the intact adult virgin rat it may be referred to as a densely collagenous connective tissue which is intimately associated with the epithelium of the uterine lumen and glands on the one hand, and the myometrium on the other. The dramatic changes exhibited by the collagenous stroma in various reproductive states and under certain endocrine influences as well as the significance of these changes with regard to various reproductive phenomena, form the subject matter of this report and others to follow from this laboratory. The investigations were aimed to throw light on the dynamics of connective tissue fibers in the reproductive tract, as well as to utilize the reproductive tract as an effective system for the study of connective tissues.

Fainstat ('60) reported that in the rat uterus the deposition, aggregation and linear orientation of molecular collagen into fibers is an important phenomenon resulting in discrete, thick collagen bundles which become the dominant structure seen in histologic sections stained with aniline blue, and which serve as an important structural supporting framework for endometrium. Clearly implicated as controlling factors involved in the appearance and maintenance of this grid framework were the ovarian hormones, especially estrogens, which were shown to be largely responsible for deposition and maintenance of dense collagenous bundles in the non-pregnant endometrium. Neural-pituitary-ovarian mediation, as in the state of prolonged suckling, was also involved. In the endometrium, discrete thick collagen bundles were infrequently seen or absent where decidual modification had occurred, in advanced pregnancy, and after long

Josiah Macy, Jr. Foundation Fellow in the Department of Obstetrics and Gynecology, Harvard Medical School.

Present address: Boston Lying-in Hospital, 221 Longwood Avenue, Boston 15, Massachusetts.

Presented in part at the First International Congress of Endocrinology, Copenhagen, July 1960.

term castration. The endometrium at the time of parturition was virtually devoid of thick collagen bundles.

Edema in the uterus

Growth wound healing, and indeed pregnancy have long been associated with the histological state of cells bathed in a sea of abundant ground substance with few visible fibers Allen ('31) observed edema of the endometrial stroma and a sparseness of stromal cells during pregnancy and Selye and McKeown ('35) wrote of the rat uterus the stroma of the mucosa is very rich in cells and relatively poor in fibers during lactation. They noted that a considerable amount of ground substance is lost during the few days immediately following parturition. Krichesky (42) reported that the development of stromal edema in the rabbit endometrium during pregnancy is a most striking histological change. He considered hormone-induced vascular premeability as a most likely edema-producing mechanism, but also considered the contributions of mechanical factors tissue injury and edema following stasis Concerning ovoimplantation Boving ('59) wrote "near the time of implantation and under hormonal control there is reduced capillary flow which causes submucosal edema, most pronounced near the epithelium.

In most mammals changes in the endometrial stroma during the initial phases of ovoimplantation are similar to those in the armadillo in which the endometrial stroma is markedly edematous at the onset of implantation (Enders, Buchanan and Talmage, '58) The cellular elements are relatively dispersed, and the stroma stains less intensely with conventional trichrome methods and with the PAS method. The authors were of the opinion that the trophoblast appeared to progress through the tissue by penetration rather than by lysis. In a discussion of ovoimplantation Rock (49) stated, access to maternal blood is the ultimate objective. While struggling on to this complete food the trophoblast must be nourished by contributions from intercellular fluid. " Wislocki and Dempsey (48) were impressed that the implanted growing blastocyst is surrounded by a zone of mucopolysaccharide which serves as nutriment. Hertig and Rock ('51) reported that implantation of the human blastocyst occurs on endometrium which is entering the physiologically edematous phase at the twentieth day of the menstrual cycle. Krafka (41) invoked imbibition of the edema fluid by the stromal cells to account for the decidual reaction in the human. Using silver stains he also noted disruption and lysis of connective tissue in the large edema-filled stromal spaces near an early implanting human ovum. Frayed reticular fibers were found in the penetration zone of the uterine stroma surrounding another early implanting human embryo (Brewer '38) Wolfe and Wright ('42) showed that during the development of deciduomata in rats a certain number of endometrial collagen fibers appeared split into much finer elements generally transitional or reticular in nature. Bartelmez ('57) suggested that, in primates, the development of edema loosens the stroma superficially and facilitates the spread of the trophoblast.

Extravascular nutrition for trophoblast and an increased ease of penetration into the endometrium were the two main functional features attributed to edema in the uterus as expressed in the histological literature with regard to ovoimplantation.

Collagen changes associated with reproductive tissues

Soon after those findings which initiated this study were made an encouraging report, "Gestational Changes in Connective Tissue in the Ewe (Bassett, '58) appeared. This paper reported extensive changes in the uterine ligaments including the disappearance of fibers staining with collagen dyes the appearance of argyrophilic fibers, and a considerable increase in ground substance. Similar though less extensive changes occurred in the other affected structures (the uterus cervix and vagina) No such changes were seen in the pubic symphysis, the lumbosacral joint, the Fallopian tubes the bladder and ureters and the connective tissue of the gastrocnemius muscle and the tendon of the deep flexor of the lower limb The activity of fibroblast cells was particularly emphasized. Bassett ('59) assumed that

the activated fibroblasts cause breakdown of the collagen fibers possibly by secreting an enzyme. He suggested that in mammals in which pelvic adaptations occur the connective tissue changes are brought about by the activity of regionally specific fibroblasts.

In '54 Harkness and Harkness first presented evidence for an increase in extractable molecular collagen (measured as hydroxyproline) which closely paralleled uterine growth during pregnancy. After parturition the molecular collagen content of the uterus fell precipitously even reaching values below the original estrus figure. (Implicit in the data was the possibility of reabsorption or mobilization of the fibers during pregnancy.) In contrast, a diminution in molecular collagen content during pregnancy was present in the area of the placental site in these same rats.

In '59 Woessner presented evidence in support of the idea that colagen is completely degraded within the uterus after parturition, and thought that a collagenase might be in operation at that time. Hydroxyproline was liberated and presumably removed by the blood. A year later Woessner and Brewer ('60) described a proteinase which was extracted from human uteri.

MATERIALS AND METHODS

Three hundred healthy virgin albino rats of the Harvard-Wistar stock were used in this study. At the onset of an experiment each rat was 95 to 105 days of age and weighed 210 to 270 gm. Throughout the experiments the animals were fed Purina Rat Chow and tap water ad libitum.

The organs studied were fixed at the time of the autopsy immediately after the death of the animal. The animals were killed instantaneously by a swift blow to the head. Animals were killed at various times during the estrous cycle, pseudopregnancy surgically induced decidual reactions, pregnancy and the post-partum period, and after various treatments, including castration and injections of estradiol 17β progesterone and relaxin. Under ether anesthesia, castrations were done through dorsolateral incisions. The pregnancy studies included observations on the non-pregnant uterus from rats which were unilaterally pregnant, and on areas of the pregnant uterus approximately midway between placental sites as well as areas near the placental sites. Unilaterally pregnant rats were obtained by performing a ligation and transection at one utero-tubal junction on the second day after coitus. Prior to injection the estradiol was dissolved in sesame oil and the progesterone in propylene glycol the relaxin was suspended either in beeswax oil or gel.

All pregnant females were primigravidas. Pregnancy was timed from the appearance of the vaginal sperm plug and the presence of sperm in the vaginal smear. Females were placed in the cage of the male in the evening and were examined between eight and ten A.M. the following morning. Day one of pregnancy was counted so as to include the 24 hours following the finding of spermatozoa in the vaginal smear during the morning screenings. The day of parturition was counted as day one in the puerperium.

Pseudopregnancy was induced by a 5-volt faradic stimulus to the uterine cervix and vagina of a rat in late proestrus or estrus. The decidual reaction was surgically induced in pseudopregnant rats during the morning of the fifth day following cervical and vaginal electrical stimulation. Under ether anesthesia the abdomen was entered via a posterolateral approach and the uterus was exposed. In some animals a very fine ophthalmic needle was used to place 6–0 surgical silk sutures in three different locations within the same uterus. The sites where suture was left in place were intentionally varied and included the mesometrial area, antimesometrial area, and both sides of the uterus. The path of the suture entered the uterine lumen in some cases and did not in others. In all cases the suture was retained in a loose tie about the uterus to serve as a marker for the course of the trauma without exerting compression on the uterus from without. In other rats, a two-inch hypodermic needle with a burr at the tip was inserted into the uterine lumen at the tubal sphincter and gently allowed to slide to the cervix. The endometrium was then scratched along its en-

Dr. Robert L. Kroc of Warner-Lambert Research Institute provided the relaxin.

tire length from cervix to tubal junction by withdrawing the needle while exerting gentle pressure against the endometrium with the burr The resulting decidual response involved the entire length of the endometrium.

At autopsy the uteri were weighed on a Roller-Smith torsion balance. Bouin s fixation was used for tissue specimens discussed in detail in this report. The following stains were applied to 6 μ paraffin sections. *Aniline blue* When it was desirable to emphasize strongly the collagenous components of the tissue while rendering the cellular components recognizable but not striking this method was most satisfactory Following mordanting in 2% phosphomolybdic acid each slide was stained for 30 minutes at 60 C in a preheated solution containing two grams each of aniline blue, orange G and phosphomolybdic acid in 100 cm of distilled water and then placed in 2% phosphomolybdic acid again for differentiation. *Biebrich scarlet-acid fuchsin:* Each slide was exposed for 15 minutes to a staining solution composed of 90 0 cm³ of 1% aqueous Biebrich scarlet, 10 0 cm of 1% acid fuchsin, and 1 0 cm of glacial acetic acid. *Green-red:* This technique was useful for demonstrating the changes in the ratio of cells to extracellular collagenous fibers, and in showing the distribution of these components within the organ. Following staining with Biebrich scarlet-acid fuchsin as above, the slide was differentiated in 5% aqueous phosphomolybdic acid, and then counterstained in "light green solution (2 grams light green stain and 2 ml glacial acetic acid in 160 ml distilled water) for 30 minutes.

Other techniques utilized were the classical Weigert s iron hematoxylin stain, Van Gieson s connective tissue stain, Masson s trichrome stain utilizing aniline blue and Wilder s reticulin stain. In some cases "light green was used following Wilder's reticulin stain (see fig 9) Some tissues were fresh frozen or freeze-dried and later stained with toluidine blue for metachromasia or with PAS by the Hotchkiss/McManus method.

Treatments for the following two experimental animals are not described elsewhere in the paper Rat number T 26 was given one injection of 3 5 cm of gel containing 8 000 guinea pig units of relaxin. The injection was given on the fourth day of pseudopregnancy and the animal was killed 72 hours later Rat number T 90 received 50 guinea pig units of relaxin in gel each day for eight consecutive days.

RESULTS

Decidual reaction location of stimulus epithelium

When 6–0 silk sutures were passed through uteri on the fifth day of pseudopregnancy decidual reactions frequently developed adjacent to the sutures. If the suture passed through serosa, myometrium, and stroma without reaching luminal epithelium, no decidual reactions resulted. In those cases in which the suture penetrated the luminal epithelium in the mesometrial portion of the uterus a decidual reaction began next to the suture (fig 6) although the trauma was distant from the usual implantation area in the antimesometrial zone.

The luminal *epithelium* covering areas of stroma which have undergone decidual modification is not merely collapsed to low cuboidal (fig. 5) or squamous (fig. 6) configurations but is also frequently elevated from the stroma in the microscopic sections (fig 12) This artifact of separation has not occurred in any of hundreds of sections of uterus in which the endometrium contains no decidua, however it has occurred frequently in sections in which decidual changes are present.

In sections of uteri (from this first experiment done in '57) stained with *aniline blue* four zones can be seen in endometrium undergoing early decidual modification (fig 7 and legend) A subepithelial densely cellular area is bordered by a zone of stroma which appears to be markedly edematous. Individual differences in the amount of stromal edema are present among animals which have received similar or identical treatments (figs. 6 and 7) Deep to the zone of marked stromal edema are areas of dispersed and split collagen fibers which stain poorly with aniline blue, and periglandular areas containing what appears to be intact dense collagen bundles which stain intensely with aniline blue.

The presence of coarse fibers which permeate the endometrium in the virgin adult non-pregnant rat was then confirmed. Dense collagen bundles clearly dominate the endometrial stroma in sections of uterus from these intact adult rats (figs. 1 and 2) In contrast, collagen bundles are absent from areas of decidual reaction (figs. 3 10 12, 19 and 20) However when these areas containing the markedly hypertrophic and hyperplastic polygonal decidual cells are studied with silver impregnation techniques, a considerable number of *argyrophilic fibers* are seen. It is not possible to distinguish the fiber changes in the decidua of early pregnancy from those in the surgically induced decidual reaction. Fibers which are thick and split, as well as fibers which are apparently splitting stain black and are seen throughout the mosaic pattern of the large, closely packed decidual cells. These fibers do not form a branching anastomosing network or reticulum such as the immediately subepithelial reticulum in the antimesometrial zone of intact rats or the argyrophilic fibrillar network in the stroma in late pregnancy (figs. 21 22 and 23)

The antimesometrial endometrium in intact animals is invariably thicker than the mesometrial endometrium. Moreover the subepithelial connective tissue in the antimesometrial area is reticular for a small portion of its depth, until it merges with the coarse collagenous bundles permeating the rest of the stroma. It is in this reticular area that stromal edema is most marked following relaxin treatments. Also edema accumulates most rapidly in this area following either blastocyst attachment to the luminal epithelium or artificial trauma to the endometrium.

In rats *castrated* six months prior to autopsy all components of the uteri have atrophied, but to varying degrees the endometrium having involuted the most. The endometrium after six months of castration is about one-sixth as thick as the endometrium during late estrus, while the myometrium has shrunk only to one-half its previous thickness (figs. 1 and 4) In cross sections (fig 4) the tissues closest to the lumen appear to involute the most. The circular muscle coat is proportionately more involuted than the longitudinal muscle layer when these layers are compared with the myometrium of intact rats. Well formed collagen bundles which stain deeply with aniline blue persist in the suspensory ligament of the involuted uterus and in the connective tissue surrounding the blood vessels which course between the muscle coats. The stroma of the castrated rats lacks the abundant deeply stained discrete collagen bundles which characterize the stroma of intact rats (figs. 1 and 2) Although perivascular areas between the circular and longitudinal muscle coats in intact rats frequently stain deeply during estrus (fig. 1), during diestrus (fig. 2) very little collagen is apparent in these areas.

In the uterine stroma of some of the rats treated with *relaxin* a markedly edematous dispersion of the fibrous architecture occurs, resulting in a loosened fibrillar pattern of the collagen bundles and in a decrement in the intensity of their staining with aniline blue (figs. 14–18) Basement membranes appear attenuated and occasionally fragmented. However the degree of these changes is unpredictably variable among similar animals given identical treatments. In some animals the only effect appears to be a slight increase in the fine fibrillations of the dense stromal bundles as seen through the light microscope These differing degrees of change are not readily explained. All uteri from relaxin-treated animals had increased wet weights in comparison to those from intact animals.

Late in pregnancy (figs. 21 22 and 23) dense collagen bundles which stain intensely with aniline blue are frequently found about basal glands (fig 23) In many sections no other deeply staining collagen fibers are present in the stroma. Abundant amorphous ground substance and widely dispersed, weakly staining fibers are visible. Basement membranes under the luminal epithelium are thinned and occasionally discontinuous. The circular coat of the myometrium, at this time stains intensely with aniline blue although in all other specimens examined, including those from early pregnancy the myometrium has virtually no affinity for the aniline blue

For more than a week following *parturition* (figs. 24–27) the endometrium is still essentially free of coarse collagen bundles. The stromal cells are large and the endometrium appears reminiscent of embryonic connective tissues or areas of wound healing Dense collagenous tissue is present in the metrial triangle (fig 27)

From the time of implantation until the time of parturition there is a progressive accumulation of ground substance in the stroma an increasing disaggregation and dispersion of the collagen bundles and a decreasing stromal affinity for aniline blue.

In animals autopsied on day 22 of pregnancy probably within 24 hours of the expected parturition, many of the stromal fibers were stained black with the silver impregnation technique. Throughout the stroma the argyrophilic fibers branched and anastomosed. Some of the branching and anastomosing fibers were single while many appeared to be composed of fibers or fibrils in close apposition. Many of the disaggregated fibers were obviously coiled rather than arranged in wavy bands Branching and coiling, with apparent anastomosing, was obvious wherever the fibers were followed for some distance. In the areas of greatest accumulation of ground substance where the most extremely disaggregated and dispersed collagen bundles were found a fine chicken wire network of faintly staining reticular fibers was present. This network had all the characteristics of a branching, anastomosing, faintly argyrophilic *reticulum*.

DISCUSSION

Decidual reactions and epithelium

Blandau (49) emphasized that the slightest disturbance of luminal *epithelium* is sufficient to instigate the *decidual reaction*. He stated "The (decidual) changes described may be observed only in those antimesometrial areas where the abembryonal poles of the ova are in contact with uterine epithelium. Knowledge of the great sensitivity of the rat endometrium to small stimuli and of the responsiveness of extrauterine connective tissues (Rubin and Novak, '56) led to an experiment intended to question the conclusion of Velardo, Dawson, Olsen and Hisaw ('53) that "Regardless of the site of traumatization of the uterine luminal wall the antimesometrial region is the first part of the uterus to undergo decidual modification. Initial changes in the antimesometrial area of the uterus occur within 24 hours after uterine traumatization. In contrast, in the experiment reported here the first decidual cells appeared near the thread regardless of the position of the thread in the uterus. In figure 6 no decidual cells have appeared in the antimesometrial region although 48 hours have elapsed since the thread was passed through the uterus.

The mesometrial endometrium is obviously not indifferent to trauma. It was in the mesometrial stroma that the first hypertrophic and hyperplastic changes occurred when the needle was passed through the mesometrial area only At the same time the antimesometrial stroma remained unchanged. The tissue did not respond to the trauma in an all-or-none manner rather the degree of response seemed to be dependent upon the site of trauma. The closer the thread was placed to the usual site of ovoimplantation at the antimesometrial end of the lumen, the larger the resulting deciduomata. However localized stimuli which failed to reach the epithelium did not produce decidual reactions, although an extensive defect in the stroma was made.

Trauma to the luminal epithelium overlying a progestational stroma induced the decidual response in the endometrium with regularity It may be suggested that trauma can cause the local liberation of a chemical transmitter whose first site of action is the neighboring progestational stroma which has a differential ability for propagating this stimulus or this tendency to excite and respond. In the rat the antimesometrial stroma has the greatest capacity to respond to trauma and to relay this excited state to contiguous stroma This region of tissue is the morphologic *pacemaker* of the rat uterus. A progestational endometrium includes cells whose integrated enzyme systems have been acted upon and modified by estrogens and progesterone in sequence and in synergism From a biochemical point of view we may consider that the progestational

endometrium contains a conditioned collection of integrated enzyme systems and substrates in a state of preparedness, awaiting a stimulus to trigger or drive reaction sequences in the direction expressed histologically by decidual modification.

The luminal epithelium is the first maternal tissue to be involved in attachment and in metabolic interchange with fetal tissue. Considering this role the collapsed degenerating epithelium which overlies decidua may be truly vestigial in the sense that it has outlived its period of usefulness once decidual modification has occurred. The failure of a blastocyst to become attached to epithelium overlying decidua probably reflects an inability of such an epithelium to convert the initial contact into attachment between blastocyst and epithelium.

In addition, the "artifact" of separation and elevation of the luminal epithelium from stroma which has undergone decidual modification (fig. 12) may reflect a newly acquired metabolic hiatus between the uterine stroma and epithelium. Interdependent metabolic relationships between connective tissue and contiguous epithelium have been demonstrated in organs other than the uterus. The function of connective tissue is to a considerable degree dependent upon and interrelated with the epithelium that covers it (Smelser '59). In cornea at least two synthetic processes in the connective tissue stroma are greatly reduced if contiguity with the epithelium is lost: (1) the incorporation of glycine-1-C^{14} into the collagen fraction (Herrmann, '57) and (2) the incorporation of S^{35} into the mucopolysaccharides of the ground substance (Smelser '59). It is through this interrelationship between the epithelium and the subjacent stroma that the epithelium can maintain synthesis of macromolecules in the stroma (Herrmann, '60). These findings can be correlated with the microscopic and biochemical findings which demonstrate a disappearance of collagen and ground substance in association with decidual modification and an apparent lack of replacement of these extracellular materials in the decidual tissue.

Permissive changes in the uterus

The extracellular changes in fibrous and amorphous endometrial constituents during pregnancy may be influential in permitting or preventing necessary uterine accomodations (Fainstat, '61). Several of the findings described in this report may represent permissive modifications of endometrial stroma. The paucity of antimesometrial subepithelial collagen bundles in non-pregnant endometrium may represent a *permissive* area anticipating ovoimplantation. As pregnancy advances and uterine contents are increased, the endometrial collagen fibers become increasingly disaggregated and considerable ground substance appears among them. At the same time the uterus becomes more plastic than in the non-pregnant state. It probably is not hazardous to guess that decaying collagen bundles in uterine stroma during pregnancy represent a "good-intentioned" activity.

Disintegration, fraying and breaking of coarse collagen bundles is almost synchronous with ovoimplantation. The wave of localized stromal edema, causing considerable fiber disaggregation and accompanied by abundant and prominent capillaries, is a prelude to the advance of the massive decidual transformation of the endometrium. Intact collagen bundles cannot be found in the wake of decidual modifications. This changed stroma is an integral part of the *nidation medium*. These changes in the uterus in early pregnancy occur immediately after contact between blastocyst and uterine epithelium and do not require penetration of trophoblast into maternal tissue. They are probably permissive of decidual modification and of subsequent intimacy between trophoblast and decidua.

Attachment of blastocysts to the uterine epithelium and surgical trauma to a progestational endometrium in the rat are both partly responsible for what we may call *induction of nidation media*. In association with ovoimplantation, a pattern of changes in the uterine stroma unfolds. For brevity we may refer to these changes collectively as the *uterine stromal CCC phenomenon*. CELL hypertrophy and hyperplasia, COLLAGEN bundle splitting, fraying, disaggregation, degeneration, and

disappearance and CAPILLARY and other blood vessel proliferation and expansion Collagen bundle disappearance may be associated with lessened rigidity or increased plasticity of the tissue thus permitting the growth of decidua and trophoblast in the implantation area while contributing to the supply of extracellular constituents used in nourishment of the growing cells. Failure of dense and rigid collagen bundles to give way to the rapid cell hypertrophy and hyperplasia associated with the decidua and trophoblast may result in implantation failures early abortions abnormal fetal development or other abnormalities of pregnancy *Nidation media* are developed as a result of the orderly interplay of a variety of changes within the stroma — a coordination of reactions concerning neighboring cells fibers and fluids and chemical energy transmission. The uterine stromal CCC phenomenon may be viewed as a key to the dynamics of the development of nidation media.

Collagen bundle disappearance during pregnancy

To account for many extracellular activities Loeven ('56) described a *tricomplex system* formed by the collagen molecules situated at the periphery of the collagen fibrils the molecular collagen between the fibrils and the mucopolysaccharides. It has been pointed out that argyrophilia may be due to a more intimate association between polysaccharide and collagen fibers than normally exists in coarse collagen bundles (Glynn, '53) or may be a reflection of the nature of the packing or the degree of aggregation of the collagen fibrils (Robb-Smith '52) As fiber formation may involve the association of soluble collagenous protein with a mucopolysaccharide the dispersion of fibers being the reverse process may involve the dissociation from the fiber of the mucopolysaccharide fraction and some collagen molecules which then become dispersed in the amorphous ground substance (Bowes Elliott and Moss '53)

In this study the appearance of argyrophilic, helically coiled fibers in the uterine stroma late in pregnancy where coarse collagenous bundles were present earlier may be the result of dissociation of the fiber complex. The split, fragmented and fraying argyrophilic fibers among the young decidual cells may be the result of local collagenase action along with mechanical breakage caused by pushing, pulling, and squeezing of the collagen bundles by the dynamic, hypertrophic hyperplastic decidua.

The stromal architecture and the staining of its fibers change greatly during pregnancy Where stromal edema is extensive the coarse collagen bundles are replaced in part by a branching and anastomosing argyrophilic reticulum and in part by larger argyrophilic coils of extracellular fiber It is likely that, except at the decidual site, the stromal fibrils of which the coarse collagen bundles are composed may persist through the pregnancy appearing in the helical coils or in the argyrophilic reticulum late in pregnancy The reticulated fibers may be an expression of extensive dispersion of helically intertwined and densely packed collagen fibrils.

Collagen molecules versus collagen bundles

Spectrum of collagen aggregates. The changes in the fibrous architecture of the uterine stroma as seen in microscopic sections should be correlated with the results of determinations of molecular collagen concentration and content in similar connective tissue systems It is sometimes not appreciated that in changing connective tissues there is a continuous spectrum of collagen aggregates with varying degrees of strength of cross-linkage. In biochemical experiments the various extraction media used remove a particular cross-section of these aggregates the specific cross-section depending upon the disaggregating ability of the medium. These extracts are biologically heterogeneous (Jackson and Bentley '60) The fraction extracted with 0 14 M NaCl contains the collagen molecules most recently synthesized in fibrogenesis. These molecules are considered to be the earliest form of extracellular collagen Where constituent molecules of the fiber are more firmly aggregated their resistance to extraction increases. Where argyrophil fibers

are visible histologically an acid buffer is required to break up the fiber complex. The mature, coarse collagen bundles, insoluble in aqueous or acid solutions can be extracted only after gelatinization (Jackson, Flickinger and Dunphy '60)

Collagen molecules from uterus The Harknesses used the method of Neuman and Logan ('50) for their determinations of collagen in the whole rat uterus. In this method the collagen is converted to a soluble form (gelatin) by hydrolysis. The collagen content is then estimated from the hydroxyproline content of the acid hydrolysates. The values obtained by this technique reflect the total molecular collagen content of the tissue, but provide no information regarding the dispersion of these molecules or their organization into fibrils or fibers.

Harkness and Harkness ('56) pointed out that the uterus has the ability to form collagen during pregnancy and rapidly absorb collagen after pregnancy They found an increase in uterine molecular collagen during pregnancy which closely paralleled the increase in uterine wet weight but was of a lesser degree. However, the collagen concentration at the placental site was only one-fourth that of the rest of the uterus (Harkness and Harkness '56) In a study in progress at The Johns Hopkins Hospital it has been found that, in practically all cases studied, the concentration of hydroxyproline in the human uterus is lower at the placental site than in the antiplacental area during the third trimester (Kumar '62) Following parturition in the rat, the rapid decrease in uterine wet weight is closely paralleled by a drop in the total collagen of the uterus these values even reaching levels below those found in intact animals (Harkness and Harkness, '54)

The total molecular collagen content of the whole uterus varies with the number of fetuses contained in it (Harkness and Harkness '54) The increase in molecular collagen is found mainly in the distended part of the uterus. The Harknesses suggested that in the pregnant uterus mechanical distention plays an important part in collagen "formation (Harkness and Harkness, '56) Edwards and Dunphy ('58) as a result of work with wound healing, pointed out that the density as well as the orientation of collagen fibers in a connective tissue regenerate appears to be related in part to mechanical forces. Cullen and Harkness ('59) found that the breaking stress of collagenous tissue is related to the quantity of collagen present. They also reported that at the end of pregnancy the collagenous tissue of the rat uterine cervix no longer acts as a continuous network but, rather acts as a mechanical system in which the ultimate links are viscous, slipping slowly under comparatively low tensions.

Enzyme action during pregnancy

A uterine collagenase? Woessner ('59) confirmed many of the findings of the Harknesses. From his data he suggested that collagen may be completely degraded within the rat uterus liberating hydroxyproline which is then removed by the blood. He found no increase in urinary hydroxyproline although there was a significant elevation in serum hydroxyproline immediately following parturition. Montfort and Pérez Tamayo ('61) confirmed the findings of the Harknesses and Woessner and showed that, although the total uterine collagen (extracted after gelatinization) increased progressively during gestation to 446% of the collagen content of intact rat uteri, the collagen content at the placental sites progressively decreased to only 9 4% of the value obtained from intact uteri.

In each of these studies the increase in uterine wet weight during pregnancy was much greater than the increase in collagen content. That is, while molecular collagen was being deposited in the expanding extracellular ground substance, other substances, probably including mucopolysaccharides, were accumulating as well. It is likely that during this same period some of the thick collagen bundles are degraded as well as dispersed. Woessner and Brewer ('60) stimulated by knowledge of the ability of the involuting uterus to effect the breakdown of the collagen molecule began an investigation of proteolytic enzymes in this organ. They described a *proteinase of the human uterus* The idea that colagen content changes may involve a composite of two processes has been expressed previously by Houck and Jacob ('61) The first process would involve the

enzymatic degradation of insoluble collagen and the second would be an attempted synthesis of new collagen to replace that being removed by this collagenase activity Evidence in support of this idea has been found in connective tissue changes in dermis where insoluble collagen decreases as a result of the inflammation which results from several forms of injury (Sethi and Houck, '61) Associated with this decrease in insoluble collagen is an increase in citrate-soluble collagen and a marked local increase in hexosamine and a non-collagenous protein. During the period of maximum collagen loss there is a significant increase in circulating hydroxyproline (Houck and Jacob '61)

The striking and rapid disruption of the coarse collagenous architecture of the uterine stroma and its microscopic change in character from collagen to reticulin provide encouragement for the concept of *enzyme action on collagen* in the pregnant uterus. The likelihood of collagenase activity in the uterus has precedent. Wislocki and Dempsey ('48) stated

> "The proteolytic activities noticed [in the uterus] have involved the product of edema, ... [and] the degradation of collagenous reticulum
>
> "The histological appearances at the margin of the trophoblastic shell of human and monkey placentas suggest that practically all of the elements of the decidua are attacked and slowly destroyed by the activity of the cytotrophoblast. In sections which have been impregnated by silver the dissolution of the reticulum fibers can be observed. Immediately adjacent to the border of the trophoblast, the fibers become broken up and the individual bits dissolve
>
> "The present observations indicate further that the metachromatic mucopolysaccharide forming the ground substance surrounding the decidual cells and reticulum fibers is also destroyed ... The multiplicity of substances seemingly dissolved by the trophoblast suggests the activity of one or several relatively powerful enzymes.

Fawcett Wislocki and Waldo ('47) wrote of cytolytic enzymes emanating from trophoblast in the early hours of nidation as the cause of edema and interstitial hemorrhages in the contiguous connective tissue In light of the above discussion it may be in order to acknowledge that reconstituted collagen has been used successfully as a tissue culture medium for several different kinds of cells both embryonic and adult (Hillis and Bang, '59; Ehrmann and Gey '56) The use of collagen as a nutritious medium and the concept of ground substance as a possible "protein storage depot" or "nitrogen depot" (Sobel Gabay Johnson and Hassan, '59) may lend support to the idea of endometrial extracellular materials as a potential source of nutriment for an implanting blastocyst.

Bassett ('59) stated, "the activated fibroblasts [of pregnancy] presumably cause breakdown of the collagen fibers possibly by secreting an enzyme. These cells may also be involved in new collagenous fibers, as argyrophilia is a well-known characteristic of developing fibers in healing wounds and tissue culture. Bartelmez ('57) pointed out that the superficial reticulum of endometrial stroma in man and in the rhesus monkey dedifferentiates and then redifferentiates during the menstrual cycle. He referred to the degeneration of reticulum as a feature of repair noting that the endometrium at the end of menstruation is characterized by fragmented reticular fibers.

The possibility of a role in parturition for such changes was suggested by Speert ('58) following a study on the uterine decidua in ectopic pregnancy He stated, "The integrity of the decidual stroma was maintained until full term or until death of the trophoblast, when dissolution of the reticulum ... and slough occurred. He suggested that these changes may initiate labor in normal intrauterine pregnancy

Myometrium

The external muscle coat extends far into the suspensory ligament of the uterus forming two arms of the metrial triangle the area through which the major placental vessels pass and in which the metrial gland develops. The outer muscle coat surrounds the whole uterus with longitudinally oriented muscle fibers. It is separated from the inner circular muscular tunic of the uterus by a vascular connective tissue layer which becomes edematous during pregnancy Further contrasts in the appearance of the two muscle tunics develop during different functional states and may lead to knowledge that the mus-

cle layers differ from one another in physiologic responses and functions.

The *circular muscle coat* displays a striking affinity for both PAS (Malbenco '60) and aniline blue near the time of parturition, in contrast with its earlier minimal affinity for these stains. The longitudinal muscle does not acquire such changes in dye affinities in any of the sections studied. It is interesting that this heightened affinity for aniline blue and PAS in the inner circular muscle occurs at a time when the adjacent endometrium displays very minimal affinity for either stain. An explanation is not at hand for the completely inverted affinities for these dyes which these adjacent muscular structures display at the time of parturition. However it may be in order to reconsider in this light, the fact that all of the reported results concerning estimations of the quantity of molecular collagen in the uterus were obtained from extractions of whole uteri in the rat and of myometrium in the human. A sizeable portion of the increase in molecular collagen in the uterus during late pregnancy may be present in the muscle. The deeply staining circular myometrium may be a reflection of an accumulation of collagenous components.

It may be of interest to mention another situation in which there is a similar interchange of stain affinity between a connective tissue and the adjacent muscle. Joseph, Engel and Catchpole ('54) demonstrated changes in connective tissue and the adjacent muscle in the intrascapular area of the rat following cortisone treatments over a period of 15 days. These changes appear to be identical to those in the rat uterus as described above.

Relaxin

The changes in the collagen fibers and in the ground substance of the uterine stroma following relaxin administration to intact rats are reminiscent of the changes which appear during pregnancy. The extracellular modifications are similar in character to the changes described earlier in stromal areas surrounding young decidua, as well as to the diffuse effects on stroma seen late in pregnancy. The looser fibrillar pattern of the fibers and the edematous infiltration of the stroma are consistent with the effects of relaxin on mesenchymal derivatives which have been reported earlier (Talmage, 47; Hall, '60). The physiology of relaxin may be concerned not merely with parturition, but also with structural changes in the endometrial stroma at the beginning of pregnancy or prior to pregnancy.

HISTOCHEMISTRY

Generally PAS stained argyrophilic fibers intensely and colagen bundles faintly. Where PAS was used the observations were in agreement with those reported by Malbenco ('60) in her discussion of the involuting rat uterus. Our studies using metachromasia unfortunately provided no significant or consistent findings in the fibrous rat endometrium. The above histochemical methods added little of significance to our knowledge of the fiber changes reported here. Attention has therefore been focused on our observations using the aniline blue and silver impregnation methods for staining fibers.

SUMMARY AND CONCLUSIONS

During pregnancy changes in connective tissue components of the uterus occur around the muscle bundles within the mesometrial triangle and between (and possibly within) the muscle layers as well as in most of the endometrium.

Collagenous fibers which are thick and dense permeate the endometrial stroma of the uterus in the virgin intact adult nonpregnant rat. Late in pregnancy many of the stromal fibers are argyrophilic and an extracellular fibrous reticulum is evident while thick fibers are much less prominent in similar microscopic sections stained with aniline blue. The argyrophilia of stromal fibers becomes widespread as the edematous dispersion of the collagen fibrils becomes marked during pregnancy.

During early decidual modification four zones may be clearly evident in the endometrial stroma:

(1) a densely cellular subepithelial area containing a mosaic pattern of large decidual cells and extracellular fibrous components which are markedly argyrophilic and consist largely of frayed and fragmented, degenerated and dissociated

collagen fibers which stain only faintly with aniline blue;

(2) an area of marked stromal edema occurring as a wave of ground substance increase in advance of he spreading decidua,

(3) a more peripheral edematous area containing poorly staining, disaggregated collagen fibrils and

(4) an area of dense collagen bundles about the basal endometrial glands forming the line of last resistance to collagen fiber dispersion.

Edematous dispersion of collagenous components of the uterus occurs in association with advancing pregnancy with relaxin treatments, and with the wave of stromal edema at the border of a decidual reaction. Thick collagenous fibers about the basal endometrial glands and adjacent to the myometrium remain relatively unchanged, while the dispersed endometrial collagen fibers nearby have lost affinity for aniline blue

Changes similar to those in the uterus about a fetal sac, but of a lesser degree occurred in interplacental and interimplantation sites and in the unilaterally non-pregnant uterus.

The edematous dispersion of endometrial colagen in rats treated with relaxin was similar to the known effects of relaxin on other connective tissues.

Endometrial collagen fibers are also compromised by long-term castration. The maintenance or laying down of thick collagen fibers may be dependent upon ovarian hormones.

During the last five days of pregnancy at the time of parturition, and during the first few days of the puerperium the endometrium is essentially free of dense collagen fibers. *At these times the circular* muscle coat is deeply stained with aniline blue and surrounds a pallid endometrium. The myometrium showed very little affinity for the aniline blue in animals which were either not pregnant or in early pregnancy The same contrast is evident when PAS staining is used

The luminal epithelium overlying decidual reactions commonly exhibited an artifact of separation and elevation from the mass of underlying decidua. This did not occur in any of the other tissues in these studies.

The decidual reaction can begin in areas of the endometrium other than the antimesometrial portion of the uterus if the decidual cell inducing stimulus is applied other than in the antimesometrial portion of the uterus.

ACKNOWLEDGMENTS

The author is deeply grateful to Professor Frederick L. Hisaw who has been inspiring and supportive since the inception of the project, to Professor Duncan E. Reid for his encouragement and guidance, to Miss Elizabeth Ann Hughes who provided valuable assistance with many phases of the work, and to Mr Leo Goodman for the photomicrography

The investigation was supported by grants from the Josiah Macy Jr Foundation and the Milton Fund at Harvard University and U.S.P.H S research grant number A-3804 to the author as well as U.S.P.H.S. grant A 2673 to Professor Hisaw

LITERATURE CITED

Allen, W M. 1931 I. Cyclic alterations of the endometrium of the rat during the normal cycle pseudopregnancy nd pregnancy II. Production of deciduomata during pregnancy Anat. Rec., 48 65–103.

Bartlemez, G. W 1957 The phases of the menstrual cycle and their interpretation in terms of the pregnancy cycle. Amer J Obstet. Gynec 74 931–955.

Bassett, E. G. 1958 Gestational changes in connective tissue in the ewe Nature, 181 196–197

——— 1959 Fibroblast cells in pregnancy Proc. U of Otago Med. School, 37 15–16.

Blandau, R. J 1949 Embryo-endometrial interrelationship in the rat and guinea pig. Anat. Rec., 104 331–359

Boucek, R. J N Noble and F Woessner 1959 The effects of tissue ge and sex upon connective tissue metabolism. Ann. N Y Acad. Sci., 72 1016–1030.

Bourne, G. H., and M. N. Golarz 1959 Human muscular dystrophy as an aberration of the connective tissue Nature, 183 1741 1743.

Boving, B G. 1959 Implantation. Ann. N Y Acad. Sci 75 700–725.

Bowes, J H R. G. Elliott and J A. Moss 1953 Some differences in the composition of collagen and extracted collagens and their relation to fibre formation and dispersion. In Nature and Structure of Collagen, J T Randall, ed. Academic Press Inc New York, pp. 199–207

Brewer J L 1938 A human embryo in the bilaminar blastodisc stage (the Edwards-Jones-Brewer ovum) Contr Embryol. Carneg. Instn., 37 85–93.

Cowdry E. V 1952 Ageing of Tissue Fluids. In: Cowdry' Problems of Ageing Biological and Medical Aspects. 3rd Edition A. I. Lansing, ed., Williams & Wilkins Co., Baltimore pp. 33–49.

Cullen, B. M., and R. D. Harkness 1959 Stimulation by distension of collagen formation in the rat' uterus. J Physiol., 148 6p–7p.

Edwards, L. C., and J E. Dunphy 1958 Wound Healing I Injury and Normal Repair N Eng. J of Med., 259 224–233.

Ehrmann, R. L., and G. O. Gey 1956 The growth of cells on transparent gel of reconstituted rat-tail collagen. J Nat. Cancer Inst., 16 1375–1404.

Enders, A. C., G. D. Buchanan and R. V Talmage 1958 Histological and histochemical observations on the armadillo uterus during the delayed and post-implantation periods. Anat. Rec., 130: 639–657

Fahmstat, T. 1960 Endocrine influences on collagen bundle deposition and maintenance in rat endometrium. In Advance Abstracts of Short Communications. First International Congress of Endocrinology ed. F Fuchs, Periodica, Copenhagen, p. 549

——— 1961 Permissive modifications of endometrial stroma. Anat. Rec., 139 227 (abstract).

Fawcett, D. W G. B. Wislocki and C. M. Waldo 1947 The development of mouse ova in the anterior chamber of the eye and in the abdominal cavity Amer. J Anat., 81 413–443.

Glynn, L. E. 1953 In Nature and Structure of Collagen. J. T Randall, ed., Academic Press, Inc., New York, p. 48.

Hall, K. 1960 Modification by relaxin of the response of the reproductive tract of mice to oestradiol and progesterone. J Endocr., 20 355–364.

Harkness, M. L. R., and R. D. Harkness 1954 The collagen content of the reproductive tract of the rat during pregnancy and lactation. J Physiol., 123 492–500.

——— 1956 The distribution of the growth of collagen in the uterus of the pregnant rat. Ibid., 132 492–501.

Herrmann, H. 1957 Protein synthesis and tissue integrity in the cornea of the developing chick embryo. Proc. nat. Acad. Sci. (Wash.) 43. 1007–1011

——— 1960 Direct metabolic interactions between animal cells. Science 132: 529–532.

Hertig, A. T and J Rock 1951 The implantation and early development of the human ovum. Amer. J Obstet. Gynec., 61A: (Suppl.) 8–14.

Hillis, W D., and F B. Bang 1959 Cultivation of embryonic and adult liver cells on a collagen substrate. Exp. Cell Res., 17 557 560.

Hisaw F L., and M. X. Zarrow 1950 The physiology of relaxin. Vitam. and Horm., 8: 151–178.

Houck, J C., and R. A. Jacob 1961 The chemistry of local dermal inflammation. J invest. Derm., 36: 451–456.

Jackson, D. S. 1957 The formation and breakdown of connective tissue. In Connective Tissue A Symposium. R. E. Tunbridge, ed., Blackwell Scientific Publications Ltd., Oxford, England, pp. 62–78.

Jackson, D S., and J P Bentley 1960 On the significance of the extractable collagens. J biophys. biochem. Cytol., 7 37–42.

Jackson, D. S., D. B. Flickinger and J E. Dunphy 1960 Biochemical studies of connective tissue repair. Ann. N Y Acad. Sci., 86 943–947

Joseph, N R., M. B. Engel and H. R. Catchpole 1954 Homeostasis of connective tissues II. Potassium sodium equilibrium. Arch. Path., 58 40–58.

Krafka, J 1941 The Torpin ovum, a presomite human embryo. Contr. Embryol. Carneg. Instn., 29 169–193.

Krichesky B. 1942 A histologic analysis of uterine growth during pregnancy in the rabbit. Anat. Rec., 82 551–564.

Kumar, D 1962 Personal Communication.

Loeven, W A. 1956 The complex binding between protein and mucopolysaccharide in connective tissue. Acta physiol. pharmacol. neerl., 5 121–146.

Ludwig, A. W., and N F Boas 1950 The effects of testosterone on the connective tissue of the comb of the cockerel. Endocrinology 146. 291–296.

Maibenco, H. G. 1960 Connective tissue changes in postpartum uterine involution in the albino rat. Anat. Rec., 136 59–72.

Masters, W H., L. E. Maze and T S. Gilpatrick 1957 Etiological approach to habitual abortion. Amer J Obstet. Gynec., 73: 1022–1032.

Montfort, L., and R. Pérez-Tamayo 1961 Studies on uterine collagen during pregnancy and puerperium. Lab. Invest., 10 1240–1258.

Neuman, R. E., and M. A. Logan 1950 The determination of hydroxyproline. J biol. Chem., 184: 299–306.

Porter K., and G. Pappas 1959 Collagen formation by fibroblasts of the chick embryo dermis. J biophys. biochem. Cytol., 5 153–166.

Robb-Smith, A. H. T 1952 The nature of reticulin. In: Transactions of the Third Conference on Connective Tissues. Josiah Macy Jr. Foundation, Charles Ragan, ed., New York, N. Y., pp. 92–116.

Robertson, W Van B., and E. C. Sanborn 1958 Hormonal effects on collagen formation in granulomas. Endocrinology 63 250–252.

Rock, J 1949 Physiology of human conception. New Engl. J Med., 240: 804–812.

Rubin, I. C., and J Novak 1956 Integrated Gynecology Vol. I., McGraw-Hill Book Co., Inc., New York, pp. 13–14.

Selye H., and T McKeown 1935 Studies on the physiology of the maternal placenta of the rat. Proc. roy Soc. B., 119 1–31.

Sethi, P., and J C. Houck 1961 Dermal collagen response to injury J invest. Derm., 37 85–86.

Smelser G. K. 1959 The importance of the epithelium in the synthesis of the sulfonated ground substance in corneal connective tissue. Trans. N Y Acad. Sci., 21 575–584.

Sobel, H., S. Gabay C. Johnson and B. Hassan 1959 Carcass nitrogen and the hexosamine-

collagen ratio of skin following starvation and cortisone administration in rats and guinea pigs. Metabolism, 5 180–184.

Speert, H. 1958 The uterine decidua in ectopic pregnancy its natural history and some biologic interpretations. Amer J Obstet. Gynec., 76: 491–514

Streeter G. L. 1926 The "Miller" ovum — the youngest normal human embryo thus far known. Contr Embryol. Carneg. Instn., 18 31–48.

Talmage, R. V 1947 A histological study of the effects of relaxin on the symphysis pubis of the guinea pig. J Exp. Zool., 106 281–297

Velardo J T A. B. Dawson, A. G. Olsen and F L. Hisaw 1953 Sequence of histological changes in the uterus and vagina of the rat during prolongation of pseudopregnancy associated with the presence of deciduomata. Amer. J Anat., 93 273–305.

White, B N M. R. Shetlar and J A. Schilling 1961 The glycoproteins and their relationship to the healing of wounds. Ann. N Y Acad. Sci., 94 297–307

Wislocki, G. B., and E. W Dempsey 1946 The chemical histology of the human placenta and decidua with reference of mucopolysaccharides, glycogen, lipids, and acid phosphatase. Amer. J Anat., 83 1–42.

Woessner J F 1959 Colagen degradation in involuting uterus. Fed. Proc., 18 461

Woessner J F., and T H. Brewer 1960 Proteinase of human uterus. Fed. Proc., 19 335.

Wolbach, S., and P R. Howe 1926 Intercellular substances in experimental scorbutus. Arch. Path. Lab. Med., 1 1–24

Wolfe, J M., and A. W Wright 1942 The fibrous connective tissue of the artificially induced maternal placenta in the rat with particular reference to the relationship between reticulum and collagen. Amer J Path., 18: 431–461

PLATES

PLATE 1

EXPLANATION OF FIGURES

Transverse sections of rat uteri in various reproductive states. Aniline blue stain. A red optical filter was used in photomicrography

1 Uterus in late estrus. The vasculature between the muscle layers is prominent. The endometrial stroma is still slightly edematous owing to fluid retention during the proestrous and midestrous phases of the cycle. Collagen bundles are evident throughout the endometrial stroma, between muscle coats and around the muscle bundles. The tall pseudostratified columnar epithelium of the uterine lumen, with abundant, large intracellular secretion vacuoles, is characteristic of the late estrous phase of the cycle. × 29

2 Uterus in late diestrus (pproximately three days later than in fig. 1) The luminal epithelium is simple low columnar without evidence of intracellular secretion vacuoles. The vasculature is no longer as prominent, and the estrous wave of stromal edema has subsided. Dense collagenous bundles permeate the entire endometrial stroma. They are scarcest in the subepithelial portion of the antimesometrial zone. The mesometrial triangle is bounded below by circular muscle fibers and on either side by longitudinal m scle fibers of the myometrium. × 29

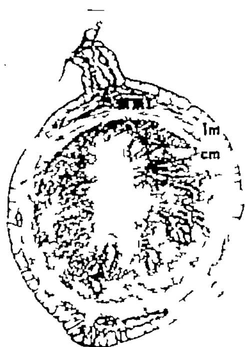
3 Uterus on the sixth day following conception (approximately 36 hours following implantation) The decidua already occupies most of the endometrium in this section. As the decidua grows, the diameter of the uterine lumen and the collagenous stroma are compromised. The collagenous stroma has not disappeared from the areas about the basal glands and adjacent to the circular muscle coat of the myometrium. Note the marked edematous dispersion of the collagenous components of the mesometrial triangle and the accompanying swelling of the triangular space. A metrial gland was destined to develop in this area within one or two days. × 18.

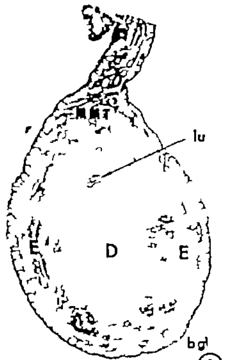
4 Uterus of rat castrated six months before utopsy Densely collagenous connective tissue is maintained in the suspensory ligament of the uterus, in the perimyometrial connective tissue of the peritoneum, and between the circular and longitudinal muscle coats of the myometrium. The endometrial collagen bundles are ill-defined and show little affinity for aniline blue. The endometrium is markedly reduced in thickness and ppears more involuted than any of the other tissues of the uterus. A striking result of long-term castration is manifested as extracellular hanges within the endometrium. × 54

Abbreviations

bgl, basal gland in endometri m
bv blood vessel
cm, circular muscle of myometrium
D decidual reaction
E, endometrial stroma
lig, uspensory ligament of utero
lm longitudinal muscle of myometrium
lu, lumen of uterus
MMT mesometrial triangle


1


lm
cm
2


MMT
lu
E
D
E
bgl
3

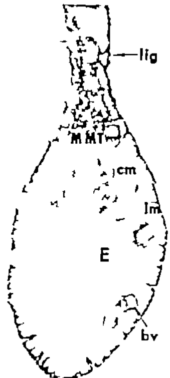

lig
MMT
cm
lm
E
bv
4

PLATE 1

EXPLANATION OF FIGURES

Transverse sections of rat uteri in various reproductive states. Aniline blue stain. A red optical filter was used in photomicrography

1 Uterus in late estrus. The vasculature between the muscle layers is prominent. The endometrial stroma is still slightly edematous owing to fluid retention during the proestrous and midestrous phases of the cycle. Collagen bundles are evident throughout the endometrial stroma, between muscle coats and around the muscle bundles. The tall pseudostratified columnar epithelium of the uterine lumen, with abundant, large intracellular secretion vacuoles, is characteristic of the late estrous phase of the cycle. × 29

2 Uterus in late diestrus (approximately three days later than in fig. 1) The luminal epithelium is simple low columnar without evidence of intracellular secretion vacuoles. The vasculature is no longer as prominent, and the estrous wave of stromal edema has subsided. Dense collagenous bundles permeate the entire endometrial stroma. They are scarcest in the subepithelial portion of the antimesometrial zone. The mesometrial triangle is bounded below by circular muscle fibers and on either side by longitudinal muscle fibers of the myometrium. × 29.

3 Uterus on the sixth day following conception (approximately 36 hours following implantation) The decidua already occupies most of the endometrium in this section. As the decidua grows, the diameter of the uterine lumen and the collagenous stroma are compromised. The collagenous stroma has not disappeared from the areas about the basal glands and adjacent to the circular muscle coat of the myometrium. Note the marked edematous dispersion of the collagenous components of the mesometrial triangle and the accompanying swelling of the triangular space. A metrial gland was destined to develop in this area within one or two days. × 18.

4 Uterus of rat castrated six months before autopsy. Densely collagenous connective tissue is maintained in the suspensory ligament of the uterus, in the perimyometrial connective tissue of the peritoneum, and between the circular and longitudinal muscle coats of the myometrium. The endometrial collagen bundles are ill-defined and show little affinity for aniline blue. The endometrium is markedly reduced in thickness and ppears more involuted than any of the other tissues of the uterus. A striking result of long-term castration is manifested as extracellular changes within the endometrium. × 64

Abbreviations

bgl, basal gland in endometrium
bv blood vessel
cm, circular muscle of myometrium
D decidual reaction
E, endometrial stroma
lig suspensory ligament of uterus
lm longitudinal muscle of myometrium
lu, lumen of uterus
MMT mesometrial triangle


E
lu
op
D
5


S
D
lu
E
amm
6


1
2
3


S
ed

PLATE 2

EXPLANATION OF FIGURES

Surgically induced decidual reactions in pseudopregnant rat uteri.

5 Transverse section through the peripheral portion of a 72-hour de ciduoma. Note the mosaic pattern within the deciduoma as result of the large, hypertrophied stromal cells and minimal visible extracellular space. The marked vascularity associated with the decidual transformation is evident. In contrast to decidual tissue, the non-decidual endometrium contains small stromal cells resembling fibrocytes, surrounded by abundant extracellular material. Also, note the wave of stromal edema t the border of the deciduoma, in advance of the spreading decidual reaction. The luminal epithelium adjacent t the unmodified endometrium is columnar whereas the epithelium adjacent to the decidual tissue ranges from low cuboidal to squamous. Biebrich scarlet-acid fuchsin stain. × 37

6 Transverse section through a uterus 48 hours after the insertion of a surgical suture on the fifth day of pseudopregnancy The 6–0 silk suture was passed through the mesometrial portion of the endometrium, the portion away from the normal site of blastocyst implantation. The decidual reaction present evidently began adjacent to the silk suture whereas the antimesometrial portion of the endometrium had not undergone decidual modification. Weigert's iron hematoxylin-Van Gieson stain. × 49

7 Transverse section through a uterus 24 hours after the insertion of surgical suture on the fifth day of pseudopregnancy As in figure 6, the 6–0 silk suture was passed through the mesometrial portion of the terus. Twenty-four hours later four zones are clearly evident in the stroma

(1) subepithelial mosaic pattern of large decid al cells;

(2) area of marked stromal edema as a wave of ground substance increase in advance of the spreading decidual reaction;

(3) more peripheral edematous area of poorly staining, disaggregated collagen fibers; and

(4) an are of dense collagen bundles bout the basal endometrial glands.

Silk suture fragments nd associated polymorphonuclea ggregates a be seen in the lumen f the uterus. Masson s trichrome stain. 49

8 Transverse section through the uterus eight hours after insertion of silk suture Fragments of silk and clumps of leukocytes are present where the suture w left in place Marked stromal edema is evident on the same ide of the teru the uture There is marked compression f the tissue around the suture Masson trichrome stain. 77

Abbreviations

amm antimesometrial rea
bv blood essel
D decidual reaction
E endometrial troma
ed, stromal edema
l uterine lumen
l ep epithelial lining of uterine l men
S p th of 6–0 surgical silk suture


E
lu
op
D
5
S
D
lu
l
a m m
6
1
2
3
7
S
ad

PLATE 3

EXPLAN TION OF FIGURES

The photomicrograph are of transverse sections through both teri of *100-day-old rat in the eighth day of pseudopregnancy. Five days after* cervical stimulation to induce pseudopregnancy burred needle was introduced into the lumen of the right uterus and the endometrium was scratched from cervix to tubal junction. Figure 9 is from the untraumat ized pseudopregnant control, the left uterus. Figures 10 11 and 12 are from sections through the three day old decidual reaction in the right uterus.

9 Transverse section of control uterus. Note the densely collagenous endometrial stroma, the argyrophilic basement membrane and subjacent reticulum and the height of the luminal epithelium. Compare these findings with those of the decid al reaction in the rat other uterus as shown in figures 10 11 and 12. Wilder' reticulin stain and "light green stain × 179

10 Transverse section through 72-hour decidual reaction in the traumatized pseudopregnant terus. The weight of this uterus wa 810 mg while the control uterus (fig 9) weighed 106 mg. The only col lagen bundles remaining intact are those in the endometrium adjacent to the circular muscle coat of the myometrium and around the basal glands. Compare with figures 9 and 2. Aniline blue stain. A red optical filter w used in photomicrography × 46.

11 Section through the same decidual reaction as in figure 10. The argyrophilic fragments of the dissociated, frayed pieces of collagen bundles are dispersed among the mosaic of decid al cells which can be seen only as sh dows. This "reticulin (by virtue of its staining haracteristics) does not form reticulum (an argyrophilic, fibrous, interlacing network) Compare with figure 9 Wilder reticulin stain. × 179

12 Transverse section through the same 72 hour decidual reaction in figures 10 and 11 The luminal epithelium overlying these decidu l reactions, which was reduced to about one-twentieth of the height of the epithelium in the control terus, commonly exhibited the artifact shown here e., separation and elevation from the mass of underlyi g decid a. The bulk of the section is decid without dense collagen bundles Compare with figure 9 Aniline bl stain. A red optical filter was used in photomicrography × 46.

Abbreviation

cm circular m scle of myometri m
D decidual reaction
E, endometrial stroma
lu ep epithelial lining of uterine lumen


lu ep
9
D
10
11
lu ep
D

PLATE 4

EXPLANATION O FIGURES

13 Sagittal section of rat terus eight days after conception. The relatively unchanged endometrium, which is composed f densely collagenou strom is from an interimplantation area. An area of decid indistinguishable from the decid al mass on the left, wa present t the right of the collagenous endometrium. The transition is rather sharp from the area of essentially intact collagenous endometrium of the interimplantation area to the area occupied by deidua. Aniline blue tain. A red optical filter was used in photomicrography × 38

14 Oblique section of uterus from rat, T 24 treated with 450 g p of relaxin daily from the fourth to the seventh day of pseudopregnancy and autopsied on the seventh day Note the marked stromal edema which is especially evident in the antimesometrial and periluminal endometrium. This stromal edema appears similar to (i) that wave of edema in collagenous stroma which occurs in advance of decidual modification (compare with fig. 7) and (ii) the edematou stroma of the non-decidual endometrium late in pregnancy (see fig. 19 through 23) Aniline blue tain. A red optical filter was sed in photomicrography × 38.

Abbreviations

amm, antimesometrial area
D decidual reaction
E, endometrial stroma
g p u., guinea pig unit of relaxin

D

E

13

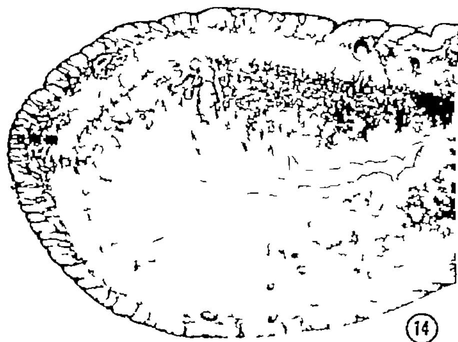


PLATE 5

EXPLAN TION OF FIGURES

Transverse sections from uteri of rats which were given 250 g.p.u. of relaxin daily for eight days. Aniline blue stain. A red optical filter was used in photomicrography

15 An edematous dispersion of collagen is most marked in area closest to the terine lumen and least marked in areas adjacent to the basal glands of the endometrium. Some myometrium can be seen in the lower right corner At the bottom of the photomicrograph are large collagen bundles which can be followed for long distances but are poorly stained in comparison t the periglandular bundles. Gradations from areas of completely dispersed collagen to areas of deeply staining collagen bundles can be seen within limited area in the center of the photograph. Compare with figures 7 13, and 17 through 23 Rat T 91 × 144

16 The integrity f the collagen bundles around the endometrial glands is retained in contrast to the varying degrees of collagen bundle dispersion in other areas of the section. The dispersion appears greater t increased distances from the endometrial glands. Compare with figures 7 13 and 17 through 23. Rat T 92. × 144.

Abbreviations

gl, endometrial gland
g p.u., guinea pig units of relaxin
lu, uterine lumen


lu
bl
15
16

PLATE 6

EXPLANATION OF FIGURES

Transverse sections from uteri of rats which have been treated with relaxin. Aniline blue stain. A red optical filter was used during the photomicrography

17 Dense collagenous bundles are evident in the lower left quadrant of the photomicrograph deep in the endometrium and immediately djacent to the endomyometrial juncture as well as in areas around the endometrial glands. The areas of greatest stromal edema and lowest collagen bundle concentration occur farthest from both the endometrial glands and the myometrium. Numerous dilated blood vessels can be seen in this photomicrograph in the areas of lowest dense collagen bundle concentration. Rat T 28. × 134

18 Note the edematous dispersion of the collagen bundles. It is more widespread but less marked than in the previous three figures. Again in this section, the lea t dispersion can be seen in areas losest to the myometrium or the endometrial glands. Rat T 90. × 134

Abbreviations

cm, circular m scle   gl endometri l gland

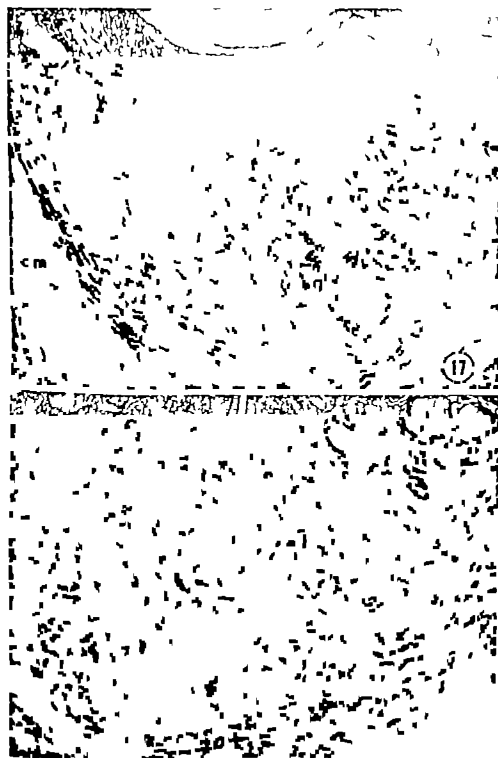

cm
17

PLATE 7

EXPLAN TION F FIGURES

Transverse sections from uteri of pregnant rats. Aniline blue stain. A red optical filter was used during the photomicrography

19 Uterus at day nine of pregnancy Note the two distinct types of rat decid the mosaic pattern of large decidual cells with homogeneous basophilic cytoplasm in the patch to the right of the letter "D" in the antimesometrial portion of the uterus; and the smaller vacuolized decidual calls to the left of the "D" on the mesometrial side. The marked vascularity is evident. In the endometrium there are dense collagen bundles contiguous with the myometrium and around the basal glands. Edematous stroma separates the dense bundles from the decidua. × 25.

20 Uterus at day 12 of pregnancy Note the periglandular dense collagen bundles, the mosaic of decidua, and the edematous stroma between the two Little dense collagen remains in the small amount of endometrium found t this stag f pregnancy × 80.

Abbreviations

cm, circular muscle of myometrium
D decidual reaction
E, endometrial stroma
ed, stromal edema
gl, endometrial gland
lm longitudinal muscle of myometrium

lm
cm
ed
D
E
C
19

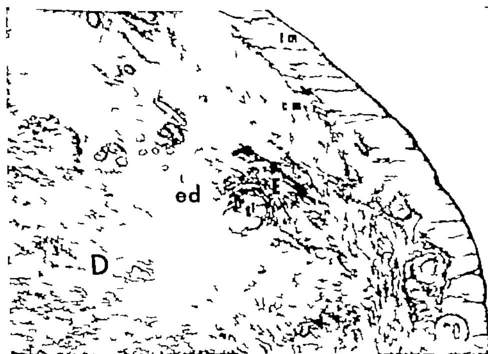


PLATE 8

EXPLANATION OF FIGURES

Photomicrographs of sections from uteri of rats late in pregnancy At the time of autopsy five days or les would have elapsed until parturition. Aniline blue stain. A red optical filter was used during the photomicrog raphy × 67

21 Non-decidual portion of endometrium on day 18 of pregnancy The stroma is markedly edematous. No coll gen bundles were seen in this section. *Faintly staining dispersed collagen fibers can be detected* throughout the non-decidual stroma. The myometrium is visible t the bottom of the picture.

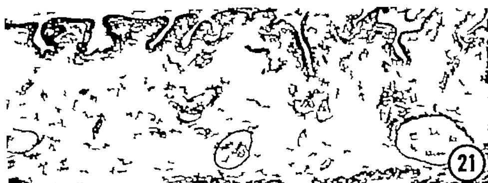
22 D y 20 of pregnancy The endometrial collagen bundles are even less pronounced than at day 18 The myometrium, as in figure 21 stains much more intensely with aniline blue than in all of the sec tions shown previously A portion of the placenta can be seen in the center of the top of the photomicrograph.

23 Day 22 of pregnancy The only dense collagen bundles which can be seen t this stage of pregnancy are the few adjacent t the endometrial gland in the lower right corner Large dilated blood vessel are visible. The myometrium as in figure 21 and 22, stained intensely with aniline blue whereas the myometrium of non-pregnant animals and of animals in early pregnancy stained only lightly with aniline blue

Abbreviations

cm circular muscle of myometrium

gl endometrial gland


21


cm
22



PLATE 9

EXPLAN TION OF FIGURES

Photomicrographs from transverse sections of rat uteri in the very early post-partum period. In figures 24 25 and 26 the aniline blue stain wa sed. I figure 27 the green red" stain was used. Photomicrography w done through red optical filter

24 Section from terus t 24 hours following parturition. At this time the endometrium is essentially free of collagen bundles. It i also completely re-epithelialized. The stromal cells are large and resemble fibroblasts in shape while the endometrium as whole is reminiscent of the embryonic state. Some myometrium can be seen t the bottom of the photograph. × 230.

25 Uteru at three days following parturition. Litter of 14 suckled dur ing the post-partum period. The endometrium is still essentially collagen bundle-free structure. The myometrium is losing the remark ble bility t stain deeply with aniline blue which it possessed during the final week of pregnancy Compare with figures 22 and 23. × 230.

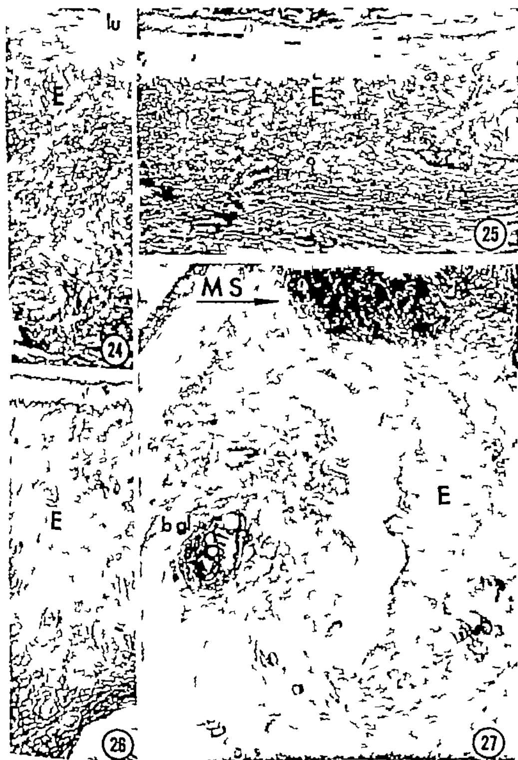
26 Uteru t five days following parturition. Litter of 14 suckled during the post-partum period. The stroma is still essentially free of dense collagen bundles. × 230.

27 Uterus t three days following parturition. Litter of 14 suckled during the post-partum period The endometrium is largely col lagen bundle-free structure. The dense fibers around a few basal gland had not disappeared during the pregnancy and are the exceptions when contrasted with the rest of the endometrium which is essentially void of collagen bundles.

The metrial scar which forms in association with the degeneration of the metrial gland during the terminal days of pregnancy is densely collagenous and stains deeply with aniline blue It is also through this area of fibrous healing, which develops in the icinity of the normal secondary implantation site, that the enlarged blood essels of pregnancy pass from maternal source to the fetal recipient. 82

Abbreviations

b gl basal gland in endometrium
E, endometrial troma
lu, uterine lumen
MS, metrial sca


lu
E
E
25
MS
24
E
E
ba
26
27

Extracellular Studies of Uterus

II. REGENERATION OF COLLAGEN BUNDLES IN UTERINE STROMA AFTER PARTURITION

THEODORE FAINSTAT

Department of Obstetrics and Gynecology of Harvard Medical School, and The Biological Laboratories of Harvard University

The focus of orientation in this series of investigations is on the endometrium as essentially a hormone-sensitive mesenchyme derivative. In the intact adult virgin rat the endometrium may be referred to as a densely collagenous connective tissue which is associated with the epithelium of the uterine lumen and glands on the one hand and the myometrium on the other. This collagenous stroma is the dominant component of the uterus in microscopic sections stained with aniline blue. The dramatic changes which it undergoes in various reproductive states and under certain endocrine influences as well as the significance of these changes with regard to various reproductive phenomena, form the subject matter of prior reports (Fainstat, '60 '61 '62) and of others to follow from this laboratory. The investigations aim to throw light on the dynamics of connective tissue fibers in the reproductive tract, and also to utilize the reproductive tract as an effective system for the study of connective tissues. The possibilities that some extracellular changes in the uterus may be vitally concerned with ovo-implantation, accommodation of the uterus to expanding intrauterine contents parturition and menstruation have been implied. In the previous reports it was shown that the thick and dense collagen fibers, which permeate the endometrial stroma of the adult non-pregnant rat and serve as an important supporting framework for endometrium are compromised by long term castration. It was therefore suggested that the maintenance or laying down of thick collagen fibers may be dependent upon ovarian hormones. In rats castrated six months prior to autopsy all components of the uteri had atrophied, but to varying degrees the endometrium having involuted the most. It was shown that the endometrium after six months of castration was about one-sixth as thick as the endometrium during late estrus, while the myometrium had shrunk only to one-half its previous thickness. In cross sections the tissues closest to the lumen had involuted the most. The circular muscle coat was proportionately more involuted than the longitudinal muscle layer when these layers were compared with the myometrium of intact rats. Well-formed collagen bundles which stained deeply with aniline blue persisted in the suspensory ligament of the involuted uterus and in the connective tissue surrounding the blood vessels which course between the muscle coats. The stroma of the castrated rats lacked the abundant, deeply stained, discrete collagen bundles which characterize the stroma of intact rats.

It was shown that during pregnancy changes in connective tissue components of the uterus occur around the muscle bundles and between (and possibly within) the muscle layers as well as in most of the endometrium. During the last five days of pregnancy at the time of parturition, and during the first few days of the puerperium, the endometrium was essentially free of dense collagen fibers. At these times the circular muscle coat deeply stained with aniline blue, surrounded a pallid endometrium, in contrast with specimens from animals which were not preg

Josiah Macy, Jr. Foundation Fellow in the Department of Obstetrics and Gynecology Harvard Medical School.

Present address Boston Lying-in Hospital, 221 Longwood Avenue, Boston 15, Massachusetts.

Presented in part at the First International Congress of Endocrinology Copenhagen, July 1960.

nant or were in early pregnancy in which the myometrium showed very little affinity for the aniline blue. The same contrast was evident when PAS staining was used. *The stroma about the basal endometrial* glands tended to retain structural integrity of the dense collagen bundles while most of the endometrial stroma nearby lost its affinity for aniline blue.

From the time of implantation until the time of parturition there was a progressive accumulation of ground substance in the stroma, an increasing disaggregation and dispersion of the collagen bundles, and a decreasing stromal affinity for aniline blue. Late in pregnancy many of the stromal fibers were argyrophilic and a fibrous reticulum was evident, while thick fibers were much less prominent in similar microscopic sections stained with aniline blue The argyrophilia of stromal fibers became widespread as the edematous dispersion of the collagen fibrils during pregnancy became marked. It was pointed out that collagen fibers exist as helices which are interwoven throughout the stroma and contain many intertwined helically coiled ...ls closely applied to one another This is in contrast to the older two-dimensional concept that collagen fibers consist of wavy bands or bundles of closely packed wavy fibrils arranged in parallel.

The endometrium at the time of parturition was virtually void of thick collagen bundles and for more than a week thereafter the endometrium was still essentially free of coarse collagen bundles. The stromal cells were large and the endometrium appeared reminiscent of embryonic connective tissues or areas of wound healing. The rat uterine stroma at term essentially depleted of collagen bundles served as the starting point for studies of collagen bundle regeneration. The previously observed compromising effects of long-term castration on the rat uterine stroma led to the use of post-parturient castrated females as controls in a study of collagen bundle regeneration under the influence of the ovaries.

MATERIALS AND METHODS

Ninety healthy virgin female albino rats of the Harvard Wistar stock were used in this study Each rat entered the experiment at 95 to 105 days of age weighing 210 to 270 gm. Throughout the experiments the animals were fed Purina Rat Chow and tap water *ad libitum*

Each *female was mated* and near the end of an apparently normal pregnancy was placed in a separate cage. Each litter was removed from the mother immediately following parturition and the mother was placed at random into one of two groups at this time. The rats of one group were left intact. Estrous cycles resumed in such females within eight hours after delivery as would be expected. Each female of the second group was castrated within nine hours following delivery Castrations were done through dorsolateral incisions under ether anesthesia.

On 1 2, 3 4 5 7 10 14 21 28 35 42, 50 and 60 days post partum uteri were obtained for study from three animals of each group The animals were killed instantaneously by a swift blow to the head. The uteri were fixed at the time of autopsy immediately following the death of the animal. The specimens discussed in detail in this report were fixed in Bouin s solution embedded in paraffin and sectioned to a thickness of 6 μ. Where it was desirable to emphasize the collagenous components of the tissue, while rendering the cellular components recognizable but not striking staining by the following method gave the most satisfactory results. After being deparaffinized and rinsed in distilled water each slide was place in a 2% solution of phosphomolybdic acid for one minute washed in distilled water for one minute and then stained for 30 minutes in an oven at 60 C in a preheated solution containing 2 gm each of aniline blue, orange G and phosphomolybdic acid in 100 cm of distilled water The slide was then washed in water placed into the phosphomolybdic acid for 30 seconds, and then washed again

Other techniques utilized were the classical Weigert s iron hematoxylin stain, Van Gieson s connective tissue stain Masson s trichrome stain utilizing *aniline blue*. and Wilder's reticulin stain. Also some tissues were fresh frozen or freeze-dried and then stained with toluidine blue for metachromasia or with PAS by the Hotchkiss-McManus method

RESULTS

Intact animals

The course of the regeneration of collagen bundles in the endometrial stroma was readily followed in the uteri of mothers which were left intact and isolated from their litters following parturition. In the absence of the suckling stimulus their estrous cycles as determined by vaginal smears, were immediately resumed and persisted with normal regularity until autopsy The endometrial stroma shortly after parturition was pallid in all cases (figs. 1 2 and 3) Except for collagen bundles in periglandular areas which had remained essentially unchanged during pregnancy (see figs. 2 and 3) the first sign of deeply staining extracellular materials in the stroma of sections stained with aniline blue occurred shortly after the second post-partum estrus, on the seventh day following parturition (fig. 4) However at this time these deeply staining materials were not organized into well-developed, multifibrillated fibers. Such fibers became clearly apparent 28 days following parturition (fig. 8)

With the further passage of time the endometrium became increasingly thick and densely fibrous. Meanwhile the constituent fibers also became thicker and more dense (figs. 9 10 and 11) The thinnest fibers were near the luminal epithelium in all sections while there was a clear-cut tendency for the thickest fibers to be furthest from the lumen, i.e., near the myometrium. A reticulated pattern of young collagenous fibers (fig 7) as well as of older thick bundles (fig 11) was apparent. Branching and anastomosing between neighboring bundles were commonly seen. Anastomoses by groups of fibrils common to the neighboring bundles, but along different portions of their length contributed to the reticulated pattern of the stromal collagen fibers in all of the specimens of this series.

When the sections were impregnated with silver salts a dark network of thin fibers became apparent in the stroma earlier in the series than when the sections were stained with aniline blue. Such a fibrous reticulum was evident subepithelially at five days post partum. At this time this reticulum was fairly prominent for a depth of about two stromal cells but was only faintly stained throughout the rest of the stroma. At seven days this reticulum was prominent throughout the stroma. Fine multifibrillations could be seen in the deeper fibers at ten days in the silver-stained sections. Where animals were autopsied and the uteri fixed while manifesting peak estrous effects i.e., the uteri were markedly ballooned, an increase in prominent argyrophilic fibers was also present, especially in the stroma immediately adjacent to the epithelium. In sections of uteri from later stages in this series the fibers were thicker and much more readily visualized when stained with aniline blue.

In none of the sections studied was there a clear-cut, continuous uniform basement membrane under the luminal epithelium. Immediately following parturition there was no evidence of fibers subjacent to the luminal epithelium. With the passage of time fibers appeared adjacent to this epithelium however they were discontinuous fragmented and irregular in thickness. At all stages a perfectly continuous basement membrane was absent. Instead there was an irregular agglomeration of fragmented fibers under the epithelium, with varying degrees of packing, resulting in a patchy and discontinuous "basement membrane. At best, this basement membrane tended to become more uniform as the stroma in general became more fibrous.

When the sections were treated with PAS the resulting pattern of the intensity of staining of the fibers was in each case the same as when Wilder's reticulin method was used. The studies using toluidine blue as a meas of identifying extracellular metachromasia were consistently unrewarding.

Myometrium

Whereas the endometrium was pallid at the time of parturition the circular muscle of the myometrium was deeply stained with aniline blue as well as by the silver impregnation technique. Regardless of the treatment of the animal prior to autopsy the deep staining of this muscle in most

cases remained prominent for about 36 hours following parturition at which time its affinity for the aniline blue began to wane. By 72 hours following parturition the circular muscle had become paler in many cases. It was pallid in all cases at five or more days following parturition In contrast, the outer longitudinal muscle did not undergo striking changes in stain affinity during pregnancy parturition, or the early post-partum period Similar findings were obtained when such sections were treated with PAS (Malbenco '60)

Castrated animals

In contrast with the progressive accumulation of thick multifibrillated collagen bundles which occurred in the stroma of intact rats the stroma of rats castrated following parturition did not undergo such a regeneration of collagen bundles (figs. 12–19) In this series as the uterus involuted the endometrium gradually shrank. A considerable amount of extracellular and intracellular water appeared to have been lost causing a condensation and compactness of the remaining extracellular and cellular components. Deeply staining poorly defined extracellular fibrous materials did appear in the endometrium in the sections stained with aniline blue (see especially fig. 18) However they were unlike the clearly defined large, multi fibrillated bundles described earlier

Some deeply staining extracellular materials as well as the markedly edematous ground substance could be seen in some portions of the stroma shortly following delivery (figs. 12 and 13) At 14 days following castration a well formed reticulum composed of fibers of relatively uniform thickness was present throughout the stroma in sections impregnated with silver At the same time the subepithelial reticulum was agglomerated into what appeared to be a thick basement membrane. Later the condensed extracellular materials continued to be argyrophilic but were irregular in thickness discontinuous and apparently not organized into either a reticulum or thick collagen bundles

DISCUSSION

The findings support the idea that the endometrial stroma is a specially evolved connective tissue with an unusual capacity to respond to the ovaries. The stromal extracellular components can be implicated as an important target or locus of ovarian activity In the absence of the ovaries the coarse multifibrillated collagen bundles were not regenerated in the endometrium following parturition In contrast, when the ovaries were left intact the estrous cycles were resumed immediately following parturition, and consequently regeneration of the stromal fibers resulted.

In '35 Selye and McKeown noted that a considerable amount of ground substance is lost from the rat endometrium during the few days immediately following parturition. This loss is an integral part of the early reorganization and involution of the uterus post partum. After three or four weeks the uterus is similar to that in the adult virgin rat in which thick collagen bundles permeate the endometrial stroma. The loss of ground substance from the endometrium is only one of a number of striking happenings during the early post partum period. As some of the ground substance is being lost from the endometrium a fibrous reticulum appears throughout the stroma and thickens. In time a densely collagenous endometrium exists. In addition, while ground substance components are being lost from the endometrium the myometrium displays a dramatic loss in affinity for aniline blue and PAS For two or three days following parturition the changes in the various tissue components in the uterus represent a remarkable recovery from the condition of the uterus at the end of pregnancy During this period the various tissue layers of the uterus essentially recover the shape and size they possessed prior to pregnancy large shifts occur in the extracellular components which accumulated during the pregnancy, the cells of the endometrial stroma and the myometrium appear to reorganize so that each tissue appears more densely cellular and reepithelialization in the denuded areas of the luminal epithelium is completed Once the pre-pregnant size and configuration of the uterus have been regained the endometrial stroma gradually changes in a manner similar to the

changes in connective tissues during the repair of wounds.

In this light it is of interest to cite Bartelmez's ('57) interpretation of the degeneration of reticulum in the superficial portion of the endometrium in the *Rhesus* monkey as a feature of *repair*. He noted that the endometrium at the end of menstruation is characterized by fragmented reticular fibers, disappearance of ground substance and an increase in the concentration of stromal cells. Later the stroma becomes reorganized and a well-defined fibrous reticulum appears. There seem to be parallel changes in the endometrium of the rat post partum and in the post menstrual endometrium in monkeys.

It is likely that during very active growth in a connective tissue new coarse bundles of collagen do not become apparent. However when a tissue stops growing rapidly the dispersed molecules and fibrils of collagen become reconstituted into coarse bundles. These phenomena become manifest in the connective tissue elements of the uterus as it grows during pregnancy and involutes post partum, as well as in the site of a wound where a rapid increase in the tissue mass occurs at first and is followed by a reduction in the tissue mass accompanied by the appearance of new collagen bundles in the healing site. In the rat it seems that the connective tissue of the uterus responds to the state of pregnancy as though it were wounded or subjected to persisting traumatic stimuli and only later *heals* completely providing ovarian function is unimpaired during the puerperium.

However in the absence of ovarian function, such as in the series of castrated mothers described in this report, a failure in the regeneration of the richly collagenous connective tissue stroma of the endometrium results. Following the initial rapid loss of most of the stromal edema acquired during pregnancy the uteri of such rats underwent gradual and continuous further shrinkage, which resulted in the appearance of a compact cellular stroma. Both cellular and extracellular compartments of the stroma were visibly condensed, the non-cellular compartment even more so than the cellular. There appeared to be a reciprocal relationship between the quantity of stromal extracellular fluid" and the staining of some extracellular materials. An argyrophilic reticulum appeared in the stroma in association with the shrinkage. After further condensation of stromal components some of the reticular fibers became thickened somewhat, but in no case did thick multifibrillated bundles appear in the endometrial stroma of a castrated rat. Such thick multifibrillated bundles appeared with regularity in all of the animals with normal ovarian function. It has become obvious that the ovaries function in part as highly potent growth promoters of extracellular constituents and thus may in turn influence some of the many metabolic functions attributed to extracellular materials.

The results of experiments involving the extraction and quantifying of molecular collagen from the uterus during pregnancy and the puerperium (Harkness and Harkness '54, '56 Woessner '59 Montfort and Pérez Tamayo '61) may be seen in better perspective in view of recent findings. In this light, respect should be paid to the reversed affinities for aniline blue and PAS present in both the endometrium and the myometrium at the end of pregnancy and for 36 to 72 hours post partum, and for the likelihood of increased collagenase activity (Woessner '59) or other proteinase activity (Woessner and Brewer '60) in the uterus at least in the early portion of the puerperium.

In view of the microscopic findings it is likely that many of the newly acquired collagen molecules in the uterus as measured biochemically near the time of parturition, may have accumulated in the myometrium, and that the deeply staining circular muscle may be a reflection of an accumulation of collagenous components. It should be kept in mind that in each of the reported biochemcial determinations of the quantity of collagen in the uterus no separation of endometrium from myometrium was made. Instead, the reported changes in quantity reflect changes in the uterus as a whole or in segments of the uterus. The separate contributions to the data by the endometrium and the myometrium are not yet known. In addition in the studies reported the uteri were gelat

Abbreviations

E, epithelium of the uterine lumen
S endometrial stroma
M, myometrium
bv blood vessel
gl, endometrial gland

PLATE 1

EXPLANATION OF FIGURES

A series of photomicrographs from transverse sections of adult rat uteri. Aniline blue stain. Litters removed from their mothers on day of birth. × 170.

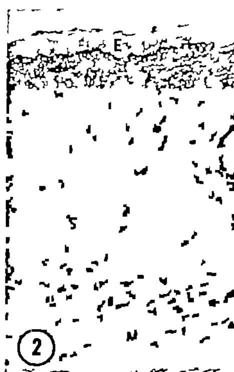
1 Twenty-four hours following parturition. There is no evidence of thick collagen fibers in the endometrium in this section. The stroma is thin and pallid. The fibroblast-like stromal cells are not oriented in any specific direction in this early stage of the reorganization of the organ. There is no evidence of even an attenuated basement membrane under the luminal epithelium. Deep in the endometrium adjacent to the circular muscle tunic are some deeply staining fibers. A considerable quantity of deeply staining material is also present in association with the extracellular fibers about the myometrial cells in the lower third of the photomicrograph. The stroma is almost entirely covered by epithelium which is either stratified or pseudostratified at irregular intervals along its length. The orientation of the epithelial cells is not consistently vertical to the underlying stroma.

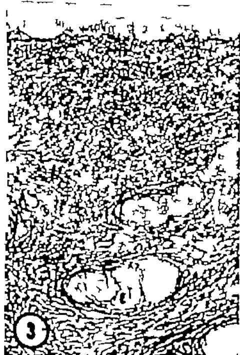
2 Forty-eight hours following parturition. In this section the only evidence of thick collagen fibers in the endometrium is found adjacent to the base of endometrial glands. These fibers had remained largely intact throughout the pregnancy The stroma is wider than in figure 1 and pallid. There is still little evidence of a specific orientation of the fibroblast-like cells in the abundant ground substance. The tissue is reminiscent of early embryonic stroma. The "basement membrane" under the epithelium is still incomplete, but is more apparent than in the previous section. The absence of deeply staining material in the circular muscle in the lower quarter of the photomicrograph is uncommon for this stage. The epithelium is pseudostratified. The orientation of the epithelial cells is now vertical to the underlying stroma.

3 Five days following parturition. The stroma is still generally pallid. It has become wider as puerperal reorganization as occurred in all the uterine tissues. Some deeply staining fibers adjacent to the deeper portions of the endometrial glands are again present. No myometrium is included in this photomicrograph.

4 Seven days following parturition and 18 hours following the second post partum estrus. The stroma is densely cellular and the stromal cells are larger than in previous sections. Deeply staining extracellular materials are widespread in the stroma for the first time in this series. No myometrium is present in this photomicrograph.


1


E
2


3


4

PLATE 2

EXPLANATION OF FIGURES

Photomicrographs from transverse sections of adult rat uteri. Aniline blue stain. Litters removed from their mothers on day of birth. × 170.

5 Ten days following parturition. Three post partum estrous periods have occured. The stroma is densely cellular. The deeply staining materials in the troma appear to be taking part in the formation of an extracellular network. The myometrium is pallid.

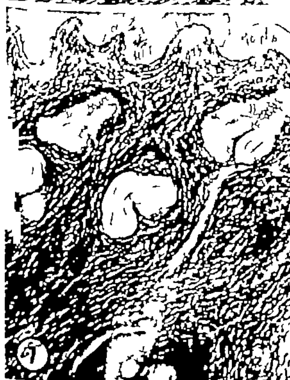
6 Fourteen days following parturition. Three post partum estrous periods have occurred. A few deeply staining extracellular stromal fibers can be seen near the myometrium.

7 Twenty-one days following parturition. Reticulated extracellular fibers are present throughout the stroma. They are thicker where the distance from the luminal epithelium is greater.

8 Twenty-eight days following parturition. The stromal fibers dominate the section. The fibrillar composition of the thick fibers is evident.


E
5
M


6


7


8

PLATE 3

EXPLAN TION OF FIGURES

Photomicrographs from transverse section of adult rat uteri. Aniline blue stain. Litters removed from their mothers on day of birth. × 170

9 Thirty-five days following parturition. Thick dense collagen bundles permeate the endometrial stroma and are the dominant feature in microscopic sections t this time.

10 *Fifty days f llowing parturition.* The less dense stroma in this section as compared with the previous one is an exampl of the individ al variability which was seen

11 Sixty days following parturition. Deep in the stroma some of the reticulated thick collagen bundles ppear t branch frequently Note the anastomoses between neighboring bundles. They are formed by groups of fibrils common to the neighboring bundles, but along different portions of their length, and contribute to the reticulated pattern of tromal collagen fibers


b v
gl


10



PLATE 4

EXPLANATION OF FIGURES

Photomicrographs from transverse sections of adult rat uteri. Aniline blue stain. Mothers were castrated and litters were removed from mothers on day of birth. × 170

12 Twenty four hours following parturition and castration. There are no thick collagen fibers in the endometrium in this section. The stroma is thin and pallid. The endometrium is similar to that seen in figure 1

13 Forty-eight hours following parturition and castration. There are no thick collagen fibers in the endometrium. The stroma is thin and pallid. Faintly staining, fine reticulated fibers like those seen in late pregnancy can be seen in the upper right quadrant of this section. A considerable quantity of deeply staining material is present in association with the extracellular fibers about the myometrial cell in the lower quarter of the photomicrograph.

14 Five days following parturition and castration. The stroma is pallid and has become wider. Puerperal reorganization of the stretched uterine tissues of pregnancy has progressed. Thin fibers can be seen most commonly near the glands and deep in the stroma.

15 Seven days following parturition and castration. Atrophy of the uterus has begun. The thinner endometrium is due largely to the loss of the abundant extracellular ground substance. There are concentrations of the deeply staining extracellular material about the glands and adjacent to the myometrium, which are not clearly organized into collagen bundles. There are no deeply staining components in the myometrium as there are in figure 13. Many large macrophages containing cytoplasmic bodies which were dark brown in the stained microscopic sections, can be seen in the endometrial stroma.


12


S
13


14


S
M
15

PLATE 5

EXPLANATION OF FIGURES

Photomicrograph from transverse sections of adult rat uteri. Aniline blue stain. Mothers were castrated and litters were removed from mothers on day of birth. × 170.

16 Fourteen days following parturition and castration. No thick col lagenou fibers can be seen in the photomicrograph. It is evident that the uteru is markedly atrophied since more than one-half of the endometrium can be seen in thi photomicrograph. All of the main cell types are reduced in size, but the cell remain compact because of the great los of extracellular constituents.

17 Twenty-one days following parturition and castration. N thick coll genous fibers can be seen in the photomicrograph. Compare to figure 7

18 Thirty-five days following parturition and castration. The uterus is contracted further tha in earlier specimens in thi series. The deeply staining extracellula material in this section ha pattern which is ery much unlike the pattern of the counterpart section (fig 9) in which collagenou fibers dominate the troma.

19 Fifty days following parturition and castration. No thick collagen bundles have ppeared in thi trophied terus. The dark lumps of variable size in the area of the endo-myometrial juncture are intracellular cytoplasmic inclu ions which were dark brown in the tained microscopic sections.


16


M
17


18


19

A Morphological Study of Fat Transport in the Normal Human Jejunum[1]

AARON J LADMAN HELEN A. PADYKULA
AND ELLIOTT W STRAUSS
Department of Anatomy Harvard Medical School, Boston Massachusetts

For more than 100 years studies of the mode of absorption of fat by the epithelial cells of the small intestine have occupied the attention of numerous investigators in experimental biology (see Palay and Karlin, '59 for a review of this literature) With the advent of methods for studying thin sections with the electron microscope it became possible to study the precise localization of particulate fat within cells during the absorptive process. In addition, the development of methods for the intraluminal biopsy of selected portions of the alimentary tract (Shiner '56 Crosby and Kugler '57; Flick, Quinton and Rubin, '61) have permitted the study of the human intestinal mucosa by a variety of techniques formerly restricted only to laboratory animals.

Recently Palay and Karlin ('59) have employed the higher resolving power of the electron microscope to examine the pathway of fat absorption in the laboratory rat. Their intensive study has suggested that fat droplets enter the epithelial cell by pinocytosis at the bases of the intermicrovillous spaces, and course through the membrane systems of the cytoplasm to be discharged at the sides of the epithelial cell into the intercellular spaces. These lipid droplets then move through the basement membrane into the lamina propria and finally into the lacteal.

At the time of Palay and Karlin s report we were engaged in a histochemical and electron microscopic study of the human jejunal epithelium in non-tropical sprue utilizing the Crosby Kugler biopsy capsule to retrieve the tissue (Padykula et al. '61) As an extension of this experience we have employed some of these methods to investigate the intracellular transport of fat in the jejunal mucosa of a normal human subject. Our findings in the human jejunum confirm those reported by Palay and Karlin in the rat. The interpretation is made that the capacity to absorb lipid increases as the absorptive cell migrates from the crypt towards the apex of the villus.

MATERIALS AND METHODS

Mucosal biopsy samples from a healthy young male physician comprise the material of this study The use of the Crosby Kugler intraluminal biopsy device (Crosby and Kugler '57) and the procedure for processing the tissues for subsequent study by light and electron microscopy are essentially similar to that which has been described in detail earlier (Padykula et al. '61) In the present work, the subject was fasted overnight, and early the next morning he swallowed the biopsy capsule. After radiological films verified that the capsule was in the jejunum, the subject swallowed 10 ml of corn oil (Mazola) and approximately 20 minutes later the capsular mechanism was triggered. The capsule was retrieved from the jejunum within five minutes after firing.

In a second experiment with the same subject, an additional patent polyethylene tube was taped to the tube of the capsular device to provide a means of monitoring the luminal contents for the presence of fat. These two tubes were swallowed by the fasted subject with seemingly little

This study was supported in part by grants B-903 (C4 and C5) and [illegible] (C7 and C8) of the National Institutes of Health, Public Health Service, Department of Health, Education and Welfare and in part by grant G-10370 of the National Science Foundation.

[1] A preliminary report of this investigation has appeared in abstract form. (Anat. Rec., 139 310, 1961).

Present address Department of Anatomy University of Tennessee Medical Units, 62 S. Dunlap St., Memphis 3, Tennessee.

Senior Research Fellow of the U. S. Public Health Service.

Special Research Fellow of the U. S. Public Health Service.

added inconvenience. After checking the position of the capsule as mentioned above the same volume of corn oil was administered and small samples (approximately 0.2 ml) of the luminal contents were withdrawn every ten minutes. These samples were mixed with an alcoholic solution of Sudan III to identify the fat in the contents. At 20 minutes after swallowing the corn oil detectable quantities of fat were recovered from the jejunum through the patent tube Forty minutes after the oil was imbibed, the capsular device was triggered and the tissue was quickly recovered. The tissue was divided into two pieces the first was fixed in 10% phosphate buffered formalin while the second was processed for electron microscopy Frozen sections (5–10 μ) of the formalin-fixed gelatin-embedded material were stained with Sudan Black B for seven minutes and compared with controls which were extracted in absolute acetone prior to staining with the Sudan dye

Sections (1–2 μ) were prepared from blocks of methacrylate embedded tissue, and stained with the periodic acid-Schiff method and hematoxylin in order to orient the specimens for thin sectioning. In addition although the lipid droplets are removed during the dehydration and clearing of the methacrylate preparations the resulting vacuolation nevertheless reflects the pathway of absorption and therefore, these sections provide a useful counterpart to the frozen sections.

Thin sections of suitable blocks were cut on a Porter Blum microtome and were stained with either aqueous lead acetate or saturated uranyl acetate in 50% ethanol and sandwiched with a thin film of celloidin. Specimens were examined in an RCA EMU 2E electron microscope or a Siemens Elmiskop I Micrographs were taken at magnifications ranging between 1,000 and 8 000 and enlarged to the desired size photographically

OBSERVATIONS

Light microscopy

Twenty to forty minutes after the ingestion of corn oil the jejunal villi have absorbed considerable amounts of sudanophilic lipid which is concentrated in the absorptive epithelium (fig 1) A conspicuous gradient in the amount of intraepithelial lipid is evident; the distal half of the villus contains the largest amount of lipid (figs. 1 2) and the amount of intraepithelial lipid diminishes progressively from the apex to the base of the villus (figs. 3 4) The cells of the villus nearest the crypts are generally free of lipid; at this level, however fine droplets of lipid occur in the region of the basement membrane (figs. 3, 4) Lipid droplets are absent in the epithelial cells of the crypt (figs. 1 3 4)

Cytologically the lipid droplets fill the apical cytoplasm of the absorptive cells near the villous tip (figs. 2, 5) In these Sudan black preparations the striated border and the nuclei are unstained, and also lipid-free cell junctions stand out as clear lines above the level of the nucleus (fig. 5) In the supranuclear Golgi region of cells near the apex of the villus lipid droplets are generally larger than those occurring elsewhere in the apical cytoplasm (fig. 5) Lipid droplets in the apical cytoplasm of cells of the lower villus are fewer in number and appear to be smaller in size; in this part of the villus the droplets accumulate selectively in the Golgi region (figs. 3 4) Lipid occurs as rows of discrete droplets between adjacent nuclei of absorptive cells and also within the lamina propria (figs. 4 5) The granules of leucocytes display an intense sudanophilia which is unrelated to fat transport.

Similar observations on lipid distribution and droplet size are found in comparable methacrylate sections from which lipid has been extracted and the intracellular vacuoles represent the site of lipid accumulation (figs. 6 7) This vacuolation further demonstrates the gradient of intraepithelial lipid in the villus. The PAS reaction in these preparations occurs in the striated border in the goblet cells and as fine granules in the apical cytoplasm.

Electron microscopy

Twenty to forty minutes after corn c
has been ingested the absorptive cells n
the apex of the villus contain nu
fat droplets in the apical cytopl
larger droplets occur in the Gol
however considerably less lipid
the infranuclear cytoplasm of

lum (figs. 8 9) In addition, at this time many droplets are free in the intercellular spaces of the epithelium at the nuclear level and in the underlying lamina propria. These observations indicate that transport across the epithelium has been effected in this short time interval.

The microvillous border and subjacent terminal web are generally free of lipid (figs. 8–16) except for occasional small droplets, approximately 50–100 mμ in diameter, which occur between microvilli (figs. 12, 15) Within the terminal web there are small, slender membrane-limited tubules which may represent invaginations of the plasma membrane or profiles of a continuous or discontinuous ectoplasmic agranular reticulum (figs. 13 15). The earliest indication of intracellular uptake was noted at the inferior margin of the terminal web where many small droplets are localized (figs. 13 14) In other sections it is evident that smooth-surfaced membranes surround such small droplets (figs. 18, 19) In general, the lipid droplets in the apical cytoplasm are enclosed by smooth membranes which appear to be a three-dimensional reticulum which ramified extensively (figs. 18 19) Occasionally the smooth-surfaced tubules with their contained lipid are disposed in a manner which suggests a helical orientation in the long axis of the cell (fig. 13) It is only rarely that lipid was found in a granular endoplasmic reticulum and this was observed in the nuclear region (fig. 16) From the endoplasmic reticular system the small droplets apparently enter the Golgi complex where they coalesce into much larger droplets (figs. 8 18 19)

Below the level of the nucleus the lipid droplets are found predominantly in the intercellular spaces, although a few droplets occur in the basal cytoplasm It is assumed that the lipid droplets have moved from the caverns of the endoplasmic reticulum into the intercellular space (fig. 17) although no clear connections of the endoplasmic reticulum with the lateral plasma membranes were observed in these preparations There is some suggestion that the lipid in the basal cytoplasm may be discharged directly from the basal surface of the cell (figs. 21 22)

All lipid whether discharged at the lateral or basal surfaces of the absorptive cells must pass through the underlying basement membrane to enter the lamina propria (figs. 8 21 22) Lipid droplets were rarely encountered in the basement membrane. Droplets are abundant in the connective tissue of the lamina propria, and are often in close association with the basement membranes of vascular capillaries (figs. 23 24) However we have not observed lipid droplets within the blood capillaries but it was common to find them within the lacteals. The lacteals are easily identified by their irregular lumens and discontinuous basement membranes (figs. 24–26) Most of the lipid droplets enter the lacteal by passing between endothelial cells. However significant quantities of lipid can usually be found within the endothelial cytoplasm suggesting that the endothelium also may participate directly in the transport of lipid into the lacteal (figs. 25 26)

The preceding cytological description was based on events which occur near the tip of the villus. As has been emphasized in our histological findings, there is a distinct gradient in the amount of intraepithelial lipid the greatest amount occurs near the tip of the villus and diminishes progressively from the apex toward the base. A comparison of the ultrastructural appearances of distal and proximal absorptive cells after the ingestion of corn oil is presented in (figs. 10 11) In the proximal cell, only the Golgi region has an appreciable amount of lipid, and the droplets tend to be smaller than that found in the Golgi regions of more distally situated cells. It is noteworthy that in this cell the endoplasmic reticulum of the apical cytoplasm is surprisingly free of lipid. These ultrastructural differences between proximal and distal cells indicate that differences in absorptive capacity may exist along the length of the villus.

DISCUSSION

From the present observations it is evident that the ultrastructural pathway for the transport of fat by the normal human jejunum is essentially similar to that described in the rat by Palay and Karlin ('59). In both these species, small lipid droplets

are seen between the microvilli and may enter the cells in droplet form by pinocytosis. However other modes of entry may exist as has been discussed by Porter ('61) Wilson ('62) and Lacy and Taylor ('62) From here the lipid passes through the terminal web in some unknown manner Droplets are only rarely seen within the web and it is possible that the transit through this most superficial cytoplasm occurs very rapidly through a tubular or vesicular membrane system (Palay and Karlin '59) or that the products of triglyceride hydrolysis enter the cell by simple diffusion and then resynthesis of triglyceride occurs beneath the terminal web (Wilson, '62 Porter '61 Senior and Isselbacher '62) Our observations suggest that a tubular system spans the terminal web although lipid droplets were not observed within it. Below the terminal web small lipid droplets are enclosed within an extensive tri-dimensional network of smooth-surfaced tubules Closer to the nucleus lipid droplets are larger and infrequently may be found enclosed by a granular endoplasmic reticulum. Within the Golgi membranes the droplets form aggregates and presumably coalesce. The various positions of the lipid droplets may be considered as markers of the physiological continuity of the cell surface with the endoplasmic reticulum and Golgi apparatus (Palay '60) A diminution in droplet size may occur as the lipid is discharged into the intercellular space at the lateral margins of the absorptive cell. The lipid droplets now devoid of membranous coverings move basally and pass through the basement membrane into the lamina propria where they enter the lacteals.

It has long been appreciated that the lipid droplets first appear within the absorptive cells at the tip of the villus (Weiner '28 Verzar and McDougall '36) These distal cells also accumulate intraepithelial lipid in greatest abundance and there is progressively less lipid in the more proximal cells of the villus. It is well established that epithelial cells of the intestine are extruded at the villus tip and are constantly being replaced by cells emigrating from the crypt (Leblond and Walker '56; Bertalanffy and Nagy '61) This gradient in lipid absorption is most likely related to the continuous replacement of the intestinal epithelium. There is morphological and histochemical evidence which indicates that the intestinal epithelium differentiates progressively during its migration (Padykula et al. '61; Padykula '62) In the normal human jejunal epithelium it has been suggested that there are changes in the distribution or amount of ribonucleoprotein during the migration of the cells from the crypt toward the extrusion zone (Padykula et al. '61; Shorter and Creamer '62) The absorptive cells at the tip of the villus are more acidophilic (Padykula et al., '61) and also have differentiated an elaborate microvillous surface (Brown '62) In a quantitative study Brown ('62) measured the microvilli of the crypt, lower villus and villus crest of the normal human jejunum. From his data it is possible to conclude that the microvilli become longer narrower and more numerous as the cells migrate up the villus. These changes in the form and number of microvilli result in an extensive elaboration of the plasma membrane with a resultant great increase in surface area at the apex of the villus. This luxuriant membranous surface may provide more numerous sites for digestive activity and transport, and also may be related to absorption by membrane flow or vesiculation as earlier postulated by Bennett ('56)

A fundamental morphological need for fat absorption may be an abundant amount of cytoplasmic membrane in the form of agranular granular and Golgi membranes for intracellular transport. In addition, cytoplasmic membranes are involved in the biochemical transformations of absorbed material. Senior and Isselbacher ('60 '62) found that the microsomal fraction of the intestinal mucosa participates in the activation of fatty acids and this is consistent with the view that fatty acids can be converted to triglycerides in the endoplasmic reticulum of the cell (Kennedy '61) It may well be that the formation of elaborate membrane systems especially agranular reticulum and Golgi membranes is another one of the principal end results of the differentiative process. In this regard there is some evidence which suggests that there may be progressive changes in the cytoplasmic membranes during epithelial

differentiation. Weiner ('28) in a study of fat absorption observed a progressive expansion of the Golgi apparatus of absorptive cells from the base to the tip of the villus, and he correlated this with the apical cell's greater capacity for lipid absorption. In the present study it was observed that in the proximal absorptive cells lipid droplets occurred mainly in the Golgi apparatus whereas in distal cells droplets filled the membrane systems of the apical cytoplasm. Also the lipid droplets in the Golgi region of the proximal cells tended to be smaller and fewer in number than in the distal cells an observation which supports Weiner's view of differences in the size of the Golgi apparatus along the length of the villus.

A cytochemical feature which may relate to the differentiation of membrane systems is the relative loss of cytoplasmic basophilia and concurrent rise in cytoplasmic acidophilia in cells proceeding toward the villus tip. The increased cytoplasmic acidophilia of the apical cells may suggest the formation of a more elaborate agranular reticulum (Fawcett, '61) Since absorbed fat droplets are always surrounded by membranes during their passage through the apical cytoplasm an extensive membrane system would appear to be necessary to handle the large volume of fat which so quickly enters the cells of the distal villus. Furthermore since the membrane system is involved in the intracellular conversions of fatty acids (Senior and Isselbacher '62) it follows also that a greater amount of membrane might result in more efficient chemical handling of lipids by the apical cells. It would be worthwhile to make a careful comparative ultrastructural study of the membrane systems of the absorptive cells along the whole length of the villus to ascertain whether cytoplasmic membranes display structural differences that could be associated with their rôle in lipid metabolism.

SUMMARY

The pathway of fat absorption by the normal human jejunum was traced in two samples of mucosa obtained by the Crosby Kugler intraluminal biopsy capsule 20 and 40 min ites after the subject swallowed 10 ml of corn oil Observations were made with the electron microscope and also on frozen sections stained with Sudan black.

A striking gradient is evident in the amount of absorbed lipid of the epithelium of the villus; the greatest amount occurs at the tip of the villus and diminishes progressively from the apex toward the base. In the distal part of the villus lipid appears as small droplets in the apical cytoplasm and as larger assemblages in the Golgi region; in the proximal part of the villus lipid is predominantly localized in the Golgi region as smaller droplets. The villous cells nearest the crypts are generally free of lipid. This gradient reflects differences in absorptive capacity and probably relates to the progressive differentiation of the epithelium during its migration from the crypt to the tip of the villus.

The intracellular pathway of lipid transport is similar to that described in the rat by Palay and Karlin. The lipid droplets within the apical cytoplasm of the absorptive cells are enclosed by smooth-surfaced membranes which are part of an extensive tridimensional agranular reticulum. Nearer the nucleus, droplets may be surrounded by portions of granular endoplasmic reticulum. Small droplets are first seen in the intercellular space at the level of the nucleus, and their course through the lamina propria and into the lumen of the lacteal has been followed.

The significance of these observations is discussed in relation to the migration and differentiation of the intestinal epithelium. In addition, a variety of evidence is reviewed which suggests that during cellular migration progressive changes occur in the properties of surface and cytoplasmic membranes which influence the cell's capacity to handle absorbed lipid.

ACKNOWLEDGMENTS

We wish to thank Dr Frank H Gardner for use of the facilities for intestinal biopsy procedures at the R. C Curtis Hematology Laboratory of the Peter Bent Brigham Hospital. Also we want to acknowledge the expert technical assistance of Miss Eileen Hall and Mr Arthur J Mitchell. The photographs with the light microscope were taken by Mr Leo J Talbert.

PLATE 1

EXPLANATION OF FIGURES

Figures 1–5 are photomicrographs of jejunal biopsies obtained 20 minutes after the ingestion of 10 ml of corn oil.

1 Jejunal mucosa, Sudan black, × 200.
Lipid droplets have accumulated principally in the villous epithelium. The greatest amount of absorbed lipid is in the upper half of the villus. The amount of intraepithelial lipid diminishes progressively from the apex of the villus toward its base. The *arrow* indicates the junction of crypt and villus. Note that the epithelial cells at the base of the villus and in the crypts are generally free of cytoplasmic droplets. The heavy staining of certain cells in the lamina propria is the result of the intense sudanophilia of granulocytes.
The boxed-in regions of the epithelium are enlarged in figures 2, 3 and 4

2 Villous epithelium (distal) Sudan black, × 500.
These epithelial cells from the upper half of the villus are filled with fine sudanophilic droplets which represent absorbed lipid. These droplets occur principally in the apical cytoplasm. The striated border and the nuclei are unstained.
This region is further enlarged in figure 5

3–4 Villous epithelium (proximal) Sudan black, × 500.
The proximal epithelium from two different villi is shown in these figures. The cells above the arrow contain lipid principally in the Golgi regions; droplets occur also in delicate rows at the nuclear level (fig. 4) and are most likely intercellular in position. Below the *arrows* the cells lack visible absorbed lipid, but fine droplets are recognizable in the region of the basement membrane.

5 Villous epithelium (distal) Sudan black, × 1,000.
The striated border is unstained. The cytoplasm immediately beneath it is also unstained, and it represents the region of the terminal web recognizable in electron micrographs (see figs. 11 13 15) Not also that the epithelial cell junctions above the nuclei appear as pale *lines due to the absence of absorbed lipid.* The droplets in the *Golgi* region are generally larger than those occurring in the remainder of the pical cytoplasm. Droplets of various sizes occur in the internuclear and basal regions of the epithelium. The *arrow* indicates the region of the basement membrane. Lipid droplets are evident also in the lamina propria.

6 Villous epithelium (distal) periodic acid-Schiff reaction, and hematoxylin methacrylate section × 500
The striated border is strongly *PAS* positive. Since the absorbed lipid has been dissolved out, the apical cytoplasm is highly vacuolated. This is another morphological representation of the absorptive tate illustrated in figures 2 and 5.

7 Villous epithelium (proximal) periodic acid-Schiff reaction and hematoxylin, methacrylate section × 500.
This region is comparable to the absorptive state illustrated in figures 3 and 4. Above the *arrow*, the supranuclear cytoplasm is vacuolated, whereas this is less evident in the call below the arrow. *The PAS reactive sites are (1) striated border (2) goblet cells, and* (3) fine granules in the apical cytoplasm.


1
2
3
4
5
6
7

PLATE 2

EXPLAN TION OF FIGURE

8 A low power electron micrograph of the distal part of the villous epithelium. The plane of section shows th apical parts of cells heavily laden with lipid droplets. The remaining apical cytoplasm is packed with droplets; in the supranuclear position, many of these are clearly larger These larger droplets are probably in the Golgi membranes (cf fig. 5) A few lipid droplets also occur in the basal cytoplasm. Numerous small lipid droplets are located in the intercellular space (icl) Occasional lymphocytes are interspersed between epithelial cells. A prominent basement membrane (bm) is usually evident A small capillary is parallel to the epithelium. × 4,200


mv
lipid
lympho-
cyte
N
bm
8

PLATE 3

EXPLAN TION O FIGURE

9 A low power electron micrograph of the distal part of the villous epithelium in an oblique plane of section. This area exhibits large intercellular spaces in the epithelium. The lipid droplets are localized predominantly in the apical parts of the cells, beneath conspicuous microvillous border (mv) Mitochondria (M) tand out noticeably in the infranuclear regions. Small lipid droplets are noticeable in the spaces between the epithelial cells as well as in the lamina propria. A venule filed with profiles of red blood cells is t the lower right. × 3,500


1
c
mv
M
L

PLATE 4

EXPLANATION O FIGURES

10 Distal absorptive cell, apical cytoplasm. Small profiles of os ophulic, round or oval lipid droplets are prominent beneath the mi ovillous border (mv) Mitochondria are interspersed mong the lipid droplets and cell junctions are free of lipid. × 10,000.

11 Proximal beorpth cell, pical cytoplasm. Both microvillous border (mv) and terminal bars (tb) are conspicuous. The apical cytoplasm is relatively free f lipid droplets when compared with figure 10 and the lipid droplets in the Golgi complex are small and relatively sparse Compare with figures 3 and 4 × 10,000.

mv

10



PLATE 5

EXPLANATION OF FIGURE

12 Distal bsorptive cell. Apical cytopl sm. Between the bases of the microvilli (mv) the *arrow* indicates small lipid particle near the surface of the plasma membrane. Below the region of the terminal web both large and small droplets, each of relatively uniform size ppear. The terminal web is generally free of lipid droplets. × 20 000.

13 Distal absorptive cell. Apical cytoplasm. The terminal web extends prominently from the regions of the terminal bar (tb). A tubular or canalicular structure courses through the terminal web (*arrow*). Beneath this tubular channel lipid is evident in two dilated canaliculi. In the upper left area of this figure ten profiles of membrane-bounded channels are filled with an opaque substance that resembles the density of lipid. These profiles give the impression of forming helical type of canal which may be continuous, being oriented in longitudinal axis. × 40,000.

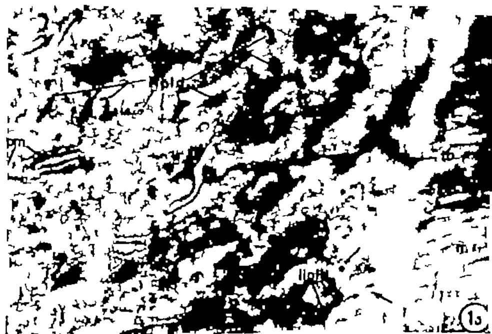


PLATE 6

EXPLANATION O FIGURES

14 Dental epithelium. Apical cytoplasm. The section is cut slightly ob liquely through the terminal web. The earliest indication absorption is found in the cytoplasm immediately benet web and takes the form f small droplets or densities v do not have any limiting membrane A little deeper in however distinct smooth-surfaced membrane (ers) ca ed enveloping the larger droplets. Two terminal bars are a ed with the pl sma membrane. × 50,000

15 Apical part of an absorptive cell. Occasionally within microvillus (mv) depressions or pits are found which correspond to original description of the caveolae (c) of Yamada ('55) These pression in the microvilli are seen infrequently I this particular micrograph particles of lipid occur t the base of the microvilli, in communication with an invagination into the region of the terminal web. In the substance of the terminal web indicated by the position of the three rrows small tubular or canalicular channel are observed. These tubulate structures are limited by smooth-surfaced membranes nd may represent portion of the endoplasmic reticulum. A mitochondrion (M) is indicated below 40,000

16 An area between two cell in the nuclear region showing the inter cellular space (icl) containing a few lipid droplets. In the cell t the left number of RNP particles occur free i the cytoplasm. I the cell at the right, areas of granular endoplasmic reticulum (erg) are found in the cytoplasm and one internal lement contains lipid droplet. The granular form of the endopl smic reticulum seems to be found in association with lipid droplets only in the cytoplasm close to the nucleus. × 50,000.


mv
lipid
15

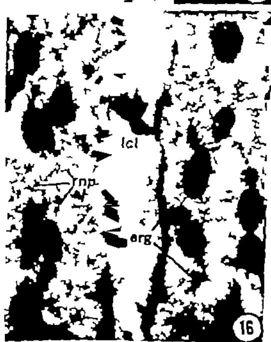

lcl
np
erg
16

PLATE 7

EXPLANATION OF FIGURE

1 The supranuclear regions of two absorptive cells and one goblet cell. In the goblet cell prominent Golgi complex (GC) is seen in association with large vacuoles containing mucus. Granular endoplasmic reticulum (erg) is prominent within the goblet cell. The two absorptive cells show evidence of the movement of lipid droplets from the cytoplasm into the intercellular space. Four instances of this activity are indicated by the *arrows*. × 20,000.

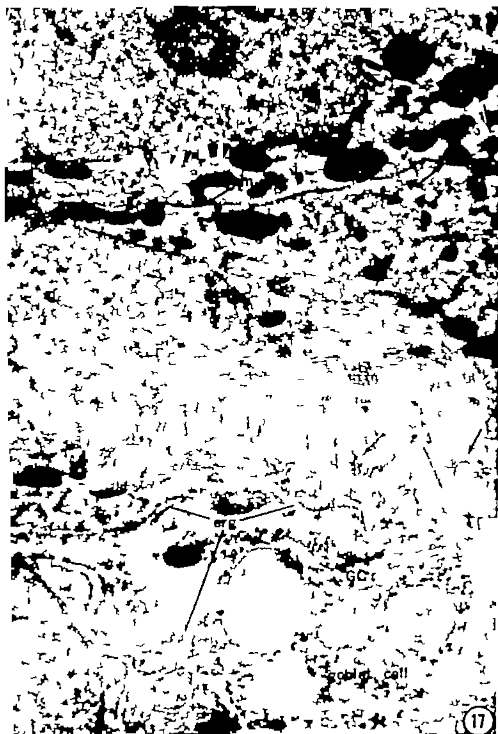

erg
GC
goblet cell
17

PLATE 8

EXPLAN TION OF FIGURE

18 An area immediately beneath the terminal web of an absorptive cell in the distal part of the villous epithelium. Small lipid droplets surrounded by smooth-surfaced membranes of the endoplasmic reticulum (ers) are bundant. Some of these small droplets are of the order f 200 A in diameter wherea others are as large 500 A. They are the smallest nit of lipid which c be identified within the confines of thi membranous, tubular system. × 50,000


ers
ers
pm
18

PLATE 9

EXPLANATION OF FIGURE

19 A region similar to that shown in figure 18 but somewhat closer t the nucleus. Small droplets occur in branching smooth-surfaced reticulum (ers) Many of these smaller lipid droplets are coalescing and forming conglomerates in the region of the Golgi complex (GC) × 50,000

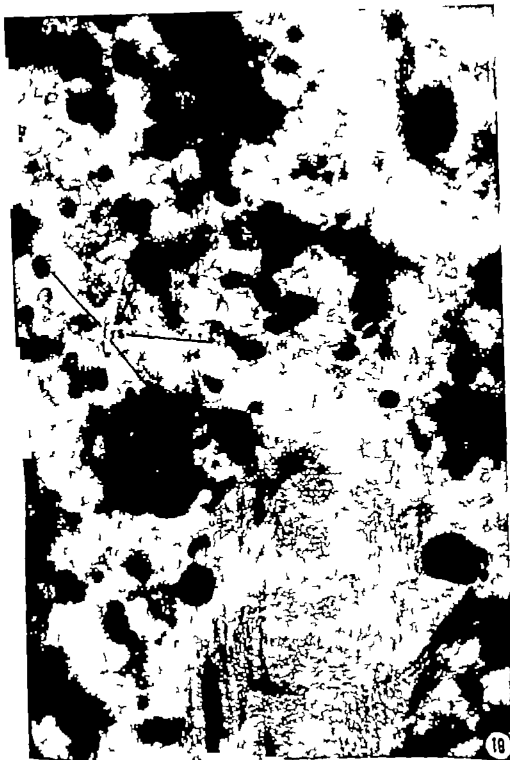

19

PLATE 10

EXPLAN TION F FIGURES

"0 A oblique section through the infranuclear portion of th howing the presence of two lymphocytes as well as coned mall lipid droplets in the intercellular space (icl) Some lipid is noted in the pper part of the figure wherea the lipid seen in the lower part of the figure is extracell the bsence of lipid droplets in the cytoplasm f lym 1..000

21 Basal oplasm of bsorptn cells near the illou tip show passag f lipid droplet through the intercell lar pace (icl) merous droplet of lipid have accumulated in the connecti e pace 12,000

22 A enlarged portion of figure 21 showing the localiz tio of lipi the baseme t membrane The position f som f the droplet gest path of egress from the cytoplasm t its inferior m rgin. lipid droplets occur both withi the basement membrane and either side of it. x 27,000.



lipid

lymphatic
lacteal

lipid

24

PLATE 12

EXPLANATION OF FIGURES

25 A portion of figure 24 showing the presence of lipid droplets beneath and between the endothelial cells. A few droplets are present in the lumen of the lacteal. × 8,000

26 Another area of figure 24 showing the endothelial lining of this lymphatic channel. The endothelium is seen as a thin cytoplasmic extension and beneath a portion of it there is a lymphocyte (L). No basement membrane intervenes between the lymphocyte and the endothelial cytoplasm (indicated by the arrows). Two leucocytes are present in the lumen. × 8,000.

lipid

E

25

endothelium

lipid

L

C

26

Index